Master of Science Thesis

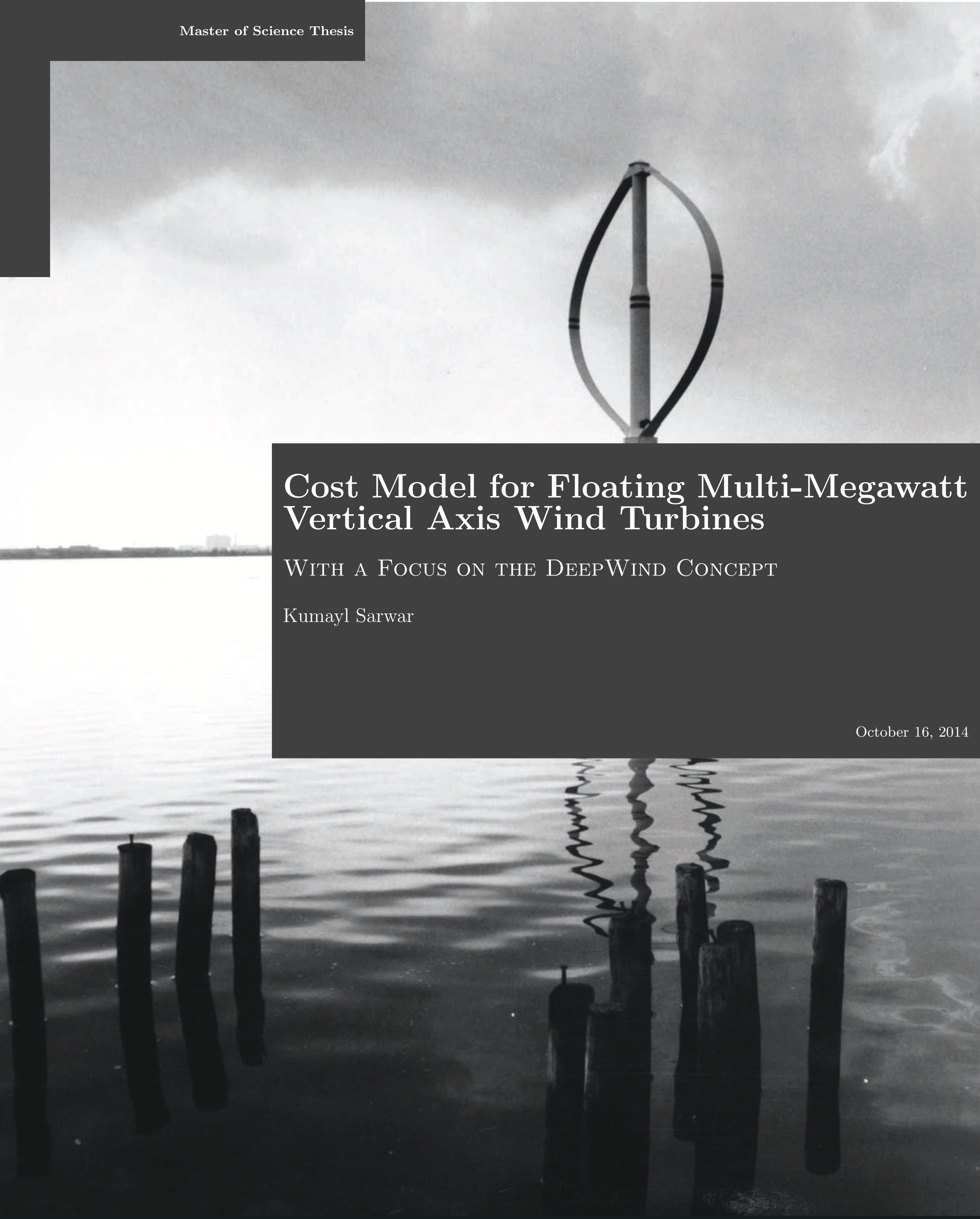

Cost Model for Floating Multi-Megawatt Vertical Axis Wind Turbines

With a Focus on the DeepWind Concept

Kumayl Sarwar

October 16, 2014

European Wind Energy Master - EWEM- Rotor Design Track

Cost Model for Floating Multi-Megawatt Vertical Axis Wind Turbines

With a Focus on the DeepWind Concept

MASTER OF SCIENCE THESIS

For obtaining the degree of Master of Science in Aerospace Engineering at Delft University of Technology and Wind Energy Engineering at Technical University of Denmark.

Kumayl Sarwar

October 16, 2014

European Wind Energy Master - EWEM
DUWIND - Delft University of Technology
Risø - Denmark Technical University
ECN - Energieonderzoek Centrum Nederland

Copyright © 2014 Kumayl Sarwar
All rights reserved.

European Wind Energy Master - EWEM
Of
Rotor Design Track

The undersigned hereby certify that they have read and recommend to the European Wind Energy Master - EWEM for acceptance a thesis entitled **“Cost Model for Floating Multi-Megawatt Vertical Axis Wind Turbines”** by **Kumayl Sarwar** in partial fulfillment of the requirements for the degree of **Master of Science**.

Dated: October 16, 2014

Committee Chair:
Prof. D r. G.J.W. van Bussel of Delft University of Technology

Supervisor:
Dr.ir. U.S. Paulsen of Technical University of Denmark

Supervisor:
Dr.ir. C.S. Ferreira of Delft University of Technology

Supervisor:
Dr.ir. J.G. Holierhoek of Energieonderzoek Centrum Nederland

Cost Model for Floating Multi-Megawatt Vertical Axis Wind Turbines

Department of
Wind Energy
Master Report

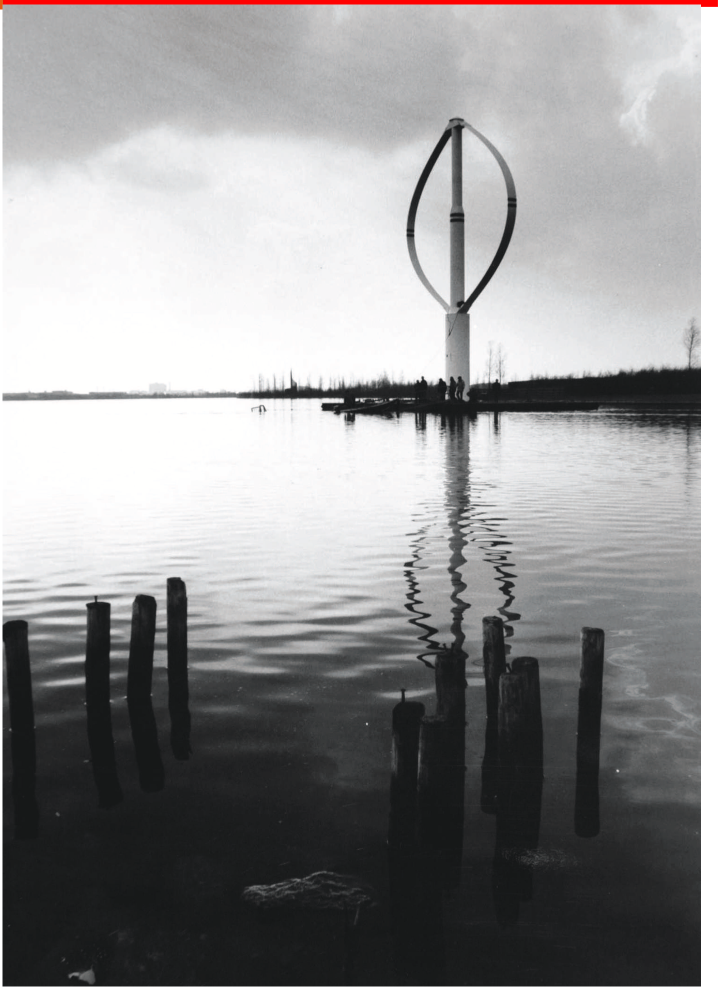

Kumayl Sarwar

DTU Wind Energy Master Thesis M-0059

October 16, 2014

DTU Vindenergi
Institut for Vindenergi

Title: Cost Model for Floating Multi-Megawatt Vertical Axis Wind Turbines - With a Focus on the DeepWind Concept

Author: Kumayl Sarwar
Department: European Wind Energy Master - EWEM

Summary (max. 2000 characters):

In an effort to achieve economic sustainability, the major challenge for offshore wind remains to bring down costs significantly before 2020. A major focus is to explore the domain of floating installations in deeper, far offshore locations. The DeepWind concept [66] is poised to demonstrate the cost savings potential for Fo-Vawt's in the multi-megawatt range. In this Master Thesis project, a cost model is designed for Fo-Vawt's focused on scaling the DeepWind concept from 5 till 15 MW in order to determine its economic viability. An analysis of the main cost and design drivers for Fo-Vawt's is presented to determine the predominant dynamic interactions and system wise cross dependencies. Scaling the baseline design with power, the mass of the systems are determined in an engineering model using the loads modelled in HAWC2. Incorporating a wind farm design optimiser, owfde, the balance of plant costs are determined to produce the final capex for a 245 MW Fo-Vawt farm in the North Sea. An O&M tool from ECN (omce) is used to simulate a parametric study of the operational environment for the wind farm. The results are combined in a economic life cycle analysis to determine the resultant LCoE and its scaling with rated power and installed capacity. For an average capex of ≈ €2650/kW and opex between €91.8 till 145.6/kW, the resultant LCoE ranges from €113.56 till 117.1/MWh. A sensitivity analysis of the LCoE and IRR for the presumptions and key elements in the model conclude that the Floater design, fixed opex and installation procedure have the strongest influence on the LCoE. Overall the DeepWind concept shows good scaling properties and a reasonable potential for cost reduction for multi-megawatt floating wind turbines.

October 16, 2014

Project Period:
2014.04.15 2014.10.15

ECTS:
30

Education:
Master of Science

Field:
Wind Energy

Supervisor:
Uwe Schmidt Paulsen

Supervisor (external):
Carlos Simão Ferreira
Jessica Holierhoek

Remarks:
This report is submitted as partial fulfillment of the requirements for graduation in the above education at the Technical University of Denmark.

Contract no.: -

Project no.:
DTU Wind Energy Master Thesis M-0059

Sponsorship: Energieonderzoek Centrum Nederland (ECN)

Front page:
Picture taken from ECN archive of a Darrieus Vawt installed at the Gaasperplas lake, the Netherlands, 1982.

Pages: 176
Tables: 33 + 3 (Appendix)
References: 74

Danmarks Tekniske Universitet
DTU Vindenergi
Nils Koppels Allé
Bygning 403
2800 Kgs. Lyngby

www.vindenergi.dtu.dk

Acknowledgements

This report marks the closing chapter of a challenging but very fulfilling journey through my master's education. I would have not been able to accomplish this if it was not for the selfless support of certain individuals close to me. I would like to start by expressing my gratitude towards all these people, all who played an instrumental role in my graduation and otherwise through my master's.

First of all I want to congratulate everyone involved in executing the EWEM programme, it is a brilliant example of knowledge homogenisation amongst renowned wind energy research institutes. I would like to thank my TU Delft supervisor, Carlos S. Ferreira, for providing me with the opportunity to work on this thesis project. Additionally I am sincerely grateful to the DTU team: Uwe S. Paulsen, Niels E. Clausen and David R. Verelst. Their collaboration on the DeepWind project, supervision in the framing of this thesis and assistance during desperate times - proved crucial towards the actualisation of this master project. More so, I am also very grateful to Michel Zaaijer for sharing his in-depth knowledge on wind farm design and Balance of Plant cost modelling.

I would like to express my appreciation to ECN in facilitating this research, especially my supervisor Jessica Holierhoek, for connecting me to the relevant people and making my time at ECN very memorable. In addition, I owe Rene v. Pieterman my gratitude for providing personal training with the OMCE tool and other valuable insights on O&M modelling.

Additionally, a big shout out to all my friends, both abroad and back home. The memories I shared with them will continue to inspire my future endeavours. Most significantly, those with my house-mate Jelmer S. Breur, a good friend that I recently lost. Also I owe a major portion of this thesis experience to Alen, Lukas and Mr. Melon.

Through all of this it goes without saying, that my master's would have not been possible without the strong backbone of my mother and brother to keep me on my feet. However, without any doubt, the most significant person has been my spouse and partner in life, *Saliha*. Without her undying support, patience and love I would be never been able to complete this masters and many other milestones in my life. To her and my departed father, I dedicate this report.

Kumayl Sarwar
Delft, The Netherlands
October 16, 2014

Preface

This Master of Science Thesis is the concluding deliverable for the European Wind Energy Master's (EWEM) programme, Rotor Design track, academic year intake 2012.

It was executed over a period of approximately nine months out of which, five months were in collaboration with Energieonderzoek Centrum Nederland (ECN) in the form of a graduation project. The work was supervised by the respective wind energy research institutes of the partner universities, Technical University of Denmark (DTU) and Delft University of Technology (TU Delft). The graduation committee consisted of

Prof.	Dr. G.J.W. van Bussel	TU Delft
	Dr. ir. C.S. Ferreira	TU Delft
	Dr. ir. U.S. Paulsen	DTU
	Dr. ir. J. Holierhoek	ECN

This Master Thesis project is primarily focused on performing an engineering cost analysis on the quantitative impacts of scaling floating vertical axis wind turbines in terms of Cost of Energy. The financial practicality of the technology was assessed with a direct focus on the DeepWind Concept developed by DTU Risø as a EU funded research under the FP7 framework - Future Deep Sea Wind Turbine Technologies. The DeepWind project was intended as a step towards improving the "technology readiness level" of floating vertical axis wind turbines.

For this project, the combination of load evaluations and existing formulations used to study the novel concept are not based on standardised procedures or measured data. Purely because the study is based on an unimplemented design and there were limited measured resources available on VAWT technology at the time of this research. This somewhat limits the viability of the findings and lead to certain presumptions where data for conventional wind turbines has been rescaled and used.

The scope of this project involved understanding all the major engineering and socio-economic aspects of wind energy. Where necessary, arguments have been presented on the system dynamics and what implications those can have on the cost of energy. Hopefully, this project will serve to provide a research directive to the growing interest in VAWT's as the future of multi-megawatt wind turbines.

Abstract

In an effort to achieve economic sustainability, the major challenge for offshore wind remains to bring down costs by approximately 35 % before 2020. With wind farm sites going into deeper waters, further from shore, with more difficult bottom conditions and rougher wave climate, costs are rising faster than the improvements in the technology are able to drive them down.

Despite these obstacles, wind farms further offshore offer better wind resource, less socio-economic restrictions and diminished environmental impacts. To satiate this need, floating wind turbines provide a feasible promise. In the wake of current Horizontal Axis Wind Turbine (HAWT) floating projects such as HyWind, IDEOL etc, the perceived positive impact of the floating system, especially for larger scale machines, is reduced due to large overturning moments and difficult accessibility of the "moving" nacelle. A possible solution to these obstacles is presented by the DeepWind project which focuses on implementing a Floating Offshore Vertical Axis Wind Turbine (FO-VAWT) on a spar structure.

In this report, the economic feasibility of a FO-VAWT concept in far offshore wind farm is assessed - from current to multi-megawatt rated power. The possible benefits of a FO-VAWT are translated into cost indicators for the main aspects of an offshore wind farm project. The difference in turbine CAPEX, perceived reductions in balance of plant costs and the impact on OPEX, is modelled into an engineering framework to determine the Levelised Cost of Energy.

Considering mass and swept area as the base factors, the mass of the baseline DeepWind turbine design [66] is approximated and broken down into material and manufacturing costs with adjustments for inflation and other financial variables over the lifetime of the wind farm. Using ECN's OMCE package, a detailed operations and maintenance (O&M) strategy is devised and implemented with respect to VAWT systems and a floating wind farm. The grid infrastructure, installation and project development costs are estimated using TU Delft's Offshore Wind Farm Design Emulator tool developed by Zaaijer [75]. All these components are combined to deduce the cost of energy for the DeepWind and the turbine capital costs for similar turbine designs.

To study the design space of the cost model, a sensitivity study of the main presumptions was done along with an evaluation of LCoE impact from rotor, floater and generator design. Using geometric up-scaling methods, the baseline FO-VAWT design was sized for higher rated power capacities and corresponding loads simulated using HAWC2. Considering a 245 MW wind farm, a workspace was created to assess where the greatest potential in cost reductions exist and provide *impact trigger's* for future research .

It was seen that the turbine capital costs for a VAWT are not significantly higher than for a comparable state-of-the-art 5MW HAWT. The reliability of a VAWT is better and subsequently the wind farm has a higher availability, assuming the same technology maturity level as a present day Hawt. Although, possible higher fixed capital costs originate for the specialised supply chain to maintain floating turbines and the DeepWind subsystems. This on average pushes the annual opex beyond €120/kW. The capex/kW extends between €2520 to €2780/ kW for the 5 to 15 MW Fo-Vawt's respectively, leading to a Levelised Cost of Energy from€113.56 to 117.1 per MWh.

Nomenclature

Latin Symbols

C_b	Centre of Buoyancy	[m]
C_d	Coefficient of drag	$[-]$
C_l	Coefficient of lift	$[-]$
C_p	Coefficient of power	$[-]$
C_t	Coefficient of Thrust	$[-]$
D	Scaling Characteristic Dimension	[m]
E	Young's Modulus	$[N.m^{-2}]$
F_ω	Centrifugal Force	$[N]$
G	Shear Modulus	$[N.m^{-2}]$
$H_{fl,s}$	Draught/height of submersed Floater	$[-]$
h_o	Measurement height	$[m]$
$h_{s,max}$	Maximum wave height	$[m]$
h_s	Significant wave height	$[m]$
I_{rated}	Current at rated wind speed	$[A]$
k_{mat}	Cost of material per unit mass	$[€/kg\,\$/kg]$
k_{sys}	System Production Price	$[€/kg]$
P_I	Power intensity	$[kW.m^2]$
$P_{WF,max}$	Maximum Power Capacity of Wind Farm	$[kW]$
r	Discount rate	[%]
r_k	Radius of curvature	$[-]$
T_z	Mean zero crossing period	$[s^{-1}]$
$U_{(z)}$	Wind speed profile	$[m.ss^{-1}]$
z_o	Roughness length	$[m]$

Greek Symbols

β	Heel Angle from vertical	$[rad]$
ρ	Density	$[kg.m^3]$
ϕ	Diameter	$[m]$
η_{elec}	Electrical Efficiency	$[-]$
ϵ	Eccentricity of an ellipse	$[-]$
ν	Kinematic Viscousity	$[N.s.m^{-2}]$
λ	Tip Speed Ratio	$[-]$
Λ	Failure rate	$[yr^{-1}]$
ω	Rotational Speed	$[rad.s^{-1}]$
υ	Poisson's Ratio	$[-]$

Abbreviations

HAWC2	Horizontal Axis Wind Turbine Simulation Code - 2^{nd} Edition
AEP	Annual Energy Production
CAPEX	Capital expenditure
CFRP	Carbon Fibre Reinforced Polymer
CF	Capacity Factor
DMST	Double Disc Multi Stream-tube
DoE	Department of Energy
DoF	Degree of Freedom
ECN	Energieonderzoek Centrum Nederland
EWII	European Wind Industrial Initiative
FCF	Fixed Cost Fraction
FLC	Fatigue Load Capacity
FTC	Fault Type Class
GDP	Gross Domestic Product
GFRP	Glass Fibre Reinforced Polymer
HAWT	Horizontal Axis Wind Turbine
IRR	Internal Rate of Return
LCF	Labour Cost Fraction
LCoE	Levelised Cost of Energy
LPC	Levelized Production Costs
LSS	Low Speed Shaft
MPL	Mature Production Level
MTBF	Mean Time Between Failure
MTTF	Mean Time to Failure
O&M	Operations and Maintenance
OMCE	Operation and Maintenance Cost Estimator
OPEX	Operational Expenditure

OWFDE	Offshore Wind Farm Design Emulator
PCC	Point of Common Coupling
PPI	Producer Price Index
RNA	Rotor Nacelle Assembly
ROV	Remotely Operated Vehicle
SCS	Spare Control strategies
STT	Surface Transition Tube
TCC	Turbine Capital Costs
TTR	Time Taken to Repair
ULC	Ultimate Load Capacity

Contents

Acknowledgements **vii**

Preface **ix**

Abstract **xi**

Nomenclature **xiii**

List of Figures **xxiii**

List of Tables **xxvi**

1 Introduction **1**

1.1 Project Goals 1

1.2 Research Question 1

1.3 Project Deliverables 2

1.4 Project Report Outline 2

2 Theoretical Background **5**

2.1 Offshore Wind Industry 5

2.2 Vertical Axis Wind Turbines 8

2.3 Vertical Axis Wind Turbine Aerodynamics 10

2.4 Floating offshore structures 13

2.4.1 Spar Buoy 13

2.4.2 Semi-Submersible 13

2.4.3 Tension Leg Platforms 14

2.4.4 Concept Analysis 15

2.5 VAWT vs HAWT 16

2.6 Scaling 18

2.6.1 Linear Scaling 18

2.6.2 Empirical Data Regression 19
2.6.3 Comparison to other Scaling methods 19
2.7 Cost of Wind Energy 21
2.7.1 Offshore Wind Farm Cost structure 21
2.7.2 Life Cycle Costing 23
2.8 State of the Art CoE Model analysis 25

3 Floating VAWT 27
3.1 DeepWind 27

4 Engineering Model 33
4.1 Model Design Methodology 33
4.2 FO-VAWT Wind Farm Initialisation 37
4.2.1 Meteorological Inputs 38
4.2.2 Material Inputs 39
4.3 Up-Scaling 40
4.3.1 Rotor Scaling Trends 41
4.3.2 Geometric Scaling with Power 43
4.3.3 Mass 45
4.3.4 Cost 46
4.4 Power estimation 46
4.5 DeepWind Simulations 48
4.6 Sizing - Static Modelling 49
4.6.1 Blade 49
4.6.2 Surface Transition Tube 54
4.6.3 Tower 54
4.6.4 Spar Buoy 58
4.6.5 Mooring 61

5 Cost Formulations 65
5.1 Model Structure 65
5.2 CAPEX - Turbine Capital Costs 66
5.2.1 Rotor 66
5.2.2 Tower 67
5.2.3 Floater & Mooring 67
5.2.4 Power-Train 68
5.2.5 Electronic Systems 69
5.2.6 Additional Hardware 69
5.3 CAPEX - Balance of Plant Costs 71
5.3.1 Electrical Infrastructure 71
5.3.2 Offshore Structures 73
5.3.3 Transport and Installation 73
5.3.4 Project Development 75
5.3.5 Decommissioning 75

5.4 OPEX - Operations & Maintenance Costs . . . 76
5.4.1 Introduction . . . 76
5.4.2 OMCE Concept . . . 76
5.4.3 Operations and Maintenance Modelling . . . 78
5.4.4 FOWT O&M Initialisation . . . 80
5.4.5 Equipment . . . 83
5.4.6 Fault Type Class . . . 83
5.4.7 Failure Rates . . . 84
5.5 Annual Energy Production . . . 88

6 Results and Analysis 91
6.1 Scaling . . . 91
6.2 CAPEX . . . 92
6.3 OPEX Parametrisation . . . 95
6.4 Economic Assessment . . . 99
6.4.1 Sensitivity Analysis . . . 99

7 Conclusions 109
7.1 Recommendations . . . 110
7.2 Final thoughts . . . 111

References 113

A Existing Cost Models 119
A.1 Definitions . . . 119
A.2 Review of CoE Models . . . 119
A.2.1 UpWind . . . 119
A.2.2 InnWind . . . 120
A.2.3 NREL . . . 121
A.3 Figures . . . 121

B Model Estimations 125
B.1 Area Mapping . . . 125
B.2 Estimation of Production Price . . . 126
B.2.1 Other Cost Parameters . . . 129
B.2.2 Labour Percentage estimations . . . 130
B.3 Cost Driven Optimisation Framework . . . 131

C Balance of Plant Cost Simulations 135

D Operation and Maintenance 141
D.1 Repair Classes . . . 141
D.2 Failure Frequencies . . . 145

List of Figures

2.1 Worldwide Installed Wind Capacity, [17] 5

2.2 State of the offshore wind energy sector as of 2013 6

2.3 Scatter of Offshore CAPEX against installed Wind Farm power capacity, [53] . . . 7

2.4 Parameter sensitivities for offshore and onshore wind Cost of Energy, [70] 7

2.5 Different Types of Wind Turbines 8

2.6 Earlier Darrieus shaped VAWT's 9

2.7 Schematic Top view of two blade VAWT showing different stage velocities U across a stream-tube for azimuth position ψ of blade 10

2.8 Variation of Angle of attack(α) across azimuth position ψ for a VAWT operating at $\lambda = 4$, Ferriera [36] 11

2.9 Forces estimations on 2D VAWT NACA 0015 airfoil pitched at $\theta= +3$, $\lambda = 4.5$ and $\sigma = 0.1$ using various aerodynamic models, [35] 12

2.10 Different types of floating foundations for offshore structures, [12] 13

2.11 Floating Spar wind turbine concepts and prototypes 14

2.12 Floating Semi-submersible design concepts and prototypes 14

2.13 Floating tension leg platform concepts and prototypes 15

2.14 Loading sources on offshore WT 16

2.15 Regressive mass scaling trends for (a) Tower, (b) Blade, (c)Rated power; as a function of characteristic dimension taken as diameter 20

2.16 Estimated Life-Cycle Cost Breakdown for an Offshore Wind Project, and prospective regions of improvement for VAWT's, Griffith [39] 21

2.17 Cost of energy overview for offshore wind, Jamieson [44] 23

2.18 Installed capital costs for onshore and offshore wind turbines based on industry averages normalised for NREL 5 MW reference turbine (source Tegen et al. [70] . . 24

3.1 Parameters influencing the outputs derived from the rotor 28

3.2 Parameters influencing the outputs derived from the tower 28

3.3 Parameters influencing the resultant outputs and size of the surface transition tube 29

3.4 Parameters influencing the response and the resultant outputs from spar bouy floater 29
3.5 DeepWind mooring system input/output and design possibilities 30
3.6 DeepWind power-train system input/output and configuration possibilities 30
3.7 Schematic Representation of the DeepWind Turbine 32

4.1 Work-flow for VAWT Engineering Cost model 34
4.2 Setup of FO-VAWT Wind Farm 37
4.3 Location of Wind Farm site close to the K13 measurement station 37
4.4 Site conditions at K13 site. 38
4.5 Non dimensional Cost and Power parameters related to height over diameter for various VAWT designs, [58] 42
4.6 Non linearity of normalised Reynold's number over a VAWT operational regime . . 42
4.7 VAWT α airfoil through a revolution, (Source: Rene Bos) 43
4.8 Power scaling relation with diameter ϕ, [44] 43
4.9 Representation of Catenary shape as a VAWT rotor blade, [56] 44
4.10 Curve fit for VAWT height vs Swept area for H/D of 1.182 45
4.11 Scaled and corrected rated aerodynamic torque represented by Shaft M_z for 10 MW VAWT 46
4.12 Power curves and rotor speed for 5 - 15 MW VAWT 47
4.13 Generator torque coupling with the rotational motion of the spar U_0=16 $m.s^{-1}$, (Source: DeepWind) 49
4.14 Ellipse Eccentricity scaling relation to map the leading edge of NACA 00XX airfoil's 50
4.15 Mapping of contours of NACA 0030 airfoil using methods mentioned in table 4.6 . 51
4.16 Cubic spline interpolation of airfoil internal structure thickness and blade t/C along blade span for TUD MSc VAWT, [62] 51
4.17 Cubic spline interpolation of blade cross sectional area along blade span of TUD MSc VAWT, [62] 52
4.18 Linear interpolation of blade cross sectional area along blade span of DeepWind VAWT 52
4.19 Input coordinates and 6^{th} order polynomial fit onto DeepWind and TUD MSc VAWT 53
4.20 Axial Forces at tower top for 5,10,5 MW turbines at rated conditions 56
4.21 Thrust Force for 5, 10, 15 MW turbines for rated U_∞= 14 [m/s] 56
4.22 Vector Schematic of DeepWind VAWT, where Z_b= C_b and Z_g = C_g [60] 62
4.23 Aerodynamic torque for 5, 10 and 15 MW VAWT's 62

5.1 Active Mass scaling trends based on un optimised designs by Leban [49] 68
5.2 5 x 5 Wind Farm Electrical Infrastructure 71
5.3 Cost of Export cable against installed wind farm capacity 72
5.4 Qualitative impact of accessibility on system availability, [45] 76
5.5 OMCE package depicting complete chain from data processing, event definition, database update and cost prediction, [28] 77
5.6 Schematic overview of the maintenance effort over the first operational years of a wind farm and the expected maintenance effort in the near future period, [29] . . 79

5.7 (a)Bathtub curve modelling the failure intensity for a repairable system against its age; (b) Impact of increased resolution in OMCE on computational effort and accuracy [45] 80
5.8 Fault type class definition based on type of maintenance 84
5.9 Processes structure for a corrective maintenance Fault type class 85

6.1 Scaling of Turbine Capital Cost Fraction with rated power for Glass fibre and Carbon Fibre Blades 92
6.2 Scaling of Balance of Plant (a) cost fractions with rated power and (b) Costs per kW with wind farm capacity 93
6.3 Scaling of Fo-Vawt (a) CAPEX with rated power and (b) Costs per kW with rated power 93
6.4 Cost fraction breakdown per GFRP rotor Vawt in a 49 * 5 MW installed capacity farm 94
6.5 O & M Results for base case with FOWT strategy, $\Lambda_{wt} = 4.33$ and $\Lambda_{bop} = 4.16$, in a 104*5 MW Fo-Vawt farm 97
6.6 O & M Results for ECN Default model, WT fail rate of 4.07 and BoP fail rate of 4.53 in a 105 * 5MW Hawt farm. 98
6.7 Avg Cost Breakdown for bottom founded Vawt in a 49 * 5 MW farm with a BH-WH fail rate 98
6.8 Life cycle cash flow for 49 * 5 MW wind farm with initial discount rate 7% and IRR of 10.33% 99
6.9 Levelised Cost of energy breakdown for 5 MW Fo-Vawt 100
6.10 Levelised Cost of energy breakdown for 10 and 15 MW Fo-Vawt, $\Lambda = 6.5$/yr . . . 101
6.11 Sensitivity diagram of LCoE and IRR 104

A.1 Levelised Cost of Energy Calculation for classical and innovation based up-scaling,([23, 51]) 122
A.2 Turbine Size influence on LCoE and its main drivers,([23, 51]) 122
A.3 Mass breakdown and Cost elements for Optimised 5,10 and 20 MW Hawt derived by Ashuri [8] 123

B.1 Illustration of area estimation error using box beam for mid section 126
B.2 historic average annual inflation rates for major wind turbine manufacturing countries , inf [2] 127
B.3 System production costs for Floater and mooring system 128
B.4 Vawt Cost Driven Design framework presented by Sarwar [63] 131

C.1 Scaling fit for BoP cable costs vs increasing WF power capacity 135
C.2 Power relations depicting the scaling of infield cable length with WF Power Intensity. 136
C.3 Cost Results for BoP simulations for 5MW and 15 MW Vawt in a rectangular grid 139
C.4 Cost Results for OWFDEsimulations for 5MW bottom foundedHawt in a 7 x 7 rectangular grid 140

List of Tables

2.1 Approximate CAPEX for European Offshore Wind projects, [17] 6
2.2 Linear Scaling laws for turbines, [22, 44] 19

3.1 Gross Specifications of the DeepWind 5 MW Baseline Turbine [66] 31
3.2 Detailed Geometric properties of final 5 MW DeepWind Turbine [66] 31

4.1 Material properties and cost 39
4.2 Gross specifications of hypothetical FO-VAWT farm 40
4.3 Scaling factor of characteristic dimension, “turbine height” 45
4.4 State-of-the art mass-diameter scaling exponents 45
4.5 Torque for 10 MW and 15 MW VAWT at different rated rotational speeds 47
4.6 Cross sectional Area estimation of airfoil section 50
4.7 Blade Volume estimations and Mass estimation for VAWT 53
4.8 Tower Sizing results 58
4.9 Mooring Sizing results 63

5.1 System production price for the tower 67
5.2 Different WF sizes based on number of turbine and turbine capacity 73
5.3 Linear scaling constants for infield cable length with WF power with turbine spacing 74
5.4 General Specifications for the OMCE tool for a FO-VAWT 82
5.5 Specification of support vessels required for 5MW FO-VAWT farm 83
5.6 Spare parts categorisation for 5 MW FO-VAWT used in OMCE 85
5.7 Estimation factors contributing towards P_{50} Net AEP 89
5.8 Range of Net P_{50} AEP and Capacity factor per unit turbine for FO-VAWT farm . . 89

6.1 Results from scaling of the DeepWind turbine 91
6.2 Parametric legend for system failure rates 95
6.3 Operation and Maintenance parametric results for FO-VAWT farm with different O&M strategies, rated power, installed capacity and location 96

6.4 Cost Results for 49 * 5 MW DeepWind Fo-Vawt farm located K13 site in the North Sea . . . 100
6.5 Influence of rated power on key economic parameters for similar installed capacity Vawt farm . . . 101
6.6 Influence of installed capacity on key economic parameters for 10 MW Vawt farm 102
6.7 Influence of variation in capacity factor on key economic parameters for 49 * 5 MW Vawt farm . . . 102
6.8 Influence of deviation in capex estimates on key economic parameters of a 49 * 5 MW Vawt farm . . . 103
6.9 Influence of wind turbine failure rates (Λ) on opex and key economic parameters of a 49 * 5 MW Vawt farm . . . 103
6.10 Influence of discount rate on LCoE of a 49 * 5 MW Vawt farm . . . 104
6.11 Influence of electricity price on key economic parameters of a 49 * 5 MW Vawt farm 104
6.12 Qualitative Analysis of system wise capex cost model to determine high impact triggers . . . 106

B.1 Hawt Cost fraction distribution from win, Blonk [6, 16] . . . 128
B.2 Fixed cost and mature production process level fractions . . . 129
B.3 System production prices corrected for inflation based on location of study, EU or USA. . . . 129

D.1 Review of failure frequencies from three European reliability surveys, a turbine manufacturer data and in-house knowledge at ECN . . . 147

Chapter 1

Introduction

The chapter introduces the goal of this Master Thesis project followed by the governing research question. Based on the derived sub-research questions, a list of deliverables are presented which define the scope of this project. Finally an overview of the project through a chapter-wise summary is provided to outline the report distribution.

1.1 Project Goals

This Master Thesis project is aimed at creating, designing and implementing a cost model to evaluate the feasibility of optimized multi megawatt offshore Vertical axis wind turbine (VAWT) designs in terms of Levelised Cost of Energy (LCoE). The focus is on evaluating the state of the art in cost modelling and implementing them on defining VAWT subsystems in terms of Design costs, Operation and Maintenance costs and Balance of Plant costs. The knowledge gained will be translated into setting up a framework model based on the detailed design of a VAWT rotor with the aim of keeping it modular and flexible enough to be adapted for other VAWT designs. By varying critical geometric/functional parameters that define the turbine and hypothetical wind farm, a workspace will be created for the scaling of key turbine and wind farm costs. The model structure will include different analytical modules handling the initialisation, performance prediction and mass estimation to determine the corresponding LCoE for a design. By studying the impact on costs for defined VAWT designs, a comparison in the variation in LCoE between VAWT and HAWT concepts will be used to supplement the feasibility and drive further research directives for the FO-VAWT concept.

1.2 Research Question

The main research question motivating this project arises due to the currently high cost of energy for offshore wind.

> "*Is it possible for optimised multi megawatt vertical axis wind turbine designs to achieve a cost/kWh less than €10 cents for far offshore implementation?*"

To answer this question, a few sub questions need to first addressed. Based on these questions, the scope of this project was defined in the next section 1.3

What are the main cost drivers for far offshore wind energy?

How do the cost aspects for vertical axis wind turbine's scale with increasing power capacity?

Which systems have the highest impact on the cost of energy?

1.3 Project Deliverables

In order to evaluate the cost applicability of a VAWT design and address the questions driving this study, a list of deliverables were derived to determine the scope of this Master Thesis project.

1. Analyse the state-of-the-art in offshore wind energy and breakdown the cost structure.
2. Review existing cost models and analyse current cost drivers for conventional multi-megawatt offshore wind turbines
3. Understand the relevance of the cost components and subsystem models for floating offshore vertical axis wind turbines (FO-VAWT). Analyse the design and cost drivers for the subsystems to determine which models can be implemented in the cost modelling of FO-VAWT's.
4. Develop an engineering framework to determine the cost of major systems for the selected FO-VAWT design(s). Prescribe scaling criteria for design.
5. Design O&M strategy and implement combined LCoE model for a far offshore wind farm.
6. Perform sensitivity analysis of main assumptions to define cost workspace.
7. Analyse scaling impacts of rated power, installed capacity and other essential parameters on the LCoE.

1.4 Project Report Outline

Based on the deliverables presented in the previous section 1.3, the outline of the chapters in this Master Thesis project are drafted to address each of these points leading towards answering the main research question. For each chapter, a small summary is presented to better identify the key elements addressed and provide the reader with a clear overview of the report.

Chapter - 1: An introduction on the research question, process and deliverables for this Master Thesis projectare presented. A chapter wise outline for the report is given.

Chapter - 2: A theoretical background on the relevant topics is provided. These include, current status of offshore wind energy sector and the factors feeding towards its growth, a state-of-the-art technological overview on VAWT's, floating wind turbine technology, current turbine mass and cost scaling techniques, a breakdown of the cost segments for offshore wind energy and a review of cost of energy modelling through the existing variations of implemented techniques.

Chapter - 3: The FO-VAWT concept is introduced with an investigation of the key design and cost drivers for the main subsystems. The design of the selected FO-VAWT concept is presented: DeepWind.

Chapter - 4: The design methodology for the cost model is developed. The framework of the engineering model is reported, encompassing estimations of the main aspects required to determine the loading and masses of the main turbine systems.

Chapter - 5: Utilising the inputs from the previous chapter, the CAPEX formulations for the Turbine Capital costs and Balance of Plant costs are explained. A parametric emulation of the Balance of Plant costs for a FO-VAWT wind farm is done using the OWFDE tool. Next the OPEX aspect of LCoE is determined. The impact on OPEX, availability and AEP for a systematic variation of base conditions is compiled.

Chapter - 6: The results from chapter 4 & 5 are illustrated. The impacts on LCoE & IRR for varying critical assumptions and important factors is evaluated via a sensitivity analysis. The results from the scaling on LCoE are also examined.

Chapter - 7: In the final chapter, the conclusions for this Master Thesis project are drafted while highlighting key assumptions impacting the results. Concurrently, future recommendations are provided towards the utilisation of the cost model and development paths for FO-VAWT 's.

Chapter 2

Theoretical Background

Through this chapter a review of the trends in the offshore wind sector and how it continues to motivate efforts in cost reduction. Following that, a brief review on the working principle of the HAWC2 aerodynamic module, an overview of state-of-the-art in floating wind turbine concepts/prototypes and a comparison of vertical axis turbines with horizontal axis machines is given. Prevalent scaling techniques for wind turbines are presented followed by an understanding of cost of energy modelling for wind turbines is developed from analysing cost structures of existing LCoE research. All these topics provide necessary elements required in the following chapters.

2.1 Offshore Wind Industry

Sustainability has been the catch phrase since the start of this century. Due to the growing awareness of the impact of human practices on the ecosystem and the possibility of insufficient resources to fuel future growth, there has been a strong surge in sustainable energy technologies and practices. Currently, the technology leading this is paradigm shift is wind energy.

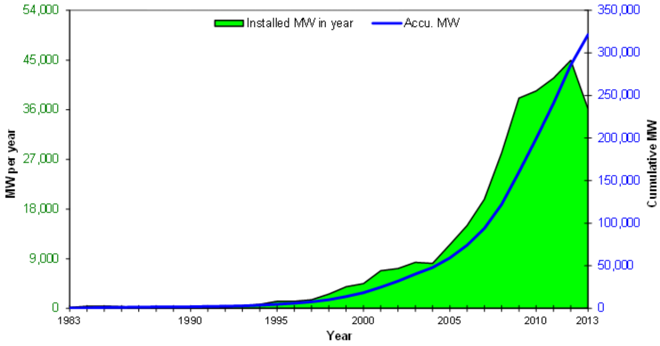

Figure 2.1: Worldwide Installed Wind Capacity, [17]

In the past years, an influx of technical developments in wind turbine technology, driven by strong political support for clean energy, has led to exponential growth of the sector, figure 2.1. The EU Member states have drawn objectives of installed wind capacity for 2020 within the context of the

EU Climate and Energy Policy. The 2013 state of installed wind capacity onshore in the EU is ≈ 120 GW while for offshore is ≈ 6.5 GW. With a 5 yr growth average of 21.4 % the goal of an additional $60\,GW$ by 2020 for onshore is attainable. However a more significant deficit of $33.5\,GW$ for the offshore targeted capacity by 2020, is developing concern towards the sustainability of the offshore sector [7, 17].

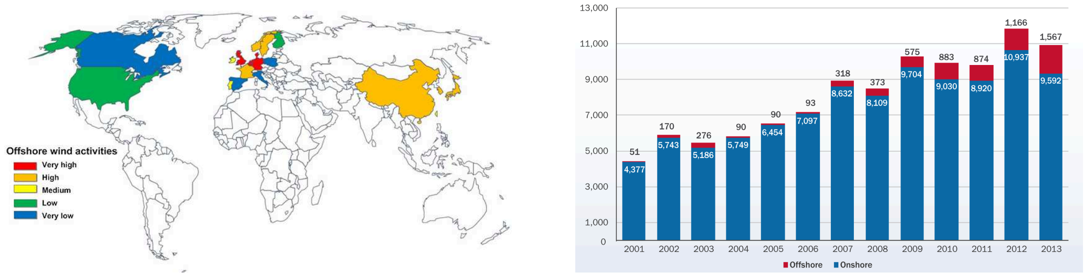

(a) Global Offshore Wind Markets, [17]

(b) Annual Wind installations (MW), [26]

Figure 2.2: *State of the offshore wind energy sector as of 2013*

It is important to note that this demonstrated progress is leveraged by the favourable state policies in place till 2020, in the form of feed-in tariffs, trade-able green certificates or favourable tendering. Nevertheless, despite current indicators and subsidies to promote the advent of wind energy sustainability, certain physical boundaries, mainly socio-economic limit the growth possibilities onshore. Thus in pursuit of better wind resource, less restrictions and more wind farm scalability freedom, the EU wind market is keen towards expanding offshore, figure 2.2a. With the advent of first offshore wind farms in 1992 at Vindeby (DK) as a modest 5 MW installation, figure 2.2b shows the global installed capacity of offshore wind energy growing exponentially to about 6.82 GW as of 2013, [17]. The reasons for this can be derived from the inherent advantages of offshore wind energy.

- Better Wind Resource: higher Capacity Factor (CF) and Annual Energy Production (AEP)
- Less problems relating to area and human interaction. Less socio-political resistance
- Steeper Wind profile (U_z) improves load distribution along the height of turbine
- Potentially unlimited wind farm scalability
- Offshore wind energy projects encouraged and strongly subsidized by EU states to deem profitable for developers
- Power needed at coastal population or island inhabitation

Table 2.1: *Approximate* CAPEX *for European Offshore Wind projects, [17]*

Online Date	Project Features	WT Rated Power	CAPEX
2000 - 2006	depth ≤ 20m, Monopiles dist ≤ 10 km from shore	$P_{WT} \leq 2.5$ MW	€1.9 M / MW
2007 - 2011	depth 10 - 30 m, Monopiles dist 10 - 35 km from shore	2.3 MW $\leq P_{WT} \leq$ 4 MW	€3.3 M / MW
2009 - 2016	depth ≤ 35 m, Jacket/tripod dist 20 - 55 km from shore	3.6 MW $\geq P_{WT} \leq$ 6 MW	€4.35 M / MW

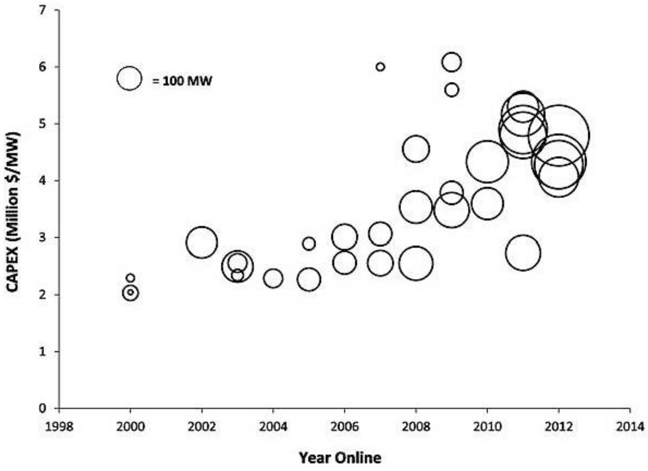

Figure 2.3: *Scatter of Offshore* CAPEX *against installed Wind Farm power capacity, [53]*

Coupling these advantages with the general understanding that development costs reduce due to *Economies of Scale*, meaning for larger wind farm installations with larger wind turbines the cost per kW/MW should be decrease, it seems straight forward to assume that the future of wind energy exists in higher capacity offshore installations. However, this assumption is disputed by observed data. According to a data compilation from EU offshore wind projects given in table 2.1 and depicted in figure 2.3, the approximate CAPEX is increasing with installed power/size. Although this rise in CAPEX per power can be attributed to the coinciding economic instability over the past few years, but the increase in commodity prices is not the lone responsible factor. Although the high cost per power is not indicative of the relative immaturity of the offshore wind sector, but of the level of impact variations in site specific parameters have on CAPEX costs. These include water depth, distance from shore, geographic supply chain maturity, severe weather, and higher foundation wave loads. This can also be deduced from figure 2.4a where a high variance in offshore Initial Capital Costs (ICC) dictate large fluctuations in the overall Cost of Energy; whereas for onshore wind (figure 2.4a) this parameter is much more constraint. It is worth noting that the relatively high baseline cost of energy is from values averaged from the limited offshore wind capacity in the USA.

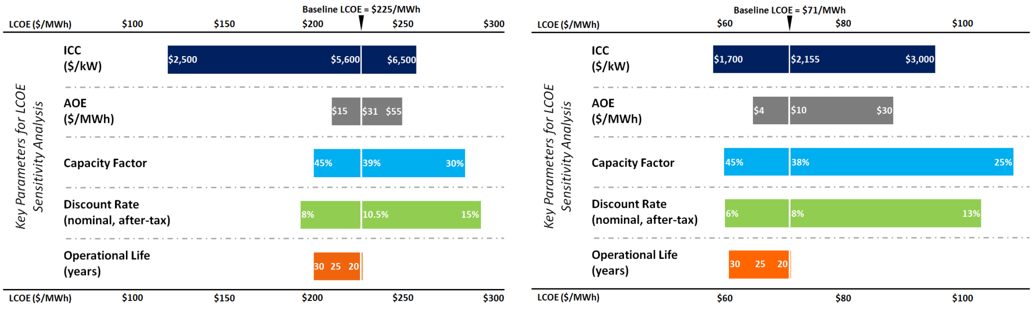

(a) Offshore (b) Onshore

Figure 2.4: *Parameter sensitivities for offshore and onshore wind Cost of Energy, [70]*

Despite the growing obstacles faced by offshore wind such as installation, expensive supply chain, difficulties in operation and maintenance, the yearly installed offshore wind continues to increase over the years, (figure 2.2b). In general the future of wind energy exists offshore. The advantages and possibilities outweigh the current financial drawbacks entailed with large offshore wind turbines. As most of the good wind resource areas near the coast or in shallow waters are being quickly assimilated, the resulting need for far offshore wind farms is inevitable. This although is not the only reason that there is a need for offshore wind turbines which can function in deep waters. Certain environments have deep water coastlines such as Norway and Japan. Deeper water's result in higher capex for bottom-founded structures with the current technical setup, while in some cases the large depth and hard sea-floor make the installation of a foundation impossible.

Therefore, *cost reduction* in the offshore wind sector is the challenge to face, with the aim to make far offshore wind farms a profitable possibility. In this Master Thesis project, the question tackled is whether floating structures, with a specific focus on Fo-Vawt technology, have more cost saving potential in comparison to the conventional Hawt designs in a deep offshore environment. This will be addressed by implementing a cost model for an optimised Fo-Vawt design.

2.2 Vertical Axis Wind Turbines

There are many theoretical Vawt designs which were conceptualised, specifically in the small wind turbine category. In this report, only those designs which have been studied or prototyped on an industrial scale are examined. There are numerous parameters differentiating the various concepts of Vawt's, but the main classification of the rotors is based on its effectiveness in extracting power. Some designs are *lift driven Turbines* such as Troposkien/Darrieus and Giromill given in figure 2.5a and 2.5b respectively while other designs are *Drag driven turbines* such as the Savonius shape shown in figure 2.5c. The difference between these two categories of turbines is in efficiency of the rotor to capture power from the wind which is denoted as the power coefficient (C_P).

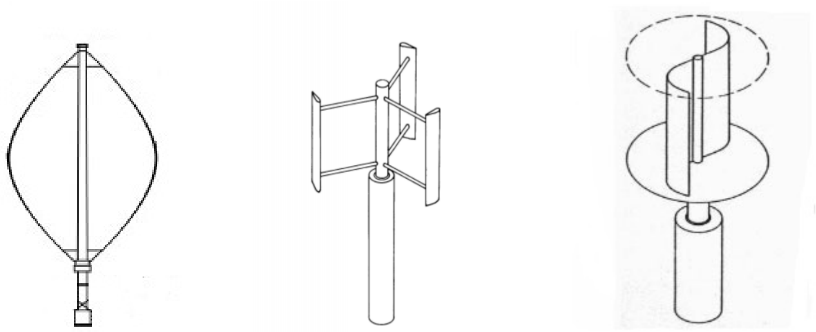

(a) Darrieus (b) Giromill (c) Savonius

Figure 2.5: *Different Types of Wind Turbines*

$$P_{Rotor} = \underbrace{1/2 \cdot \rho S U_\infty^3}_{\text{Power in wind}} \cdot \underbrace{C_p}_{\text{Rotor Efficiency}} \tag{2.1}$$

The power coefficient is a function of the tip speed ratio ($\lambda = \frac{\omega.R}{U_\infty}$), solidity of the rotor ($\sigma = \frac{B \cdot c}{R}$) and the aerodynamic efficiency of the rotor blade(C_l/C_d). For an idealised rotor modelled as an actuator disc with an area S, we assume for C_l/C_d and $\sigma \rightarrow \infty$, the maximum power coefficient is limited to 0.593 according to the Betz Limit, [44].

- Drag driven: $C_l \equiv C_d$ which ≤ 1, $\lambda_{opt} \leq 1$

- Lift Driven: $C_l/C_d >> 1$, $\lambda_{opt} > 1$

This gives a power coefficient for a lift driven devices to be higher than that for drag based machines, where C_l/C_d is a function of the optimum tip speed ratio.

Rotor Configuration: Darrieus

Known by the surname of its inventor, George Darrieus, is one of the most recognisable and researched configurations of the vertical axis category. In the early 1970's, and early 1980's, the National Research Council of Canada and the Sandia laboratories USA respectively launched intensive research programmes into VAWT's. Most of the actualised prototypes were based on this configuration, such as the Sandia 17 and 34-m [10], Flowind turbines, 1981's Fokker prototype and the 1987's EOLE project 4 MW wind turbines shown in figure 2.6. The troposkien shape for the Darrieus concept was predominantly adopted which physically results when a perfectly flexible, uniform cable is spun around a vertical axis at a constant speed. If gravity effects are disregarded, the shape can be described with a hyperbolic cosine function, *cosh* like a catenary. The curved blade shape mitigate bending loads on the blade due to centrifugal forces but add longitudinal stiffness from internal tension being transmitted along the blade span.

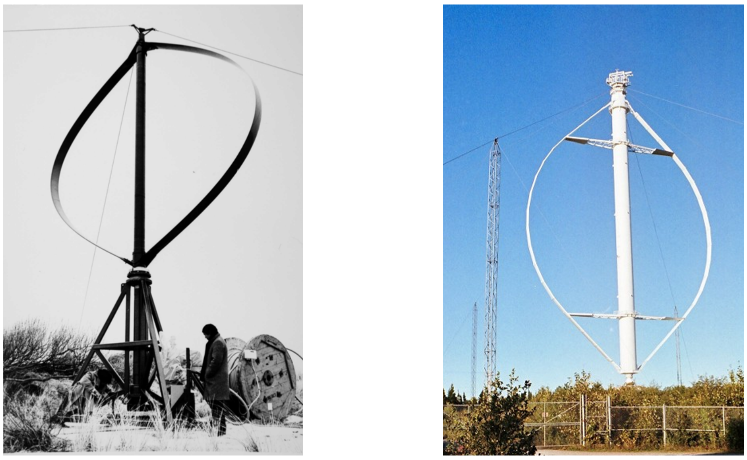

(a) Fokker Schipol 15kW, [33]

(b) Eole 4 MW, [4]

Figure 2.6: *Earlier Darrieus shaped* VAWT*'s*

The reduction in radius at the ends results a variation of tip speed ratio along the span, reducing power generation near the base and top of the rotor. The Darrieus rotor is stall controlled as it is difficult to incorporate a pitching mechanism to control the blade orientation. The configuration permits housing the electrical power systems closer to the ground, consequently diminishing inertial effects due to height on the support structure while allowing for easier access and in general removing nacelle space constraints. This is especially important because a larger generator and brake is needed in the absence of pitch braking. Although, the Darrieus rotor has a better torque performance at lower smaller tip speed ratio's, the start up characteristics remain as a design drawback for VAWT's and most turbines have an independent mechanism to restart the turbine.

Rotor Configuration: Giromill

The Giromill shape for VAWT's (figure 2.5b) is a simplified version of the Darreius rotor with straight blades. It has similar fundamental mechanism of operation however the straight blades and radial supporting struts introduce new dynamics. Straight blades maximize the area capture and allow the whole blade to operate at λ_{opt} normal to the plane of rotation, leading to an increased power extraction. However there are added stresses on the blade and tower due to distributed span-wise normal load and bending moments. Tip vortices interaction and the parasitic drag from supporting struts impart a loss in power conversion efficiency of the rotor. The H-rotor shape has more prominent start up problem than the Darrieus but its simplicity of blade design and effectiveness in power generation make it a more attractive option for small scale implementation, especially in urban environments. Helically twisting the blades, cambered airfoils and the provision to add a blade pitching mechanism can be used address the start up problem, smoothen the torque pulsation and add a back-up braking system. However the effectiveness of these modifications have not been thoroughly examined for larger rated VAWT's. The aerodynamic advantages of active/passive pitching mechanisms are possibly out-weighed by the technical complications, increased mechanical friction and added mass(cost) of the pitching system according to Kirke and Lazauskas [46]. The complexity in a helical geometric blade shape is perceived to require expensive tooling to manufacture but the LCoE for this concept (figure 2.12b) can be soon evaluated with the proposed completion of Nenuphar's pilot wind farm in 2016, [1]

2.3 Vertical Axis Wind Turbine Aerodynamics

In this sections, a short explanation about the aerodynamics of VAWT 's is presented. The working methodology of an adapted momentum based model by Madsen [50] used in HAWC2 is presented. The performance of the model is discussed in comparison to the more accurate Vortex models. The basics of 2D momentum models for VAWT's was derived from the work of Paraschivoiu [56].

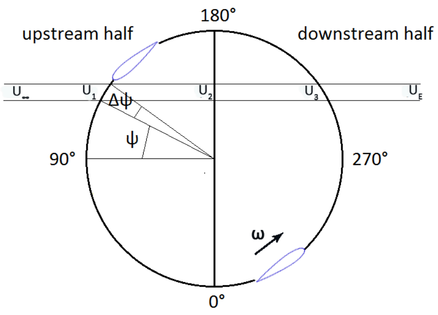

Figure 2.7: *Schematic Top view of two blade* VAWT *showing different stage velocities* U *across a stream-tube for azimuth position* ψ *of blade*

The aerodynamics of a VAWT are more complex to model than that of a HAWT . This is mainly because almost 2/3 of the rotor is operating in the wake of the upstream section. The blade wake interactions coupled with the unsteady aerodynamics including dynamic flow effects and trailing vorticity make it difficult to estimate the induced velocities (U_1, U_2, U_3, U_E) along a stream tube, especially for the azimuthal positions $180° < \psi < 360°$ as depicted in figure 2.7. The fluctuating relative velocities along the azimuthal position result a coinciding variation in angle of attack given in figure 2.8.

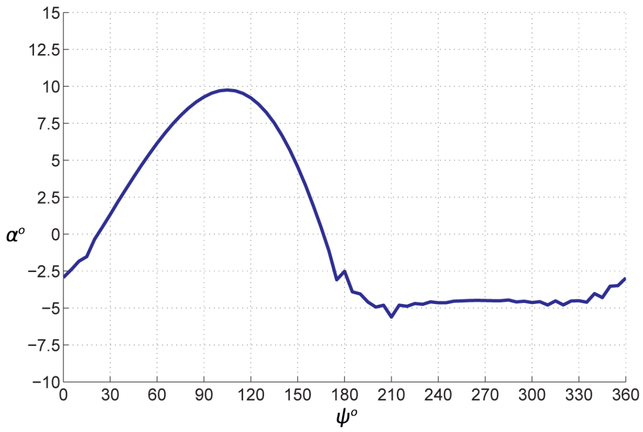

Figure 2.8: *Variation of Angle of attack(α) across azimuth position ψ for a* VAWT *operating at $\lambda = 4$, Ferriera [36]*

It is necessary for a tool simulating VAWT aerodynamics to capture these fluctuations accurately to predict the loading to determine the effective torque generated. To study how HAWC2 simulates VAWT aerodynamics, the *actuator cylinder* model used is compared with the results from various VAWT vortex models.

Actuator Cylinder

The AC model implemented in the HAWC2 software to calculate the induction field for VAWT's was developed by Madsen [50]. Unlike the Double disc Multiple Stream-Tube momentum model (DMST) by Paraschivoiu [56], the AC model uses a cylinder instead of a disc to emulate the swept area of the turbine. The decelerations on the flow due to the forces reacting upon it from the blade are approximated based on the following simplifications

- There is no interaction between the actuator discs, so inflow velocity is neglected
- The wake is assumed to be fixed
- Viscous effects are neglected as Euler estimations are used for the Navier Stokes Equations.

The AC model assumes the rotor as a *H-type* configuration but corrections have been applied so that it does not underestimate the body forces, especially in the vertical directions for the darrieus configuration. The turbines swept area is reduced into discs, divided into arc segments along the azimuthal position $\delta\psi$, discretised as a thin cylinders of height δh, for the length of the blade. Geometric inputs along with freestream wind velocity and rpm are only needed to determine the blade loading per height interval (δh). These blade forces are inverted to act as body forces. The Actuator cylinder model provides a reasonable trade-off for accuracy with computational requirements. It calculates the quasi steady induction velocities within a sufficient accuracy which are coupled with a dynamic inflow model to estimate the dissipation in induction velocities due to wake interactions. These both in combination are implemented in HAWC2 which is used for the load calculations in the succeeding sections.

Vortex Models

Although momentum models are simpler to implement and more widely used to estimate the C_P curves, they fail to account for dynamic effects downstream and lateral expansion of the wake, Ferriera [36]. Vortex models can be used instead for better accuracy. They are potential flow models based on the calculation of the velocity field about the turbine through the influence of vorticity in the wake of the blades. By accurately determining the wake and its effects on the velocities experienced by the blades, the loads exerted upon them can be calculated. The VAWT blade element is replaced by a "bound" vortex filament assuming bound circulation is conserved. A spanwise vortex is shed whose strength is equal to the change in the bound vortex strength as dictated by Kelvins theorem. Here also the interaction of the downstream blade with the vortex filament of the upstream section calls for a time based model where every vortex element interacts and influences each other at each step of the revolution. This results in large computational efforts but accurately captures the angle of attack oscillations and subsequently the C_P for the downstream region, giving the force coefficients shown in figure 2.9.

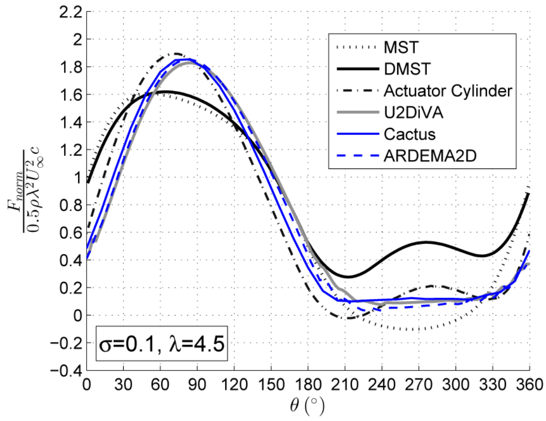

(a) F_{norm}

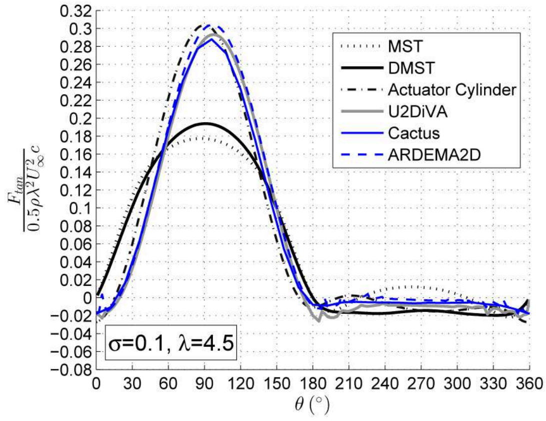

(b) F_{tan}

Figure 2.9: *Forces estimations on 2D* VAWT *NACA 0015 airfoil pitched at* $\theta = +3$, $\lambda = 4.5$ *and* $\sigma = 0.1$ *using various aerodynamic models, [35]*

The dynamic inflow model used in HAWC2 to add wake corrections to the induction factors is based on weighted factors derived for HAWT cases. However, a recent study by Ferreira et al. [35] provides a thorough comparison between DMST, AC and vortex models to demonstrate the similarity of results for various blade pitch, rotor solidity σ and tip speed ratio λ. According to the study, the AC implementation in HAWC2 (figure 2.9) code shows good agreement with the vortex models while the DMST model proves to be inadequate from approximating VAWT performance.

2.4 Floating offshore structures

The domain of offshore wind farms include regions with deep sea floors or difficult underwater soil conditions/terrain. These situations prohibit bottom founded structures either due to financial infeasibility or installation limitations, even if wind resource and energy demand is high. This has promoted research on the concept of floating wind turbines as plausible solution. Currently there are many pilot projects looking into various concepts for floating wind turbines, either for HAWT's or VAWT's. From figure 2.10, the different concepts for floating structures are illustrated. These concepts are explained in the following sections with reference to existing research projects.

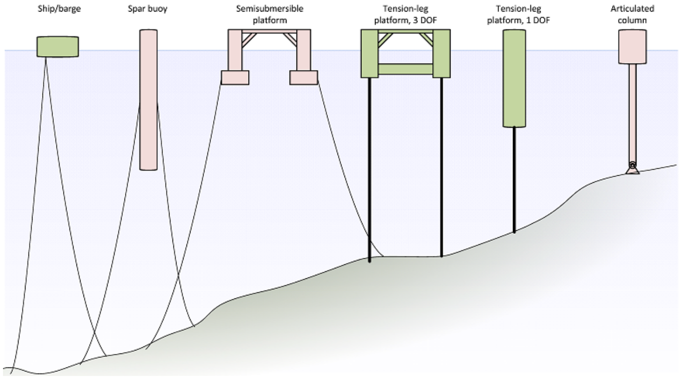

Figure 2.10: *Different types of floating foundations for offshore structures, [12]*

2.4.1 Spar Buoy

The spar buoy concept is a ballast stabilised, *freely* floating platform. Using ballast weights below the central buoyancy tank, a high inertial resistance to angular motion is achieved. This is one of the most favoured concepts with the better dynamic performance. Currently a prototype is being tested in a joint development project between StatOil-hydro and Siemens under the "HyWind" project. The concept consists of a cylindrical draft submersed for approximately twice the length of the tower height with a internal ballast and anchored lines holding it in place, figure 2.11. A Siemens 2.3 MW turbine is nested on top of the 100m deep draft anchored with three flexible mooring lines to the sea bed at a depth of 210 m, [64].

The VAWT variable with a spar-buoy Floater is the DeepWind concept shown in figure 2.11b. It is also spar-buoy design which is gravity stabilised by a heavy ballast weight. However, the structure is rotating with the rotor instead of having an internal low speed shaft (LSS), [12, 66]. The DeepWind concept differs from other spar-type concepts as the generator is placed at the bottom of the structure which is held in position by a flexible wire mooring system. There is possibility of reduced O&M costs with the exclusion of a LSS and related bearings while housing the generator at the bottom can have stronger adverse impacts on O&M.

2.4.2 Semi-Submersible

Semi-submersibles are common concepts derived from the family of buoyancy barge platforms, figure 2.10. The stability in the system is achieved through distributed buoyancy, taking advantage of weighted water plane area to create a restoring moment. The semi submersed concept is widely used in the oil and gas industry or for large offshore installations. They involve elevated platforms resting on vertical half submersed platforms anchored to the bottom. These can be in a tri-floater configuration as for the "Drijfwind" project for HAWT 's, figure 2.12a or the "Nenuphar" concept

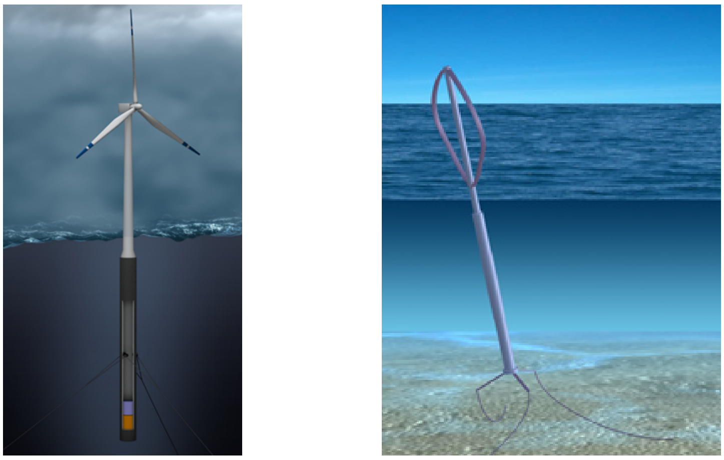
(a) HyWind, [34, 64] (b) DeepWind, [59]

Figure 2.11: Floating Spar wind turbine concepts and prototypes

implemented for vertical axis machines, figure 2.12b. Other concepts which have actually gone into pilot project production include "IDEOL" which has a taut mooring system holding a ring shaped concrete Floater which has a unique damping pool stabilising mechanism , figure 2.12c

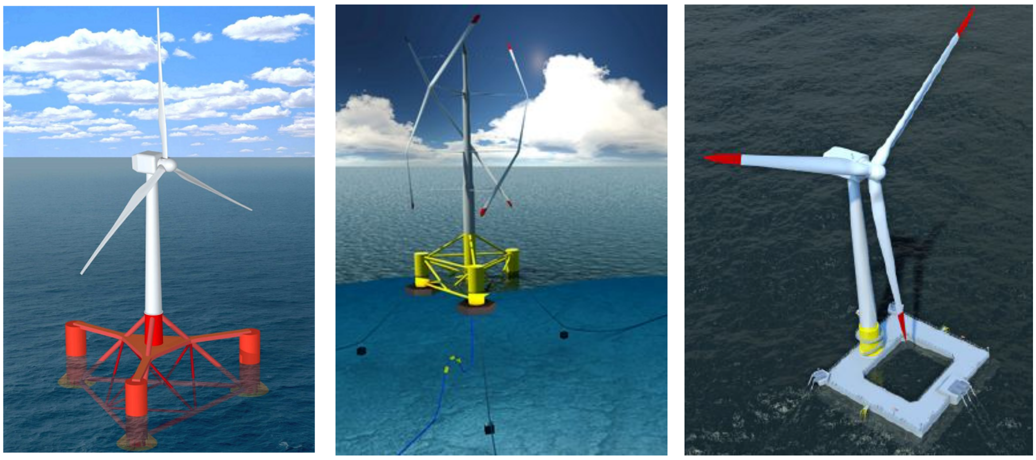
(a) Drijfwind, [54] (b) Nenuphar, [1] (c) IDEOL, [3]

Figure 2.12: Floating Semi-submersible design concepts and prototypes

2.4.3 Tension Leg Platforms

Tension leg platforms (TLP) are designed to eliminate vertical motions by maintaining high tension through a highly buoyant Floater. TLP's are mostly implemented for large oil rigs offshore as the loads on oil rigs are mostly vertical with limited offsetting or over-turning moments. The simpler classical 1 DoF TLP concept, as in figure 2.10, has been implemented with a downwind turbine design by a Norwegian based company "Sway A/S" in collaboration with Areva and NREL. The 1 DoF TLP is a combination of a spar buoy design with tension rod connecting the base of the floater to a gravity anchor on the sea floor figure 2.13b. Also the tower is stiffened using a patented taut wire and spreader-beam system design while a passive yaw system for the entire turbine is nested at a universal joint at the bottom of the floating structure, [40]. As for 3 DoF TLP systems applied to wind turbines, the work of Crozier [27] and Matha et al. [52] provide initial designs, however further work on improved technology readiness level were not found.

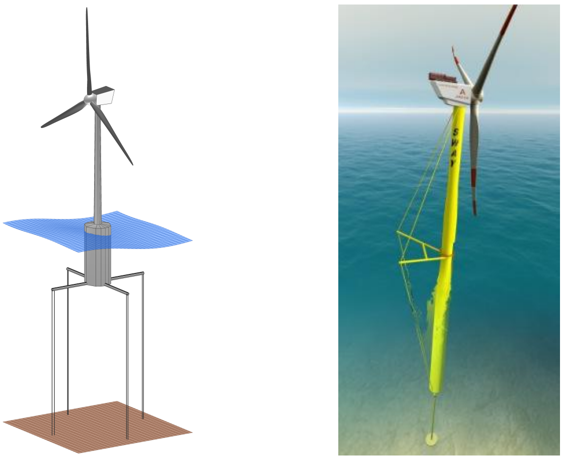
(a) 3 DoF TLP, [27]

(b) 1 DoF TLP: Sway, [40]

Figure 2.13: *Floating tension leg platform concepts and prototypes*

2.4.4 Concept Analysis

The spar buoy is designed as a heavy deep structure which adds large inertial resistance to the loads generated on the Floater and turbine from the wind and wave climate. This reduces sensitivity of wave loads on the system dynamics, keeping the motion frequencies low. Considering cases for large wind turbines (>5MW), the required stiffer tower and spar buoy structure will give rise to higher natural bending frequencies. Normally the natural frequency of a bottom founded structure is designed around 0.2 to 0.3 Hz. Designing in this space can result in coincidence with the 1P frequency of a turbine with a low rotor speed. However, the added freedom in motion results in more pronounced aerodynamic and hydrodynamic damping influences. The heavier design, depth dependence and ballast tank complexity can contribute to higher system costs and logistic difficulty. Whereas independence from bottom founded conditions, less dynamic coupling of system to wave motion [13], less stress-baring anchor assembly, good installation/decommissioning and maintenance potential and overall simpler construction [19] are all positive performance indicators for the spar-buoy system. Nevertheless the response of a VAWT turbine design space to the increased DoF of the spar buoy requires detailed analysis.

The other two concepts, semi-submersible and TLP, have the advantage of being more independent from depth restrictions as compared to spar-buoy concept. In static conditions the semi-submersible design seems stable but the dynamic response of the system is sensitive to the wave climate and resulting in possible dynamic coupling of the turbine design space to the wave loading, [54]. The scalability of the semi submersible means a wider weight-water plan area is required for larger turbines, [12]. The logistic viability of a semi-submersible can be better but larger area percentage exposure to water and air might make the system more prone to corrosion. For the 3 DoF TLP, the results from Matha et al. [52] show high variance in loads and deflections on the support structure due to tilting motion and strong yaw instability due to the inherent compliance in horizontal motion and yaw. With respect to design, the high longitudinal stresses in tethers make the mooring a critical system which would requiring careful design and maintenance [19].

A strong pretension would be needed to prevent large slacks in the tethers during high sea state which can result in high accelerations on the turbine systems, [12]. Thus structural design of the anchor foundations would need to balance these high vertical loads and need consistent maintenance. Both of these factors would result in added costs.

Based on the literature review, it was seen that the VAWT concept serves to achieve better results when implemented with a Spar buoy platform. Although the CAPEX for a spar buoy can be higher than a semi-submersible, the dynamic influence on the turbine design is limited for the high inertial spar-buoy. This can provide for more stable design solution for a FO-VAWT's. This was in concurrence with the design used for the DeepWind project which was also a spar buoy.

2.5 VAWT vs HAWT

The lack of data to validate any cost estimations for VAWT designs makes it difficult to devise an engineering cost model from the ground up. Thus based on analysing the key systems of HAWT's and a hypothetical VAWT, the loading profiles and the overall dynamics are cross examined to create an exploratory model space for VAWT's with similar systems to HAWT's. Figure 2.14 illustrates the spectrum of forces incident on a floating turbine. The impact of the environmental loads are evaluated for the respective turbine system through an enumerated explanation of the load drivers.

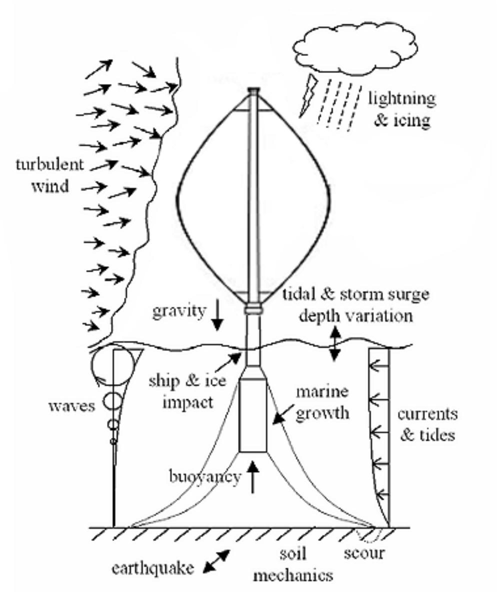

Figure 2.14: Loading sources on offshore WT

.

1. Wind: Aerodynamic loads

   Cases Turbulence, irregular wind shear effects, gusts, misalignment
   Impact Size of rotor, tower, Floater, mooring system and power-train

2. Inertia: Gravitational, centrifugal loads

   Cases Design specific, operational speed
   Impact Size of blades and tower

3. Waves: Hydrodynamic loads

   Cases Regular waves, irregular sea state, extreme wave height
   Impact Floater, mooring system, tower

4. Bouyancy: Hydrostatic loads

   Cases Constant
   Impact Floater, rotor, mooring system

5. Corrosion, marine growth
6. Lightning, Earthquake
7. Icing,
8. Scour

The first four load generating sources dictate the design of every turbine system. The remaining load sources are ignored in this report due to their limited or inconsistent impact. The rotor system encompasses both the blade and hub assembly for a conventional HAWT.

The *Wind* creates aerodynamic loads on the blades, which determine the combined axial shear force and bending moment for sizing the tower. The combined weight and overturning moments from both systems and other physical constraints determine the size of the Floater and consequently that for the mooring system. For VAWT's, the wind load propagation is quite similar, only that there are less systems concentrated in a hub-nacelle assembly like in a HAWT.

The *Inertial* induced loading for bottom founded HAWT's is primarily incident on the blades which results in higher leading or trailing edge mass due to the higher edgewise moments. The cyclic nature of the load induces a side to side motion in the tower and increased edgewise bending for the blade, [74]. For the VAWT, gravitational forces are evenly distributed due to the centrifugal stiffening during operation but result in large compressive stresses during parked conditions [62]. Centrifugal loads are more prominent rotor strucutral design drivers for *h-type* VAWT's, [30].

Hydrodynamic loading is represented through modelling the sea surface and the relative motion of the platform. It is a complex environment to simulate. Apart from the regular waves and current shear layers, the remaining forces on the Floater and tower originate from irregular sea states and surge waves. However, far offshore and for large inertial structures, these loads can be ignored, [52, 64]. Overall hydrodynamic loads influence the dynamic response for all systems and is key in determining the dynamic properties of the sub- sea systems. For a VAWT however an initial statement on how these load environments impact the turbine is difficult to formulate. Especially as the Floater is rotating in water which will also give rise to a Magnus force when interacting with a current stream as modelled by Vita in his Phd.

The hydrostatic loads comprise of the buoyancy forces which rise from the submersed part of the Floater, incident at the centre of buoyancy, C_b. This is optimised with the size of the systems for both VAWT 's and HAWT's and induces a restoring moment to the turbine tilting displacement.

These design criteria feed into the design costs of the turbine and Floater but do not indicate the impacts on external works and maintenance which are established from different parameters. It is perceived that the operation and maintenance as well as the balance of plant cost potential for a FO-VAWT is better mainly in terms of smaller floater, power-train accessibility and no motors.

2.6 Scaling

Scaling implies basing similarities between the properties of a set of objects so that their difference is only dependant on size. To assess the possible future prospects of larger wind turbine size on the reduction of Cost of Energy, many research projects have been carried out to predict the trends of mass, loads and cost scaling effects, discussed in section 2.7 The *classical scaling techniques* used are either based regression analysis of existing data or linear scaling relations (geometric similarity) to study the effect of size on certain characteristics. A review of the predominantly practised method for conventional wind turbines is given below.

2.6.1 Linear Scaling

Linear scaling implies formulating analytical relations between important parameters of system as a function of a characteristic dimension D, such that for different sizes of the system, variations in D are geometrically linear. For different sizes of wind tubrines, the important geometric and functional parameters defining the wind turbine subsystems are modelled to vary as a function of the characteristic dimension. The relations defining the dependant parameters can be reduced to vary with, or as a combination of, the length (D), area (D^2) or volume (D^3). This method is used frequently as a first approach to derive up-scaling effects on load and mass of the system sub components. Linear up-scaling as a design tool for wind turbine can be distinguished by some assumptions as described by Ashuri:

- The core design of the machine inherently stays the same such as number of blades, airfoil type, drive-train and support structure
- All other geometric parameters vary linearly with the top design variable, usually selected as rotor radius
- Aerodynamic similarity is controlled by keeping tip speed ratio constant

Using these linear scaling assumptions, basic physical relations between the characteristic dimension and the parameters of interest for the concerned component/subsystem can be used to estimate the variations in components design and essentially performance/cost etc. These relations are a function of the mathematical relation defining the parameter in question for that subsystem. A very thorough linear scaling study was performed in the "*UpWind*" project by Chaviaropoulos [22] and can be found in Jamieson [44]. The basic scaling relations for geometry, system masses, loads and other properties as a function of characteristic dimension (radius = R) are given in table 2.2.

The 'Scale' dependency in table 2.2 are derived by linking parameters to the radius by a simplifications of the respective mathematical formulations. This also forms the basis for the "square-cube" law implemented to wind turbines, where the power of a turbine is proportional to the swept area, thus scaling power with R^2, while the mass of a system depends on the volume, thus mass scales with R^3. For the relations given in table 2.2, it can be defined that generator size/power rating depends upon the torque driving the system [44]. As power of the WT scales with R^2 while the rotational speed scales with R^{-1} in order keep a constant tip speed ratio. The torque scales with R^3 for $Q = \frac{P}{\omega}$. Conventional generators are independent of the rotor torque due to the presence of a gear box, thus their mass scales with R^2 while Direct drive generators do not have one thus their mass scales with R^3.

Category	Parameter	Description	Scale
Geometry	C	Blade Chord	[R]
	t	Thickness, Internal Blade segments	[R]
	t/C	Blade Airfoil thickness	[−]
	A	Swept Area	[R^2]
Mass	m_b	Blade Mass	[R^3]
	$m_{gen,DD}$	Direct Drive Generator Mass	[R^3]
	m_{gen}	Conventional Generator Mass	[R^2]
	$m_{b,sec}$	Blade mass per cross section	[R^2]
Forces	T	Thrust	[R^2]
	P	Power	[R^2]
	Q	Torque	[R^3]
	F_ω	Centrifugal Force	[R^2]
	F_{ax}	Axial Force	[R^2]
	M	Moment	[R^3]
Other	I_{xx}	Area Moment of Inertia	[R^4]
	ω	Rotational speed	[R^{-1}]

Table 2.2: *Linear Scaling laws for turbines, [22, 44]*

2.6.2 Empirical Data Regression

The most adopted method for establishing scaling trends of technology, or in this case turbine subsystems, is by regression analysis by fitting average trend-lines using existing data across a spectrum of power ratings. These methods are possible if data sets of industrial designs are available as under the framework of large collaborative state funded projects. In Jamieson [44], a very comprehensive and detailed study is compiled on mass, loads and cost trends for wind turbines over a range of rotor diameters. However, the variation of manufacturer-wise turbine designs, limitations in extracting model properties, parameter dissimilarities(tip speed ratios) and constraints from changes in technology learning curve, all add uncertainties in the ability to extrapolate to larger scales from trend-lines derived from empirical regression, [8].

2.6.3 Comparison to other Scaling methods

Based on linear scaling, the mass of systems vary with cube of the characteristic dimension. This however was found to be not valid when comparing to actual wind turbine data trends in figure 2.15a, b. Technological advances in airfoil design, materials engineering as well as better manufacturing techniques have brought the scale dependency close to ≈ 2 for blade mass while for ≈ 2.7 for tower mass. Additionally for the tower, the mass does not scale with the cube of the characteristic dimension for two reasons. The non linearity in the scaling of the geometric dimensions for optimised towers and because all towers are not the same height for the same turbine power rating. Non linear interactions between the subcomponents for most subsystems reduce the mass scaling exponents from cube closer to with the square of the characteristic dimension. Nevertheless when comparing existing engineering practices with the concepts designed with linear scaling, relative similarity in results do exist. Especially when considering the scaling of energy with the swept area of turbine, a strong similarity with practical data and linear scaling predictions was found in the results of Chaviaropoulos [22], Jamieson [44] and compiled values from Ashuri [8] in figure 2.15c. Classical scaling methods have a limited direct use when calculating representative large offshore wind turbine designs using linear laws. Mainly due the inability to define the performance of a subsystem as a function of characteristic dimension in a linear closed

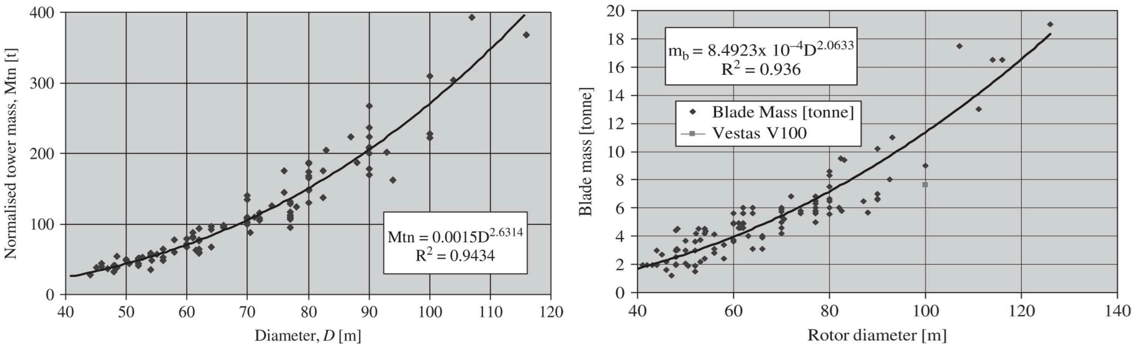

(a) HAWT tower mass scaling by [44]

(b) HAWT blade mass scaling [44]

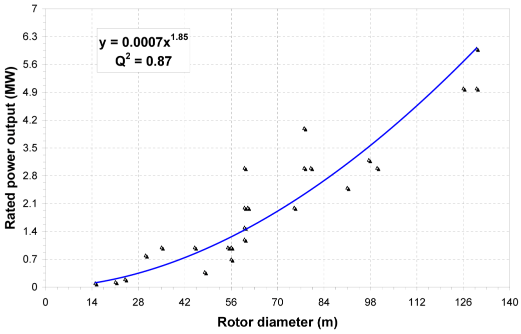

(c) Rated power output scaling compiled by Ashuri [8]

Figure 2.15: *Regressive mass scaling trends for (a) Tower, (b) Blade, (c)Rated power; as a function of characteristic dimension taken as diameter*

loop form. Especially in offshore conditions where site specific wind farm factors impact the size and cost of the systems dramatically.

Thus “load-based” scaling methods are used to construct optimised designs which are technically plausible and possess feasible economic characteristics. This involves modelling of system couplings and dynamic interactions using accurate engineering models to simulate the relative impacts of scaling for the complete turbine. Generally load based scaling is a complicated and time consuming process, but it is deemed a more accurate and commonly applied method to estimate the progression of loads and inherently the structural mass on the basis of a multi disciplinary optimisation. Recent mass/cost estimations have been performed in this method, such as for the “InnWind” project, Chaviaropoulos et al. [23] and by Ashuri [8]

Linear scaling laws have a very limited application due to the inherent oversimplification and assumptions it is based upon. However, it can be used for a conceptual estimation to understand the scaling behaviour of the components. In application to this report, physical relations for the scaling of VAWT systems are assumed to be based on scale dependency given in table 2.2.

2.7 Cost of Wind Energy

Introduction

In the economic optimisation of wind energy, there are two aspects which can be improved to increase the revenue from the electricity produced. One addresses the technical and financial variables while the other looks at the socio-economic and political aspects. The focus of this section will be to provide a high level overview of existing and prospective turbine technology with the aim to present a methodology to dimension for cost optimisation of large floating vertical axis wind turbines.

2.7.1 Offshore Wind Farm Cost structure

Cost estimations for technology remain vulnerable to fluctuating external impacts which are difficult to predict and quantify. This makes it specifically more challenging to create an engineering cost model as it forms a union between high fidelity load computations with relatively vague cost relations. To better judge the cost drivers, figure 2.16 gives a breakdown of the elements in cost of energy for offshore wind energy.

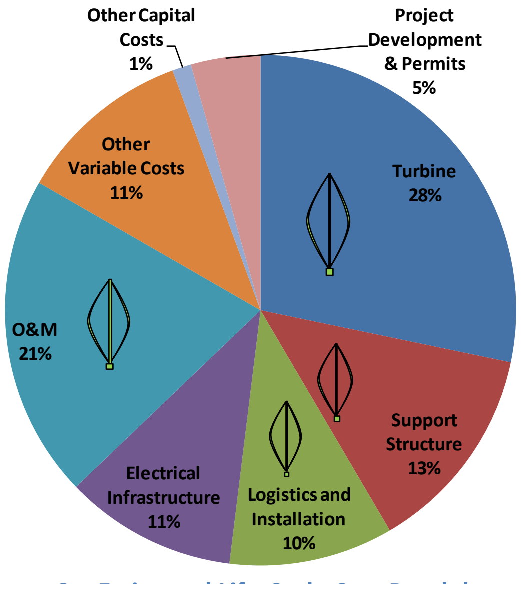

Figure 2.16: *Estimated Life-Cycle Cost Breakdown for an Offshore Wind Project, and prospective regions of improvement for* VAWT*'s, Griffith [39]*

The respective contribution and source of this generic cost breakdown figure 2.16 is build upon, focusing more on the specific cost during the life cycle of an offshore wind farm and the factors contributing to it. These parameters will be later reflected upon in application to the vertical axis concept.

1. **Design Costs**
    - Costs of complete Rotor Nacelle assembly and related elements
    - Geometry dependant

   - Extra factor depending on maturity of technology (testing, proving of concept, risk factor)
   - **Manufacturing**;
     - Prices of constituting material's fluctuate.
     - Labour costs

2. **Operation and Maintenance**
   - Repair and Maintenance of moving parts
   - **Site specific**
     - Turbine and sub structures design depends on location
     - Site conditions: wave and wind forecasting
     - Loading design cases built from site conditions
   - Electrical up-keep
   - Overhaul costs (based on condition monitoring or component design where fatigue or extreme loads deteriorate system)

3. **Balance of Plant/Station**
   - **Supply chain**
     - for RNA, foundations, cables and installation services have large impact
     - for installation supply chain, the installation vessels are the biggest constraint if fixed structures used (M.J. Kaiser [53])
     - lack of market transparency adds to high level of uncertainty in installation costs (M.J. Kaiser [53])
     - technology development leads to new supply chains for customised components, incurring niche technology costs, (Berry [11])
   - Foundation or Support Structure (for FOWT's implicates the Floater)
   - Electrical infrastructure
   - Installation, dependant on soil, depth and distance from shore

   Wind farm layout optimisation can be implemented to improve array efficiency, in terms of both grid layout and lesser wake effects,(Heath [41])

4. **Economics**
   - Fixed charge rates, *f(financing fees. return on debt/equity, depreciation etc)*
   - Commodity prices which effect installation, material costs etc , such as Oil,(M.J. Kaiser [53])
   - Return on investment and parameters linked to that
   - Risk, uncertainty of estimation

The difference in cost of energy estimations between HAWT 's and VAWT's result from a different distributions of costs between the parameters listed above. The drivers for the design costs for vertical axis machines are different as compared to horizontal machines. These are also dependant on the type of configuration chosen and very closely coupled to site conditions, rather than just a difference in concept. Thus based on design details, CAPEX can vary significantly. Operation and maintenance for the *DeepWind* concept depend mainly on the chosen design. An inherent advantage of VAWT's is the accessibility to the moving components. However, the anchor-type generator design of DeepWind leaves this aspect as a source of concern and further research.

Major differences in cost come from the manufacturing and Balance of Plant aspects. The technical immaturity of VAWT's, supply chain deficiencies for specialised components and being a niche technology implicates large uncertainties in cost and risks hitting high costs of energy. However, development of the technology will push the large advantage of the limited on-site infrastructure needed to setup FO-VAWT farms. Balance of Plant comprise of almost 30-45% of the costs incurred by hypothetical multi megawatt wind farms based on the HAWT technology, [8, 23, 75].

2.7.2 Life Cycle Costing

Wind energy is a investment which returns revenue. In retrospect, all technical improvements are measured by the effort put into them compared to the increase in efficiency they output. For the case of wind energy, financial payback is a major factor of the industry's sustainability. The principles affecting the Cost of Wind energy can be derived from its formulation, outlining the major factors contributing to lowering turbine costs and reducing the overall cost of energy. The structure of the cost of energy is illustrated in figure 2.17. Three methods of evaluating the economic profitability of wind energy: simple cost of energy, life cycle analysis(LCoE), and utility based financial analysis. For this report, the model is based on a life cycle analysis focusing on the levelised cost of energy

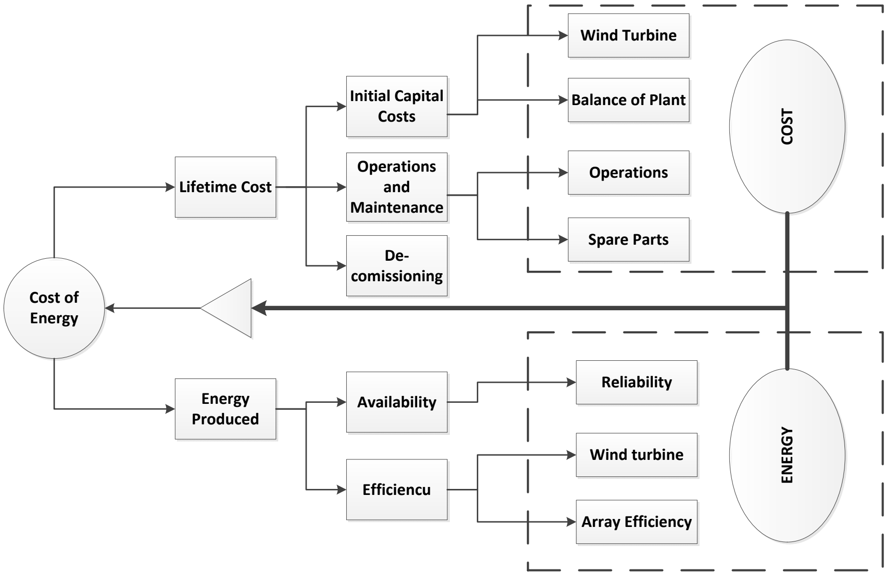
Cost of Energy
Lifetime Cost
Initial Capital Costs
Operations and Maintenance
De-comissioning
Wind Turbine
Balance of Plant
Operations
Spare Parts
COST
Energy Produced
Availability
Efficiencu
Reliability
Wind turbine
Array Efficiency
ENERGY

Figure 2.17: *Cost of energy overview for offshore wind, Jamieson [44]*

Economic Analysis

The formulation of the simple cost of energy is given in equation (2.2)

$$sCoE = \frac{(ICC) + O\&M}{AEP} \tag{2.2}$$

Where ICC constitutes of the capital expenditure CAPEXform the turbine capital costs and the balance of plants while the O & M costs summate into the operational expenditure, OPEX. A closer examination of the breakdown of CAPEX is given in figure 2.18

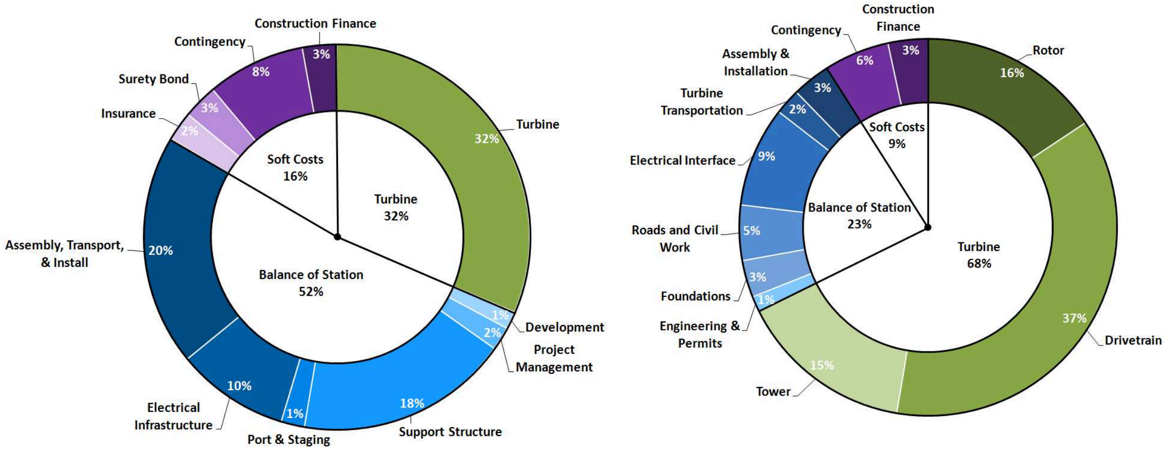

(a) Offshore (b) Onshore

Figure 2.18: *Installed capital costs for onshore and offshore wind turbines based on industry averages normalised for NREL 5 MW reference turbine (source Tegen et al. [70]*

$$LCoE = \frac{\sum_{i=-2}^{0} \text{CAPEX}_i + \sum_{i=1}^{T} \text{OPEX}(1+r)^{-i} + C_{end}(1+r)^{-T}}{\sum_{i=1}^{T} AEP_{50}(1+r)^{-i}} \tag{2.3}$$

Where CAPEX is the combined Turbine Capital costs (TCC) and Balance of plant (BoP) investment needed to establish the wind farm, OPEX represents the levelized sum of revenue losses and total costs of repair per year, C_{end} are the decommissioning costs the wind farm incurred in the last year of operation and AEP_{50} is the mean electricity production derived in section 5.5 . The discount rate 'r ' depends on the project stakeholders, terms of the project financiers and economic constraints of the country. The factors influencing the cost of capital comprise include *a*) inflation (disregarded in this study), *b*) Risk, *c*) Time Preference. Risks are project and country specific, where variation comes from the reliability of the technology, maturity of the project supply chain, stakeholder risk and economic support The time preference factor is determined from the stability of the electricity market. For this study, the discount rate is taken at 7% for an offshore project without considering GDP inflation. This is considered relatively reasonable as the general risks associated with offshore wind are quite high with respect to onshore wind.

Based on the time value of money changing based on the inflation and perceived risks, Net Present Value (NPV) is used as a measure of the economic value of an investment. NPV is the sum of the initial investment and value of the revenue stream for the life cycle (T years) of the wind park using a deprecating present value of money for an assessed discount rate, r. The formulation for NPV is similar to the terms used in equation (2.3).

$$NPV = \sum_{i=1}^{T} \left(\frac{CF_i}{1+r} \right)^{i} + CF_0 \tag{2.4}$$

The net cash flow CF stream is the annual levelised difference between the revenue generated and the OPEX. The first cashflow symbolises the CAPEX investment. The revenue is the product of the electricity provided at the PCC and the electricity tariff provided.

Another important parameter used to determine the economic performance of an energy system is the Internal Rate of Return, (IRR). It is a strong indicator of the potential the profitability of an investment. The discount rate for a project when the sum cash outflow is equal to the sum cash inflow is called the IRR, or quite simply the discount rate when NPV $\rightarrow 0$.

2.8 State of the Art CoE Model analysis

There have been many recent European projects over the years under the Research and Innovation policy to collaborate academic and industrial resources to deliver technological reports on the future in the Wind energy sector. The projects are focused on the current three bladed upwind HAWT rotor. To name some of the major ones

UpWind: FP6, focused on the establishing the limits to up-scaling till 25 MW machines (Sieros et al. [68])

InnWind: FP7, objective to provide an innovative offshore design performing in the 10 - 20 MW range (Chaviaropoulos et al. [23])

DOWEC : Evaluate the feasibility of offshore wind in the Netherlands (Bussel et al. [18])

NREL - WindPACT: A comprehensive study to define empirical cost scaling relations, (Fingerish et al., Griffin [37, 38])

Phd Research

- M. Zaaijer: TU Delft, Offshore wind farm design Emulation, [75]
- T. Ashuri: TU Delft Cost Scaling optimisation of multi megawat HAWT's, [8]

A more thorough review of these models is presented in the Appendix A.2. The understanding gained related to the cost models under EU and DoE funded projects both stipulate the similar methods and conclusions. The UpWind project paved the way to focus research for large horizontal axis machines with a detailed aero-elastic analysis of the turbines components and a fatigue loading induced cost optimisation of wind farms. The mass and cost were scaled using time based technology factors extrapolated from existing data trends and linearised weight factored cost models. The focus of the InnWind project was build upon the results of the UpWind project. The design parameters which were focused upon to continue to drive the trend for innovation in technology, especially for large deep offshore wind farms, were:

- Reduction of weight scaling of the turbine tower head mass
- Reduce gravity loads
- Reduce axial induction by having less specific thrust
- Improved manufacturing processes and materials used for rotor.
- Higher specific power drive train
- Adaptive smart pitch control to mitigate loads
- Design of wind turbine based on site specific conditions

The detailed optimisation model for up-scaling and the associated power specific cost including probabilistic failure costs was performed only for the support structure. The resulting mass and cost scaling conclusions state that up-scaling with the current technology level leads to unfavourable mass increase. This assumption holds valid for with similar research conclusions from Ashwill, Chaviaropoulos et al., M.J. Kaiser, Xudong et al. [9, 23, 53, 74].

The InnWind project emphasized on LCoE optimisation of a 10 MW offshore light weight rotor and the ad-joint BoP, scaling upto 20 MW, [23]. The model, like in UpWind, every reduction in up-scaling coefficient for the turbine below the classical assumptions of ($\lambda_c = 3$) is related to a technological improvement. The idea is that cost reductions occur as greater experience is gained in the technology with respect to manufacturing, installation and operation. In a study done by Ibenholt, experience curve studies revealed varied cost drop for doubling in cumulative installed capacity in certain wind energy markets but not all. This makes this hypothetical assumption weak. Secondly, the cost models were designed taking fixed sub sea structure height in BoP(foundation) cost calculations allowing for a BoP CAPEX scaling factor of 1.7.

Although economies of scale do seem to begin to positively effect as size of wind turbines exceed 15 MW; improvements such as more power output per area, less subsidies needed, larger return cash flow (better IRR) and increased wind farm capacity factor begin to surface, [23]; the optimum sizing of turbines still remains a trade-off between BoP and Turbine cost per MW for bottom founded designs. No validated cost models for different turbine subcomponents hence cost/mass proportionality is used for deriving the scaling components. Out of the main design drivers focused upon, reduction in thrust yielded the highest impact on reducing cost of energy. Having a higher rotational speed resulted in less gearbox cost and weight (smaller permanent magnet generator), but this reduction in tower nacelle mass had a limited effect on overall cost. The major assumptions made included design limits based on ultimate deflection and not on fatigue loading as well as the assumption that technological innovation will continue in an “increasing” trend to achieve the EWII CoE goals. The CAPEX scaling was also eventually favourable due to the assumption that the foundation can be founded at the same depth as the reference turbines.

Chapter 3

Floating VAWT

This chapter introduces the DeepWind Fo-Vawt is more detail, building up from the understanding of design and cost drivers from previous sections. Input-Output diagrams are determined for the main systems to understand the system drivers and system cross dependencies. In the end, the concept schematic and tabulated specifications are provided

3.1 DeepWind

The DeepWind project is a current research initiative spearheaded by DTU Risø under the EU FP7 programme, 'Future emerging technologies'. It is focused on developing the troposkien Darrieus concept on a floating structure. The project is intended as a pilot to establish a detail design for a 5 MW concept that builds upon Vawt research from the 1980's and 1990's done by Sandia, Flowind, EOLE project and many other similar endeavours. In the following sections, a system wise description for the most optimised design, the 5 MW baseline, are given.

5 MW baseline

The core configuration definition for the project was set to a troposkien shaped, single tubular, rotating spar floating turbine connected to the sea bed with drag/suction anchors and moor lines. The rotor H/ϕ ratios and spar structures were optimised amongst different options for specific driving options such as efficiency, loads, production, transportation and installation, Pedersen et al. [60]. A preliminary cost and mass scaling analysis was done from 200 kW upto 25 MW and a design optimisation for a 5 MW baseline model as the baseline to exponent trends for the current technology level. The design optimisation was performed using HAWC2 with a actuator cylinder (AC) model, gravity loads and a constraint subsea mooring model, [59]. However, a complex model coupling hydrodynamic loading and mooring system was linked with the AC model to investigate the coupling effects in the DeepWind design, Vita [72]. The **key** subsystems of the DeepWind Rotor include

- Rotor
- Tower
- Surface Transition tube

- Spar buoy Floater
- Mooring system
- Power train

Rotor

The shape of the rotor blade is chosen on the basis of load efficiency and design simplicity. The constraints are generic for wind turbines; load mitigation, floating stability and less costs. The rotor is also one of the primary drivers for the turbine, having downstream effects[1] on all other subsystems. Apart from operational conditions; other parameters effecting the rotor mass distribution and loads generated include the blade design, wind turbine operational conditions, heave angle of FOWT and hydrodynamic influences. A schematic showing the inputs affecting the *outputs* from the rotor subsystem are illustrated in figure 3.1

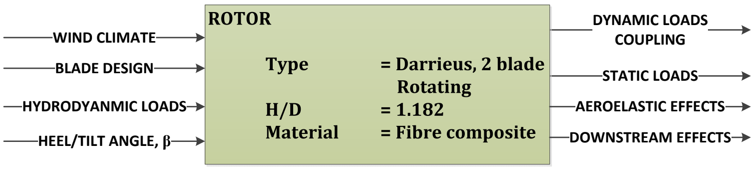
ROTOR
WIND CLIMATE
BLADE DESIGN
HYDRODYANMIC LOADS
HEEL/TILT ANGLE, β
Type = Darrieus, 2 blade Rotating
H/D = 1.182
Material = Fibre composite
DYNAMIC LOADS COUPLING
STATIC LOADS
AEROELASTIC EFFECTS
DOWNSTREAM EFFECTS

Figure 3.1: *Parameters influencing the outputs derived from the rotor*

To reduce the mass of the blades, rotor shape optimisation is necessary by varying solidity and the thickness of the blade along with better material selection to mitigate dynamic loading and aeroelastic effects on the blades as well as directly coupled structures like the tower and if applicable, the struts. For the DeepWind rotor, a two blade troposkien inspired, Darrieus rotor shape was designed, [66]

Tower

The pulsating loading due centrifugal and aerodynamic forces along with the hydrodynamic loading from the Floater adds some complex aero-hydro elastic fluid structure interactions on the tower. *The entire tower is a rotating* structure transferring power from the rotor to the generator and loads through the surface transition tube from the rotor to the Floater and subsequent mooring/anchor systems. A schematic summarising the inputs and main *functions* of the tower are illustrated in figure 3.2

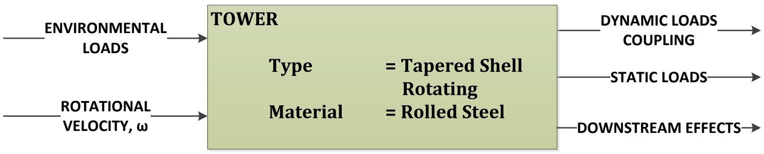
TOWER
ENVIRONMENTAL LOADS
ROTATIONAL VELOCITY, ω
Type = Tapered Shell Rotating
Material = Rolled Steel
DYNAMIC LOADS COUPLING
STATIC LOADS
DOWNSTREAM EFFECTS

Figure 3.2: *Parameters influencing the outputs derived from the tower*

The tower functions to sustain the aerodynamic and hydrodynamic loading(environmental loads), transferring loads in between subsystems, but primarily downstream from the rotor towards the power-train. A modal analysis of the tower design after scaling is deemed important to examine the impacts of aero-hydro-elastic effects.

---

[1] Downstream effects symbolise the impact of the loads generated by the Rotor as they propagate through all the subsystems **down** till the mooring system

Surface Transition Tube

The surface transition tube consists of a tapered continuation of the tower through the water surface into the spar bouy foundation structure. The section functions as the pivot. It is a critical component which is highly loaded, possibly with unsynchronised loading from aerodynamic and hydrodynamic forces. This subsystems' design is driven by having an appropriate wave transition zone as splashing of water on a large area can have significant force impact on the structure. The water displacement area of the tube should not result in heave resonance with the wave motion. This could result in the water touching the rotating blades.

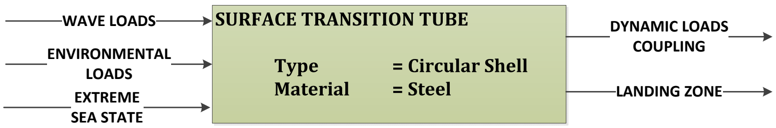
WAVE LOADS
ENVIRONMENTAL LOADS
EXTREME SEA STATE
SURFACE TRANSITION TUBE
Type = Circular Shell
Material = Steel
DYNAMIC LOADS COUPLING
LANDING ZONE

Figure 3.3: *Parameters influencing the resultant outputs and size of the surface transition tube*

Spar buoy Floater

A spar buoy functions as a high inertia, free floating structure, anchored with a mooring system, to counteract the weight and forces generated by the aerodynamic loading and the mass of the entire turbine. Normally, Floater's are compliant in on direction or more, allowing for the possibility of dynamic wave induced loading or system resonance in one or more DoF. Such upstream effects [2] influence the sizing of the turbine and the Floater, [12]. The DeepWind Floater is a spar buoy comprised of a hollow mono hull and ballast connected to the mooring system via a bottom founded bearing and shaft. The monohull is a continuation of the tower and surface transition tube, and similarly is rotating.

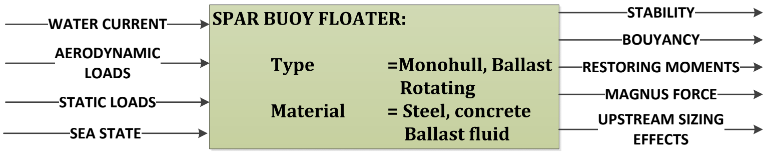
WATER CURRENT
AERODYNAMIC LOADS
STATIC LOADS
SEA STATE
SPAR BUOY FLOATER:
Type =Monohull, Ballast Rotating
Material = Steel, concrete Ballast fluid
STABILITY
BOUYANCY
RESTORING MOMENTS
MAGNUS FORCE
UPSTREAM SIZING EFFECTS

Figure 3.4: *Parameters influencing the response and the resultant outputs from spar bouy floater*

The spar buoy Floater are mainly gravity stable from its deep draught and inertial mass from the integral ballasts, designed to keep the centre of buoyancy above the centre of gravity of the turbine. The other important aspect to address while scaling for Floater designs is to ensure that the wave motion does not coincide with the motion of the floating turbine. The bearing and the shaft connected to the mooring system are critical components which experience the culmination of the VAWT's thrust and torque loading, [72]. The rotating spar buoy induces a Magnus force due to the current flow over it.

Mooring System

The motion of a floating structure has 6 degrees of freedom, making stability an important aspect. To ensure the floating VAWT does not drift away or tilt over due to the forces, a mooring system is implemented to maintain the turbines position and provide a restoring force to counteract the environmental loads. For floating structures, taut or catenary systems are either implemented. For the DeepWind design, a catenary system with drag anchors is used, where the weight and catenary shape of the long mooring wires add restoring stiffness and provide compliance to wave-induced resonance, [13]. A critical requirement for the DeepWind mooring design is to counteract the torque from the rotating turbine so as to prevent rapid accelerations on the power-train, [59]. The restoring forces have to be able to counteract the combined influence of the aerodynamic and hydrodynamic loading, including the rotational friction and Magnus force on the Floater, Vita [72].

---

[2] Upstream effects symbolise the progression of hydrodynamic loads and other effects through the subsystems upwards towards the tower

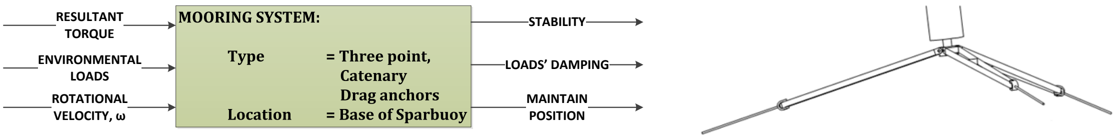
RESULTANT TORQUE
ENVIRONMENTAL LOADS
ROTATIONAL VELOCITY, ω
MOORING SYSTEM:
Type = Three point, Catenary Drag anchors
Location = Base of Sparbuoy
STABILITY
LOADS' DAMPING
MAINTAIN POSITION

(a) Parameters influencing the response and the resultant outputs (b) Mooring configuration

Figure 3.5: *DeepWind mooring system input/output and design possibilities*

Power-train

A direct drive, permanent magnet setup is the preferred design as it reduces maintenance and cost for incorporating a drive-train. The generator is situated at the base of the floating spar buoy, functioning to lower the centre of gravity, adding to inertial stability and controlling the rotor speed to maintain optimum power production The generator also functions as a start-up motor to help with 'self-start' problems faced by VAWT's, [56, 72]. The housing of the generator remains to be optimised as access and maintenance are a key factor for deep seas installations. This needs to be weighed in when finalising the placement of generator as either inside/outside the rotating foundation or underneath the Floater in an isolated anchor type housing seen from figure 3.6b. For the current baseline design, it is presumed the power-train is housed as the last modular compartment at the base of the Floater, connected to the mooring via a shaft and bearings marked in figure 3.7.

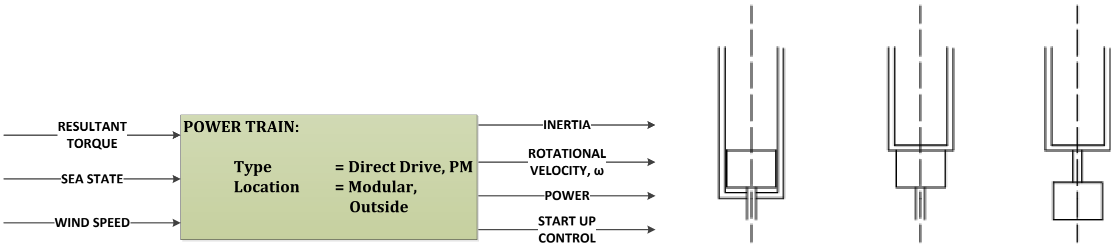
RESULTANT TORQUE
SEA STATE
WIND SPEED
POWER TRAIN:
Type = Direct Drive, PM
Location = Modular, Outside
INERTIA
ROTATIONAL VELOCITY, ω
POWER
START UP CONTROL

(a) Parameters influencing the response and the resultant outputs (b) Possible power-train placements, [60]

Figure 3.6: *DeepWind power-train system input/output and configuration possibilities*

Table 3.1: *Gross Specifications of the DeepWind 5 MW Baseline Turbine [66]*

Property	**Unit**	**Specification**
Rotor Type	Vertical Axis	Optimised Troposkien
Foundation	Floating	Spar-bouy
Mooring	Tri-arm	non-taut lines
Power Train	Submersed	Direct Drive
N° blades	[-]	2
Rated power	[MW]	5.0_{ltd} (5.62)
Rotor radius	[m]	60.5
Rotor height	[m]	143
Chord	[m]	5.0
Solidity σ	[-]	0.1653
Swept Area	[m^2]	11996
Blade Mass	[kg]	4.85E5
Rated rotational speed	[rad.s^{-1}]	0.62
Centre of Gravity, h_{cg}	[m]	-67.7
U_{rated}	[m.s^{-1}]	14
U_{cut-in} , $U_{cut-out}$	[m.s^{-1}]	4 to 25

Table 3.2: *Detailed Geometric properties of final 5 MW DeepWind Turbine [66]*

Geometric Specifications					
Rotor			**Tower**		
h_{rotor}	[m]	143	$\phi_{\text{sec},1}$	[m]	4.62, Δt: 0.015
$R_{\text{b,max}}$	[m]	60.49	$\phi_{\text{sec},2}$	[m]	5.32, Δt: 0.017
Chord	[m]	5	$\phi_{\text{sec},3}$	[m]	5.84, Δt: 0.018
Swept Area	[m^2]	11996	$\phi_{\text{sec},4}$	[m]	6.4, Δt: 0.0219
Airfoil t/c	[%]	18,25	$h_{\text{sec,i}}$	[m]	35.75
m_{blade}	[kg]	48030	m_{tower}	[kg]	3.54 E5
Material	[-]	GFRP (Protrusion)	Material_{tower}	[-]	Rolled Steel
Floater					
$\phi_{\text{fl,top}}$	[m]	7.32, Δt: 0.5	ϕ_{ballast}	[m]	8.3
$\phi_{\text{fl,botom}}$	[m]	8.3, Δt: 0.5	h_{ballast}	[m]	27
$h_{\text{fl,top}}$	[m]	15	$\text{Material}_{Floater}$	[-]	Construction Steel
$h_{\text{fl,trans}}$	[m]	10	$\text{Material}_{ballast}$	[-]	Olivine_{aq}
$h_{\text{fl,main}}$	[m]	64.5	m_{tower}	[kg]	3.76 E6
m_{fl}	[kg]	1.126 E6			
Mooring			**Generator**		
$N°$ arms	[-]	3	h_{Gen}	[m]	2.608
m_{arm}	[kg]	1.709 E4	R_{Gen}	[m]	6.5
m_{chain}	[kg]	1.089 E6	m_{Gen}	[m]	2.90 E5

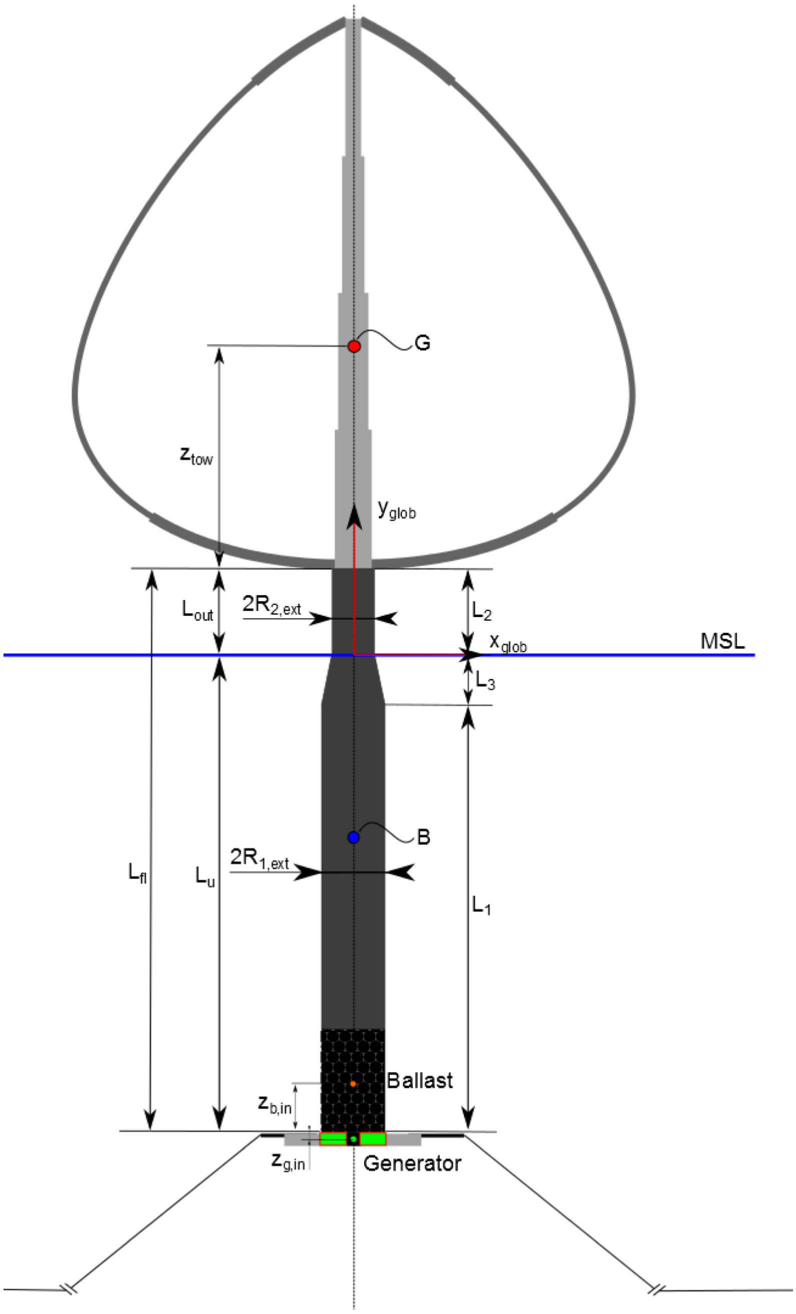
G
z_{tow}
y_{glob}
L_{out}
$2R_{2,ext}$
L_2
x_{glob}
MSL
L_3
B
L_{fl}
L_u
$2R_{1,ext}$
L_1
Ballast
$z_{b,in}$
$z_{g,in}$
Generator

Figure 3.7: *Schematic Representation of the DeepWind Turbine*

Chapter 4

Engineering Model

This chapter describe the process used in calculating the necessary inputs towards estimating the mass of the VAWT. It involves using existing blade design information from DeepWind and the research work of previous master's thesis projects at TU Delft [62, 65], to calculate the loading on a VAWT structure. The complexity arises from the increased degree of freedom of the DeepWind concept. The engineering model presents the framework adopted to estimate the mass of the rotor, tower, Floater and mooring lines based on certain load cases. The load simulations, model processes and subsequent mass estimations are performed for the 10 and 15 MW scale versions of the baseline 5 MW turbine as well. The results from the following sections are fed into the design cost calculations of the succeeding chapter.

4.1 Model Design Methodology

The state-of-the-art and novel technology being considered for the cost model was studied in detail in a Special Course project [63] and incorporated in chapters 2 and 3 respectively. The aim of the Special Course project was to review existing design methodologies in order to develop an engineering framework to perform a cost driven optimisation for a specific VAWT design, (figure B.4). It provided a strong indication on the process required when performing an iterative cost of energy optimisation.

However, that findings entailed efforts beyond the scope of this Master Thesis project and therefore was reduced to a more linear framework. The main limiting factor encountered was the ability to accurate capture the downstream and upstream effects of load propagation. Capturing the dynamic coupling effects of a freely floating system rotating about its axis requires a multidisciplinary analysis and optimisation (MDAO) where the piecewise results are captured in the form of cost of energy. Due to the limitations in cost modelling for VAWT's, as mentioned in the preface, it was not possible to verify the results with industrial data on VAWT's. In lieu of these constraints, the DeepWind 5MW Baseline design would serve as an input as well as a datum of verification for the engineering model. A framework is illustrated in figure 4.1

The engineering cost model is built upon calculations from three software packages to determine the design costs, operations and maintenance costs and the balance of station costs for offshore

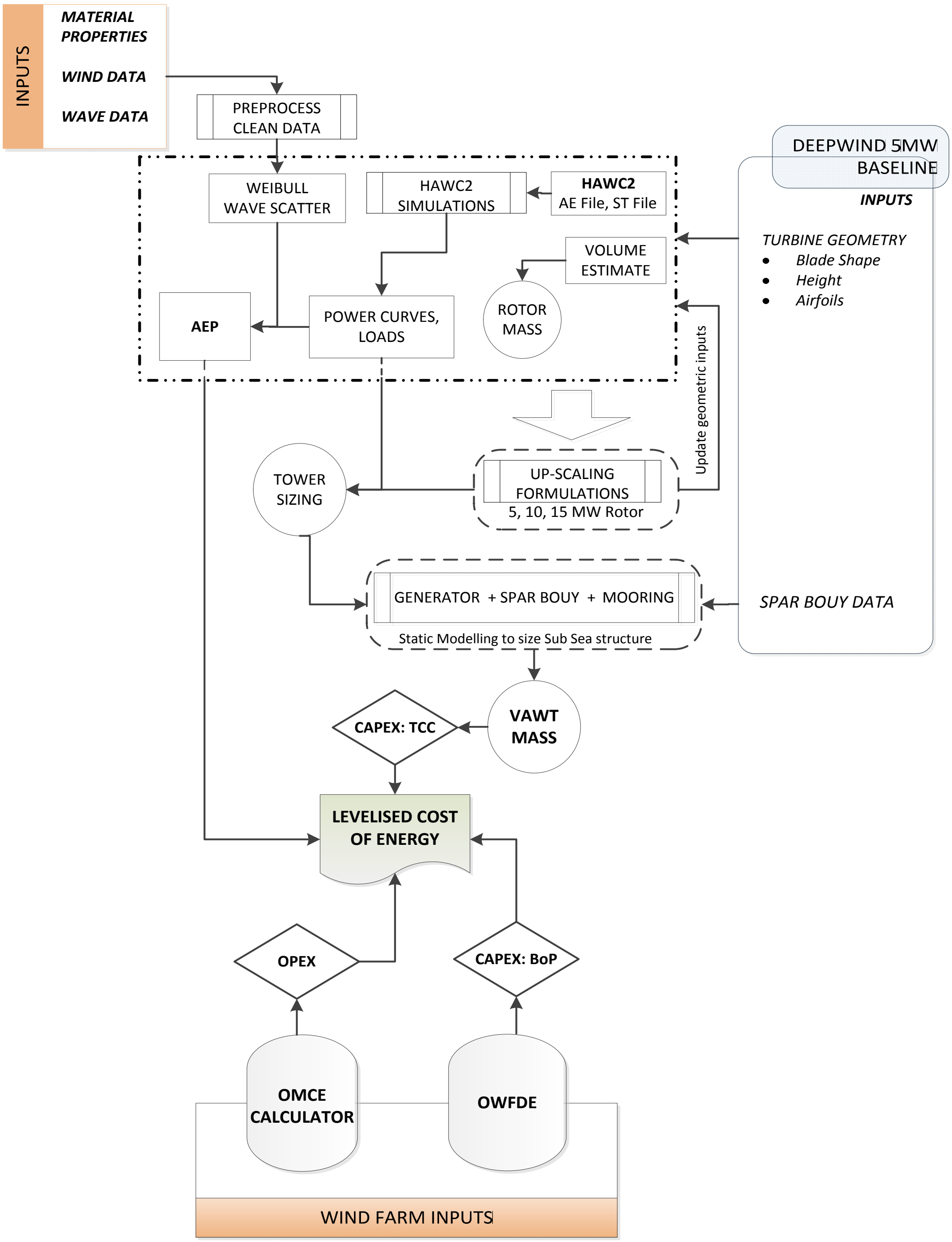
INPUTS
MATERIAL PROPERTIES
WIND DATA
WAVE DATA
PREPROCESS CLEAN DATA
WEIBULL WAVE SCATTER
HAWC2 SIMULATIONS
HAWC2 AE File, ST File
VOLUME ESTIMATE
ROTOR MASS
AEP
POWER CURVES, LOADS
DEEPWIND 5MW BASELINE
INPUTS
TURBINE GEOMETRY
Blade Shape
Height
Airfoils
Update geometric inputs
TOWER SIZING
UP-SCALING FORMULATIONS
5, 10, 15 MW Rotor
GENERATOR + SPAR BOUY + MOORING
Static Modelling to size Sub Sea structure
SPAR BOUY DATA
CAPEX: TCC
VAWT MASS
LEVELISED COST OF ENERGY
OPEX
CAPEX: BoP
OMCE CALCULATOR
OWFDE
WIND FARM INPUTS

Figure 4.1: *Work-flow for* VAWT *Engineering Cost model*

wind installation. The model is setup in a modular manner using MATLAB where each step of the design work flow is called into the model as a function. This provides the freedom for modification and improvement at any step of the model. For the design costs, the aero-elastic wind turbine simulation tool, HAWC2 is used. At this time it was the only commercially available tool that can be used to simulate the performance of a VAWT. This adaptability is possible through the implementation of an actuator cylinder model that was developed and used to design the DeepWind rotor. The operations and maintenance costs are estimated with a tool provided by ECN called

Operation and Maintenance Cost Estimator". For the final aspect of the Balance of Plant estimates, a package developed by Zaaijer [75], *Offshore Wind Farm Design Emulator* is implemented to estimate the grid connection and related infrastructure costs. For the other remaining aspects, various formulations are adapted from literature and derived from the DeepWind work packages. To determine the LCoE , a discounted cash flow for economic life cycle of a far offshore 245 MW wind farm is calculated. Emphasis is given on using the OMCE and OWFDE tools to generate a cost trends by varying key assumptions in a semi-limited workspace. Where possible, parametric relations will be derived to describe the scaling of system costs to analyse the scalability of the FO-VAWT concept.

Implementation Process

The algorithm applied in reference to figure 4.1 is outlined here. To determine the necessary masses for the cost model (chapter 5), certain geographic and design inputs are required. A detailed rotor structure definition for the base turbine (5MW) serves as the top design variable which dictates the sizing of the downstream subsystems. The inputs, criterion/load cases established to size the systems, along with the simplifications made using presumptions, are given in detail through the rest of the chapter

1. Inputs
   (a) Specific Parameters
      - Meteorological Inputs
      - Material Properties (ρ, E, G,€/kg)
   (b) Design Parameters
      - Rotor Geometry
      - Spanwise geometric distribution
      - Support structure heights
      - Turbine Operational spectrum
   (c) Cost Parameters
      - Manufacturing: Mature production process level(yrs),System Production Prices, Fixed Cost Fraction
      - Economic: Discount rate
2. Pre-processing of specific parameters: Outliers, clean data
3. U_z extrapolation
4. HAWC2 simulation (section 4.5)
   ▷ Bottom fixed rotor modelled
   ▷ Input files modified for scaled turbines (aerodynamic, structural)
   ▶ *Results*: Turbine power curve and loads
5. Wiebull distribution and wave scatter (section 4.2.1)
6. Annual Energy production is calculated (section 4.4)
7. Up-Scaling of geometry with swept area for higher turbine power rating(section 4.3)

   Steps 3-7 are repeated for Up-Scaled 10 and 15 MW turbines

8. Sizing of turbine systems (section 4.6)
    (a) Blade: Volume and mass is estimated from input, (section 4.6.1)
    (b) STT: Sized using linear scaling, height determined from wave climate, (section 4.6.2)
    (c) Tower: Shell dimensioned to satisfy Euler buckling criteria, (section 4.6.3)
    (d) Floater: Spar buoy sized to balance mass with buoyancy and maintain separation ratio between turbine centre of gravity and Floater centre of buoyancy, (section 4.6.4)
    (e) Mooring: elastic catenary wires satisfy maximum yaw moment, arms scaled as a linear parametric function of aerodynamic torque, (section 4.6.5)
    (f) Generator: derived from Direct Drive design presented by Leban [49], (figure 5.1)
9. Parametric models used for remaining systems such as bearings, brake and power electronics, [16, 18, 37]
10. Capex - Turbine Capital Costs determined with mass estimations and other inputs form preceding sections for 5, 10 and 15 MW, (section 5.2)
11. Wind Farm specifications [53, 75]
    ▷ Distance from Point of common coupling
    ▷ Wind Farm capacity and number of turbines
    ▷ Turbine Spacing
12. Capex - BoP Costs estimated: Owfde tool used to create workspace varying major wind farm specifications, (section 5.3)
    (a) Electrical infrastructure
    (b) Transportation and Installation Cost
    (c) Decommissioning
13. Opex - Operations and maintenance effort for wind farm life cycle using Omce, (section 5.4)
14. Geometric Scaling relations used for
    (a) Variation in fixed costs: number of technicians based on number of wind turbine units
    (b) Rising costs of spare parts with higher rated power turbines
    (c) Higher equipment costs as larger vessels needed
15. Parametric study of modelling assumptions, (section 6.3)
16. Economic assessment of wind farm project using key parameters
    ▷ Net Present Value
    ▷ Internal Rate of Return
    ▷ Levelised Cost of Energy
17. Analyse influence of constituting elements and assumptions on LCoE

The algorithm provided summarises the working process of the cost model and adds more step wise detail to the work-flow shown in figure 4.1. The three different models involved results in the linking of different assumptions and conditions when translating data to get the final cost of energy. The basic assumptions used in all the models to stream-line and simplify the cost formulation process are given in Section 4.2.

4.2 FO-VAWT Wind Farm Initialisation

As shown in figure 2.17, the levelised cost of energy comprises from investment and levelised yearly costs as a ratio of the annual revenue for the life time of the wind farm. The formulation of each aspect involves certain assumptions, while for some factors, the effect on LCoE does not seem to differ much for VAWT's from HAWT's. For this reason, the wind farm, its layout and other associated factors, which will be required in later chapters, are introduced together.

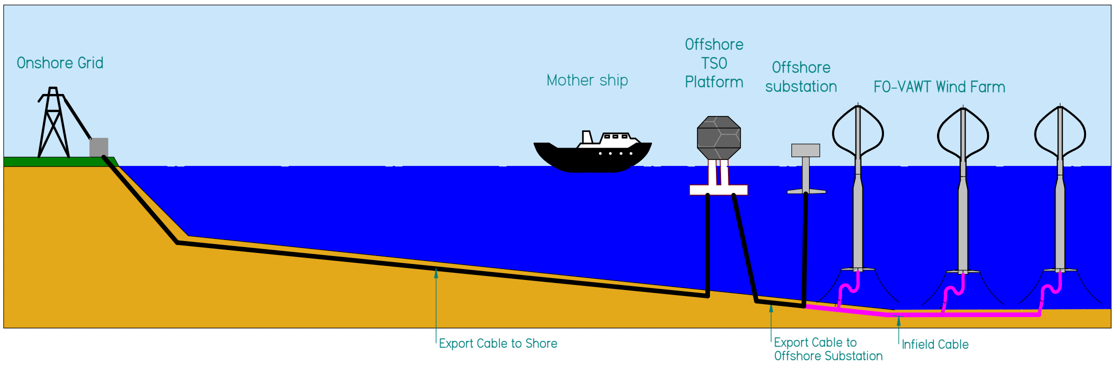

Figure 4.2: *Setup of* FO-VAWT *Wind Farm*

The base case of the wind farm is a 245 MW installation comprised of 498 turbines with a rated power of 5 MW. The location of the wind farm site is chosen at a location over 70 km from the closest shore the North sea, figure 4.3. Concurrently, a matured supply chain infrastructure and location specific requirements such as deep seabed are assumed to be satisfied. A critical but necessary assumption for far offshore wind farms is the provision of a grid coupling point 25 km from the wind farm by the Transmission Service Operator (TSO). This will be probably as a large floating HVDC substation platform, depicted in figure 4.2.

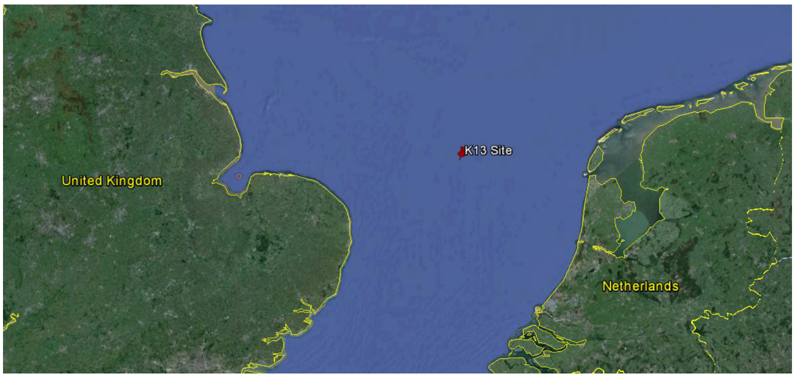

Figure 4.3: *Location of Wind Farm site close to the K13 measurement station*

In similar context, the operations and maintenance control/deployment is from an offshore ship stationed around 15 km from the wind farm. The vessel is customised with specialised equipment specific to FO-VAWT's, explained in section 5.5. It is assumed that all the structural turbine systems are fabricated at the port staging facility for ease of deployment. The generator evaluated is a direct drive design provided by Leban [49]. The wind farm capacity is scaled according to a square grid layout for the specific wind turbine rating compiled in table 5.2. The electricity feed-in tariff is taken at a fixed rate of €0.13/kWh, while the real discount rate is taken at 7%. A summary of the input parameters based on these assumptions is given in table 4.2.

The focus of the turbine capital costs are limited to Darrieus VAWT designs. The costs of the systems are evaluated for constructing the turbine out of standard materials for the structural masses sized from the load simulations or using parametric functions. For the O&M, the reliability of the turbine systems is derived from existing HAWT technology (appendix D.2) and adapted for VAWT's. The System Production Price (SPP), k_{sys} compiled in table B.3, include the contribution of manufacturing complexity on top of the material costs, k_{mat} given in table 4.1. A sensitivity analysis of the critical inputs is performed in order to to quantify the respective impact of the assumptions on the LCoE .

4.2.1 Meteorological Inputs

Site specific data influence the turbine design and energy production simultaneously. Reliable wind and wave data is needed for AEP estimations, to determine the design criteria and in O&M modelling. The fictitious site considered is located $\gtrsim$ 70 km offshore of the coast of the Netherlands, (N 53°10′, E3°10′) at the K13 measurement station of the Royal Dutch Meteorological Institute. Data was acquired on a 3 hourly time series of wind and wave parameters from 1995 to 2004 at a reference height, $z_0 = 10\,\text{m}$. Wind data is provided by ECN.

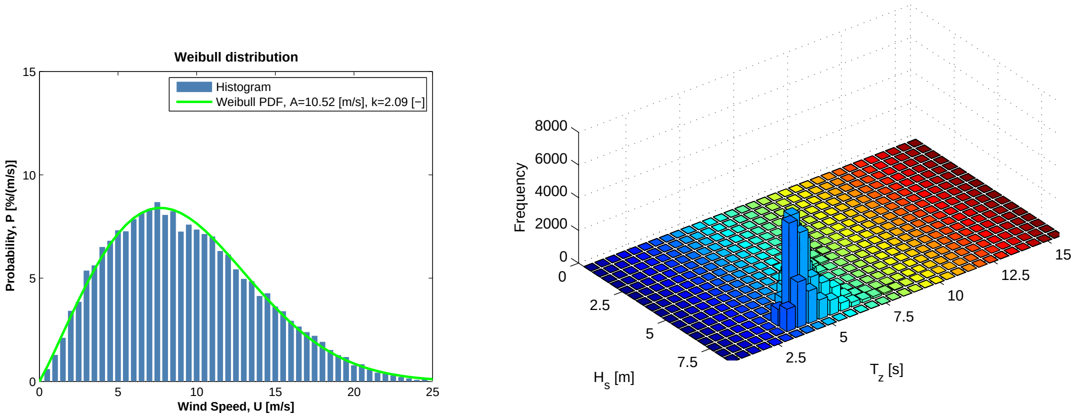

(a) Weibull Distribution (b) Wave Climate

Figure 4.4: *Site conditions at K13 site.*

Although the mean water depth at this height is 27 m, in this study the sea floor is presumed to be at-least 50 m *below* the Floater draft. The wind resource has to be transformed to the turbine equator height before it can be processed to generate a Weibull distribution. Assuming neutral atmosphere conditions, wind speed at equator height can be computed by means of;

$$U(H)\,[\text{m/s}] = u(h_0) \cdot \left(\frac{H}{h_0}\right)^{\alpha} \tag{4.1}$$

Where the power law exponent, $\alpha = 0.1$. The equator height for the base 5 MW case is derived from table 3.1 to be 88.1 m. This is based upon the understanding that the rotor is mounted on a surface transition tube of a 17 m height. The mean wind speed measured in sustained hourly periods during the measurement years can be approximated by a Weibull probability density function (pdf_W) defined as follows;

$$\text{pdf}_W(u) = \frac{k}{A}\left(\frac{u}{A}\right)^{k-1} \exp\left(-\left(\frac{u}{A}\right)^{k}\right) \tag{4.2}$$

The resource data from a specific site can be grouped in different bins of wind speed in order to fit a Weibull distribution function and obtain the two parameters A and k. Once the density function is fitted, several variables can be assessed such as the mean wind speed of the site, given by;

$$\overline{U}\,[\mathrm{m/s}] = \int_0^\infty \mathrm{pdf}_W(u)\mathrm{d}u \tag{4.3}$$

Similarly, the wave data is sampled into pockets for the significant wave height (h_s) and the mean zero crossing period (T_z), to determine a scatter diagram of the wave climate as given in figure 4.4b.

4.2.2 Material Inputs

The materials input to the model depend on what is primarily used in the turbine. For the cost estimations, material density, production costs k_{mat} and mechanical properties are needed. The material composition used along with other associated properties are given in table 4.1

Table 4.1: *Material properties and cost*

System	Material	$\rho\,[kg.m^{-3}]$	k$_{mat}$[€/kg]
Blade	CFRP	1570	22
	GFRP	1860	10.5
	Polyurethane Foam	125	5.12
	metal fasteners	8200	2.8
Floater	Rolled Steel	7800	3.5
Tower	Concrete	2450	0.10
	Aluminium	2700	1.8
	Steel Wire	7800	3.75
	Construction Steel	7850	0.62
Power Train	Copper	8900	5.2
	Iron	7050 - 7450	3

For historic prices, commodity based inflation rates were acquired from Producer Price indexes monitored in the United States[1]. The specifications of the relevant offshore turbine systems were acquired from literature [8, 12, 37, 38, 48, 49] . The material prices, k_{mat} were taken from the CES software package [31] with related estimations of some system production costs given in the appendix B.2. Where required, the average yearly GDP inflation rate of 2.5% per year was used if the commodity price index could not be acquired. A summary of the input parameters and other gross LCoE specific properties for the Fo-Vawt are given in table 4.2.

---

[1] `http://www.bls.gov/data`

Table 4.2: Gross specifications of hypothetical Fo-Vawt *farm*

Specification	Properties	Details
Geographic Inputs	[Site, Location]	Site K13, N 53°10′, E 3°10′
Rotor Type	[Darrieus]	DeepWind Fo-Vawt
Material Properties	[ρ , k_{mat}]	System Specific, table 4.1
System Reliability	[Failure rate Λ]	Adapted from Hawt's, section D.2
Wind farm layout	[MW, # Turbines]	245 $\pm$5MW, $f(\mathrm{P}_{WT})$
	[Layout, Spacing]	Square Grid, 5 & 7 ϕ_{turb}
Economic Factors	[SPP, k_{sys}]	Appendix B.2
	[Price of Energy]	€130/MWh
	[GDP Inflation]	Avg 2.5% yr^{-1} (B.2)
	[Real Discount Rate]	7 %

4.3 Up-Scaling

As mentioned in section 2.6, predicting how the loads and costs increase with larger sized WT's depends on the level of detail that needs to be captured. The common practice is to work back from load simulations to size the structures for higher power ratings. However, this requires a multi-disciplinary aero-elastic model to predict the dynamic interactions of the systems and the subsequent influences of sizing the structures. As there is a lack of standardisation and empirical data available on Vawt design, most of the scaling relations implemented are translated from existing Hawt research or based on geometric similarity rules.

From the *Square-Cube* law introduced in section 2.6, the power of a scaled rotor can be correlated to swept area, while the cost to the blade mass. Both depend on the blade shape which is a function of material properties and blade length (s). The starting point for the scaling calculation is the turbine rated power, with mass estimations as the necessary goal.

- A combination of *geometric upscaling relations* from Jamieson [44] are used along with *load based estimations* to size the mass of the tower and mooring system
- The 5 MW rotor geometry is pre-defined, upscaled as per design while maintaining geometric and aerodynamic similarity
- Static Load estimations on main systems are essential: aerodynamic loads on rotor, hydrostatic loads on spar- buoy and resultant operational loads on mooring system.
- Determine the critical load cases driving the system design
- For the power-train, a detailed design and upscaling study for the DeepWind rotor by Leban [49] is utilised

Characteristic Dimension

In classical wind turbine up-scaling, the square-cube law based relations are employed based on a characteristic dimension D. The Rotor swept area, S increases with the square of D which correlates to the energy yield. While the mass of turbine increases with the cube of D correlating to cost. In conventional Hawt scaling, D is taken as diameter of the rotor with which all systems are related based on a scale dependency, (refer to section 2.6). However for VAWT's, the swept area is not a exclusive function of radius R or diameter ϕ

$$\phi = f(h) \tag{4.4}$$

The radius of the blade varies along the height of the VAWT. Thus the swept area is also a function of the height.

$$S = \int_{h_\circ}^{H} \left(\frac{\delta}{\delta h}\right) \phi \tag{4.5}$$

Considering these aspects, the **turbine height** 'H' was selected as D while the Height-to-diameter (H/ ϕ) ratio was kept constant at 1.182, value obtained from table 3.2. This simplified relations connecting power to rotor area, where an increase in tower height was coupled with more downstream effects [2] on mass and cost scaling of other systems.

4.3.1 Rotor Scaling Trends

The rotor is one of the primary drivers for wind turbine design, having downstream effects on all other subsystems. When designing, it is essential to reduce the mass of the blades, while maintaining a high C_p efficiency. Rotor optimisation procedures involve varying rotor solidity, blade dimensions and the segment wise shape, within certain constraints, to mitigate dynamic loading and aero-elastic effects on the blades as well as directly coupled structures like the tower and struts. The increased freedom of motion with a floating structure adds another layer off complexity as the turbine stability is a function of aerodynamic and hydrodynamics loading, Paulsen et al. [59], Pedersen et al. [60]

According to the work of Schelbergen [65] and Roscher [62], successive rotor optimisation were performed on 5 MW VAWT's and the design scaled up to 20 MW. The blade structure was optimised but the height of the rotor was fixed at 180m for the 5 and 10 MW and increased to 260m for the 15 and 20 MW. This lead to a subsequent change in the rotors H/ϕ ratio. In figure 4.5, a correlation presented by de Vries [30] is used to compare the area factor B_δ (equation (4.6)) and the blade shape ratio S_δ (equation (4.7)) for various old VAWT designs,[30, 58].

$$B_\delta = \frac{S_{ref}}{s \cdot R_{max}} \tag{4.6}$$

$$S_\delta = \frac{S_{ref}}{R_{max}^2} \tag{4.7}$$

It is normally perceived by Paraschivoiu [56], that the optimum H/ϕ ratio lies around ≈ 1.2 - 1.4. However, analysing figure 4.5 for the blade shape S_δ and area factor ratio B_δ , shows that a H/ϕ (where $R_0 = \phi/2$) ratio slightly above 1.1 proves to be optimum giving a S_δ close to π, [58]. For the iterative rotors designed by Roscher, Schelbergen, the H/ϕ for the upscaled rotors is not constant. Aerodynamic similarity is not maintained if the all geometric properties are not scaled in parallel [68]. In conclusion, it was chosen to analyse scaling effects of VAWT's with the DeepWind 5 MW design as the base topology

---

[2] Downstream effects symbolise the impact of the rotor generated loads as they propagate through the turbine systems

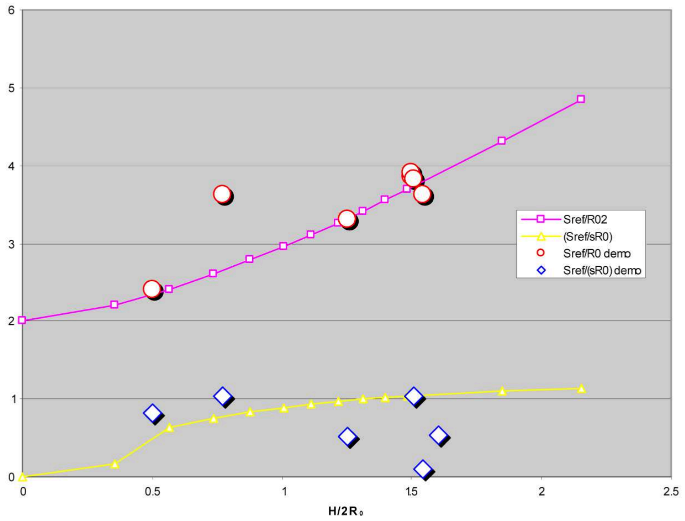

Figure 4.5: *Non dimensional Cost and Power parameters related to height over diameter for various* VAWT *designs, [58]*

System Similarities

It is necessary to maintain the performance envelope of the turbine by not altering the rotor aerodynamic similarity, [22]. This means maintaining the same tip speed ratio ($\lambda = \frac{\omega R}{U_\infty}$) by reducing the rotational speed (ω) so that the Reynolds number (Re) is more or less constant for the upscaled turbines. This however, is difficult to ensure for VAWT's. Reason being that the Reynolds number scales along the blade height for decreasing diameter while it also varies along the operational envelope with wind speed. Considering the change in azimuthal angle as an example. The extreme cases are for $\theta = 0°$ and $180°$ (figure 4.7), the free stream wind U_∞ is either added or subtracted from the local velocity on the airfoil, ($\omega.R - U_\infty \geq U_{rel} \leq U_\infty + \omega.R$).

$$U_{rel} = U_\infty \cdot \sqrt{(\lambda - \sin\theta)^2 + (\cos\theta)^2} \tag{4.8}$$

$$Re = \frac{U_{rel} \cdot C}{\nu} \tag{4.9}$$

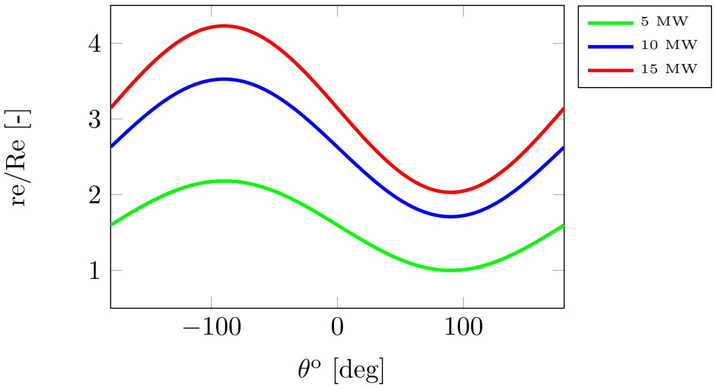

Figure 4.6: *Non linearity of normalised Reynold's number over a* VAWT *operational regime*

As the VAWT radius scales with height, the local Reynold's number on the blade scales proportionally, $Re \propto Re_{ref} \cdot \frac{H}{H_{ref}}$. Considering a fixed λ= 2.7 and $U_{rated} = 14m/s$, Re variations with

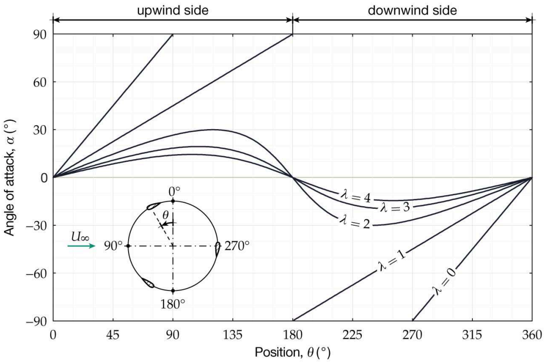

Figure 4.7: VAWT *α airfoil through a revolution, (Source: Rene Bos)*

the turbine power ratings P_{wt} = [5, 10, 15] MW are given in figure 4.6 for radii (R_{max}) of [61, 84 and 103] respectively. With a operational envelope of $6\text{E}10^6 \geq Re_{5MW} \leq 1.4\text{E}10^7$, the blade performance, such that $\frac{C_l}{C_d}$ and stall properties of the airfoil vary with azimuthal position (θ), rotor height and evidently rated power.

To maintain aerodynamic similarity across the power scale spectrum, the chord length and power coefficient for the scaled rotors was kept constant to the base case. This meant assuming a very stiff blade material for the HAWC2 simulations. Arguments with respect to this assumption will be made in the conclusions, chapter 7.

4.3.2 Geometric Scaling with Power

The scaling factor for the *characteristic dimension* is determined by solving with the power of a wind turbine to calculate the swept area of the turbine. As introduced in section 2.6.1 the 'Square-Cube' law adheres well in estimating the power of a turbine. From equation (2.1), the power is proportional to the swept area, thus for HAWT's the rated power increases with ≈ square of the diameter as in figure 4.8.

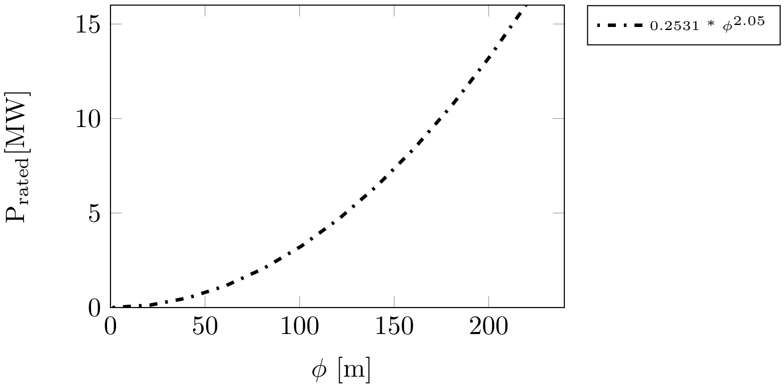

Figure 4.8: *Power scaling relation with diameter ϕ, [44]*

The equation of the curve in figure 4.8, can be related to the power equation equation (2.1), where the constant 0.2531 represents the power intensity normalised with the cube of the velocity, and the extra power exponent $\phi^{0.05}$ can be a correction factor to account for the variation in U_{rated} and $C_{p,max}$ for different HAWT designs.

However for VAWT's this relation is not directly applicable as the area is not a lone function of the diameter, equation (4.5). Evaluating figure 4.5, the power intensity (P_I) and the rotor power coefficient (C_P) can be considered to depend on H/ϕ, [30]. To scale the DeepWind design for larger power ratings, the H/ϕ is fixed at 1.18, [66]. Maintaining the same P_I as for the baseline design, the swept area of the upscaled turbines is determined.

$$P_I = P_{rated}/S = 416.7\,W.m^{-2} \tag{4.10}$$

To determine the area of a Darrieus VAWT, the rotor shape is modelled as a 'catenary'. A catenary shape is obtained by rotating a perfectly flexible cable of uniform density under the action of a constant force, e.g. 'gravity'. In this case, the equation of a catenary is modified to approximate the area under the curve and thus the swept area of a Darrieus VAWT.

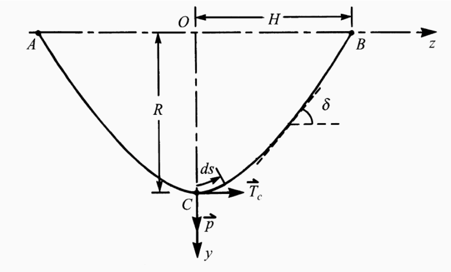

Figure 4.9: Representation of Catenary shape as a VAWT *rotor blade, [56]*

$$y = a\cosh(z/a + C_1) + C_2 \tag{4.11}$$

Where a is the radius ($\phi/2$) and z is turbine height from -h/2 → +h/2. The equation is modified for a rotated vertical axis.

$$\begin{aligned} val =& -\phi/2 \cdot \frac{cosh(H)}{\phi/2} && (4.12)\\ C_2 =& |val|_{max} + \phi/2 && (4.13)\\ Y_{cat} =& val + C_2 && (4.14) \end{aligned}$$

With the coordinates of the blade known, the area is approximated using trapezoidal approximation. For H/ϕ ratios from 1→2, $\delta H/\phi = 0.05$, an array of swept areas is calculated. Using a power regressive fits on the results, it was noticed that the size dependency remained constant at 0.5 but the constant was dependent on H/ϕ. The equation was re-formulated to correlate how the height of the VAWT varies with area (S) for a certain H/ϕ ratios.

$$H = Const(f(H/\phi)) \cdot S^{1/2} \tag{4.15}$$

$$H = \big(0.4576 \cdot (H/\phi)^2 - 0.2(H/\phi) + 0.858\big) \cdot S^{1/2} \tag{4.16}$$

With the swept area's scaled using equation (4.10), for 10 and 15 MW and equation (4.16), for a fixed H/ϕ, the respective heights are determined in table 4.3. This provides the scaling factor for the characteristic dimension against which all other geometric relations are based for the size dependencies given in table 2.2.

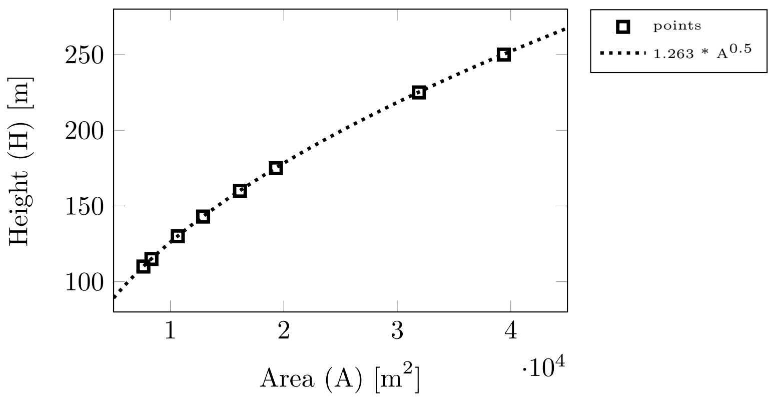

Figure 4.10: *Curve fit for* VAWT *height vs Swept area for H/D of 1.182*

Table 4.3: *Scaling factor of characteristic dimension, "turbine height"*

Parameter	Unit	Values		
Power Rating	$[MW]$	5	10	15
Area	$[m^2]$	12000	24000	36000
Height	$[m]$	143	200	243
Scaling Factor	$[-]$	1	1.4	1.7

4.3.3 Mass

The loading and mass of the blade increase with greater exponential relations than formulated by Chaviaropoulos as part of the "*UpWind*" project. Designers work to beat the Square-Cube law and with time as the technology matures, designs get better and more refined. A compilations of relevant mass scaling studies for the rotor, tower top mass and tower are given in table 4.4.

Subsystem	**Linear**	**UpWind** [22]	**InnWind** [23]	**Loads** [8]
Blade	3	2.09	2.5	2.64
Tower Top	≈ 2.5	2.39	2.25	2.41
Tower	3	2.78	2.7	3.22

Table 4.4: *State-of-the art mass-diameter scaling exponents*

In this study, mass estimations are based upon geometric scaling dependency (sd) where the ratio of parameters is scaled to the power of the size dependency, taken as 3 under the *cube* law. Mass scaling is only needed in order to determine the cross sectional area of the blade for the HAWC2 structural file . In this case, in adherence to the geometric relations, the mass per blade length (m_b) is scaled with the size dependency for H of 2.

$$\frac{m_b/l}{m_{b,ref}/l} = \left(\frac{H}{H_{ref}}\right)^2 \tag{4.17}$$

4.3.4 Cost

For the cost scaling, mass is taken as a direct correlation to cost of material, while other percentage factors such as manufacturing complexity account for a portion in the total production cost aswell. The initial cost analysis done in Paulsen et al. [57] is based on scaling the turbine with respect how deep the floating spar should be to counteract the weight of the rotor of a certain power rating. The cost functions developed in this report will be specific to each turbine system and wind farm aspect, covering the following aspects.

- The material usage as a percentage of the internal composition of the subsystem. For eg: blades are made of a combination of resin, composites, foam etc.
- The mass of the systems, determined from the relevant load cases given in section 4.6.
- Other factors such as manufacturing complexity taken as scalar multipliers to the final cost estimation
- The operation and maintenance cost inputs are modelled for 5MW but scaled for higher rated power turbines and wind farms
- Wind farm infrastructure costs are scaled for a fixed farm layout topology for all three turbine rated powers.

Direct cost scaling is utilised in the O&M model, section 5.4. The costs for spare parts, labour equipment are derived as a function of the main characteristic dimension/parameter which varies for the higher rated turbines or larger wind farms.

4.4 Power estimation

The scaling factors determined intable 4.3 give the approximate geometric size of the 10 and 15 MW turbines. To verify the power output, HAWC2 is used to simulate the turbines. The FoVawt is implemented as a bottom fixed Vawt , with the rotor speed is reduced according to linear scaling relations given in table 2.2, where the characteristic dimension D was the height of the rotor.

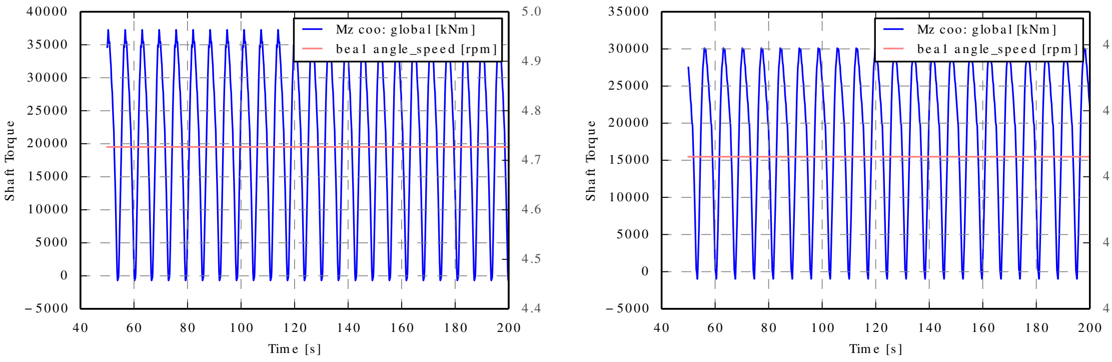

(a) $M_{z,mean}$ = 20300 kNm, ω = 0.494 rad.s^{-1} (b) $M_{z,mean}$ = 17910 kNm,= 0.443 rad.s^{-1}

Figure 4.11: Scaled and corrected rated aerodynamic torque represented by Shaft M_z for 10 MW Vawt

For the 10 MW turbine, this results in a scaled rated rotational speed of 4.24 rpm or $\omega = 0.443$ rad.s^{-1} for a fixed tip speed ratio, $\lambda = \dfrac{\omega R}{U_\infty}$. It was however noticed that the product of the mean torque ($M_{z,mean}$) and ω did not scale proportionately with the geometry to the expected rated power using the scaling factors derived in table 4.3. An adjustment (e_{wt}) in the tip speed ratio or ω_{rated} was made for both up-scaled turbines given in table 4.5.

$$\omega_{10mw} = e_{wt} \cdot \omega_{5mw} \cdot \left(\frac{H_{10mw}}{H_{5mw}}\right)^{-1} \tag{4.18}$$

Table 4.5: *Torque for 10 MW and 15 MW* VAWT *at different rated rotational speeds*

Property	**Unit**	**10 MW**	**15 MW**
$\omega_{5MW,rated}$	[rad.s^{-1}]	0.62	
Scaling Factor	[–]	1.4	1.7
ω_{scaled}	[rad.s^{-1}]	0.443	0.365
Q_{mean}	[kNm]	17910	27000
Power	[MW]	7.93	9.86
e_{wt}	[–]	1.116	1.2
ω_{corr}	[rad.s^{-1}]	0.494	0.438
$Q_{mean,corr}$	[kNm]	20300	34250
Power	[MW]	10.0	15.0

These corrections will be discussed in the conclusions (7). Thus assuming the same operational wind speed limits, the aerodynamic power curves for the up-scaled turbines came out to be

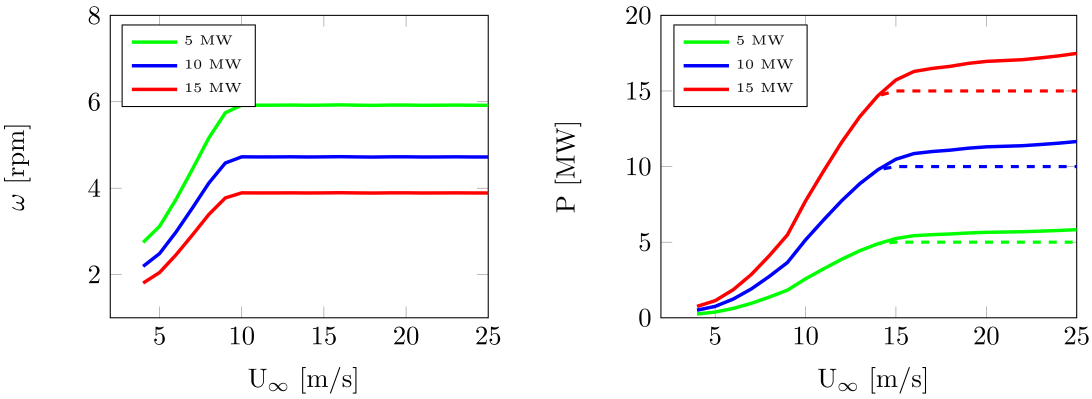

(a) Rotor Speed

(b) Power Curves

Figure 4.12: *Power curves and rotor speed for 5 - 15 MW* VAWT

Annual Energy Production

Utilising a Weibull distribution as generated in figure 4.4(a), Weibull factors for the 10 and 15 MW turbines were also calculated at equator heights 126 and 153 respectively.

- Mean wind speed, ($\overline{U}$)or Scale factor A

5 MW = 10.52 $\mathrm{m.s^{-1}}$
10 MW = 10.85 $\mathrm{m.s^{-1}}$
15 MW = 11.09 $\mathrm{m.s^{-1}}$

- Shape factor k = 2.09

The overall annual electrical energy yield curve of the wind turbine is a product of the aerodynamic power and cumulative probability of the Weibull distribution

$$AEP = 8760 \cdot \sum_{i=1}^{N} P_i \cdot F_W(U_{\infty i}) \tag{4.19}$$

where, N is the number of velocity segments, P_i denotes the power in kW for each velocity segment and $F_W(U_{\infty i})$ is the cumulative probability difference. The Weibull cumulative distribution was determined using the Matlab function *wblcdf.* The predicted annual energy production for three scaled Vawt came out to be:

AEP $_{5MW}$ = 19.574 [GWh/yr]
AEP$_{10MW}$ = 40.817 [GWh/yr]
AEP$_{15MW}$ = 62.962 [GWh/yr]

Nevertheless, the previous result does not consider many elements contributing to the uncertainty in AEP estimations. In order to account for this, a value for availability of the wind turbine has to estimated. The recalculated net AEP for an exceedance probability of 50 % can be found in the section 5.5

4.5 DeepWind Simulations

As introduced in section 4.3.3, the mass scaling for the blade to input into the HAWC2 files was done based on equation (4.17). However for the cost modelling mass estimation, the method used to determine the volume of the blades internal structure is explained in the following section 4.6.1. The blade geometric properties are varied with a linear geometric size dependency (sd = 1) in equation (4.17) for the height scaling factors presented in table 4.3.

.

The first aspect in modelling the cost of energy is the calculation of the loads and do a model analysis of the system. The DeepWind design involves a high level of dynamic substructure interaction. According to Berthelsen [12], modelling the hydrodynamic behaviour linked with the fluctuating loads generated from a Vawt rotor, some critical resonance problems can occur. Especially because of the added modelling of a rotating submersed spar. From the simulations of the complete HAWC2 model, certain instabilities were noticed as shown figure 4.13

It can be seen from the figure there is a large fluctuation in the generator torque resulting in negative rpm's and oscillatory motion around the vertical axis to the factor of $\pm 20^0$. This could be due to coupling of the generator torque control with the motion of the rotating spar or this could be attributed to either the torque ripple creating a lead lag with the generator rotation resulting in resonance occurring at certain wind speeds. In either case, such divergent motion means the controller is not optimised over the whole velocity profile of the turbines operation. Thus using the complete DeepWind HAWC2 model to analyse and upscale the Vawt design loads was abandoned as an option. The adopted approach was based on modelling the wind turbine as a bottom fixed Vawt without a cylindrical tower. The loading resultant from the rotor simulations fed to calculate the mass of the supporting structure.

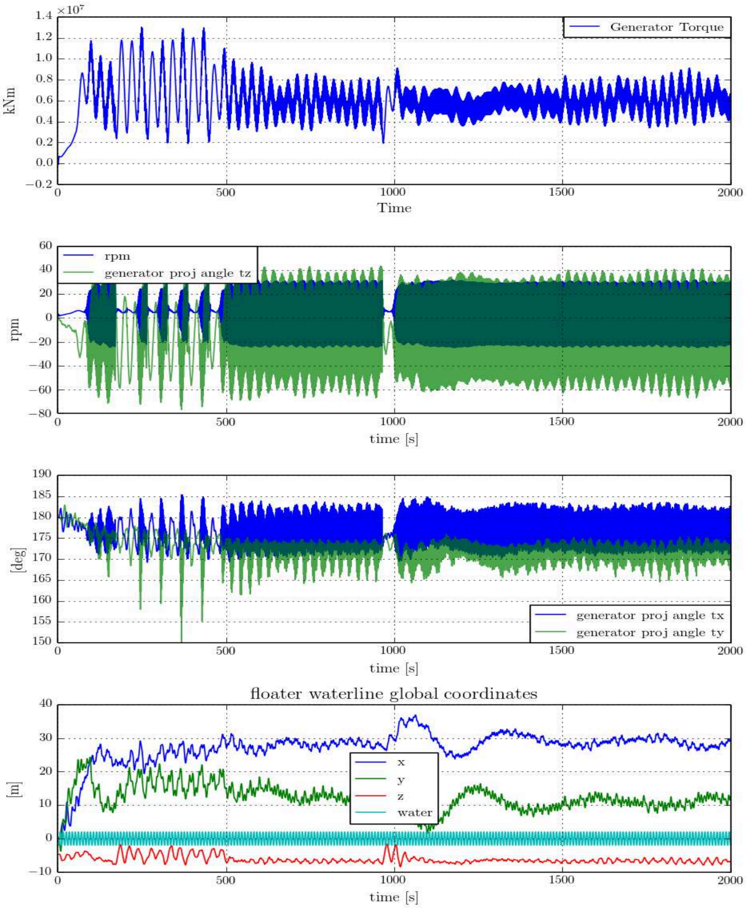

Figure 4.13: Generator torque coupling with the rotational motion of the spar U_0=16 m.s^{-1}, (Source: DeepWind)

4.6 Sizing - Static Modelling

Using the relevant inputs from the preceding sections and HAWC2 simulations for a bottom fixed Fo-Vawt, the required dimensions of the system downstream to the baseline and scaled rotors will be determined in this section. For the baseline DeepWind case, these systems have already been designed. However it is interesting to assess how the systems scale in terms of mass and cost. These are determined based on the governing aerodynamic loads inflicted on the system. The driving load case will primarily determine the standard mass required to fulfil the structural requirements of the loadings induced. Fatigue driven load cases and other dynamic stability modelling are not considered. Although these are presumed to have a strong impact on the mass estimations and are important design criteria to consider, but currently are beyond the scope of this project.

4.6.1 Blade

The aspects covering the structural design of the blade were beyond the scope of this thesis. To predict the airfoil, chord distribution and curvature of a Vawt rotor, a multi-disciplinary optimisation is needed in order to capture the aero-elastic behaviour of the rotor to refine the structural distribution. The purpose of this is to achieve a low mass to area ratio while maintaining a high

Cp. For VAWT's, rotor design optimisation to improve the LCoE is strong topic of focus for many research institutes including DTU Risø under the DeepWind Project [66], by Sandia National Laboratories [39], as well through consecutive master project's by Roscher [62], Schelbergen [65] at TU Delft. For the purpose of this project, the optimised structure of the DeepWind rotor from section 3.1, is utilised.

Volume Estimation

To estimate the mass distribution along the blade length accurately, the volume of the blade skin, spar caps and shear webs is to be calculated. For this process, the cross section of the airfoil is divided and modelled according the geometric approximations given in Table 4.6.

Airfoil Section	**Mapping Estimation**	**Blade structure**
Leading Edge	Half Ellipse	Skin
Mid Section	Rectangle	Shear web, Spar Cap
Trailing Edge	Triangle	Skin

Table 4.6: *Cross sectional Area estimation of airfoil section*

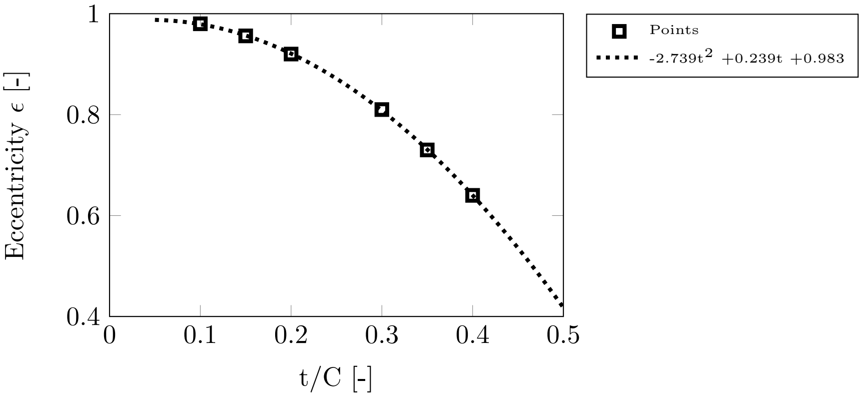

Figure 4.14: *Ellipse Eccentricity scaling relation to map the leading edge of NACA 00XX airfoil's*

The eccentricity of the ellipse 'ϵ' is scaled as a function of the airfoil thickness, t/c. The eccentricity can also be interpreted as the fraction of the distance along the semi-major axis, denoted by 'b', at which the focus ($f = \sqrt{a^2 + b^2}$) lies, where the semi-minor axis is taken as 'a'. An eccentricity of 0 gives the shape of a circle. The equation of the curve fitted in figure 4.14 defines the curvature of the leading edge with respect to the increasing thickness of symmetrical airfoil's from the NACA 4 digit series. This airfoil cross section shape mapping is only valid for $[0.05 \geq t/C \leq 0.5]$ with the formulation illustrated in figure 4.15. More detail on the area estimation and possible errors can be found in Appendix B.1.

For the blade internal structure, the inputs are at a discrete number of' n' points along the blade span, where there is a change in airfoil's thickness, 't/C'. The internal thickness distribution and airfoil thickness from Schelbergen and Roscher's optimised rotor[3] is shown in figure 4.16. The DeepWind rotors' blade distribution is more constant, sectioned for two airfoil's with a fixed

---

[3] For future reference, Roscher, Schelbergen's optimised rotor design will be referred to as the TUD Msc VAWT

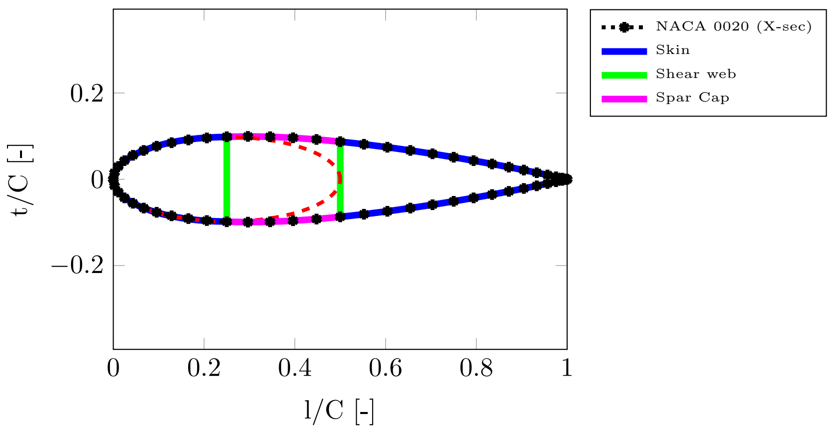

Figure 4.15: *Mapping of contours of NACA 0030 airfoil using methods mentioned in table 4.6*

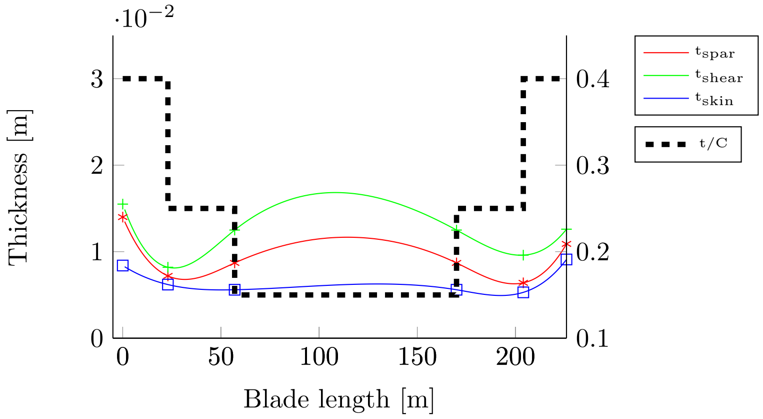

Figure 4.16: *Cubic spline interpolation of airfoil internal structure thickness and blade t/C along blade span for TUD MSc* VAWT*, [62]*

thickness for the internal blade structure.

The cross sectional area of the blade is also determined at 'n' points along the blade length using the relations given in the Appendix B.1. To define the blade area more precisely, a *cubic spline interpolation* is implemented, figure 4.17. The interpolation is performed over the length of the blade for a discrete number of fixed points, 'N' along the height-wise axis. The points are determined by fitting the rotor blade coordinates to a high order polynomial. Negligible errors can be seen in the accuracy of the mapping from figure 4.19.

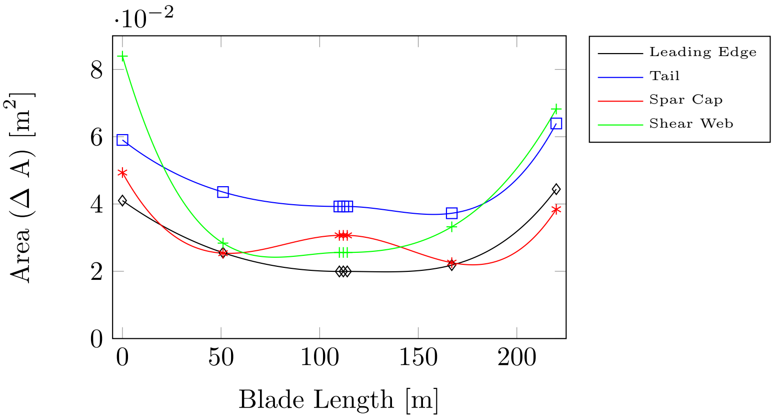

Figure 4.17: *Cubic spline interpolation of blade cross sectional area along blade span of TUD MSc* VAWT, *[62]*

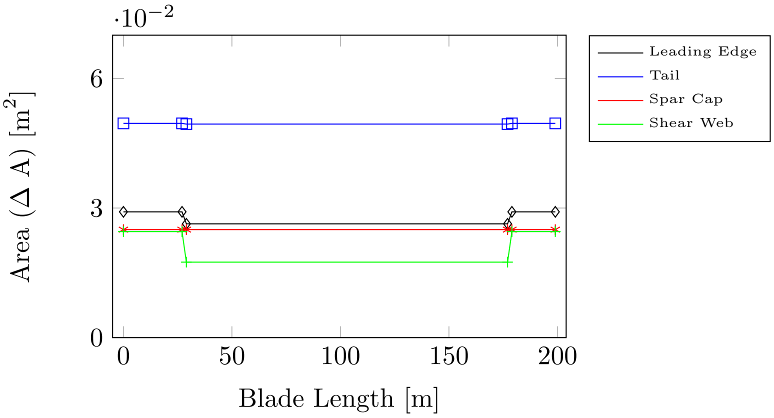

Figure 4.18: *Linear interpolation of blade cross sectional area along blade span of DeepWind* VAWT

However, for the volume of a tapered shell, a function defining the variation in shell thickness and radius needs to be integrated along the height H for the variation in area to determine the volume. If the difference between the points $\delta h_N \leq 1$, trapezoidal integration can be used to find the volume at every 'δh_N'. The method used is shown in equation (4.20) till equation (4.24).

$$V = \int_0^H A(h)\,\delta h \tag{4.20}$$

$$where : A = A_i + (A_{i+1} - A_i) \cdot \frac{h}{H} \tag{4.21}$$

$$A_i\,h + (A_{i+1} - A_i) \cdot \frac{h^2}{2H}\bigg|_0^H \tag{4.22}$$

$$V_{i+1} = \frac{1}{2} \cdot (A_i + A_{i+1}) \cdot h_i \tag{4.23}$$

$$V_{tot} = \sum_{i=1}^{N-1} \left(\frac{A_i + A_{i+)}}{2} \cdot \delta h_i \right) \tag{4.24}$$

The results for the volume estimation in table 4.7 show a dependence on the accuracy based on the method used and the defined blade structure. As for the DeepWind blade, the internal

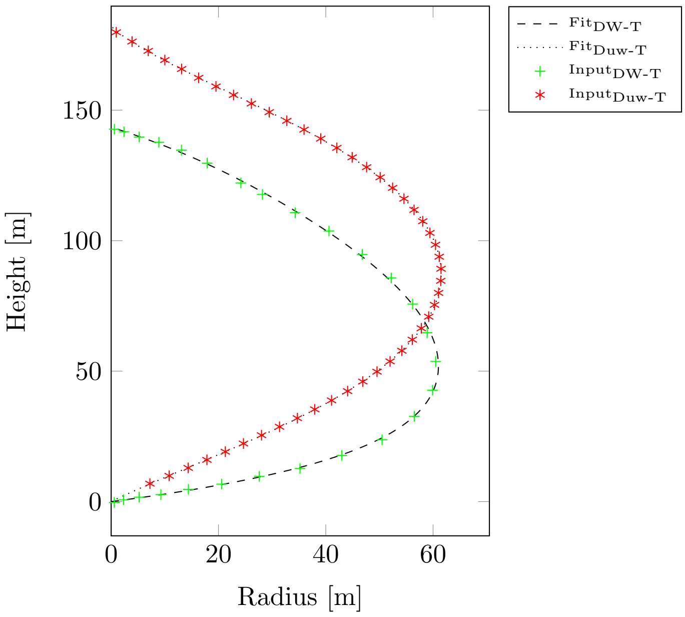

Figure 4.19: *Input coordinates and* 6^{th} *order polynomial fit onto DeepWind and TUD MSc* VAWT

dimensions are fixed, the area scales with the thickness of the blade only. In this case a higher order interpolation produces *negative* volumes for the constant mid section. However, for a tapered internal and external blade structure, using polynomial piecewise interpolations increase area mapping accuracy and consequently improve the volume estimated.

Volume Interpolation [m^3]					
Blade	Length [m]	Linear		Spline	
		Skin	Box Beam	Skin	Box Beam
DeepWind - 5 MW	200	15.219	8.712	10.2176	-3.3097
DeepWind - 10 MW	280	44.783	25.643	31.097	-7.123
DeepWind - 15 MW	341	83.902	48.036	56.435	-17.555
TUD MSc VAWT- 5 MW	225	16.217	15.702	15.5502	14.5376
TUD MSc VAWT- 10 MW	260	42.189	31.480	29.7294	40.1439
TUD MSc VAWT- 15 MW	290	42.134	62.678	40.2289	59.8830
Mass Estimates [kg]					
		GFRP	CFRP		
		2000 [$kg.m^{-3}$]	1650 [$kg.m^{-3}$]		
DeepWind - 5 MW	200	4.8020E+04	3.9617E+04		
DeepWind - 10 MW	280	1.414E+05	1.166E+04		
DeepWind - 15 MW	341	2.649E+05	2.185E+05		

Table 4.7: *Blade Volume estimations and Mass estimation for* VAWT

4.6.2 Surface Transition Tube

There is a high level of loading on this structure, for this reason a very conservative design was done for the baseline DeepWind turbine. A shell thickness, t_{stt} of 50 mm kept for a constant ϕ of 7.63 m along the height of the surface transition tube (STT). These dimensions will be scaled linearly with the turbine height. The height of the STT however is based on the sea state. From figure 4.4(b), the maximum significant wave height came out to be 7.24 m. Based on this, the maximum extreme wave height possible

$$H_{wav,max} = 1.86 \cdot hs_{max}$$

Based on IEC 61400-3 standards ([25]), a minimum height is 1.2 times $H_{wav,max}$ = 16.157 m. Thus the h_{stt} was taken as 17 m. The mass of the structure was made from construction steel with density ρ_{cs} of 7850 kg.m^{-3} from table 4.1

$$m_{STT} = \rho_{cs} \cdot (A_{shell} h_{stt})$$

The thickness of the STT is taken to scale with a linearly size dependency on D.

$$\frac{t_{stt}}{t_{stt,ref}} = \frac{H}{H_{ref}}$$

4.6.3 Tower

The tower design module is based on determining the mass of the tower required to cope with the loading incident on it. As explained in model methodology, (section 4.1), the aerodynamic load simulations from the rotor are only considered while the hydrodynamic influences are disregarded. However to verify the design, the mass estimated from the criteria/load cases considered will be compared with the final mass of the tower from the baseline DeepWind design.

Design Load Cases

The design of the tower thickness distribution is normally based on the fatigue load capacity (FLC) and ultimate load capacity (ULC) at the tower root as the determinant case. For conventional turbine design, load cases for emergency shut-down, rated operational, parked, high turbulence and extreme wind are chosen to investigate the thickness needed for the tower to safely operate through its life cycle. In this study, only ultimate load cases are considered for rated operational conditions. The limit states of the tower thickness will be based on the ultimate load capacity of the material for the following criteria

- Operational Loads at rated wind speed at Heel angle β= 0°
- Addition of Static blade mass effects at Heel angle β= 10° on bending moment
  Criteria: Euler local Buckling strength

Based on these conditions and the formulations published by DNV and DTU Risø in [32] and from the work of Zaaijer [75], the diameter and thickness distribution was determined along the turbine height. A partial safety factor of 1.55 was chosen from the DNV-GL offshore standard for the Design of Floating Wind turbines, Veritas [71].

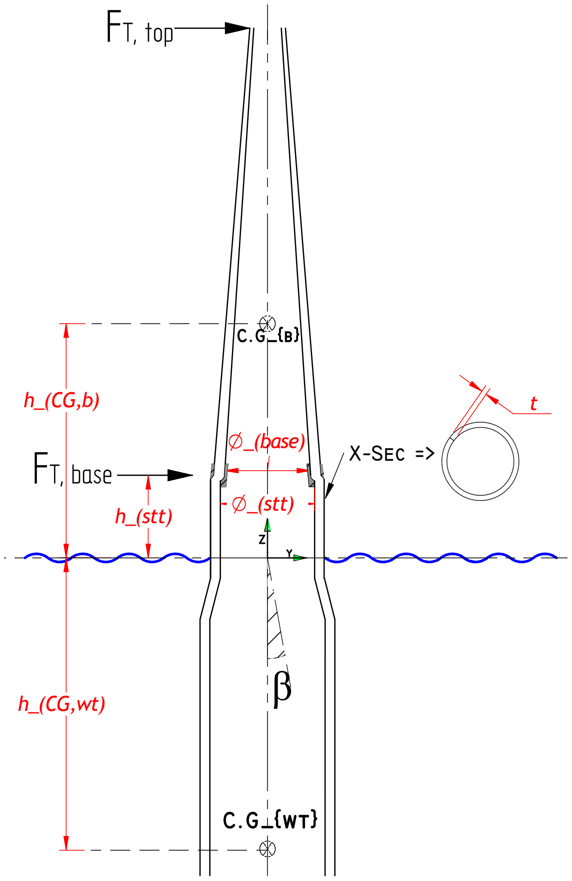

H_t :- Tower height
ϕ_{base} :- Tower base Diameter,
ϕ_{top} :- Tower top Diameter
ϕ_{STT} :- STT Diameter
t :- Tower shell thickness,
β :- Heel Angle

$\delta\phi\,,\,\delta t \Rightarrow \mathrm{fn}(H_t)$
Origin at MSL

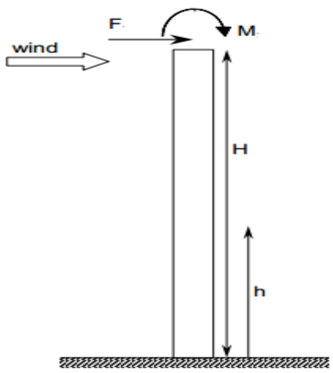

The load simulations are taken from modelling the turbine in HAWC2. The tower is modelled as an infinitely stiff beam with a cross sectional area comparable to the DeepWind specifications but with a negligible mass. This provides forces/moments along the tower due rotor and tower wind loads and centrifugal effects but no gravity or dynamic coupling of the tower on the turbine. Gravitational effects of the blades for the turbine tilting at a maximum static heel angle of 10° are incorporated as well. The limit state for the heel angle β was taken from the design criteria established for DeepWind by Berthelsen et al. [13].

As the tower was modelled as a single body and wind shear effects were neglected, the axial forces are constant over the structure. The forces from HAWC2 are evaluated at the tower base and top, with the bending moment (BM) determined by measuring the sum of the resultant forces at the tower top and multiplying it with the height (H).

$$\text{At Time t} \rightarrow BM = \left(\sqrt{F_{x,i}^2 + F_{y,i}^2}\right) \cdot H$$

where i signifies the time step Δt. These loads are used to estimate the thickness and diameter. A tapered distribution is assumed till the tower top. The axial forces F_x and F_y are resolved to generate cumulative mean thrust force taken over a simulation time length as shown in figure 4.20. The incident mean thrust = 380.85, 637.46, 867.15 kN for the scaled turbine with a standard deviation of 130, 252 and 309.1 kN[4].

---

[4] Generated with Pdap, HAWC2 post processor

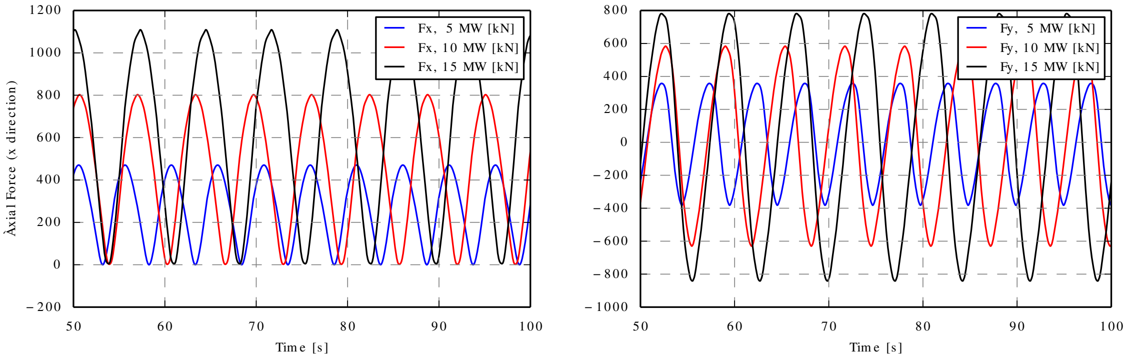

(a) F_x (b) F_y

Figure 4.20: *Axial Forces at tower top for 5,10,5 MW turbines at rated conditions*

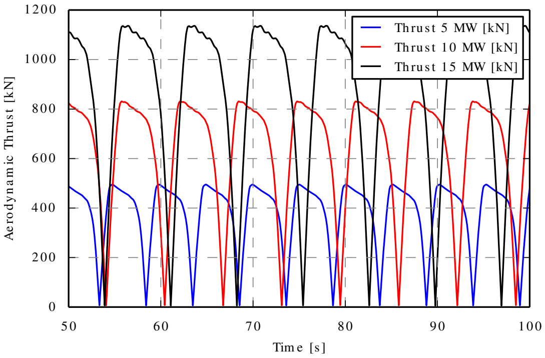

Figure 4.21: *Thrust Force for 5, 10, 15 MW turbines for rated U_∞= 14 [m/s]*

Mass Estimation

The tower mass is estimated by determining the tower base sectional area as a function of the thickness and diameter necessary to sustain the loads. As an initial guess, a ratio factor of diameter to thickness, $f_{t/\phi_{out}} = 0.0067$ is chosen, [16]. The design material considered is *rolled steel* with a density $\rho_{rs} = 7800$ kg.m^{-3}, Elastic modulus $E_{rs} = 220$ GPa, Poisson's ratio $\upsilon_{rs} = 0.287$ and Elastic stress limit $\sigma_{lim} = 220$ MPa. The stresses from axial force and bending moment are calculated by

$$\sigma_F = \frac{F_{Res}}{\pi\phi t} \tag{4.25}$$

$$\sigma_{BM} = \frac{4 \cdot M_{Res}}{\pi\phi^2 t} \tag{4.26}$$

Where F_{Res} and M_{Res} are the loads obtained from the HAWC2 simulations on the VAWT at a heel angle β= 0. To establish the criteria for Euler buckling due to critical compressive stress σ_{cr}, the theory of elasticity is implemented

$$
\begin{aligned}
sigma_{eu} =& \frac{E_{rs}}{f_{t/\phi_{out}}\sqrt{3\,(1-\upsilon_{rs}^2)}} && (4.27)\\
sr_b =& \sqrt{\frac{\sigma_{lim}}{\sigma_{eu}\varepsilon}} && (4.28)\\
\text{where } \varepsilon_F =& \frac{0.83}{\sqrt{1+0.01\dfrac{\phi_{out}}{t}}} && (4.29)\\
\varepsilon_{BM} =& 0.1887 + 0.8113\varepsilon_F && (4.30)\\
\varepsilon =& \frac{\varepsilon_F\sigma_F + \sigma_{BM}\varepsilon_{BM}}{\sigma_F + \sigma_{BM}} && (4.31)\\
F_{eu} =& \frac{1/4\cdot\pi^3 E_{rs}(\phi/2)^3 t}{H^2} && (4.32)
\end{aligned}
$$

where if the slenderness ratio for local buckling $sr_b \leq 0.3$, then $\sigma_{cr} = \sigma_{lim}$ other wise

$$\sigma_{cr} = (1.5 - 0.913\sqrt{sr_b})\sigma_{lim}$$

Equating equation (4.27) and equation (4.32) for E_{rs} and rearranging to make the thickness subject of the function, where $\phi = \dfrac{t}{f_{t/\phi_{out}}}$ was estimated to be

$$t_{base} = f_{t/\phi_{out}} \cdot 2\sqrt{2} \cdot \sqrt[4]{\frac{F_{eu}H^4}{\pi^3\sigma_{eu}\sqrt{3(1-\upsilon^2)}}} \qquad (4.33)$$

The moment acting on the tower base due to the weight of the blades $M_{bld,g}$ at a heel angle β= 10°, is added into the M_{Res}, along with the impact of the bending moment due to the mass of the Floater and generator. The centre of gravity location of the blades was calculated to be 6 m below the midpoint of the tower height along the z -axis due to the co-eccentricity of the DeepWind blade. This is transferred into a fraction of H. The location of the centre of gravity for the entire turbine other than the rotor is assumed to be at the actual location calculated in the DeepWind project for the baseline model.

$$
\begin{aligned}
h_{CG,b} =& H/2 - 0.042\cdot H && (4.34)\\
M_{bld,g} =& m_{bld}\cdot g\cdot h_{CG,b}\cdot\sin(\beta) && (4.35)\\
M_{spr,g} =& (m_{flt}+m_{gen})\cdot g\cdot |h_{CG}|\cdot\sin(\beta) && (4.36)
\end{aligned}
$$

Once all these values have been evaluated, the initial assumption for $f_{t/\phi_{out}}$ is iterated until the following inequality is satisfied

$$\frac{F_{Res}}{\pi\phi t_{base}} + \frac{F_{eu}}{F_e u - F_{Res}}\cdot\frac{M_{Res}+\sum M_g}{0.25\cdot\pi\phi t_{base}} \leq \sigma_{cr} \qquad (4.37)$$

Once equation (4.37) is satisfied, the diameter and thickness distribution is discretised as a taper ratio of the property w.r.t the height of the turbine.

$$\text{Diameter Taper Ratio} = tr_\phi = \frac{\phi_{top}/\phi_{base}}{H} = 0.72343$$

$$\text{Thickness Taper Ratio} = tr_t = \frac{t_{top}/t_{base}}{H} = 0.68493$$

The mass of the tapered tower

$$m_{tower} = \rho_{rs} \sum_{i=h_\circ}^{H} \cdot A_i \cdot \delta h \tag{4.38}$$

The maximum critical stress $\sigma_{cr}$was reduced by a factor of 1.55 to account for the lack of fatigue analysis and as a conservative safety factor as taken from Veritas [71]

Table 4.8: *Tower Sizing results*

Property	**Unit**	**Values**		
Power Rating	[MW]	5	10	15
ϕ_{base}	[m]	6.54	8.63	9.83
ϕ_{top}	[m]	4.73	6.25	7.11
t_{base}	[mm]	23.1	32.1	41.4
t_{top}	[mm]	15.8	22.0	28.3
Mass	[kg]	3.97E+5	10.20E+5	18.41E+5

The model over estimated the mass of the tower by $\approx 12\%$, compared to the DeepWind design. This can be due to the higher aerodynamic thrust from the HAWC2 simulations as compared to the DeepWind results and also the high safety factor used. This lead to thicker tower shells beyond the expected initial guess range $f_{t/\phi_{out}}$ of 0.0067.

4.6.4 Spar Buoy

The process of optimising the mass of the Floater for a static case with increasing turbine scale in a high fidelity tool was deemed to be an inefficient approach. It brought about uncertainties in the design with respect the spars stability during the operational state of the wind turbine. Thus a review of the system dynamics and design considerations was done to reduce the problem to a determinant load case.

System Dynamics

A wind turbine on a spar buoy Floater is a flexible multi-body system operating in a multi-fluid environment. This can result in the structural deformation frequencies from the coupled hydrodynamic and aerodynamic loading to resonate with the free body motion of the structure. Simultaneously, the higher density water induces hydrodynamic damping coefficient in the equation of motion making the problem non-linear. An example of the equation of motion for a FOWT is

$$(\mathbf{M} + \mathbf{A})\,\overline{\ddot{X}} + \mathbf{b}\overline{\dot{X}} + \mathbf{K}\overline{X} = \sum_{i}^{n} \mathbf{F}_i + \overline{m}g \tag{4.39}$$

where

$\mathbf{M} + \mathbf{A}$: Mass matrix and Added mass matrix
$\mathbf{b}$: Damping matrix
$\mathbf{K}$: Stiffness matrix
$\overline{\ddot{X}}$: Acceleration vector
$\overline{\dot{X}}$: Velocities vector
$\overline{X}$: Displacement vector
F_i : 'n' Force/Moment vector contributions
$\overline{mg}$: Gravitational component due to mass vector

The forcing inputs to the system include Wind, Current, Wave loads (inertial and viscous), hydrodynamic forces, along with restoring forces which include hydrostatic force. Even though the problem was simplified by assuming a rigid system, hence disregarding structural damping, the hydrodynamic influences induce damping apart from the added mass and displacement(drift) term. This leads to system behaving non-linearly and requires discretisation into linear sub problems which are resolved through iterative *frequency domain analysis* to include the non-linear effects. The *time domain analysis* of the loads involve direct numerical integration of the differential equations, [12, 13]

Considerations for Design Load Case To solve equation (4.39), general design considerations are reviewed to dimension the spar buoy. The deep structure and low centre of gravity adds a high inertial resistance to wave motion along with a strong restoring moment to heeling/tilting. However it is important to note that the frequency of wave motion does not coincide with the free motion of the Floater to avoid resonance. Hence the shape/size of the Floater depends upon

1. The natural tilting motion period be above the energetic wave period range
2. STT diameter ϕ_{stt} optimisation:
    - ULC: Narrow cross-sectional area to reduce wave loads
    - FLC: Large wave plane intersection to reduce heave frequency below median wave period T_z
3. Longitudinal stiffness to counter compressive stress from weight of turbine & tower
4. Centre of buoyancy, C_b well above mas centre of gravity, C_g to impart large restoring moment to avoid heel angle $\beta > 10°$. Normally, calculating with this case also involves considering the inertial resistance of the mooring system
5. Main spar shell diameter
    - Bending stiffness compliant enough to avoid resonance with median wave, T_z
    - Bending stiffness high enough to prevent buckling at rated U_∞ for maximum, β
6. System motion should not induce damage to turbine/machinery

These are some of the important general design considerations for a spar buoy Floater. For the DeepWind concept, an added specific requirement due its rotating structure was a significant yaw stiffness, especially for the mooring system. The impacts of this design requirement were reflected upon in section 4.5. Also the added effects of Magnus forces due to the spar rotating in current can add a permanent operational tilt (and higher bending loads) based on the current. This entails that the spar bouy sizing is very dependant on the turbine performance and site specific. Thus when scaling the spar-buoy geometrically for larger rated power, then design would need to consider stability and all the 6 consideration presented. For this a refined physical aero-hydro-elastic model coupled with a optimisation loop is required.

Case Selection

The results from the HAWC2 simulation for the complete system, shown in section 4.5, depict a complex interaction between in the system dynamics and the machinery, a possible violation of design consideration 6. The stability constraints in heave, pitch and roll motion of the floater involve a frequency domain analysis, which are considered beyond the scope of this Master Thesis project. Optimisation of the spar shell is not deliverable while the ϕ_{stt} is scaled from existing design with the height of the turbine, section 4.6.2.

The original problem is to determine a realistic, determinant mass to maintain a high inertia with a low C_g so that the hydrostatic force can counteract the weight. The design driver and subsequent scaling criteria is kept as the mass of the rotor and tower. The size of the spar buoy is determined to balance the weight of the turbine and itself, where the diameter and thickness of the structure are initially constraint to scale with the height of the tower. The size of the spar buoy sections are kept in equal proportion as initiated from the DeepWind design. The constraint is to maintain the same proportional distance between C_b and C_g according to the 5MW design.

Mass Estimation

The Floater is sized based on only vertical equilibrium of forces for the immersed systems and the total weight. To establish a vertical equilibrium, the weight forces should balance the buoyancy force through an iterative parametrisation of a constant hull thickness and spar-buoy height. The buoyancy force is based from *Archimedes* law using which the depth of the Floater is derived for the scaled turbines.

$$\Delta F_z = B - W \tag{4.40}$$
$$B = \rho_l g \cdot \nabla \tag{4.41}$$
$$W = g \cdot \sum m_{sys} \tag{4.42}$$

where B is the buoyancy force acting at C_b, ∇ is the displaced water volume, ρ_l is the density of water and m_{sys} are the masses of the turbine systems. Initially, the diameter and thickness of the Floater are scaled with the turbine height as a linear size dependency. This will give us the volume of the spar in terms of H_{fl}. For the different sections: STT height is fixed while the hull and ballast lengths are defined as a ratio to submersed floater $H_{fl,s}$ from the original DeepWind design.

For		K_i
i = 1	h_{stt}	= 17 m
i = 2	$h_{hull,t}$	= 0.096*$H_{fl,s}$
i = 3	$h_{hull,c}$	= 0.646*$H_{fl,s}$
i = 4	$h_{ballast}$	= 0.258*$H_{fl,s}$
i = 5	h_{foot}	= 0.025*$H_{fl,s}$

Where $h_{hull,t}$ symbolises the region in spar-buoy with a variable diameter.

$$V_{fl} = \sum_{i=i}^{5} V_i \tag{4.43}$$

$$\text{for i} = 1,\ 3 \rightarrow 4 \tag{4.44}$$

$$V_i = \pi \frac{\phi_i^2}{4} \cdot K_i H_{fl} \tag{4.45}$$

$$\text{for i} = 2 \tag{4.46}$$

$$V_i = \frac{A_{i,top} + A_{i,base}}{2} \cdot K_i H_{fl} \tag{4.47}$$

$$\therefore \nabla = \sum_{i=2}^{5} A_i \cdot K_i H_{fl} \tag{4.48}$$

The mass of the immersed floater is also derived in the similar manner. The density considered for the hull and STT is the same while the ballast is high density liquid, *olivine* with a density $\rho_{ol} = 2600\ kg.m^{-3}$ as taken from Berthelsen et al. [13]

$$m_{fl,i} = \sum_{i=1}^{5} \rho_i \cdot V_i \tag{4.49}$$

$$m_{ballast} = \rho_o \left(\pi \frac{\phi_4^2}{4} \right) \cdot K_4 H_{fl} \tag{4.50}$$

The area formulation for the hull shell is of a hollow cross sectional area

$$A = \frac{\pi}{4} \left(\phi_i^2 - (\phi_i - t_i)^2 \right)$$

The mass is also determined in terms of the H_{fl}. Based on the understanding that 17 m of the spar buoy or the h_{stt} should be out of water. The draught of the Floater contributes to the buoyancy only, $H_{ft,s}$. Then using equation (4.40), the vertical equilibrium is achieved such that

$$H_{fl,s} = \frac{\Delta F_z}{\rho_i g \sum_{i=2}^{5} A_i} \tag{4.51}$$

Adding all terms for weights and water displacement in terms of H_{fl} will give us the depth of the scaled Floater needed to balance the weight of complete turbine and the Floater itself. However it is important to keep a constraint on the Floater so that the optimisation does not push the C_g to high. Using a balance of forces at the maximum heel angle, the restoring moment can be calculated and the location of C_g kept below the C_b position.

4.6.5 Mooring

The mooring system is an elastic catenary system. The weight of the wires adds stiffness while compliance to system dynamics is provided by slack in the mooring lines. From figure 4.22, the wire is connected with drag anchors at the seabed. The special design consideration for the DeepWind concept due to its rotating structuring proved to be the driving case for the mooring design. As the system is constrained at the base of the Floater, it is necessary for the mooring system to have enough stiffness to resist the yaw moment without ensuing accelerations on the generator. While the stiffness must not be result in resonance due to the periodic load from the turbine.

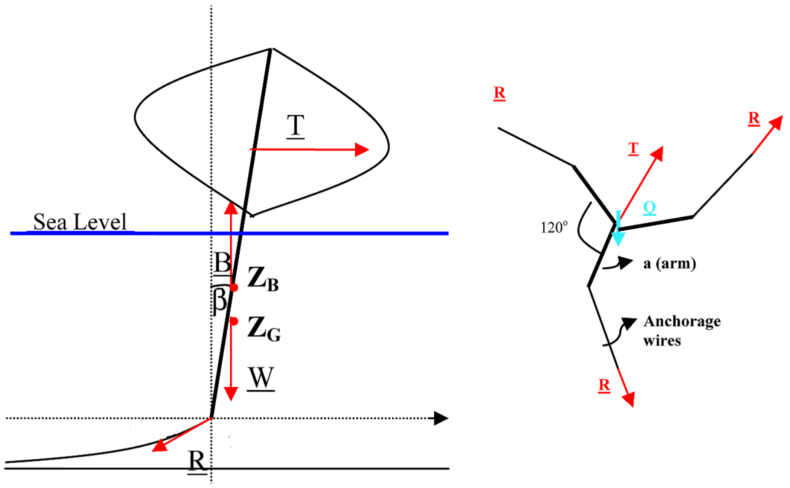

Figure 4.22: Vector Schematic of DeepWind VAWT, *where* $Z_b = C_b$ *and* $Z_g = C_g$ *[60]*

It is assumed that the torque generated at rated wind speed at the rotor plane area is incident on the mooring system without any damping or reduction. Using the results for the torque, the weight of the mooring cables was determined by modelling the wires as a linear elastic catenary's following the schematic representation in figure 4.22 For the mean torque at rated power of 5 MW, the minimum break load(N_{ml}) of 6500 kN is taken. As there is a high torque incident on the mooring system, a initial pretension of 1000 kN is assumed from Berthelsen et al. [13] which is scaled as a ratio of the yaw moment.

$$T_{pre} = Q_{mean}/a = M_z$$

$$T_{pre} = T_{pre} \cdot \frac{M_z}{M_{z,0}}$$

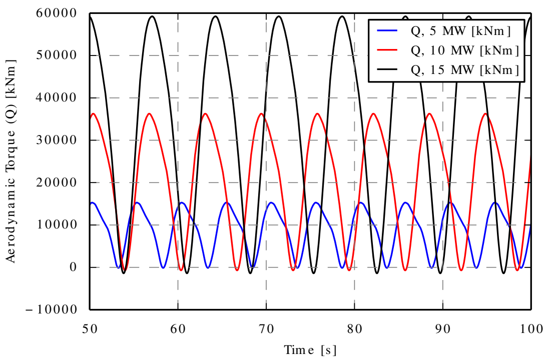

Figure 4.23: Aerodynamic torque for 5, 10 and 15 MW VAWT*'s*

The mean ratio of the mean torques are used to scaled the dimensions of the mooring arms. For the baseline case, the mass of one arm was approx 17 tonnes. The mass of the arm is scaled with the ratio of the yaw moment M_z at the moor arm radius a. The radius of the arm is scaled with the turbine height.

$$\begin{aligned} a &= a_{ref} \cdot \frac{H}{H_{ref}} \\ M_z &= \frac{Q_{mean}}{N_{lines} \cdot a} \\ m_{arm} &= m_{ref} \cdot \left(\frac{M_z}{M_{z,ref}} \right) \end{aligned}$$

Table 4.9: Mooring Sizing results

Property	**Unit**	**Values**		
Power Rating	[MW]	5	10	15
H/H_{ref}	[–]	1.0	1.4	1.7
a	[m]	9.0	12.6	15.3
Q_{mean}	[MNm]	8.83	20.30	34.25
M_z	[MNm]	0.327	0.537	0.746
$M_z/M_{z,ref}$	[–]	1.0	1.64	2.28
Mass	[kg]	1.09E+05	1.79E+05	2.48E+05

The results show that a decreasing non linear behaviour for the mass scaling of the mooring system.

Chapter 5

Cost Formulations

This chapter discusses the realisation of the cost model while emphasizing on the relevant inputs and limitations of its application. The prior chapters entail the necessary calculations and modelling required to implement a cost model. Initially the structure of the cost model is introduced in terms of its components. The assumptions used are presented leading into the CAPEX section which comprises of the turbine design CAPEX (TCC) and wind farm infrastructure CAPEX (BoP). The cost modelling formulations used for the main turbine systems is presented along with parametric functions for the BoP costs against key wind farm factors. Next, for the OPEX section, an introduction on the role of O&M, followed by explanations on the O&M strategy modelled in the OMCE tool. Finally the power production from the wind farm is corrected for uncertainties and errors to develop the mean exceedance probability of AEP.

5.1 Model Structure

To assess the potential economic viability of a wind turbine design, a *Life Cycle Cost* model design is developed to determine the 'Levelised Cost of Energy'. The components of the cost model include estimation of the CAPEX of key systems, OPEX and project revenue based on the energy production through the farm lifetime.

- Capital Expenditure (CAPEX)
  - Turbine Capital costs
  - Balance of Plant costs
- Operational Expenditure (OPEX)
- Annual Energy Production

The cost categories for offshore wind energy have a more equal distribution, as discussed in section 2.1 and figure 2.16. However, the complex interactions between the all the environmental and socio-economic factors with the wind turbine systems and wind farm supply chain makes it essential to compile a complete package tool where all the inputs are read in and translated downstream along the different components of the model. The primary interest was to see the impact of the different systems on the overall cost of energy by dimensioning the system with the loads to get the mass and translate the mass based on the manufacturing process/configuration to cost numbers.

Modelling Assumptions

The confidentiality encompassing cost modelling makes it difficult to access reliable information necessary to validate the model. Cost estimations are complicated due to the number of unquantifiable factors shaping the cost. Hence, data regression of industry data is the common practice used. Parametric cost functions are calibrated to real data to determine the scaling patterns of costs and also mass. These are used to derive system production prices (€/kg) and scaling constants for exponential cost relations. A review of existing cost models is presented in Appendix A.2. Due to the limited publicly available data, this cost model was formulated based upon NREL reports, (Fingerish et al. [37], Griffin [38]) in combination with reports from the DOWEC project, (Bussel et al. [18], B.H.Bulder et al. [15]). Due to the lack of industry data to calibrate estimations, key factors are taken variable in a parameter study to evaluate the impact of any inaccuracies. The turbine capital costs include the Floater and mooring system which in essence replaces the bottom founded support structures counted in with the BoP costs. The following assumptions are considered in establishing the cost estimations for the FO-VAWT.

- A mature production process level (MPL) of 10 years
- System Production Prices (k_{sys}) used are given in appendix B.2 and in the respective sections for the system-wise cost formulations
- Fixed Cost Fraction (FCF) are taken in some cost formulations based on the rational provided in [38]
- The material specific prices are given in table 4.1, adjusted for inflation with average GDP or producer price inflation index, PPI

5.2 CAPEX - Turbine Capital Costs

The turbine capital costs (TCC) are also known as the design costs. The impact of design variations are captured in the mass estimation which is fed in as the prime factor for the cost estimation. The load simulations are explained in chapter 4 and the subsequent geometric estimations in section 4.6

5.2.1 Rotor

For a VAWT, due to the absence of complicated hub assembly and associated machinery for the pitch mechanism, it is unnecessary to model the blades independently. Although a mature manufacturing process of 10 years is assumed for the blade production, it is necessary to take into account the complication of manufacturing a curved blade which is over 200 metres long. For a mature production process, the material and manufacturing are directly proportional to the mass(Griffin [38]). Thus the cost structure can be decomposed into *material, manufacturing* costs while *financial* costs are kept at a fixed at 28% (Fingerish et al. [37]).

$$C_{blade} = \left[\sum_{i=1}^{n}(f_{mat,i}(m_i) \cdot (1 + PPI_{mat,i}) + f_{lab}(m_{blade} \cdot GDP)) \cdot (1 + FCF)\right] \cdot MPL \tag{5.1}$$

$$f_{mat,i}(m_i) = k_{mat,i} \cdot (V_i \cdot \rho_i) \tag{5.2}$$

$$f_{lab}(m_{blade}) = k_{blade} \cdot m_{blade} \cdot LCF \tag{5.3}$$

The first element of the equation captures the cost of the material per section (i) of the blade cross section. Based on the material composition taken, the mass of the section, $m_i = V_i \cdot \rho_i$, is multiplied with k_{mat} which is adjusted to present day value with PPI inflation,[1]. The type of materials n comprising the blade include Fibre Reinforced polymer (either carbon or glass fibre) and Resin (65%), LD Foam (25%) and metal fasteners (10 %), [37]. The The second element of equation (5.1) is an adjustment made to the blade production price to segregate the impact of manufacturing from the cost of the material. The labour cost fraction can be varied to account for added complexity in fabrication for blades with a higher radius of curvature or lower height to diameter ratio. FCF and MPL (table B.2) are percentages dependant number of blades, power rating and year of production experience to account for effects of economies of scales and maturity of the technology, Appendix B.2.

5.2.2 Tower

The load simulations and static modelling for the tower explicitly determine the size and mass of the tower per section. Estimating the tower costs arise from an accurate prediction of the mass. In essence the tower does not comprise of any moving parts or complicated assemblies and the developing an engineering cost model simply arises from multiplying the mass of the structure with a cost per kg. As for the other systems, this cost includes all aspects leading onto towards the fabrication of the tower apart from just the material cost.

To estimate the cost of the tower different formulations for the system production prices of the tower were consulted. As the labour costs for the tower construction were not clearly defined, a direct formulation for cost with mass was used to estimate the cost of the tower. A compilation of different cost per kg for the tower are given

Table 5.1: *System production price for the tower*

Source	k_{sys} (Cost/kg)	Year	Adjusted k_{sys} (Cost/kg)
Zaaijer [75]	$2.04	2002	€1.96
Fingerish et al. [37]	$1.5	2002	€1.43
Bussel et al. [18]	€1.8	2000	€2.34
Blonk [16]	€3.5	2010	€3.81

Based on these results, a final aggregate value of **€3**/kg was selected for the tower.

5.2.3 Floater & Mooring

The Floater implemented in the DeepWind design is considered as the standard “spar buoy” configuration. The spay buoy consists of sections comprised of different materials and functions. For the cost estimations, three different data sources were found and the optimum is selected based on heuristic knowledge. The details about the system production prices are given in Appendix B.2

From Blonk [16], the cost of a simple floating structure was taken as €1.2/kg while for complex floaters, the cost is quoted as €11/kg in M.J.Wolf [54]. These seem adapted to tri-floaters and un-realistic to implement for a floating spar. In the initial cost estimations done by Vita, linear relations of mass were used to scale the cost of the spar similarly to the cost of the tower.

---

[1] Producer Price Index tracked via `http://www.bls.gov/data`

Using the adjusted k_{spar} for the spar tabulated in table B.3, [14], the cost of the spar was divided over the substructures. A general cost for marinisation protection coating was taken from Herman [42] at an adjusted k_{coat} of €$3.63/m^2$

$$C_{spar} = \left[\sum_{i=1}^{n} k_{spar,i} \cdot (V_i \cdot \rho_{mat,i})\right] \cdot MPL \tag{5.4}$$

$$C_{coat} = \left[k_{coat} \cdot \sum_{i=1}^{n}(A_i)\right] \cdot GDP \tag{5.5}$$

$$C_{moor} = k_{moor} \cdot \sum_{j=1}^{n}(m_j) + C_{fixed} \tag{5.6}$$

As there is limited data available on the system production cost for floating structures, the k_{sys} for the different components of the Floater is based on single estimates encompassing both material and manufacturing costs. The MPL factor is kept to encompass the impact of technology production knowledge and is set at 2% assuming similar production maturity as for semi-submersibles in the Oil and Gas Sector. For the mooring system, the materials used is taken as general steel anchored with steel cable wires, [13]. The fixed costs (C_{fixed}) for the mooring installation were taken from the Drijfwind project [54] and are included separately as *Misc* costs in the results (table 6.4) to segregate the more gross approximations as a percentage of the total CAPEX.

5.2.4 Power-Train

The power train used for the DeepWind concept is generically a customised design presented by Leban [49] in her Phd thesis. Several cost relations were found for the generator but as direct drive permanent magnet generators are an emerging technology whose price is dictated by a very volatile market of rare earth materials, the cost estimations given by Leban can be used for a engineering model as the system production price for the active mass in the generator. Using values from table 4.1 and table B.3 for a generic breakdown of the system masses taken to be ≈ 60 % iron, 17 % PM material and 23% copper

$$C_{gen} = \left[\sum_{i=1}^{n}(k_{gen,i} \cdot (m_{i,mat}) \cdot (GDP)\right] \tag{5.7}$$

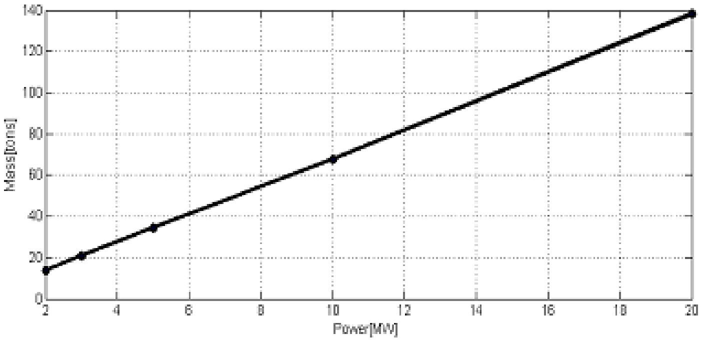

Figure 5.1: *Active Mass scaling trends based on un optimised designs by Leban [49]*

Linear relations for cost and mass of the 6 MW and scaled 20 MW Direct Drive generator design by Leban were made. The costs and mass were scaled against the rotor power and on the recommendation of the author, the optimised generator design and subsequent costs were chosen.

05 MW Total Mass: 56.6 tonnes, Cost = €750k

20 MW Total Mass: 190 tonnes, Cost = €2.8 M

However, many additional elements constituting as the inactive mass, cooling systems and hydraulics are not accounted for. From the comparative study done by Polinder et al. [61] on various 3MW wind turbine generators, the overall generator system cost (apart from the converter, controller and power electronics) was on average ≈ 1.5-2.5 time the active mass/generator cost. Hence, based on this gross assumption, the cost of the remaining structural and support elements were incorporated as miscellaneous costs.

$$C_{misc,gen} = C_{gen} \cdot 2 \tag{5.8}$$

5.2.5 Electronic Systems

The direct drive generator unit is coupled with power electronic systems such as a converter capable of carrying the full power output. The mass of the system is not estimated but the costs of the power electronics and other systems apart from the transformer are taken via a direct relation with the power rating by Fingerish et al. adjusted from 2006 value to present day.

$$C_{pow,elec} = (79 \cdot P_{WT}) \cdot (1 + PPI_{pow,elect}) \tag{5.9}$$

Where the average $PPI_{pow,elect} = 3.07\%$ per year

5.2.6 Additional Hardware

For the selected turbine, the major components contributing into the design have been modelled. The costs of some other remaining subsystems which are an essential component of VAWT's have not been determined and difficult to estimate for other than regression analysis from existing designs.

Mechanical Brake A very important aspect of vertical axis machines is a robust mechanical brake which can be deployed to save the generator in high wind speed occurrences. According to a rough estimates, the mechanical brake on a VAWT is thrice as big as one in a HAWT , especially because it is situated on the LSS. Hence base on the cost estimations done in Fingerish et al. [37] in 2006

$$C_{brake} = 5.968 \cdot (P_{WT}) \cdot (1 + PPI_{brake}) \tag{5.10}$$

where the average $PPI_{brake} = 1.71\%$ per year

Main bearing The main bearing is critical component of the DeepWind design and should be estimated through load estimations. However due to the dynamic instabilities in the HAWC2 model, the bearing is also assumed to be thrice as heavy for a FO-VAWT turbine.

$$m_{bearing} = 0.03 \cdot (0.0133 \cdot R - 0.033) \cdot R^{2.5} \tag{5.11}$$

As the power rating of a VAWT does not necessarily scale with its radius like in the case for a HAWT. It is better to estimate the mass of the bearing based on a loads formulation, [38], involving its diameter and the maximum moment incident on it. The $\phi_{bearing}$ is known from where it is housed below the ballast region of the Floater.

$$m_{bearing} = 0.0152 \cdot \left(\frac{M_{z,max}}{\phi_{bearing}}\right) \cdot (\phi/2)^{1.489} \tag{5.12}$$

$$C_{bearing} = k_{bearing} \cdot (m_{bearing}) \cdot (1 + PPI_{bearing}) \tag{5.13}$$

where the average $PPI_{bearing}$= 5.1% per year, and in 2001 $k_{bearing}$ =$17.6/kg. Thus the inflation adjusted SPP of a bearing$k_{bearing}$ = €21.66/kg

5.3 CAPEX - Balance of Plant Costs

The Balance of Plant costs comprise of all CAPEX related to the Wind farm project and execution with respect to offshore support structures, infrastructure and development other than the rotor-tower assembly costs. This also includes offshore transportation and installation, electrical infrastructure, substation, grid connection, project engineering and decommissioning. However, for this cost model, the cost of support structure such as the Floater and mooring system are not included with BoP.

The offshore wind farm design emulator(OWFDE) tool from Zaaijer [75] (TU Delft) was used to simulate theoretical wind farm scenarios for 5 MW, 10 MW and 15 MW VAWT's. The selected square wind farm configuration shown in figure 5.2 is kept geometrically similar by maintaining the aspect ratio, as the wind farm capacity scales with the product of turbine number in the rows and columns, a compilation is given in table 5.2. Two different turbine spacing are considered, 5 and 7 times the turbine diameter. It is important to note with the OWFDE simulations, no layout optimisation was implemented to minimize LCoE. The reason being that the OWFDE tool works to optimise both the array and electrical efficiency for the BoP CAPEX. It can not be assumed that the wake effects in a VAWT wind farm will be similar to a HAWT wind farm. Hence the calculation method used in OWFDE to determine array efficiency of a wind farm was not applicable. The tool is used to generate initial guesses for establishing scaling patterns while maintaining as much similarity as possible to the operations and maintenance cost modelling assumptions.

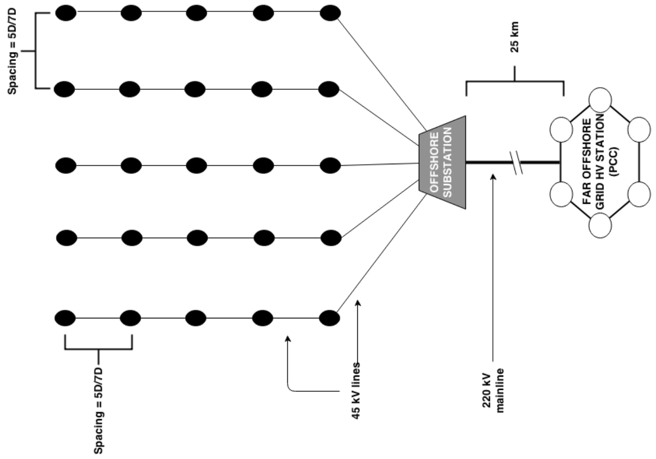

Figure 5.2: *5 x 5 Wind Farm Electrical Infrastructure*

As for most cases before, the lack of data on implemented floating wind farms means that in some cases existing assumptions/formulations for bottom fixed HAWT's are used. These along with the initialisation of the different components of the tool are explained in the succeeding sections.

5.3.1 Electrical Infrastructure

Infield Cable infrastructure CAPEX is taken as a function of conducting and insulating material masses. This is dependant on the dimensions of the cables and the wind turbine spacing. A base representation of the electrical infrastructure shown in figure 5.2. In a normal simulation of the OWFDE tool, an optimisation of the infield gird cable dimensions with respect to the layout of the wind farm and the rated power capacity between two nodes is implemented. As for this case, only the initial guess results are used to estimate all subsequent BoP costs, thus the results from the simulation are rather conservative. As the array layout is not optimised, a fixed turbine spacing was selected at either 5 or 7 times the turbine diameter (ϕ). With the length of the cable and power rating of the cable fixed based upon the size and rated power of the turbine, this only leaves the internal dimensions of the infield cable to be dependant upon the rated power capacity. The rated power capacity of a cable prescribes how much current the cable can carry without overheating. For the initial guess, a conservative infield voltage definition of 45 kV is used to determine the rated current, I_{rated}.

Upon accumulating the results for the simulations (table 5.2) under the stated assumptions, a unified scaling expression was determined for the cost of infield cable infrastructure as a function of wind farm power rating [kW]. The results can be found in appendix C

$$C_{cab,5\phi} = \left[94.82 \cdot (P_{WF,max})^{2.09} - 2.3\text{E}+5\right] \cdot GDP \tag{5.14}$$

$$C_{cab,7\phi} = \left[101.5 \cdot (P_{WF,max})^{2.13}\right] \cdot GDP \tag{5.15}$$

The average annual GDP inflation is taken from table 4.1 as the OWFDE result outputs are in 2012 Euro. The lack of case specific optimisation does add a higher than expected scaling value to equation (5.14) for the overall cable costs. Having two or more voltage rating infield cable's is the common practice, [53].

Export cable length is distance from the wind farm substation to the offshore TSO grid HV station/platform or the point of common coupling(PCC). For this case, the cable length is fixed at 25 km with a voltage rating of 220 kV. The current at rated power, I_{rated} determines the size of the conducting core and insulation based upon heat dissipation, power losses and surrounding environment constraints. However for the initial guess, the cross sectional area of the cable conducting material is defined based upon a regression fit of different ABB cable ratings and corresponding sizes done by Zaaijer [75]. The corresponding materials in the cable are determined as a function of conductor cross sectional area and the infield voltage. By reducing the number of variables and keeping the case definition streamlined by con straining turbine spacing and the distance to the offshore TSO platform, the export cable costs becomes a function of the turbine rated power and number of turbines in the wind farm.

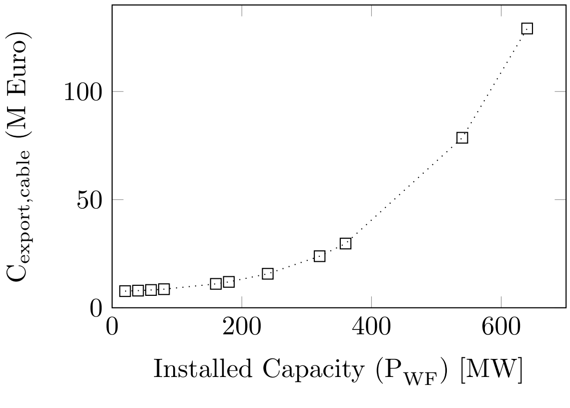

Figure 5.3: *Cost of Export cable against installed wind farm capacity*

Electrical Efficiency

The electrical efficiency of the infrastructure can be subdivided based on two types of losses. Electrical losses due to the internal grid and transmission losses from the wind farm till the PCC.

The electrical losses in the cable dependant. The initial guess for the electrical efficiency for each of the wind farms varies per WF size. However an average value was derived by considering all variations at $\eta_{elec} = 0.982$. The complete tabulation of the results is given in Appendix C.

5.3.2 Offshore Structures

Site Assessment Equipment such as a meteorological measurement tower is taken at a fixed price[2]. Although it is deemed unnecessary at the location as the existence of an offshore grid platform means that there are existing wind farm installations nearby with sufficient wind resource data.

Operations Control as presumed for a far offshore wind farm during the model initialisation in section 4.2, is from a "mother-ship". It will serve as the point of base operations for the O & M crews and day to day procedures. Any onshore premises are assumed to be located at the TSO platform if necessary, otherwise the mother-ship serves as the base of operations. This effectively removes BoP CAPEX linked to operation control room and site assessment.

Floating Substation Similar to the wind turbine, the wind farm's substation also needs to be afloat in the deep water. Floating semi submersible platforms are an existing concept especially in the Offshore Oil & Gas industry. Typical substations are have a topside payload from 500 - 2000 tonnes [53], however floating semi-submersibles are costly as compared to the average bottom founder structures. This is mainly due to the large displacement needed to provide sufficient vertical stability and due to the installation large complex mooring systems, Butterfield et al. [19], Cermelli et al. [21]. As a conservative assumption, the costs for the offshore substation from the OWFDE simulations was multiplied by a factor of 1.3 to account for the higher costs of a semi-submersible platforms.

Table 5.2: *Different WF sizes based on number of turbine and turbine capacity*

Array Size	Power rating (MW)		
	5	10	15
2 x 2	20	40	60
3 x 3	45	90	135
4 x 4	80	160	240
5 x 5	125	250	375
6 x 6	180	360	540
7 x 7	245	490	735
8 x 8	320	640	960

5.3.3 Transport and Installation

For the BoP model, onshore transport is neglected. It is assumed that the port staging site serves as the location for fabrication, assembly and offshore transport of the turbines' subsystems. This serves to eliminate the prediction of onshore transport costs and any affiliated constraints. In summary the major subsystems connected to offshore installation costs include

(a) Electrical Infrastructure :- apart from the substation

---

[2] Zaaijer [75] takes $C_{meteo} = 2.12$ M€, & $C_{onshore} = 1.59$ M€

(b) Foundation installation :- mainly involves anchoring the mooring system for FOWT's
(c) Meteorological equipment - neglected
(d) offshore works: transportation and installation of Turbine
(e) Harbour use :- Assume port staging site is at the coast.

The electrical infrastructure installation is dependant on the layout of the WF. As no optimisation is implemented and the WF shape is constraint by an equal aspect ratio while the size is limited with the prescribed 5ϕ or 7ϕ. The electrical infrastructure installation can be kept linearly proportional to the length of the cable, Zaaijer [75]. The formulation implemented in OWFDE tool for the cable costs are

$$C_{cab,ins} = (a_{cab,inf} \cdot L_{inf}) + (a_{cab,exp} \cdot L_{exp}) + C_{fixed} \tag{5.16}$$

Where:

$a_{cab,inf}$	= Infield Cable cost per length	138.3[€/m]
$a_{cab,exp}$	= Export Cable cost per length	145.4 [€/m]
C_{fixed}	= fixed cable costs	1.232 M[€]
L_i	= Cable length of 'i' component	[m]

The length of the transmission cable is fixed. For each turbine rating, the length of the internal cable scales with varying linear gradient for different wind turbine power ratings P_T, table 5.3.

$$L_{inf} = M(P_{WF,max}) + K \tag{5.17}$$

Turbine spacing = 5ϕ		
P_T [MW]	M	K
5	153.5	-1162
10	105.3	-1683
15	84.3	-2069
Turbine spacing = 7ϕ		
P_T [MW]	M	K
5	214.2	-1716
10	147.1	-2441
15	117.8	-2980

Table 5.3: *Linear scaling constants for infield cable length with WF power with turbine spacing*

To install floating turbines far offshore, tugging a upright Floater is not conceived to be a pratical solution in terms of time consumption. A proposed method would be use large vessels which can carry the complete spar buoy on its deck or tug a platform carrying them. A tanker would be needed with the ballast fluid to weigh down the spar buoy once it is offloaded. A possible problem would be coordinating the extraction of ballast liquid once the rotor-tower is place on top while engaging the anchoring vessels to harness the mooring system and the electrical umbilical cord.

In general it is perceived that the installation of floating strucures can be faster with less resource intensive machinery needed per turbine, [19] as compared to normal bottom founded monopile foundation installation. The lack scour protection and "hammer driving" cranes gives a presumed financial advantage to FOWT's . The exact process and its cost is difficult to quantify. Hence as an added compensation, the cost of installation is kept similar to how the OWFDE tool estimates turbine installation.

5.3.4 Project Development

The estimations for offshore project management and engineering costs are kept similar to existing cost measurements based on existing WF's. These estimations are taken from Fingerish et al. [37] and Zaaijer [75]. Offshore project engineering costs comprise of permits, engineering plans and site assessment. While project management costs sum towards the organisation of labour and contractors for the project execution.

$$C_{mgmt} = 0.03 \cdot (TCC + (BOP - C_{decom})) \tag{5.18}$$

$$C_{engg} = [37 \cdot (P_{WF,max})] \tag{5.19}$$

C_{engg} has to be adjusted for currency exchange rate from USD to Euro and is a function to wind farm capacity while C_{mgmt} is assumed to a fraction of total CAPEX.

5.3.5 Decommissioning

Decommissioning of offshore installations is a low-tech routine as suggested by M.J. Kaiser [53], however the higher number of structures encompasses a high level of activity and large overall cost. There can be different methodologies used for the removal and transport of the wind turbines back to shore. As the installation for a floating turbine does not encompass resource intensive processes such as pile driving, similarly the removal should also not encompass any major operation other than a high vessel activity. From the models proposed by M.J. Kaiser [53]

Self-Transport: Removal and transport vessel is the same

Barge Model: Removal and transport vessels are seperate

Felling: Turbine is cut off from foundation and transported back

According to Zaaijer [75], the cost of decommissioning a wind farm is estimated to be around 80-90 % of the cost incurred during installation. Thus, a reasonable estimation of the installation costs for a floating WT will coincide with a linearly proportional decommissioning approximation. Considering a Barge model removal method, a possible removal process for the mooring system would be based on the depth of the ocean floor from where the wires are cut. The other heavy sub-sea modules (power train, transformer) can be removed and lifted via a heavy lift vessel. The Floater can be lifted by extracting the ballast fluid and let the hydrostatic force lift it out of the water, mount it on floating platform and tow it back to port.

As the installation costs for the turbines are retained from the OWFDE tool, decommissioning costs are taken to be 80 % of the installation costs for the turbines. The electrical removal costs are linearly dependent on the length of the cables in OWFDE, while site clearance is dependent on the number of turbines. The execution of the decommissioning project is presumed to cost 3 % of the total decommissioning costs.

$$C_{decom,elect} = 53 \cdot L_{inf,cab} + 49 \cdot L_{exp,cab} \tag{5.20}$$

$$C_{decom,site} = 12500 \cdot N_{wt} \tag{5.21}$$

$$C_{decom,mgmt} = 0.03 \sum C_{decom} \tag{5.22}$$

Where the infield cable length is given by equation (5.17)

5.4 OPEX - Operations & Maintenance Costs

This section entails an Operation and Maintenance cost evaluation for a far offshore wind farm with specific adaptations to FO-VAWT. To model the operational and maintenance effort, ECN's *O&M Cost Estimator* (OMCE) tool was used to study the impact on OPEX from the variation of key assumptions. The modelling methodology is explained along with key presumptions made while defining the different types of maintenance, the repair strategies, fixed and running costs, infrastructure required and approximations for the wind turbine systems reliability. A parametric study of key assumptions is given in the results section 6.3

5.4.1 Introduction

Accessibility and reliability are two key words when discussing offshore wind farms from an operators point of view. It is common understanding that far offshore wind farms give access to better wind resource and more freedom in layout optimisation to maximise AEP. However, being unable to maintain a smoothly operating wind farm, can significantly impact the profitability and LCoE for offshore wind farm. The infrastructure requirements, specialised equipment and weather related constraints scale the OPEX at approximately 20 - 30% of the LCoE [24, 70]. These key words factor in to determine the availability of the turbines in the wind farm. As a strong indication of the importance for a comprehensive O&M model, a qualitative assessment presented in the Opti-OWECS report in figure 5.4 presents an example of how weather and a high systems failure rate can cut availability down to approximately half.

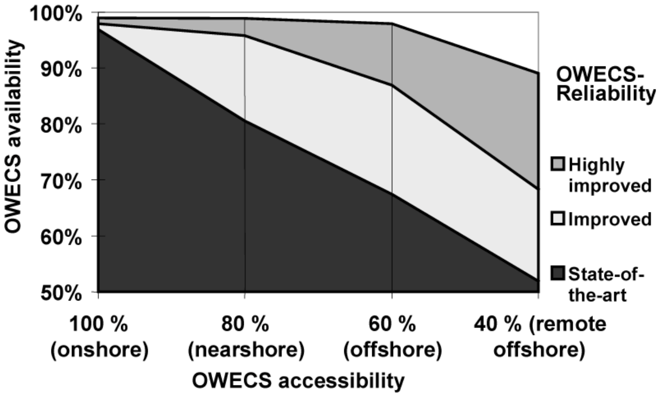

Figure 5.4: *Qualitative impact of accessibility on system availability, [45]*

O&M costs affect the LCoE both through the direct expenditure from accessing and repairing the wind turbine as well as energy costs incurred from the downtime of the turbine. This can be explained if a situation is considered where poor weather conditions coupled with daily working hours and consistent failures can lead to a simple manual restart operations from the turbine to be delayed for days. Thus, in retrospect of operational data, an approximate yearly OPEX constituting to be 1% of the total CAPEX , can translate into an energy cost of 11 % over the course of a wind farm's life cycle, [24].

5.4.2 OMCE Concept

The OMCE package provided by ECN summarises a six year long development programme driven to optimise offshore OPEX through monitoring the actual O&M effort and controlling future OPEX.

It involves the processing of operational data for prediction of future costs and improved strategies. To handle these aspects, the package can be divided into two parts,

- 'OMCE Building Blocks' processing specific raw data sets to obtain useful trends for either cost prediction or monitoring
- 'OMCE-Calculator' which implements information from the building blocks towards the assessment of the expected O&M effort and associated costs for the coming periods

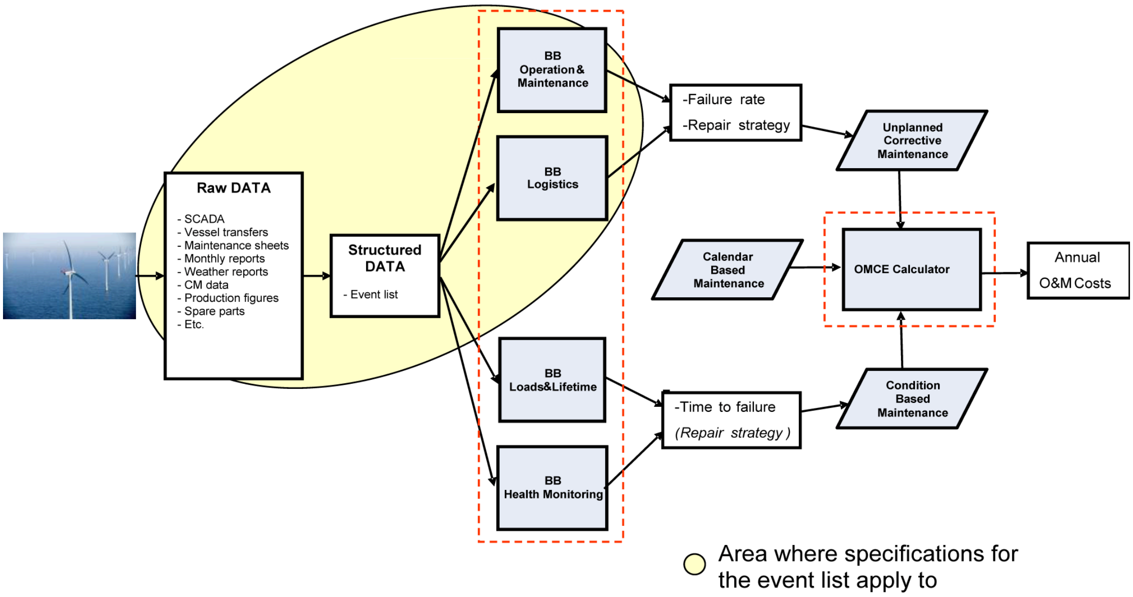
Raw DATA
- SCADA
- Vessel transfers
- Maintenance sheets
- Monthly reports
- Weather reports
- CM data
- Production figures
- Spare parts
- Etc.
Structured DATA
- Event list
BB Operation & Maintenance
BB Logistics
BB Loads&Lifetime
BB Health Monitoring
-Failure rate
-Repair strategy
-Time to failure
(Repair strategy)
Unplanned Corrective Maintenance
Calendar Based Maintenance
Condition Based Maintenance
OMCE Calculator
Annual O&M Costs
Area where specifications for the event list apply to

Figure 5.5: OMCE *package depicting complete chain from data processing, event definition, database update and cost prediction, [28]*

The work flow in figure 5.5 defines an iterative process where data from existing wind farms is fed into the tool to better predict the maintenance requirements and costs of the future. The OMCE-Calculator is based on a Monte-Carlo approach, where system failures are simulated in a time domain analysis using the Poisson process, accounting for the random statistical behaviour of the weather and systems failure probability to produce short term cost predictions[3]. The structure of the tool is focused around a sound understanding of the behaviour of the wind turbine and its systems. This allows for it to be used as an operational tool to predict future events or as a design tool for hypothetical cases. A detailed input about the wind farm setup and its systems is required to simulate the OPEX effectively. The O&M strategy for this report is 'built-upon' by adapting the existing default wind farm model for conventional HAWTs to the DeepWind concept representing a FO-VAWT wind farm. When establishing the maintenance model each of the following factors had to be considered due to their impact on O&M costs.

1. Geographic Location
2. System reliability and failure rates
3. Availability and constraints of vessels required
4. Supply Chain maturity

For (1), geographic location is synonymous for the site conditions, distance from the shore and distance to Grid/PCC. These shape the infrastructure necessary to access the wind farm for maintenance which impacts the accessibility for the support infrastructure and subsequent availability of the turbines. The site data also feeds in to calculate the AEP of the WF and corresponding revenue/energy losses for the time period when the turbine(s) is unavailable. As the OMCE tool involves a time domain based analysis, it is difficult to create a model setup where distance can be related directly to time. This is an assumption in the model where the access time is independent of site conditions, it is fixed based on the average speed of the vessel and the opening of a *minimum repair window*. For (2), this is a prevailing limitation in VAWT analysis. Design's have not been implemented to such a mature production level that any reliable information on failure rates can be attained. Due to this limitation, knowledge based engineering and consultations were used to develop a feasible reliability of the wind turbine and Balance of Plant system's, especially with a focus towards Floating concepts. Aspect (3) and (4) are assumed constant to a favourable site of conventional wind turbines with good resources and reliable contractors.

---

[3] The functional details of the OMCE tool are confidential

5.4.3 Operations and Maintenance Modelling

Wind farm O&M strategy is designed to tackle the two main constitutes of the wind farm, the *wind turbine systems* with its sub-assemblies and the *Balance of Plant*, consisting of all remaining systems in the wind farm. Even though the O&M strategy for both systems is executed similarly, the repair processes are different. The impacts on cost of energy of the downtime for a wind turbine system failure is less and more localised, but a BoP related can affect a whole row or portion of the wind farm, significantly reducing the availability of the wind farm and increasing the cost of energy.

The operational strategies are generalised based on the stimuli for the maintenance. This can be either reactive: *corrective maintenance* or pre-emptive: *preventive maintenance*. Corrective maintenance is necessary to repair or replace a component or system which has failed or is not fulfilling its function properly. While preventive maintenance is performed in order to mitigate the possibility of a component or system failing in the future. In a wind farm, the system is operated under a combination of preventive and corrective maintenance procedures. Depending on the detail of the model, each subsystem of the wind farm can be modelled to be maintained both as prescribed by the manufacturer and as observed from monitoring. With respect to this, the maintenance strategies can be divided into three distinct categories.

- *Calendar based maintenance*, based on a fixed yearly period where minor and semi major work is done on the wind turbine or wind farm.
- *Condition based maintenance*, based on the observed condition of the system derived from monitoring or the expected time to failure known from design
- *Unplanned Corrective maintenance* Necessary after an unexpected failure occurs. Each component has a prescribed type of failure mode and an annual failure rate. Refer to appendix D.2 for more information

For Calendar based maintenance, a yearly preventive procedure is defined or a more intensive 5/10 year major overhaul. It follows all the steps highlighted above but is focused towards preventive maintenance and keeping the turbine running smooth. However, for Unplanned Corrective Maintenance, each system in the wind turbine, its components can suffer a random failure. The annual failure rate of the system, denoted by Λ_{sys} (equation (5.24)) has to be specified. Based on data processed through the OMCE Building Blocks, a detailed understanding exists on the types of failures that each system can incur and the distribution of the types of failures as a percentage of the total failure rate of the system. For each system, a Fault type Class (FTC) is specified for each sub-assemblies. Within an FTC, the kind of maintenance or repair that has to be carried depends on the subsystem which failed, the probability of the failure and the repair process needed to fix it, all of which are defined. The following list represents a breakdown for a FTC:

- Maintenance type:
  1. Preventive Maintenance
     - Calender based
     - Condition based
  2. Corrective Maintenance
- The Repair Class, (refer to Section 5.4.6)
  - Phases of the Repair strategy: inspection, repair, replacement
  - The Equipment needed, labour deployment and logistic constraints of each phase
- The Spare Control Strategy (refer to Section 5.4.6) adopted depends on the system and type of Repair Class

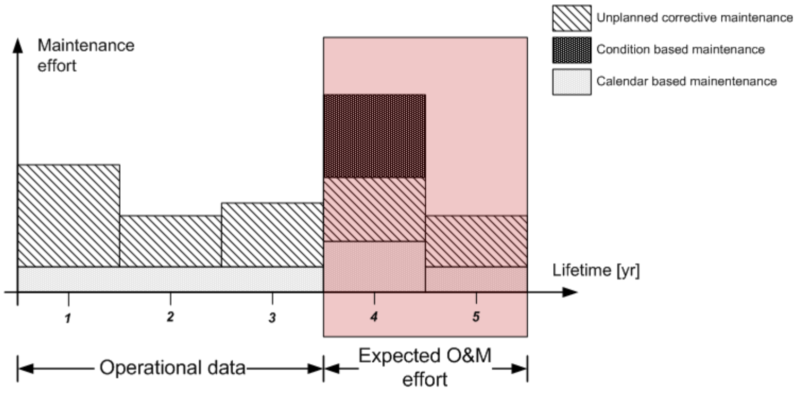

Figure 5.6: *Schematic overview of the maintenance effort over the first operational years of a wind farm and the expected maintenance effort in the near future period, [29]*

As the implementation of the OMCE Calculator is for a design case in this Master Thesis project, it is safe to assume no differentiation between calendar based and condition based maintenance, especially as no operational data is being used to monitor and predict the future O&M effort. An example of a typical maintenance simulation for the initial three years of an operational wind farm is given in figure 5.6. The number of FTC's per system are variable. The annual failure rates of components Λ_{comp} the systems were derived from analysing wind turbine reliability studies such as ReliaWind Project, [47, 73] and the heuristic knowledge gained through discussing with de Pieterman et al. [28]. A reliability study can be found in Appendix D.2. Systems which were not existent in a VAWT were excluded and the total failure rate of the wind turbine comprise of the remainder. The total number of failure that the entire wind turbine Λ_{WT}, including the balance of plant, suffers for a year are between 4 and 6 [28]. These do not account for remote resets due to operational conditions which are also modelled to capture the downtime. The failure rate ($\Lambda_{comp,x}$) of a component x is calculated as the sum of the number of failure types (n_k)over the lifetime of the wind farm (T) minus the downtime durations per failure, D_k . These add up to the combined system failure rate Λ_{sys} which add into the entire wind turbine failure rate Λ_{WT}. This determines is the reliability of the wind turbine.

$$\Lambda_{comp} = \frac{\sum_k^K n_k}{T - \sum_k^K D_k} \tag{5.23}$$

$$\Lambda_{sys} = \sum_x^X \Lambda_{comp,x} \tag{5.24}$$

$$\Lambda_{WT} = \sum(\Lambda_{sys,i}, \ldots \Lambda_{sys,N}) \tag{5.25}$$

5.4.4 FOWT O&M Initialisation

The strategy defined for the maintenance and operational control of Fo-Vawt's is denoted by FOWT in the respective OPEX sections. The precision of the OMCE tool can be varied for different time resolutions, allowing for the interaction of the site conditions and the time/cost of the maintenance teams/vessels to be resolved till an accuracy of 1 min. However, such high precision modelling is only useful if the site data used is also sampled at similar time intervals. It was observed that the difference in the results for single digit resolutions was less than 5 % but it led to much larger surge in computational effort as shown in figure 5.7b. Thus for this project a resolution of 20 min was chosen to be an optimum trade-off between

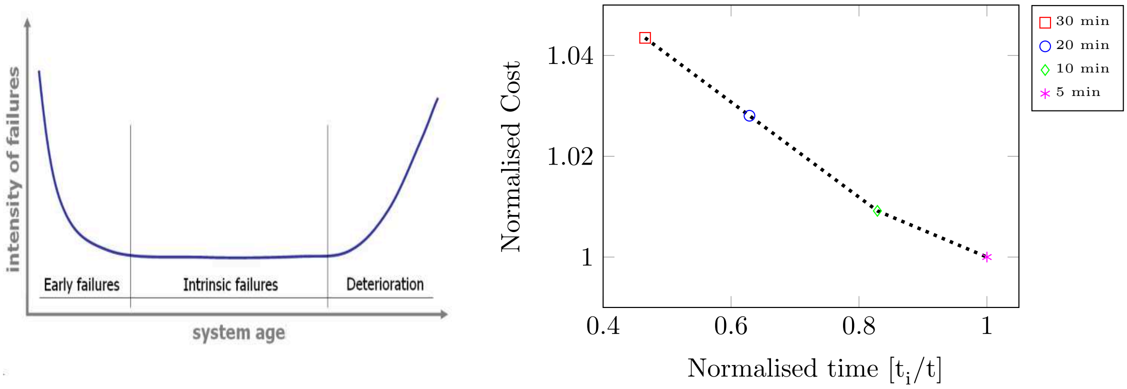

(a) Age wise system failure intensity [73]

(b) Computational expense vs accuracy

Figure 5.7: *(a)Bathtub curve modelling the failure intensity for a repairable system against its age; (b) Impact of increased resolution in OMCE on computational effort and accuracy [45]*

The OMCE tool is setup to function with average failure rates and mean conditions. The reliability of a systems do not account for the non linear behaviour in the early 'burn-in' and later 'wear-out' stages of a mechanical system as depicted in figure 5.7a's 'Bathtub' curve . Thus the O&M simulations were modelled for failures from the 3rd year of the wind farm operation uptil the 8th year. This 5 year simulation period is repetitively superimposed for the complete 20 yr life cycle of the Fo-Vawt wind farm to determine the total OPEX.

Power Capacity The scaling of the Fo-Vawt's was taken at discrete steps of 5 MW, 10 and 15 MW. To study the impact of increasing wind farm rated power on OPEX , the layout criteria used in the BoP CAPEX in section 5.3 was followed for the O&M setup as well. In table 5.2 no common power capacity exists where an equidistant square WF layout for all rated power can be formed. A relaxation is made and the closet wind farm capacities selected are 245 and 490 MW for 5,10 and 15 MW Vawt's

Logistics The "Minimum Repair Window" is the least time period required to perform the simplest maintenance task or even a phase of the total maintenance job. Resources affecting this window are wind speed and wave height being within the operational regime of the vessel/equipment and vessel availability. Travel time to and from the turbine is included in this period. The "work clock" for the technicians is a 12 hr day.

Geographic Inputs The explanation of the site location was introduced in section 4.2.1. The K13 site in the North Sea is 120 km from the nearest port. In this model, the site of operation for the maintenance teams is presumed to be from a "Mother Vessel" anchored 15 km from the wind farm. However, the wind farm site is still 120 km offshore to nearest port and staging harbour from where large spare parts/specialised vessels can be deployed. The distance from shore in essence is translated as the time taken for large equipment and spare parts to be transported to the site.

Costs

To determine OPEX , it is essential to first have reliable information on the prices of the spare parts, the charge for the equipment and vessels as well as good estimations for the labour. All these aspects are addressed based on information from ECN from the OMCE default model or through discussion. The scaling relations used are highlighted in the following text

Spare parts From section 5.2 the TCC came out to be €5.203 Million for GFRP blades without considering marinisation costs, in-active structural generator mass and Floater related costs, apart from the mooring system. The reason being as only the rotor-nacelle assembly, tower and mooring undergo maintenance requiring need spare parts. The spare parts were broken into categories defined from de Pieterman et al. [28] based on the mass and turbine cost structure. The turbine cost structure for the 5MW VAWT were based on CAPEX model in section 5.2 and correlated to the decomposition of the turbine capital cost given in tableB.1. Insight about the spare parts control strategy and cost structure is given in section 5.4.6 with the category definition for the base 5MW in table 5.6.

$$\frac{C_{spare}}{C_{spare,ref}} = \left(\frac{H_1}{H_{ref}}\right)^{1.57} \tag{5.26}$$

Where C_{spare} is the cost of the specific spare parts of the scaled turbine. For the cost scaling relations from Ashuri [8] are used. A size dependency of 1.57 is considered to the characteristic dimension, 'D' for the increase of CAPEX for the turbine spares. D is taken as the rotor height, H.

Fixed Costs The fixed costs in the O&M module comprise of mainly the labour costs to operate and maintain the wind farm. The labour costs are based on the number of turbines in the wind farm. The number of technicians per turbine is based on practical engineering knowledge. In the default O&M model 36 technicians manage 130 machines, meaning approximately 3 turbines per technician [28]. However working bi-weekly shifts, twice the number of technicians are needed.The cost scaling is a function of the number of technicians required per turbine and the number of turbines based on $P_{WF,rated}$ while adhering to the lower limit constraint. The ratio of technicians needed per turbine is also scaled with turbine height.

$$\frac{tech_{WT}}{tech_{WT,ref}} = \left(\frac{H}{H_{ref}}\right) \tag{5.27}$$

Where the ratio of (combined) technicians needed per turbine from the reference case is $tech_{WT,ref}=$ 0.55, while is C_{tech} are the cost per technician per year. The total number of turbines is $\propto P_{WF,rated}/P_{WT,rated}$, however $tech_{WT,min} \geq 24$ so that at least two workboats can be manned at any given time.

$$C_{fixed,1} = N_{WT} \cdot (tech_{WT,1} \cdot C_{tech}) \tag{5.28}$$

Equipment Costs Similarly, to account for larger equipment required for larger scaled wind turbines and parts, the resources required were also scaled in terms of costs. However, the increase in equipment rental/daily rates was also based on a linear size dependency with the turbine height. The base equipment/vessel costs were from obtained from ECN and upscaling relations were applied to the Operations Control and Installation vessels only.

$$\frac{C_{equip}}{C_{equip,ref}} = \left(\frac{H}{H_{ref}}\right) \tag{5.29}$$

A summary of the above factors and the general wind farm specifications taken in section 4.2 are given in table 5.4. The factors are given as a range or discrete steps, indicate the variables for the parametric study, which is discussed in section 6.3.

Table 5.4: *General Specifications for the* OMCE *tool for a* FO-VAWT

Specification	**Unit**	**Value**
Wind Farm Capacity	[MW]	245,490
Wind Turbine Rating	[MW]	5, 10, 15
Wind Profile	[-]	Power, 0.1
Electricity Tariff	[€/kWh]	0.13
Labour Costs	[M€]	4.2 - 8.6
Minimum Repair Window	[hr]	2
Work Clock	[hrs]	0700 - 1900
Maintenance Periods	[−]	01-04 till 01-09

The wind farm efficiency is the combination of the wake losses, technical losses and electrical losses incurred by a wind farm other than the downtime due turbine non availability.

Assumptions

To reduce error of assumption, the model is adapted from existing ”Default” model taken from ECN. The distance from shore denotes that all turbines are around 120 km from the closest port.

1. VAWT production and supply chain is at the same MPL as modern day HAWT’s
2. The operational strategies and expertise are cross applicable from HAWT to VAWT’s
3. The TSO “can” be responsible for maintaining the wind farm substation in terms of costs as well.
4. The pitch and roll motion of the FO-VAWT is minimal when off-line and allows for easy access by boat
5. The underwater Power-train and mooring system are modular systems which can be removed and replaced independently of each other
6. Most minor and medium underwater repairs can be performed via an underwater ROV
7. The top and bottom of the FO-VAWT is accessible by elevators and parts ($<$ 2 Metric Ton) can be transported in these elevators which are loaded by a service crane in the surface transition tube platform.

5.4.5 Equipment

The vessel and equipment used to perform the maintenance are based on standard practice and compiled in table 5.5. The basis for this assumption was made after consultation with the engineers with the *HyWind* project, the current testing prototype for FO-HAWT's. It was attained from Eugster [34] from StatOil[4] that the maintenance protocol for floating structures is not too different from bottom fixed offshore structures in terms of regular small maintenance Eugster [34]. However, there is a need for specialised vessels to operate around a deep sea wind farm. The problems arise for "condition based" quarter life overhaul maintenance and for larger scale "unplanned corrective maintenance". However in this study, no hindrance to the execution of larger maintenance procedure is assumed. The vessel resources utilised are based on standard O&M fleets used offshore given in, [28, 53].

- **Work Boat**: Lease costs based from standard rates used by de Pieterman et al. for *WindCat* workboats[5]. The cost is increased by 50% to account for specialised ROV equipment and diving support. The range of crewmen is set from 6 -12, which also forms the lower limit constraint for a minimum of 24 technician employed in bi-weekly shifts so that two boats (6 each) are always ready for deployment.
- **Operation Controls - Mothership**: Functions as the base of operations, accommodation for max 36 technicians and a spare parts buffer storage. Lease costs for 'SeaEnergy' vessels[6] with an 'Ampelmann' system taken from [28] . A 35% increase in annual costs is added for a submarine unit or large load bearing ROV adaptation needed for external parts replacements.

Table 5.5: *Specification of support vessels required for 5MW* FO-VAWT *farm*

Vessel	Response time	Availability	Weather Limits	Costs [€]
WorkBoat	*Unchanged*	2 boats	*Unchanged*	500000/boat fuel = 200/hr
Helicopter		*Unchanged*		
Jack Up		*Removed*		
Diving Support		*Removed*		
Cable Laying		*Unchanged*		
Operation Controls	*unchanged*	1 boat	*Unchanged*	14000000/yr
Dynamic Position Vessel		*Similar to Jack Up Vessel*		187500/day 525000=mobilise

In table 5.5, the operational limitations of the equipment are assumed similar for all adapted vessels. The major adaptation, and subsequently cost, are for the Workboat, the 'Operations Control Mother-ship and the Dynamic Position Vessel. As the water depth > 100 m, a Jack-up vessel for major repairs is not applicable, thus a " Dynamic Positioning Vessel" is needed which is assumed to be 30% more expensive than a Jack-up.

5.4.6 Fault Type Class

This section basically addresses establishing the supply chain for the maintenance. Fault type classes are defined for the corrective procedure for failed components or preventive measures for a planned procedure as shown in figure 5.8. Depending on the system, many types of failures can occur which are a percentage f_{comp} of the total failure rate, Λ_{sys} or the number of repairs to be executed in the maintenance period .For both types of maintenance, the FTC is based on the component that failed or needs to be replaced before failure. Each FTC points to a level of failure/damage which correlates to a size of the component with a respective repair process along with a spare control strategy. Both the repair process and spare strategy is based on the size, cost and availability of the corresponding parts, supplementary resources and consumables needed to perform the maintenance.

---

[4] StatOil is the operating partner in the HyWind demonstration project

[5] http://www.windcatworkboats.com/

[6] http://www.seaenergy-plc.com/

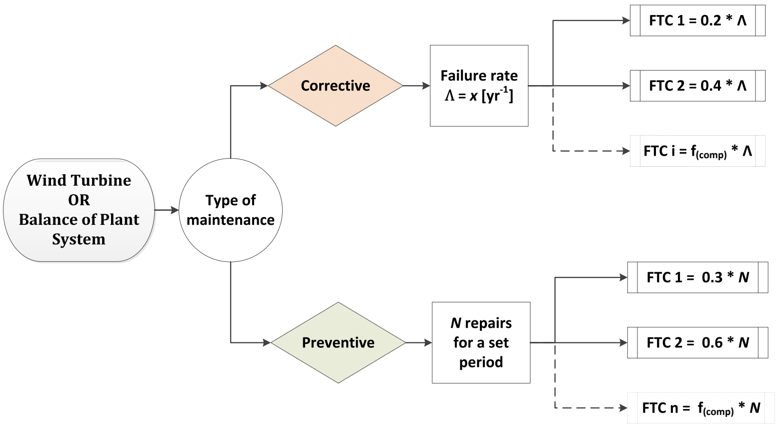

Figure 5.8: *Fault type class definition based on type of maintenance*

FTC: Repair Class

Different failure/maintenance categories are modelled as *Repair Classes*. These denote for a specific type of failure or maintenance work, a sequence of phases with the corresponding amount of work, required equipment and time needed to organise for each phase. For the larger parts, the strategies are kept similar to the ones used in the default model by de Pieterman et al. [28] but for the distinct Fo-Vawt systems, new repair classes were created. The changes and their corresponding effects on the default repair classes are given in Appendix D.

FTC: Spare Control Strategies

Spare Control Strategies are the categorisation of the parts required with respect to a FTC. They are grouped based upon the turbine capital cost and according to the mass distribution for a typical wind turbine system. For each spare part class, there can be a corresponding cost, size and stock delay for the part required. It is assumed that the supply chain is mature enough to provide parts within the same time interval as for a Hawt farm located at the same location.

5.4.7 Failure Rates

Failure rate or the mean time between failures is the average number of times a component fails in a year. However, the mean time between failure(MTBF) assumes that there is no downtime in between. Adding a downtime which is the time taken to repair (TTR), the mean time between failure (MTBF) becomes dependant on TTR. As this can not be known before the simulation, a new parameter is defined, mean time to failure (MTTF). Initially the MTTF is assumed equal to

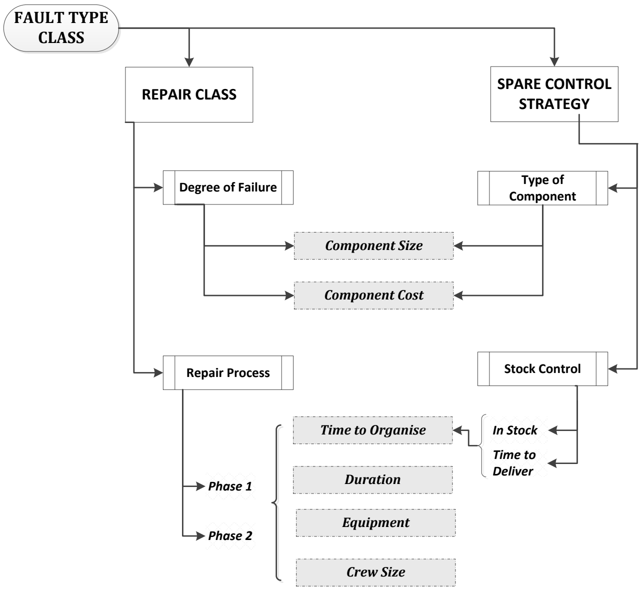
FAULT TYPE CLASS
REPAIR CLASS
SPARE CONTROL STRATEGY
Degree of Failure
Type of Component
Component Size
Component Cost
Repair Process
Stock Control
Time to Organise
In Stock
Time to Deliver
Duration
Phase 1
Equipment
Phase 2
Crew Size

Figure 5.9: *Processes structure for a corrective maintenance Fault type class*

Table 5.6: *Spare parts categorisation for 5 MW* Fo-Vawt *used in* omce

Classification	Logistic Time [days]	Cost [€]	Category
Consumables	0	< 500	1
WT small parts	0	5000 - 50000	8
WT large parts	7-14	100000 - 500000	3
BoP electrical - power	30	250000	1
BoP electrical - cable	10	350000	1

the failure rate per year(Λ) and input in to the omce tool which estimates the TTR and corrects the MTBF.

$$MTBF = TTR + MTTF \tag{5.30}$$

$$\therefore MTBF = f(TTR) \tag{5.31}$$

$$\text{Assume, } TTR \rightarrow 0 \tag{5.32}$$

$$MTBF \approx MTTF \tag{5.33}$$

According to the VTT study cited in [28, 67], the average downtime for an onshore turbine is estimated to be 170 hrs/year. As the downtime is dependant on all the factors affecting O&M, it is difficult to estimate for a non-implemented technology based on regression of statistics. A comparison of different reliability studies was conducted by Sheng. The failure rates and associated failure frequency distributions from this survey are provided in the Appendix D.2.

Based on values used in the omce default model and the trends understood from the survey (Appendix D.2), heuristic engineering knowledge was used to define the failure percentage of the different subsystems for a Fo-Vawt. The overall failure rate is varied through the simulations such that the failure frequency vs distribution for the subsystems remains the same. The FTC are kept similar to the default model for common systems. From the wind turbine reliability report,

[73], it was noticed that there is a trend for downtime and number of failure to increase with larger power rating turbines. Key failure and components contributing to the downtime include:

- Pitch and yaw system
- Drive train assembly
- Converter and power electronics
- Generator control

Wind Turbine Systems

The main aspect to address for establishing the OMCE model was presuming with reasonable understanding the differences between a HAWT and VAWT . The challenge posed were there can be no verification of the presumptions as there is no operating commercial VAWT wind farm presently. Thus utilising information from the ReliaWind reports by Lange et al. [47] and in house information from ECN, the data from the default model is adapted [28] to develop failure percentages for a VAWT. From Appendix D.2, a generic understanding of the failure distribution across the subsystems is given. The failure rates of the WT subsystems are adapted to the FO-VAWT design based upon the existence of the system and the operational environment it has to function in. The overall chosen failure rate was adapted to a failure distribution adapted to VAWT's after removal of certain elements such as Drive-train, Rotor Hydraulics and actuator motors. The wind turbine system breakdown is based on the guideline from BV [20] on Reference Designation System for Power Plants.

Considering an overall failure rate of the wind turbine system $\Lambda_{WT} = x[yr^{-1}]$, the following list provides the distribution of the subsystem wise failures a percentage to the combined Λ_{WT}. It should be noted that this annual fail rate does not incorporate BoP or remote resets due to operational emergencies/requirements. In this model the base case for Λ_{WT}= 3.302 [yr^{-1}]. This value was derived by removing systems from the framework which are unique to HAWT's such as drive-train, motors, hub assembly and yaw system. However, the MTTF for the common subsystems was kept constant. Based on this, as the overall fail rate scaled for a VAWT, the time taken for the subsystem to fail remained the same. This rearranged the subsystem's failure contribution to the overall wind turbine fail rate.

$$\frac{\Lambda_{subsys,HAWT}}{\Lambda_{WT,HAWT}} \neq \frac{\Lambda_{subsys,VAWT}}{\Lambda_{WT,VAWT}} \tag{5.34}$$

1. **Rotor**

   Overall Failure percentage = **4.1 %**
   No pitch mechanism which accounts for 90 % of rotor failures [67]
   MTTF = 65000 [hr]
   Blade Adjustment subsystem for the Rotor is removed as there are no pitch motors.

2. **Drive-Train**

   Overall Failure percentage = **1.1 %**

   The DeepWind rotor incorporates a Direct Drive Generator

   Still modelled with negligible fail rate as part of brake system. As turbine is primarily torque controlled, brakes are an essential and regularly used component of the turbine

3. **Nacelle**

This system is not applicable to VAWT's as no yaw motor's/nacelle

4. **Power-train**

   Overall Failure percentage = **30.8 %**

   Scales up as overall WT faire rate reduces

   Transformer and Converter considered along with "Transmission" WT subsystems

   Switch gear considered in "Control and protection"

   Machine enclosure gives higher failure rate as it functions as a submerged nacelle enclosure.

5. **Control and Protection System**

   Generator *Overall Failure percentage* = **27 %**

   The power train controller failure is kept high as the turbine's rotational speed is torque controlled. Direct drive machines are also attributed to higher electronic failures due to the higher number of coils, difficulty to seal and less technology standardisation according to Tavner et al. [69]

   Turbine *Overall Failure percentage* = **24 %**

6. **Turbine Structure/tower**

   Overall Failure percentage = **7 %**

   As the DeepWind design involves a rotating tower spar structure, it will definitely experience wear and tear.

7. **Mooring Bearing**

   Overall Failure percentage = **6 %**

   New Wind Turbine subsystem

   Type of Failures include

   - Repair Class 2, frequency 65%
   - Repair Class 4/6, frequency 15%
   - Repair Class 12, frequency 5%

   Calendar based Maintenance for BoP Mooring system added as WT system to model for each WT in wind farm. It is assumed that on average a turbine mooring system needs operational repairs every 4 years.

   - Repair Class 18, Regular Bi-annual Inspection
   - Repair Class 19, Regular Bi-annual inspection and repair if inspection deems necessary.

8. **Auxillary & Misc**

   Overall Failure percentage = **7 %**

   Ventilation subsystem failure = 2 %

   Crane subsystem failure = 2 %

   Hydraulic subsystem failure = 1 %

   Miscellaneous failures = 2 %

Some critical elements such as the yaw and pitch systems are removed, which weighs towards the advantage of VAWT's. However, the overall complete turbine failure range is kept high to replicate the immaturity of the technology. This is evident in the higher failure percentage attributed to the Generator and Control modules. It was concluded from de Pieterman et al. [28] and it was also stated in Tavner et al. [69] that direct drive power trains have more breakdowns and failures than a conventional gearbox generator assembly as the technology is less matured.

Balance of Plant

In the OMCE model, the Balance of Plant failures are kept very high to account for the damage to the foundation primarily. As the turbine is floating, the scour protection failure class is replaced by mooring line failure. The other failure is at the WF offshore substation where the main transformers are housed. An initial assumptions was made that the transformers at the wind farm substation were maintained by the TSO. The BoP transformer repair is modelled such that no costs are induced during a transformer failure but half of the wind farm suffers downtime. This results in a loss of energy captured but not costs to repair the failure. However in the parametric study, section 6.3, this assumption is switched on and off to evaluate the impact on the O&M effort.

1. **Transformer 1 & 2**

   Overall Failure percentage = **32 %**

   Case 1: No costs or labour work required as work performed by TSO.

   Case 2: Costs and labour work responsibility of wind farm operator.

   Results in 50 % of wind farm non-operational.

2. **Mooring System**

   Overall Failure percentage = **65 %**

   Regular maintenance and repair jobs to keep the mooring connectors, lines and sea floor connections secure and strong.

   Accounts for major maintenance related to the BoP system

   - Repair Class 11, frequency 95%
   - Repair Class 10, frequency 5%
   - Repair Class 15, Condition Based maintenance

   BoP Calendar based maintenance was modelled in WT system "Mooring Bearing".

3. **Cable Replacement**

   Overall Failure percentage = **5 %**

   Specialised equipment and resources required

   Results in 13 % of wind farm un-operational.

5.5 Annual Energy Production

The reference annual energy production for the 5 - 15 MW turbines was determined initially in section 4.4. Now with more accurate estimations about the losses incurred due to technical, operational, and site conditions, a worst case calculation of the net AEP can be estimated. As the wind farm is offshore, so terrain losses are neglected. The main elements constituting to a probability in the AEP are

- Wind farm array efficiency
- Electrical losses, infield and transmission
- Data/Instrumentation uncertainty
- Wind Variability
- Wind farm Availability

Table 5.7: Estimation factors contributing towards P_{50} Net AEP

Type	**Difference**[%]	**Sum Range**	**Source**
Wake Losses	-5	-5	Mortensen [55]
Electrical Losses	-1.8	-6.8	Section 5.3.1
Instrumentation Error	± 2.5	-4.3 → -9.3	Mortensen [55]
Vertical Spatial Variation	± 1.5	-2.8 → -10.8	Mortensen [55]
Mean WF Availability	-5.15	-7.95 → -15.95	table 6.3

From table 5.7, availability from the O&M effort constitutes as a major contributor of the exceedance probability between predicted and actual AEP. The wind farm availability was averaged for the all the cases from the downtime in table 6.3. The P_{50} net AEP could lie between -7.95 → -15.95 of the reference AEP. This also provides a reference to the capacity factor (CF) of the wind farm and subsequent full load hours for the wind farm can be determined based on the final AEP approximation

$$\text{CF} = \frac{AEP_{P_{50}}}{8760 \cdot P} \tag{5.35}$$

$$\text{Load Hours} = \text{CF} \cdot 8760 \tag{5.36}$$

Based on this the limits of net AEP and capacity factors per rated turbine are given in table 5.8. The lower values seem more indicative of realistic capacity factors of modern wind farms. However both the value will be used to gauge the impact on LCoE.

Table 5.8: Range of Net P_{50} AEP and Capacity factor per unit turbine for FO-VAWT *farm*

Rated Power	Ref AEP [GWh/yr]	Max AEP [GWh/yr]	Min AEP [GWh/yr]
5 MW	19.574	18.018	15.144
10MW	40.817	37.572	31.579
15MW	62.962	57.957	48.712

Rated Power	Full Load AEP [GWh/yr]	Max CF[%]	Min CF [%]
5 MW	43.8	41.14	34.58
10 MW	87.6	42.89	36.05
15 MW	131.4	44.11	37.07

Chapter 6

Results and Analysis

The mass calculations and cost estimations are given in this chapter. The resulting CAPEX and OPEX for the FO-VAWT concept is examined for a staple 240-250 MW wind farm depending on the power rating. The scaling of the mass fractions and cost fraction of the different wind turbine and balance of plant systems are assessed. To determine the viability of the design, the LCoE and IRR is presented with a sensitivity analysis of certain key assumptions and contributing elements.

6.1 Scaling

The calculations methods used for the system wise masses are based on the engineering model implemented or parametric approximations outlined in section 4.6. The geometry size of the characteristic dimension was taken from correlating the area needed to operate at higher rated powers for the same operational strategy. However, aerodynamic similarity was difficult to ensure as seen from the incoherent downscaling of λ with $(\mathrm{H}/\mathrm{H}_\circ)^{-1}$ from table 6.1

Table 6.1: *Results from scaling of the DeepWind turbine*

Property		**Unit**	**5 MW**	**10 MW**	**15 MW**
Tip Speed Ratio	λ_{opt}	[–]	2.7	2.99	3.21
Rotational Speed	ω_{rated}	[rad.s^{-1}]	0.621	0.495	0.437
Height	H	[m]	143	200	243
Swept Area	A	[m^2]	12000	24000	36000
Mean Torque	Q_{mean}	[MNm]	8.83	20.30	34.25
Rotor Mass (GFRP)	m_{rotor}	[t]	48.02	141.35	264.86
Tower Mass	m_{tower}	[t]	397	1019.6	1840.9
Floater Mass	m_{flt}	[t]	1201.2	2460.4	3932.2
Ballast Mass	m_{blt}	[t]	3707.3	7762.6	12516.2
PM DD Gen. Mass	m_{gen}	[t]	56.6	123.3	156.7
Mooring & Arm Mass	m_{moor}	[t]	378	637.1	893.8

It can be seen that the torque decreases for the larger sized wind turbines. This is attributed to the Reynolds number effects. As the turbine is scaled to operate at such high Re, data was correct to model the loads properly. Hence in order to maintain the power from the torque measurements, the rotor speed was increased which decreased torque while increasing C_P. this in essence reduces the aerodynamic similarity of the system. This is also based on the approximation that the swept area doubles as the power doubles. An interesting trends is the reducing increase in tower mass which is contrary to HAWT scaling, where the tower mass scales with exponent higher than 3.

The rotor mass increases with an exponent less than the cube of characteristic dimension scaling factor (H/H$_\circ$) . The mass is however not based on the loading, as the thickness distribution of the baseline blade is linearly increased with (H/H$_\circ$). This lack of structural optimisation can result in much heavier blades than expected, especially when changing materials to CFRP. The mass of the rotor and tower have downstream effects on floater sizing. The static vertical equilibrium is based on the hydrostatic force from the water displacement pushing the weight of the VAWT out of the water by at least 17m(height of STT) while maintaining the baseline designs static margin between the centre of gravity and center of buoyancy at maximum heel. The hydrostatic force scales faster than the mass of the structure and the ballast combined, leading to the draught ratio(L/L_{ref}) being less than (H/H$_\circ$). It should be noted this optimum is not the global optimum as it is constraint by the slenderness ratio ϕ_{max}/L of the baseline model and the ratio of section-wise heights tot he total draught.

6.2 CAPEX

In figure 6.1, the scaling of the cost fractions fro turbine capital costs while incorporating the Floater are shown. The turbines design entails a mutual dependency between the rotor and the Floater. Although in the LCoE analysis, the Floater is considered as a segment of the BoP CAPEX and not TCC. In this section the Floater CAPEX is explicitly examined with respect to the TCC. From 6.4, the TCC with the Floater are €10.3M, €22.4M and €34.7M for the 5, 10 and 15 MW FO-VAWT respectively.

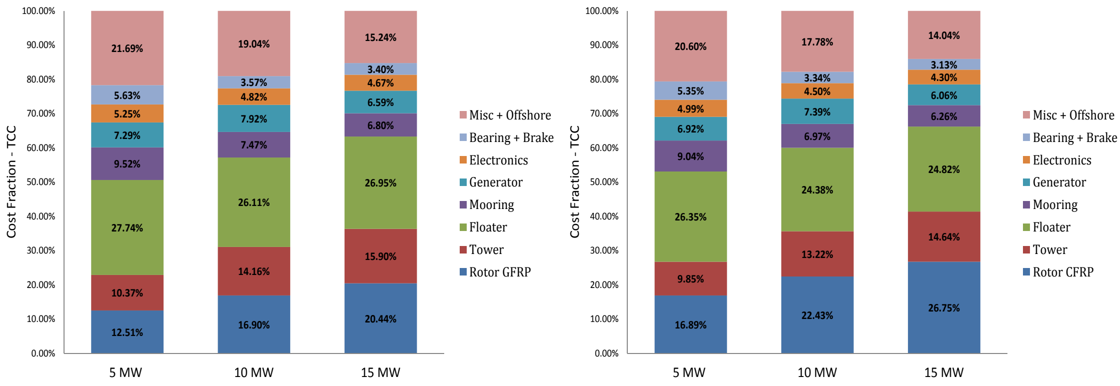

(a) Cost Fraction GFRP (b) Cost Fraction CFRP

Figure 6.1: *Scaling of Turbine Capital Cost Fraction with rated power for Glass fibre and Carbon Fibre Blades*

It can be noted that the Floater does not scale in terms of mass or costs with increasing proportion to the volume/mass. This is perceived to be based on the sizing criteria mentioned in the previous section. This is an important trend as the large increase in foundation costs for higher rated bottom founded HAWT's is a key cost driver, [8]. The rotor cost fraction rises due to the non optimised structural distribution for higher rated powers and length of the blade scaling much faster than that for HAWT's. The tower costs fractions scales with the most favourable ratios. The tower mass is another key cost driver for HAWT's, [8] mainly due to the high tower top mass. For VAWT's however the tower cost driver is perceived to be the aerodynamic thrust. The low C_G and equator height prove to be intrinsic qualities of the VAWT which improve its scaling trends.

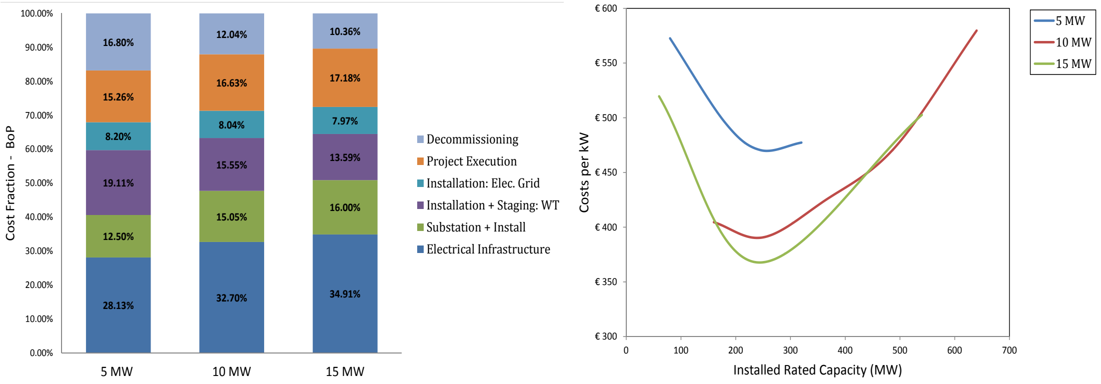

(a) Cost Fraction (b) Costs per kW

Figure 6.2: *Scaling of Balance of Plant (a) cost fractions with rated power and (b) Costs per kW with wind farm capacity*

The fixed grid structure used for the wind farm layout prevented a common wind farm capacity for all rated powers, (refer to table 5.2). For the BoP CAPEX analysis, the installed wind farm capacity's used when comparing the 5,10 and 15 MW are 240. 250 and 245 MW respectively. From 6.4, the BoP costs per turbine including decommissioning without the Floater and mooring are €2.35M, €3.91M and €5M for the 5, 10 and 15 MW FO-VAWT respectively. For the BoP CAPEX in figure 6.2a all cost fractions tend to increase apart from the installation and decommissioning costs. It should be expected for the ratios to stay some what constant, but the installation costs as mentioned earlier are difficult to estimate for FO-VAWT's. Thus if kept as for bottom founded structures while removing the cost for foundation installation, the installation CAPEX decrease by more than > 50 %.

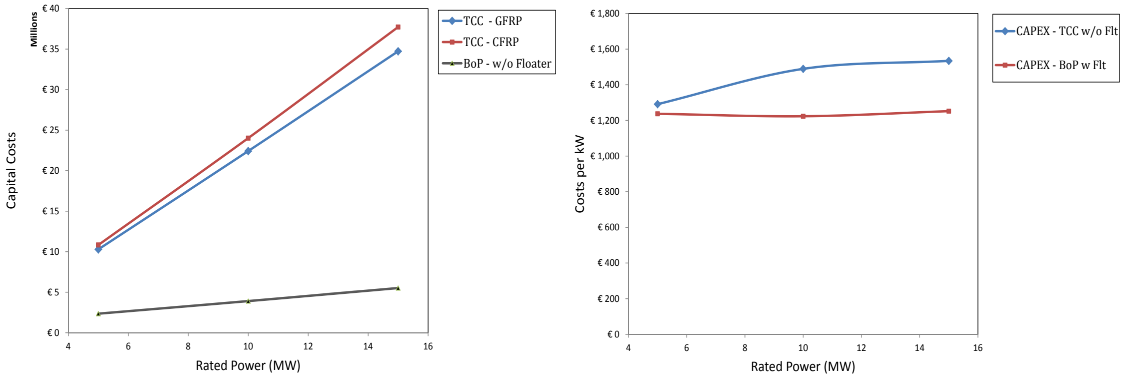

(a) CAPEX (b) CAPEX per kW

Figure 6.3: *Scaling of* FO-VAWT *(a)* CAPEX *with rated power and (b) Costs per kW with rated power*

After a certain wind farm capacity, the BoP costs begin to rise rapidly in figure 6.2b. This was seen to be due to a large increase in the electrical infrastructure costs. Mainly as a result of lack of optimisation resulting in the export cable and infield cable costs scaling with the installed capacity and not the load between turbines. These results can be seen in appendix C. It should be noted, there is a lower number of higher rating turbines in smaller installed capacity wind farms but the cost per turbine is still rising with rated power. Despite this, the cost per kW for higher rated turbines for similar installed capacities is less as seen in figure 6.2b.

In figure 6.3a, the costs are shown for GFRP and CFRP rotors for increasing rated power. Despite the structurual thickness of CFRP is percieved to scale better than for GFRP, the overall cost impact of CFRP rotors is not such a large cost driver as was anticipated. In figure 6.3b, the convention of TCC and BoP is different as mentioned before. Here the CAPEX for the turbine excludes the Floaterand mooring costs, which are added into the BoP costs. This counter acts the favourable scaling of BoP costs with rated power from figure 6.2b while improves the scaling pattern for TCC.

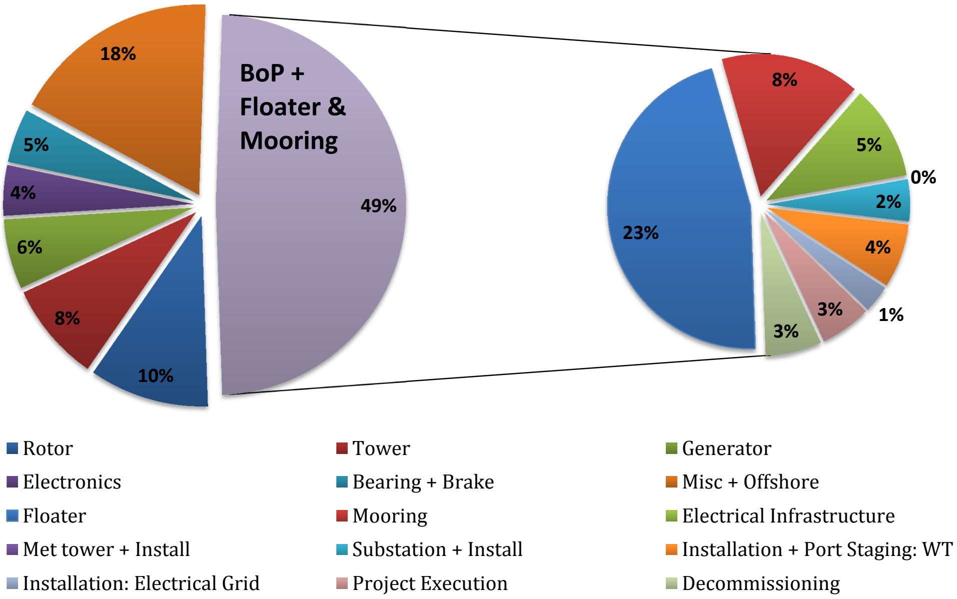

Figure 6.4: *Cost fraction breakdown per GFRP rotor* VAWT *in a 49 * 5 MW installed capacity farm*

The complete CAPEX pie for the FO-VAWT is given in figure 6.4. The BoP includes the Floater and mooring costs which comprise to almost 31% of the total CAPEX. This makes the Floater design a key aspect. The *Misc-Offshore* costs comprise of a simple interpolation of the inactive mass costs needed to house the generator which in itself is the interpolation of the DeepWind generator design. The other elements in the *Misc-Offshore* costs are fixed costs for the installation of the mooring system (€0.72M) as explained in the respective section and the marinisation costs of protecting the Floater . These elements are also main contributors to the CAPEX (≈ 22%) making them key aspects to address and improve.

6.3 OPEX Parametrisation

The purpose of the parametric study is to reduce any uncertainty in results arising from assumption which might not hold in practice. For this reason, a sensitivity analysis is done for the important parameters to generate a workspace of effects that major assumptions, statistics and model implementations have on the cost spectrum of a FO-VAWT wind farm. First of all, to create simplicity in the understanding the overall failure rate parametric process, a legend is created to refer from when reading through the table 6.3

Table 6.2: *Parametric legend for system failure rates*

Fail rating	High	Medium	Low	Para 1	Para 2
BoP	4.16	3.16	2.16	3.16	2.16
WTS	4.33	3.33	2.33	2.33	3.33
Legend	BH-WH	BM-WM	BL-WL	BM-WL	BL-WM

The legend in the table will be refereed to in the main result tabulation. Apart for variation in Overall failure rates, installed capacity and rated power, the other cases are studied to asses the impact on O&M effort from tinkering with certain scenarios mentioned in section5.1 and 4.2. For all the cases considered, geographic and site conditions are kept constant unless otherwise indicated. The analogy used to indicate them are

- **TSO** The assumption that the TSO will have a fast response team to amend any wind farm substation failures is switched *ON* and *OFF*
- **Strategy** The O&M strategy (repair classes, spare parts control, labour and vessel costs) is changed from the one modelled specifically for **fowt**'s and to the one used by *ECN*(TSO off) for normal bottom founded turbines
- **Default** The complete O&M model and strategy including failure rates for a 5MW HAWT is used for the same location
- **SSW** Location of new site right at the mouth of the Rotterdam port, N 52°0′, E3°75′) acquired on may 2012 for a times series from 1992 to 2010 [1]
- Variation of individual system failure rates $\Lambda_{max/min}$, rotor and generator

The assumption that the substation failures are maintained by the TSO was taken as the wind farm is 120 km offshore. With the TSO taking care of the wind farm substation repair costs, it reduces a significant portion of the cost impact. In this case only a loss in energy production is felt. The strategy variation was brought about to study the influence of the O&M model on the overall OPEX. The one used for the majority of the study is FOWT unless otherwise stated. For all the cases presented in table 6.2, the maintainence strategy and failure system definition are the kept as to the one modelled.

---

[1] `www.waveclimate.com`

Table 6.3: *Operation and Maintenance parametric results for* FO-VAWT *farm with different O&M strategies, rated power, installed capacity and location*

DW 245 MW, Site K13, 5 MW VAWT							
Fail Case Λ	Case /Strategy	CoE [€cents/kWh]	Rev/MW.yr [€/(MW.yr)$^{-1}$]	Downtime	Prod loss[MWh]	Repair Cost [€/kW]	Rev loss/MW.yr [€/(MW.yr)$^{-1}$]
BM-WL	FOWT	4.29	4.41 e+05	2.22E+04	5.33E+04	146.6	2.89E+04
BM-WM	[-]	4.28	4.41E+05	2.23E+04	5.36E+04	145.2	2.90E+04
BL-WM	[-]	3.69	4.49E+05	1.62E+04	3.82E+04	127.6	2.07E+04
BL-WL	[-]	3.73	4.49E+05	1.63E+04	3.88E+04	128.9	2.10E+04
BH-WH	[-]	4.68	4.35E+05	2.67E+04	6.45E+04	156.4	3.49E+04
B -WM	$\lambda_{Gen,min}$	3.69	4.49E+05	1.65E+04	3.88E+04	127.0	2.10E+04
BM-W	$\lambda_{Rotor,max}$	4.78	4.07E+05	2.82E+04	6.33E+04	149.4	3.43E+04
BM-WM	FOWT,TSO off	4.56	4.09E+05	2.59E+04	5.85E+04	143.0	3.17E+04
BLL-WM	[-]	3.72	4.47E+05	1.83E+04	4.29E+04	127.6	2.33E+04
Scaled VAWT's, Site K13							
BM-WM	24*10MW, FOWT	4.44	4.46E+05	1.12E+04	5.38E+04	152.2	2.91E+04
BM-WM	49*10MW, FOWT	3.08	4.45E+05	2.34E+04	1.13E+05	105.2	2.99E+04
BM-WM	16*15MW, FOWT	4.67	4.56E+05	7.66E+03	5.58E+04	163.7	3.02E+04
BM-WM	32*15MW, FOWT	3.05	4.56E+05	1.53E+04	1.12E+05	107.2	3.04E+04
DW 520 MW, Site K13							
BH-WH	FOWT,TSO off	3.35	2.17E+06	5.75E+04	1.41E+05	112.0	3.53E+04
BM-WM	ECN Strategy	1.62	6.27E+05	5.57E+04	1.78E+05	78.0	4.46E+04
ECN Default	ECN Strategy	2.94	4.67E+05	8.47E+04	1.70E+05	104.0	4.24E+04
DW 490, Site K13							
BM-WM	FOWT,TSO off	2.70	4.46E+05	3.86E+04	9.08E+04	92.6	2.41E+04
BL-WL	[-]	2.66	4.49E+05	3.37E+04	8.00E+04	91.8	2.12E+04
BL-WL	FOWT	3.10	4.40E+05	4.53E+04	1.11E+05	105.0	2.95E+04
DW 490 MW, Site SSW							
BM-WM	FOWT	4.82	3.65E+05	3.81E+04	3.81E+04	135.4	2.06E+04
BM-WM	[-]	4.88	3.62E+05	2.27E+04	4.42E+04	135.6	2.40E+04

From table 6.3, the costs for 240 MW wind farm increase with same size wind farm capacity. This is predictable as the number of machines installed against the cost of the effort is not justified by the power production. It is better to install more larger machines for a higher capacity turbine as the resources required till a certain installed capacity and turbine number does not scales in large steps.

Then overall system break down for a VAWT wind farm involved the removal of many systems which attributed towards major cost impact and downtimes towards the an offshore wind farm. Although there were many assumptions held to push the overall O&M effort towards a feasible solution for both types of wind turbines, a VAWT does remove major components of system failures from the overall wind farm such as BoP and design inherent advantages. Less BoP failures are intrinsic to any sort of spar Floater turbine.

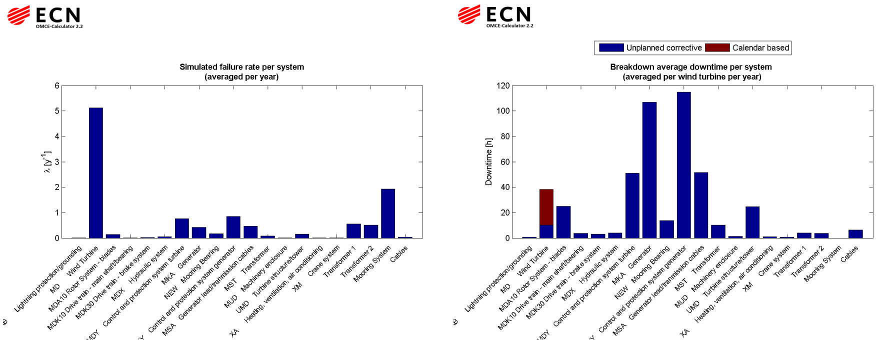

(a) Failure Rate (b) Avg System Downtime

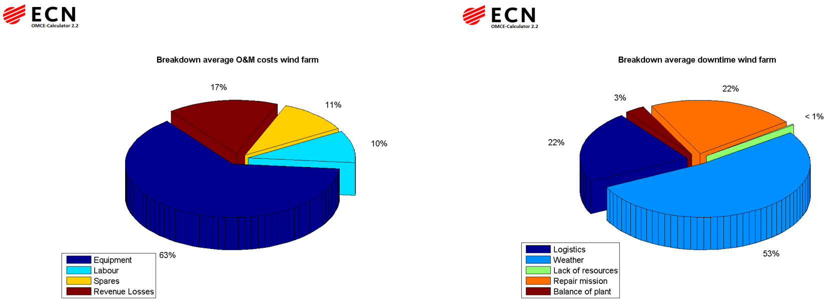

(c) Avg Cost Breakdown (d) Avg Downtime breakdown

Figure 6.5: *O & M Results for base case with* FOWT *strategy,* $\Lambda_{wt} = 4.33$ *and* $\Lambda_{bop} = 4.16$*, in a 104*5 MW* FO-VAWT *farm*

O & M results for a FO-VAWT strategy in figure 6.5 refers to the Fail case BH-WH for a 520 MW farm at K13 with the TSO relaxation off in table 6.3. For the ECN default case in figure 6.6can be found in the table 6.3 as ECN Default. The figures show to compare the difference in cost breakdown for a bottom founded HAWT and VAWT installation. The most major cost factor was due to the high captial costs of the specialized equipment that presumably would be needed to maintain the FOWT's. The difference in failure rates is attributed to VAWT's having less critical systems which fail more as can be seen in figure 6.5a in comparison to figure 6.6a. The large peak in failure rates under the category "MD Wind Turbine" are attributed to remote resets due to environmental events or grid unavailability.

In general it is a big assumption that the technicians have the same expertise in maintaining the turbines as there as no existing VAWT wind farm in operation. Also how the repair will be actually

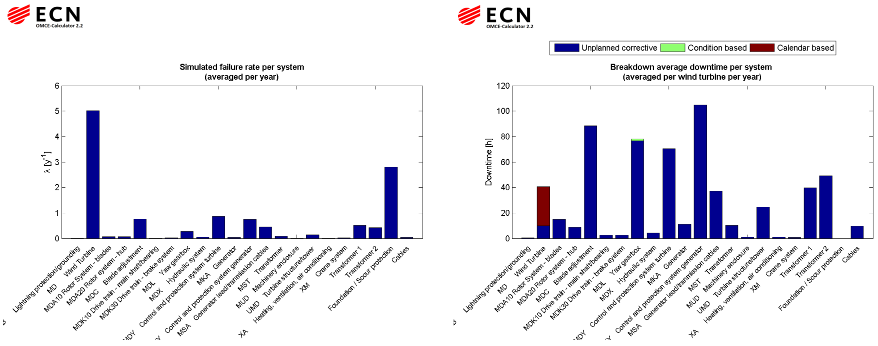

(a) Failure Rate (b) Avg System Downtime

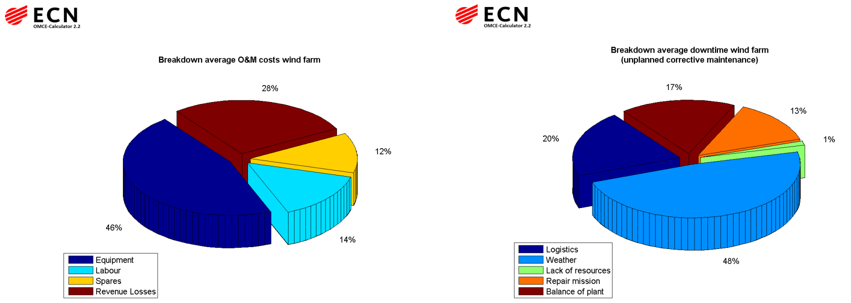

(c) Avg Cost Breakdown (d) Avg Downtime breakdown

Figure 6.6: *O & M Results for ECN Default model, WT fail rate of 4.07 and BoP fail rate of 4.53 in a 105 * 5MW* Hawt *farm.*

carried out is very difficult to estimate. So it is hard to deviate form the repair classes other than default. The only adaptations are improvisations on accessing the areas of fault which are based on self conceptualised ideas in reference to the design of the Deep wind rotor. The increase in annual costs for the vessels contributes to a major portion of the overall annual cost if we compare figure 6.7 to figure 6.5b especially for smaller wind farms. This is the reason why there is such a high OPEX/kW as the resources used for the 245 and 490 MW are the same.

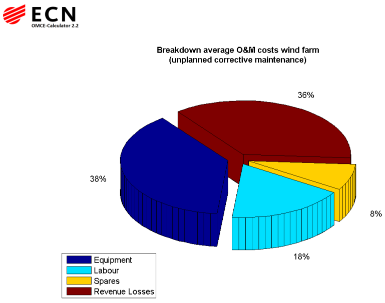

Figure 6.7: *Avg Cost Breakdown for bottom founded* Vawt *in a 49 * 5 MW farm with a BH-WH fail rate*

6.4 Economic Assessment

To address the economic factors, a discounted, cash flow for an economic project life cycle (T) of 20 years is drafted. To assess the viability of a Fo-Vawt farm, the NPV and IRR are interesting parameters to address as well. For the NPV, revenue stream is an essential components for which the electricity price needs to be established. In the Netherlands, a flat rate is provided by the TSO of ≈ €58/MWh, however the government has in place many load hour based subsidies, providing a Feed in Premium starting €88/kWh uptil €153.4 /kWh, more information can be found on sde [5]. For the initial economic evaluation, the favourable case scenario is chosen, resulting in a constant average electricity tariff of €130/ MWh for the economic lifetime. These along with other major assumptions are addressed in section 6.4.1.

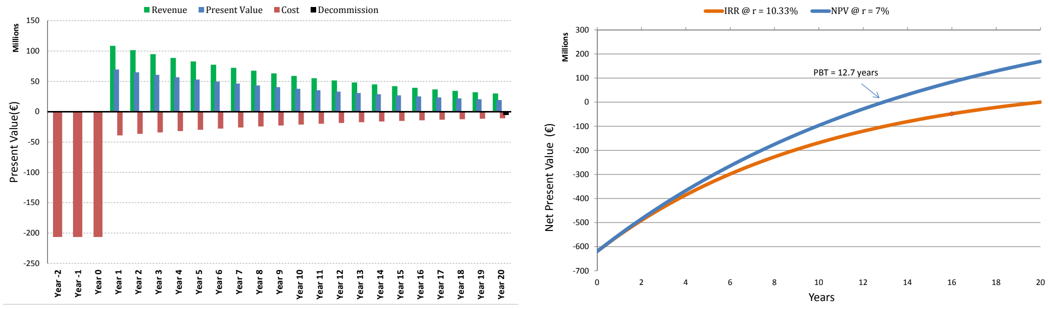

(a) Discounted cash flow, $r = 7\%$ (b) Accumulated discounted cash flow

Figure 6.8: *Life cycle cash flow for 49 * 5 MW wind farm with initial discount rate 7% and IRR of 10.33%*

Energy rates escalation and general inflation is not considered in this economic analysis. Similarly the real discount rate 'r ' considered removes the effects of inflation on the time value of money and on the OPEX . Financing options, tax incentives and payback schemes are also not considered. The CAPEX or initial investments needed to setup the farm are distributed over three years before the economic commencement.

If the IRR is higher than the discount rate, then the investment is profitable. According to figure 6.8a, an IRR of 10.82%, the project provides a sufficient buffer in case of an unforeseen risk to break even. However, the return on investment is not high with a discounted pay back time is **12.7 year** with a $r = \mathbf{7}\%$. The simple payback time for this project

$$\text{PBT} = \frac{\text{CAPEX}}{\text{Rev} - \text{OPEX}} = \mathbf{8.35\ years}$$

The complete table for the results from scaling with rated power are given in table 6.4, where the miscellaneous costs comprise of the in active mass costs approximated in section 5.2.4, marinsation costs and fixed mooring arm installation costs discussed in section 5.2.3.

6.4.1 Sensitivity Analysis

According to the equation (2.3), the main constituents describing the LCoE and other economic factors of the Fo-Vawt wind farm are based on certain uncertainties. To assess the impact of the model assumptions, the major elements influencing the LCoEare varied within a range defined by the uncertainty of the presumptions made. The influence of the assumptions on the listed elements is discussed through the sensitivity analysis.

Table 6.4: *Cost Results for 49 * 5 MW DeepWind* Fo-Vawt *farm located K13 site in the North Sea*

245 MW Fo-Vawt, K13			Cost(€)		
System	**Classification**	Unit	**5 MW**	**10 MW**	**15 MW**
Rotor	CFRP	€22.00/kg	1,829,706	5,386,080	10,091,858
	GFRP	€10.50/kg	1,287,493	3,789,818	7,101,318
Tower	Steel	€3.0/kg	1,066,674	3,175,458	5,522,824
Floater	Hull	€2.19/kg	2,668,782	5,466,568	8,736,613
	Ballast	€0.05/kg	185,364	388,132	625,812
Mooring	Arms	€4.06/kg	208,156	407,986	601,571
	Chain	€2.36/kg	771,224	1,266,450	1,759,672
Generator	Direct Drive	[49]	750,000	1,775,000	2,287,500
Power Electronics	Refer 5.2.5	€	540,518	1,081,036	1,621,554
Bearing	Refer 5.2.6	€	437,532	517,479	756,843
Brake	Refer 5.2.6	€	141,856	283,712	425,568
Miscellaneous		€	2,231,722	4,270,000	5,295,000
Turbine Capital Costs	CFRP		10,831,535	24,017,902	37,724,815
	GFRP		10,289,321	22,421,640	34,734,275
Balance of plant costs		M€	95.9	85.9	79.1
Decommissioning costs		M€	19.4	11.8	9.15
CAPEX		M€	619.5	658.2	644.0
OPEX		M€/yr	41.8	45.6	47.8E
Electricity Tariff		€/kWh		0.13	
AEP P$_{50,max}$		GWh	18.02	37.57	57.96
AEP P$_{50,min}$		GWh	15.14	31.58	48.71
Capacity Factor		%	34.57	36.06	37.07
LCoE		€/MWh	113.57	114.69	117.10

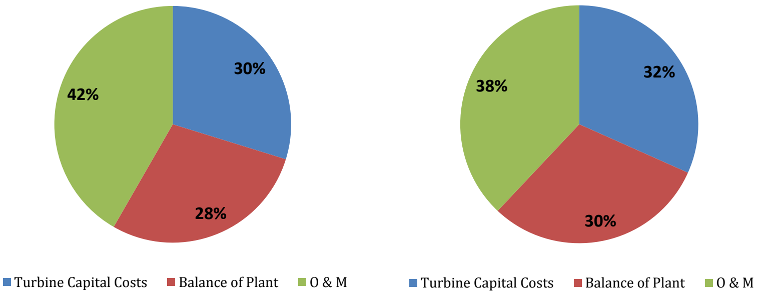

(a) 5 MW, $\Lambda = 6.5$/yr (b) 5 MW, $\Lambda = 4.5$/yr

Figure 6.9: *Levelised Cost of energy breakdown for 5 MW* Fo-Vawt

1. Wind turbine rated power
2. Wind farm installed capacity
3. Capacity Factor
4. CAPEX

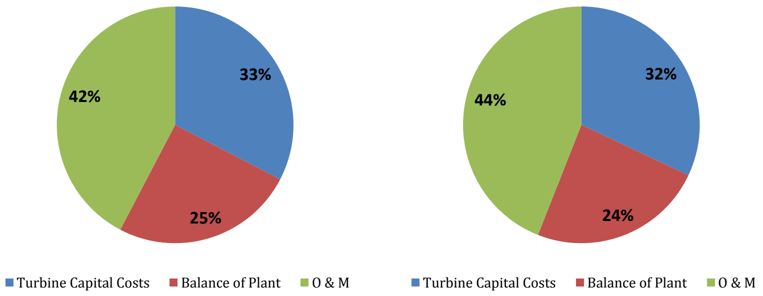

(a) 10 MW (b) 15 MW

Figure 6.10: *Levelised Cost of energy breakdown for 10 and 15 MW* FO-VAWT, *Λ= 6.5/yr*

5. OPEX
6. Electricity price
7. Discount Rate

For all analyses, the AEP is taken as $P_{50,max}$ from table 5.7 and the rotor blades are GFRP with the average electricity price at €0.13/ kWh. The LCoE values are at a discount rate of 7% The O&M strategy used is assuming that the costs of the substation failure are incurred by the TSO (TSO on). A graphical representation of the sensitivities is given in figure 6.11.

Wind Turbine Rated Power

There is a slight dissimilarity when comparing the effect of wind turbine rated power on LCoE. The installed capacity of the different turbine ratings vary by ± 5 MW from each other. The influence of this on the overall LCoE is considered negligible.

Table 6.5: *Influence of rated power on key economic parameters for similar installed capacity* VAWT *farm*

Rated Power (kW)	**WF Capacity** (MW)	**Capacity Factor** (%)	**OPEX** (M €)	**IRR** (%)	**LCoE** (€/kWh)
5000	245	41.1	41.8	10.33	0.1136
10000	250	42.9	45.6	9.54	0.1147
15000	240	44.1	47.8	8.72	0.1171

In table 6.5, the LCoE increases slightly for higher rated power for an ≈ installed capacity. The increase in OPEX is deemed the necessary reason even though theCAPEX/kw is relatively constant , figure 6.3. The rise in OPEX is due to the higher cost of repair per kW as even though labour costs are less, capital lease costs for the vessels are the same for both a 49 * 5 MW farm and a 16 * 15 MW farm.

Wind Farm Installed Capacity

The 10 MW turbine was used to estimate the change in LCoE when installed capacity is increased. Both the wind farms are square grids with a a 5*5 and 7*7 configuration with 5 ϕ spacing.

Table 6.6: *Influence of installed capacity on key economic parameters for 10 MW* VAWT *farm*

WF Capacity (MW)	**Capacity Factor** (%)	**OPEX** (M€)	**OPEX/kw** (€/kWh)	**IRR** (%)	**LCoE** (€/kWh)
250	42.9	45.6	182.4	9.94	0.1147
490	42.9	66.3	135.30	11.26	0.1042

The LCoE drops significantly in table 6.6 due to the much lower OPEX/kw for larger installed capacity. This again can be linked to the reducing annual lease costs per kW for the vessels needed in O&M.

Capacity Factor

The capacity factor of a wind farm is based on annual energy production . AEP is a dependent on the interaction of the site resource, wind turbine reliability and the response limits of the O &M. From section 5.5, a range of the mean exceedance probability of the wind farm energy production was estimated, table 5.7. From OMCE, the worst case of the capacity factor was attained from the simulations.

Table 6.7: *Influence of variation in capacity factor on key economic parameters for 49 * 5 MW* VAWT *farm*

Case	**Capacity Factor** (%)	**AEP/turbine** (GWh)	**IRR** (%)	**LCoE** (€/kWh)
OMCE worst case	32.5	14.235	6.72	0.1438
AEP $P_{50,min}$	34.6	15.144	8.09	0.1351
AEP $P_{50,max}$	41.1	18.018	10.33	0.1136
AEP predicted	44.7	19.574	11.08	0.1045

The annual energy production has a very high influence on the LCoE. High turbine availability can greatly improve the profitability of the wind farm. In the current state, the FO-VAWT farm modelled is not a viable financial option if the worst weather case persists for too long, pushing the IRR (6.72 %) below the average discount rate (7%). The availability of the turbines can be improved with better condition monitoring, wind resource assessment and sustained grid availability.

CAPEX Variation

Change in CAPEX due to major elements such as Floater, Misc generator cost is investigated in this analysis. . The sensitivity to LCoE was seen with a range of ±15%. This can relate to account for inaccuracy in estimates for the *Misc-Offshore* costs and Floater design which constitute almost 39% of the CAPEX fromfigure 6.4.

A ± 15 % change in baseline CAPEX of €620 M for a 49 * 5MW wind farm brings a substantial impact on the LCoE, with a variation of almost 9.6% per step. To put this in perspective, a 25 % increase in Floater and mooring costs results in a 7.2% rise in wind farm CAPEX, thus increasing LCoE by ≈ 4.1%.

Table 6.8: *Influence of deviation in* CAPEX *estimates on key economic parameters of a 49 * 5 MW* VAWT *farm*

Case	**Capacity Factor** (%)	**OPEX** (M €)	**IRR** (%)	**LCoE** (€/kWh)
CAPEX-15%	41.1	41.8	12.88	0.1036
CAPEX	41.1	41.8	10.33	0.1136
CAPEX+15%	41.1	41.8	8.34	0.1235

OPEX Variation

The cases chosen are from the tabulated (table 6.4) simulations performed with OMCE. The highest failure rate for all the wind turbine and BoP systems (WH-BH) from table 6.3 gives a repair cost of€156.4/kW while a low failure rate results in a cost per kW of €127.6. The base case repair cost is €145.2/kW. consequently changing the failure rate effects the downtime of the turbines, thus the less availability also effects the AEP. Hence the corresponding capacity factor was used for the different failure rates. The analogy for the O&M cases can be taken from table 6.2.

Table 6.9: *Influence of wind turbine failure rates (Λ) on* OPEX *and key economic parameters of a 49 * 5 MW* VAWT *farm*

O&M Case	**OPEX** (M€)	**Capacity Factor** (%)	**IRR** (%)	**LCoE** (€/kWh)
WL-BL	35.6	41.9	11.72	0.1045
WM-BM	41.8	41.1	10.33	0.1136
WH-BH	45.9	40.3	9.32	0.1206

The increase in combined failure rates from 4.5/yr to 8.5/ yr sow a reasonable variation in LCoE. This is attributed to both the higher number of repair activities thus resources and spares consumptions but mainly also from the reduced availability on average of the wind farm. This adds to lost revenue due to higher downtime. The decrease in respective capacity factor is indicative of this.

Electricity Price and Discount rate

Both these factors encompass assumptions taken on the economic conditions of the location where the farm is situated. A real discount rate of 7% is an optimistic assumption of the viability of this project to investors. However it is a safe assumption when considering offshore projects on a level field. The electricity price is although very fluid and depends on daily spot prices and market demand. A major portion is based on subsidy from the government especially until for the onshore wind industry in the Netherlands, sde [5]. The estimate taken depends on the commissioning month of the project as there are different feed in premiums per quarter and similarly what is the production level per quarter. For full load hours higher than 3200, high subsidies are given by the Dutch government, [5]. If for the most favourable case, the revenue is divided by the production, an average tariff of €0.13/kWh is acquired.

The difference in discount rate is specific to the risks involved in the project. Specifically, the technological risks for FO-VAWT's and far offshore installations will be perceived to be high. The electricity price has more of an effect on the economic feasbility of the project rather than the

Table 6.10: *Influence of discount rate on LCoE of a 49 * 5 MW* Vawt *farm*

Discount rate (%)	LCoE (€/kWh)
5	0.1036
7	0.1136
10	0.1298

design superiority of the concept. The internal rate of return is very dependent on the return on investment. The variation in electricity price is based on the four cases of feed in premium offered by the government, where the case if the wind farm operates constantly at the lowest feed in premium, capacity factor below 2800 full work load hours per year, then the net present value will be negative 280 M, where the simple payback time is 19.3 years. Meaning without discounting the project is barely able to break even.

Table 6.11: *Influence of electricity price on key economic parameters of a 49 * 5 MW* Vawt *farm*

Electricity Price (€/kWh)	IRR (%)	NPV (r = 7%) (M€)
0.085	0.35	-279.0
0.105	5.36	-76.5
0.115	7.2	9.92
0.135	10.92	200.0

The sensitivity of IRR and LCoE to the various parameters tabulated from table 6.5 till table 6.11 are summarised in figure 6.11b and figure 6.11a respectively. The bars signal the range of variaion in LCoE and IRR from the lowest to the highest value for the parameter considered. The base line values are given next to y-axis data labels.

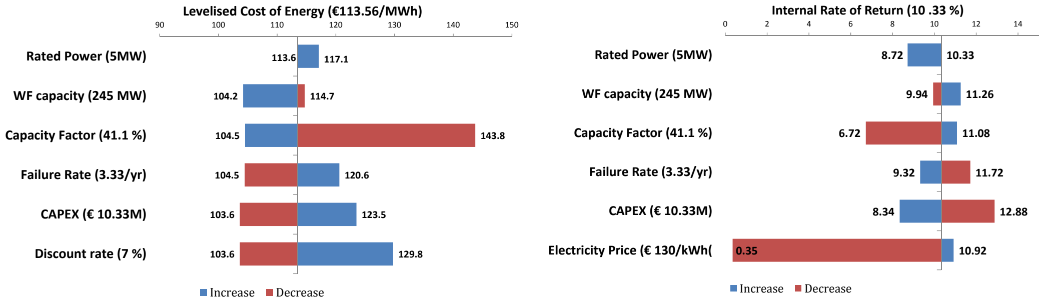

(a) LCoE senstivity

(b) IRR senstivity

Figure 6.11: *Sensitivity diagram of LCoE and IRR*

Critical Review of Cost Model

The sensitivity analysis provide a overview of the different factors influencing the LCoE of a Fo-Vawt. Based on the cost fractions in figure 6.1 and 6.4, the appropriate impact triggers can be determined for future work. Apart from the simulation results from OMCE and OWFDE, there were three model types or methods used to derive the LCoE . These are first explained after which a system wise cost model analysis is presented. The criterion considered when evaluating system wise models are *a*) Resource intensive: speed and time to setup *b*) Error from baseline design *c*) Verified source *d*) Adaptability *e*) Scaling

Engineering Model: focus on determining the mass of a system based on the load/ load spectrum it experience. Depending on the criteria used, the mass can be determined to a high level of accuracy. However making the step from mass to cost still involves estimations on the average cost per unit mass $k_{sys}$to fabricate the system. If accurate numbers are known, this allows for precise adjustments of the financial factors effects each aspect of the cost. Example the inflation of the material and inflation of labour can be treated independently. Provides freedom to adapt to design specific cost and thus allows for better scaling predictions, especially to capture the influence on other systems. However when scaling the design, it is important to consider the aspect of production process maturity and reduction in cost of production and labour per mass changes with size. Resource intensive

Parametric Model: are used by regressively analysing the cost trend of a system and derive a common factor with which the cost is scaled for example rotor power density, rotor radius etc.. The influence of mass is neglected and the cost of the systems is determined directly. Build up averaging thus making it less design specific. However it accounts for small unquantifiable aspects of the system cost and other geographic specific deviations. For financial analysis, this is the most common method used however it is limited that a large spectrum of existing data is needed and scaling is usualy direct extrapolation of the trends. Also does not capture the individual system or material based cost inflation or depreciations.

Linear Scaling: such estimations are usually only valid if the system considered matches the system used for interpolation. Direct interpolation is based on scaling systems in connection to the top design parameters. In essence it provides crude estimations and does not account for any design specific or geographic variations. The possibility of error depends completely on the coherence of the system estimated to the known costs and great care has to be taken when using such methods. It is definitely the fastest way to estimate cost.

OPEX

The operations and maintenance modelling was done with in OMCE. The model accuracy depended on the number of simulations made to reduce statistical errors in the Monte Carlo simulations. The costs were highly dependent on the cost of the labour and equipment used for the maintenance. This ofcourse would be relevant to any FOWT. The operations and maintenance contributed to the much larger contribution to the overall LCoE as seen from figure 6.9a. This was somewhat expected considering the far offshore location of the farm and with the high rate of failure. The overall impact of OPEX on LCoE is quite significant from figure 6.11a. However, modelling this in a different way will not result in much difference as the main factors dictating OPEX is the supply chain. OPEX is very situation specific and the results in 6.3 give us a good indication of how it fluctuates based upon the weather mainly followed by the resources needed to support the O&M and in last the cost of the spare parts. Downtime and revenue lost incur a combination cost deficit with the repair effort. A better failure rate understanding of VAWT's would make the O&M modelling more reliable.

Impact: *Medium*

CAPEX - TCC

The capex aspect of the model is built upon a combination of engineering mass estimations, linear scaling laws and parametric models. All the systems in the engineering cost model are built from estimations on the cost per mass to fabricate the part. This value depends on literature evaluation and trends understood from industry. The cost per mass is build upon the market price of the material and the average are or mass based cost of manufacturing the part or the labour costs. The formulation for major sections is mainly addressed and smaller/ systems are neglected. A system wise analysis if given in table 6.12.

Table 6.12: *Qualitative Analysis of system wise* capex *cost model to determine high impact triggers*

System	Type	Inputs	Application	Limitations	Impact	Trigger
Blade - Rotor	Geometric mapping, Parametric, Linear Scaling	○ Material properties ○ Baseline Rotor thickness distribution, ○ Radius of Curvature	+ Accurate approximation of baseline mass, $\Delta m \leq 2\%$ + Quick, setup time consuming + Adaptable: variation in k_{sys} and other economic/financial factors + independent of environment influence	– Area taken from parametric scaling of HAWTpower to area trend, unverified results – Linear scaling: based on height f(Area) ratio – Detailed inputs needed – No structural optimisation in scaling	Top design system Scaling constraint High downstream effects on other systems Cost fraction 10 → 20 %	Medium
Tower	Engineering Model	○ Material properties ○ Rotor Mass ○ Load Case Constraints	+ Static modelling + High partial safety factor for conservative approximation of mass + Adaptable to variation in k_{sys} and other economic/financial factors + Reliable Approximation of baseline mass, $\Delta mleq12\%$	– Dynamic influences disregarded, No modal analysis – Design criteria adapted from HAWTS – bottom founded case considered – Resource Intensive – Over predicts when compared to 5MW DeepWind baseline	Significant mass Contribution Cost fraction 10 → 16 %	Low

System	Type	Inputs	Application	Limitations	Impact	Trigger
Floater	Engineering Model - simplified	○ Material properties ○ Turbine Mass ○ Power-train Mass ○ Baseline Floater geometry	+ Draught and diameter optimisation for Static equilibrium at max heel angle + Adaptable to variation in k_{sys} and other economic/financial factors + Quick	– Stability of Floater and extreme waves loads not considered – Magnus forces ignored – Thickness scaled linearly – Influence of mooring pretension ignored	Largest mass and cost contribution Conservative hull thickness Cost fraction $\approx$ 27%	High
Mooring	Engineering Linear Scaling	○ Turbine torque ○ Baseline Mooring Geometry	+ Elastic catenary method for cable mass/length + Static case + Mooring arm geometry and mass scaled lineally + Good approximation of cable mass $\Delta mleq5\%$	– Unverified k_{sys} data – Installation costs taken as fixed value – Influence of added mass ignored – Dynamic influence on yaw stability not considered	Influence Floater design Low cost contribution<9 %	Low
Power - Train	Linear Scaling	○ Linear Scaling	+ Direct interpolation of mass and cost of DD PM DeepWind Generator between 5 and 20 MW + Inactive mass % estimated from Polinder et al. [61]	– Optimised specifically to DeepWind design – not interchangeable to different concept	High Upstream effects Floater design effect Significant cost fraction $\approx$ 17%	High
Electron - ics	Parametric	○ Based on HAWT cost model ○ Rated power, radius	+ Direct drive generators electronics + NREL cost model [37]	– HAWT based – VAWT controller differences not accounted – Accuracy Limited to sub 5MW designs	small Cost fraction $\leq$ 5%	Low

System	Type	Inputs	Application	Limitations	Impact	Trigger
Hardware	Parametric Linear scaling	○ Based on HAWT cost model ○ Power, radius	+ brake mass corrected with high safety factor for VAWT + Empirical approximation of Yaw bearing used + Reliable baseline mass bearing mass approximation $\Delta m \leq 10\%$	– HAWT based – Brake sizing inconsistent with requirements	small Cost fraction $\leq 5\%$	Low
Miscella-neous	Linear Scaling Knowledge based engineering	○ Referred from FOWT design studies	+ Marinsaton, Inactive mass estimations, Mainframe mass estimation + fixed mooring costs + Assumed fixed value for unknown costs	– Fixed values independent of site conditions – Lack of verifiable references	Second Largest Cost Fraction 20→15%	Medium

CAPEX - BoP

The balance of plant costs are derived from simulations made in OWFDE. The cost formulations used are derived from a combination of engineering and empirically derived parametric HAWT models. Care was taken to use those elements which can be generalised for both turbine concepts, however detailed analysis can reveal more important variations which can provide reliable estimates. . The approximation for the electrical infrastructure are perceived to be at a substantial level of accuracy but the installation costs, specifically for the mooring and consequently the linked decommissioning costs need to be re-evaluated. Comprising of $\leq 45\%$ of the CAPEX. The decommissioning costs when accounted for in the LCoE sum up to a very discounted value, but the CAPEXinvestment for the turbine and mooring installation can weight the LCoE in either direction by $\approxeq 8$ %. The relative inaccuracy coupled with the LCoE influence gives rise tot he following impact triggers.

Installation cost:	*High*
Grid Infrastructure	*Low*
Project Development	*Low*
Offshore substation	*Medium*

Chapter 7

Conclusions

The results for the LCoE show that there is substantial potential for the Deepwind FO-VAWT to demonstrate good economic feasibility if the technology is developed to the status of current state of the art wind energy technology. A LCoE from €113.56/MWh to €117.1/MWh for 5 to 15 MW turbines demonstrate a good scaling properties with rated power. A bit too optimistic in some regards but seem plausible when compared to the LCoE simulations at Horns Rev for a 49 * 5 MW HAWT farm using OWFDE. For those simulations a LCoE of €49/MWh was achieved whose results can be found in the Appendix, figure C.4. With respect to this, a thorough scaling process is needed to re-design the rotors and wind turbine systems specifically for the higher rated powers to attain a more accurate understanding of cost scaling with rated power.

The assumption that the H/ϕ remains constant for optimum performance for larger scales seems inaccurate as it is difficult to maintain aerodynamic similarity for the higher rated turbines. High Reynolds effects are perceived to be a problem for the 15 MW turbine, making the airfoil data used unreliable. Disregarding these effects and just concentrating on the mas escalations, the rotor mass increased more than would be expected with a refined design. Especially if the higher stiffness of a CFRP blade and consequent optimised internal thickness distribution is derived, however the thickness for both materials was kept the same in this study. It was observed that the chord has a significant impact on the mass scaling. Keeping the chord constant and scaling the rotor by 1.7 for the 15 MW scale resulted in a mass increase from 9.62e+05 to 5.297e+06. When scaling, the solidity should be reduced and tip speed increased from a cost perspective, but the added loading could result in different mass additions.

Despite this, the overall system mass did not scale with the same proportion of a HAWT as demonstrated by Ashuri [8] in figure A.3. The removal of pitch, yaw, hub assembly, low speed shaft, drive-train and overall lack of large tower top mass contributed positively to the mass scaling of VAWT's. Initially, the higher drive-train costs for VAWT's in order to manage the torque ripple made them an unattractive alternative to the HAWT concept [44], but the extensive adoption of DD generators has diminished this disadvantage substantially for both systems.

The Floater is seen to be a key cost driver in terms of independent systems contributing to the CAPEX. A variations in the Floater and mooring costs by 25% can bring about a LCoE variation by almost 5%. The Floater shows good scaling trends and when compared to the HyWind floating HAWT [64]. The overall draught length is less due to the lower over turning moment and lower turbine C_g. The ballast weight has majority of the mass component in the under water structure. Although having long structures adds to transportation and installation complexity, increasing the ballast mass is an effective way to reduce the weight and cost significantly. The implications of this on the stability of the structure are not clear thus making it an important aspect to drive future research.

The TCC CAPEX for the generator seem optimistic especially as the inactive mass costs have not been added. This basically accounts for the strucutral body housing. Auxiliary system costs were not estimated such as cooling systems, pumps, generator housing, main frame costs and sea level hub costs. Similarly the BoP costs per kW around €1200/kW are much lower from reality for an offshore wind farm. The lower price for the BoP was due to the inaccuracy of certain elements such as not considering any land transport cost, floater specific installation costs and operational permitting costs. However at the same time, the non optimised infield grid cables pushes the cost higher than it should be. As only one voltage is prescribed for the infield cables and not optimised between turbines, the diameter is overcompensated, meaning material cost is high . The dimensions of the cable are based upon the highest load connector resulting in the whole cable is the diameter of the point which has the highest power rating. The trade-off between having higher electrical infrastructure costs while having lower installation costs was not clarified through this study. Similarly, the cost implications of a floating wind farm substation can also be more adverse than estimated in this study.

With a specific focus to the DeepWind design, the mooring bearing is highly loaded system. As equations of motion were not modelled, it was difficult to explicitly correlate the load impacts due to gravity, wind, waves and rotation at the lower fixed point. Thus the estimation for the bearing mass and connected mooring system requires a deeper understanding in order to quantify the results in terms of cost effects.

In the LCoE parametric study with OPEX, the variation of the systems failure rate did not have the highest OPEX impact. Rotor failure incurs the biggest setback as the repair effort along with the increased downtime and reduced AEP, increase the LCoE significantly. Similarity generator reliability has a sufficient impact on the LCoE. DD machines are newer and suffer from a higher failure rates due to many reasons. These include the incorporation of more complex power electronics,, less design standardsiation thus less mature technology production rate and difficulty to sealing from environmental exposure due to large size, all are factors that currently hamper the reliability of direct drive generators [47]. However on the other hand, electrical failure incur less downtime as the repair procedure involves less complicated physical maintenance. Thus DD machines do have a higher yearly availability. The OMCE model is a good piece of simulation tool but more reliable cost estimations are needed to accurate capture the impact of a downtime. The failure rates for VAWT systems are not well compiled this a high failure rate of 4 was taken.

7.1 Recommendations

The novelty of vertical axis technology resulted in lack of appropriated standards, data and reliable cost modelling approximations/techniques. The methods used to estimate the cost were based on linear scaling and estimations made from existing HAWT technology. This lead to costs which in certain aspects are perceived to be low. The overall LCoE of €113.56/MWh is seen to be a very optimistic estimate by the author. This arises from reading the LCoE pie shown in figure 6.9a. Certain financial aspects such as tax depreciation, financing procedures, inflation, etc can also be considered to determine the nominal Cost of Energy which might give a more realistic estimate of the LCoE.

System design	**Impact**
Cost Reductive	
Fixed Blade	No pitch system
Omnidirectional	No Yaw system
Equal gravity loads	Low m_{blade}/length
Lower Power density	Distributed aerodynamic loads
Low C_g	Reduce Floater mass and draught, Better stability
Centrifugal stiffening	Low m_{blade} at R_{max}
No Yaw/Pitch Motors	Low OPEX, less Downtime
Power-train near MSL	Low OPEX
Cost Additive	
Longer Blades	High m_{blade}
Novel Technology	High Manufacturing costs, Project costs
Start up issues	Reduced AEP, energy input
Torque Ripple	System coupling, Resonances
Fixed Blade	High brake CAPEX
Low ω_{rated}	High Torque, Power Train CAPEX
Turbine Mass	Higher Floater mass

For the design load cases, rotational spar and torsion was disregarded. This could also have an impact on the tower and the generator design which should be investigated for the engineering cost modelling, especially when considering the downstream effect on the Floater. It is possible to look at HAWC2 simulations for a non rotating spar and a operational turbine in order to assess the impacts on stability from environmental loads. This could also make a better comparison against the dominant Floater design driver for the Floater sizing. A design study involving MDAO to analysis the scaling of the Floater and rotor is necessary to verify the possibility of FO-VAWT's having a lower LCoE than its HAWT counterpart.

The failure frequencies compiled from various sources give a distribution with respect to major systems for the rotor-tower and not the BoP. For FOWT or far offshore wind farms, this can be a source of repetitive problems. It leaves an area of presumption in lieu of lack of available reliability data for the impact on overall maintenance efforts and costs. Failures linked to the BoP, especially far offshore can lead to costly underwater repair efforts. To analyse the impact of the equipment costs on the OPEX, better estimates for the system reliability and supply chain costs are needed for a detailed study

The installation process for a FO-VAWT requires further research. The limiting factor for larger turbines is the large mass of the floater. Mid sea installation is unlikely to be cost effective. Whether the Floater is towed to location or assembled there is a question that requires answering and the procedure needed. The influence of depth of grid infrastructure and mooring installation are important aspects to consider for future research.

7.2 Final thoughts

Installing HVDC stations offshore are a necessary step forward in accessing far offshore wind resource while driving down the CoE for offshore wind. The vitalisation of far offshore grid connections through floating platforms is currently being realised under the framework of projects such as DolWin or BorWin. To realise the possibility of wind farms existing in a deep water environment, strong infrastructural support is required from the public bodies.

The future of offshore in the authors perspective is promising mainly where it is needed. Having favourable sea soil conditions (low depth) as in the North Sea is rare, making floating turbines more of a necessity than eventuality. However, for VAWT's to overtake current conventional turbines, strong academic and industrial R & D is necessary.

With respect to the DeepWind design, the concept requires more detail designing for proof of concept, especially with respect to the influence of friction drag for a rotating spar. The omission of LSS and a bearing does not justify the complications involved in accessing a generator housed >100 m below sea level. The cost and time needed to repair it will be too high to justify. The weight can be counteracted by heaving mooring wires or a bigger ballast.

More cost optimisation studies need to be done to verify the results of this thesis. The lack of experimental data and the novelty of the design leave a blank mark on the validity of the findings. Certain operational conditions such as wake losses and start-up losses should be considered when modelling a FO-VAWT farm.

References

[1] Nenuphar- offshore wind turbines, 15 August 2014. URL http://www.nenuphar-wind.com/company.

[2] Historic Inflation, 15 July 2014. URL http://www.inflation.eu.

[3] Ideol- moving the wind energy offshore, 17 August 2014. URL http://www.ideol-offshore.com/en.

[4] Structurae, 28 July 2014. URL http://structurae.info/ouvrages/eole.

[5] Rijksdienst voor ondernemend nederlands- Subsidies & Financiering wind sde+ 14, 3-09-2014. URL http://www.rvo.nl/subsidies-regelingen/wind-sde-2014.

[6] Supply Chain - the race to meet demand, 30 June 2014. URL http://www.altenergystocks.com/assets/Wind%20Directions.pdf.

[7] R. L. Arantegui. *2013 JRC Wind Status Repor.* European Commision Publications, 2014. ISBN 9789279344992.

[8] T. Ashuri. *Beyond Classical Upscaling: Integrated Aeroservoelastic Design and Optimization of Large Offshore Wind Turbines.* Ph.D. Thesis, Delft University of Technology, Delft, Netherlands, 2012.

[9] T.D. Ashwill. Developments in Large Blades for Lower Cost Wind Turbines. Technical report, Sandia, 2004.

[10] D. E. Berg. Structural Design of Sandia 34-meter Vertical-Axis Wind Turbine. Technical Report SAND84-1287, Sandia National Laboratories, 1985.

[11] David Berry. Innovation and the Price of Wind Energy in the US. *"Energy Policy"*, 37(11): 4493–4499, 2009. ISSN 03014215, 18736777, 0301-4215.

[12] P. A. Berthelsen. Floating spar bouy for the DeepWind Concept. Internal-unpublished 580239.00.01, Marintek, 2013.

[13] P. A. Berthelsen, L. Vita, I. Fylling, and U.S. Paulsen. Conceptual Design of a Floating Support Structure and Mooring System for a Vertical Axis Wind Turbine . In *"Conference Proceedings of OMAE 2012 "*, Rio De Janeiro, June 2012.

[14] B.H.Bulder, editor. *Future Innovative Solutions*, 2005. ECN. URL `http://wind.nrel.gov/public/SeaCon/Proceedings/Copenhagen.Offshore.Wind.2005/documents/papers/Future_innovative_solutions/B.Bulder_FloatingSystems_pp.pdf`.

[15] B.H.Bulder, S.A.M Barhorst, J.G. Schepes, and F. Hagg. *Theory and User Manual-BLADOPT*, 2001.

[16] D. L. Blonk. Conceptual Design and Evaluation of Economic Feasibility of Floating Vertical Axis Wind Turbines, 2010.

[17] Ringkøbing (Denmark) BTM Consult ApS. *International wind energy development - Offshore report 2013.* 2014.

[18] G.J.W. Van Bussel, B.H.Bulder, M.B. Zaaijer, and F.Hagg. Duch Offshore Wind Energy Covnertor - Task 12: Cost Comparison of Selected Concepts. Internal report, ECN, 2000.

[19] Charles P Butterfield, Walt Musial, Jason Jonkman, Paul Sclavounos, and Libby Wayman. Engineering challenges for floating offshore wind turbines, 2007.

[20] VGB PowerTech BV. Guideline- Reference Designation System for Power Plnats RDS-PP: Application explanation for wind power plants. Technical Report VGB-B 116 D2, 2007.

[21] CA Cermelli, DG Roddier, CC Busso, et al. Minifloat: A novel concept of minimal floating platform for marginal field development, 2004.

[22] Chaviaropoulos. Similarity rules for Wind Turbine Upscaling. Technical report, UPWIND, 2007.

[23] P.K. Chaviaropoulos, A. Natarjan, and P.H. Jensen. Key Performance Indicators and Target Values for Mulit-Megawatt Offshore Turbines. In *"Conference Proceedings of EWEA 2014 "*, Barcelona, March 2014.

[24] T.T. Cockerill. *Cost Medelling of Offshore Wind Energy Systems in Northern Europe*. Ph.D. Thesis, University of Sunderland, United Kingdom, 2005.

[25] International Electrotechnical Commission et al. Iec 61400-3. *Wind TurbinesPart 3: Design Requirements for Offshore Wind Turbines*, 2009.

[26] G. Corbetta and T. Miloradovic. Wind in Power: 2013 European Statistics, February 2014.

[27] Aina Crozier. Design and dynamic modeling of the support structure for a 10 MW offshore wind turbine, 2011.

[28] R.P. Van de Pieterman, H. Braam, and T.S. Obdam. OMCE-Calculator - Description of model "Default' 2.0'. Confidential ECN-Wind memo-12-003, Energy Research Centre of the Netherlands, 2012.

[29] R.P. Van de Pieterman, H. Braam, and T.S. Obdam. *OMCE - Calculator*, 2012.

[30] O. de Vries. Fluid Dyanmic Aspects of Wind Energy Conversion. Technical report, NLR, 2007.

[31] Granta Design. CES Edupack software, 2014.

[32] DTU RisøDNV. Guidelines for design of wind turbines, 2001.

[33] ECN. Image Data Archive, 15 June 2014.

[34] Andrea Eugster. Statoil – Presentation on HyWind at EWEM Summer School, 12 June 2014.

[35] C Simo Ferreira, H Aagaard Madsen, M Barone, B Roscher, P Deglaire, and I Arduin. Comparison of aerodynamic models for vertical axis wind turbines. *Journal of Physics: Conference Series*, 524(1), 2014.

[36] C.S Ferriera. *The near wake of a VAWT: 2D and 3D views of VAWT aerodyanmics.* Ph.D. Thesis, Delft University of Technology, Delft, Netherlands, 2009.

[37] L. Fingerish, M. Hand, and A. Laxson. Wind Turbine Design Cost and Scaling Model. Technical Report NREL/TP-500-40566, National Renewable Energy Laboratory, 2006.

[38] Dayton A. Griffin. WindPACT Turbine Desing Scaling Studies Technical Area 1 - Composite Blades for 80 to 120-Meter Rotor. Subcontractor report, NREL, 2001.

[39] D. Todd Griffith. Innovative Offshore Vertical Axis Wind Turbine Rotors Project, 17 June 2014.

[40] Koh Jian Hao, Amy N. Robertson, Jason Jonkman, Frederick Driscoll, and Eddie Y. K. Ng. Building and calibration of a fast model of the SWAY prototype floating wind turbine. pages 788–793, 2013.

[41] M. Heath. Deliverable 8.6: Lifetime Cost Modelling. UpWind Project 019945 (SES6), “Garrad Hassan and Partners Ltd”, Feb. 2011.

[42] S.A. Herman. DOWEC Cost Model - implementation. Technical Report DOWEC 068, ECN, 2005.

[43] Karin Ibenholt. Explaining learning curves for wind power. *Energy Policy*, 30(13):1181–1189, October 2002. URL `http://goo.gl/vFXeYql`.

[44] P. Jamieson. *Innovation in Wind Turbine Design.* Wiley, 2011. ISBN 9781119975458. URL `http://goo.gl/lJdO5l`.

[45] M. Khn, W. A. A. M. Bierbooms, G.J.W. van Bussel, M. C. Ferguson, B. Gransson, T.T. Cockerill, R. Harrison, L.A. Harland, J. H. Vugts, R. Wiecherink, and Kvaerner Turbin Ab. Structural And Economic Optimisation Of Bottom-Mounted Offshore Wind Energy Converters. 1999.

[46] BK Kirke and L Lazauskas. Enhancing the performance of a vertical axis wind turbine using a simple variable pitch system. *Wind Engineering*, 15(4):187–195, 1991.

[47] M. Lange, M. Wilkinson, and T. van Delft. Wind Turbine Reliability Analysis. In *“10th German Wind Energy Conference ”*, Bremen, November 2010.

[48] E. Lantz, R. Wiser, and M. Hand. IEA Wind Task 26: The Past and Future cost of Wind Energy. Technical Report NREL/TP-6A20-53510, National Renewable Energy Laboratory, May 2012.

[49] K. Leban. *Design tool for Direct Drive Wind Turbine Generators.* Ph.D. Thesis, Aalborg University, Aalborg, Denmark, 2014.

[50] H. A. Madsen. Actuator cylinder: A flow model for vertical axis wind turbine. *Proceedings of the BWEA Wind Energy Conference (British Wind Energy Association)*, pages 147–154, 1985.

[51] E.H.M. Mast. *Scenarios for Offshore Wind Power Development in the Netherlands; an Agent-Based modelling approach.* Ph.D. Thesis, Delft University of Technology, Delft, Netherlands, 2014.

[52] Denis Matha, Tim Fischer, Martin Kuhn, and Jason Jonkman, editors. *Model Development and Loads Analysis of a Wind Turbine on a Floating Offshore Tension Leg Platform*, February 2010. National Renewable Energy Laboratory.

[53] B.F. Snyder M.J. Kaiser. *Offshore Wind Energy Cost Modeling.* Green Energy and Technology. Springer, 2012. ISBN 1865-3529.

[54] M.J.Wolf. studie naas haalbaarheid van en randvoorwarden voor drijvende offshore windturbines. Technical Report NOVEM 224.721-0003, ECN, MARIN, TNO, TUD, MSC Gusto, Lagerwey the Windmaster, Decemeber 2002.

[55] Niels G. Mortensen. Planning and Development of Wind Farms: Wind Resource Assessment and Siting. Technical report, DTU Wind Energy, 12-2013.

[56] I. Paraschivoiu. *Wind Turbine Design: With Emphasis on Darrieus Concept.* Polytechnic International Press, 2002. ISBN 9782553009310. URL `http://books.google.nl/books?id=sefVtnVgso0C`.

[57] U.S. Paulsen, T.F. Pedersen, and L. Vit. Floating Vawt Wind Farm Concepts. Internal (2615), RisøDTU, National Laboratory for Sustainable Energy, February 2008.

[58] U.S. Paulsen, T.F. Pedersen, and L. Vita. Existing Vawt Technologies. Internal (2613), RisøDTU, National Laboratory for Sustainable Energy, February 2008.

[59] Uwe Schmidt Paulsen, Helge Aagard Madsen, Jesper Henri Hattel, Ismet Baran, and Per Horlyck Nielsen. Design Optimization of a 5 MW Floating Offshore Vertical-Axis Wind Turbine. *10TH DEEP SEA OFFSHORE WIND R&D CONFERENCE*, 35:22–32, 2013.

[60] T.F. Pedersen, U.S .Paulsen, and L. Vita. Floating Vawt Concepts. Internal (2614), RisøDTU, National Laboratory for Sustainable Energy, January 2008.

[61] H. Polinder, F.F.A van der Pijl, G.-J. de Vilder, and P.J. Tavner. Comparison of direct-drive and geared generator concepts for wind turbines. *Energy Conversion, IEEE Transactions on*, 21(3):725–733, Sept 2006. ISSN 0885-8969.

[62] B. Roscher. Structural Optimisation of a Vertical Axis Wind Turbine with Aeroelastic Analysis, 2014.

[63] K. Sarwar. Cost driven optimisation framework for vertical axis wind turbines, 04-2014.

[64] L.B. Savenije, T. Ashuri, G.J.W van Bussel, and J.W. Staerdahl. Dynamic modelling of spar-type floating wind turbine. In *"Proceedings of 2010 European Wind Energy Conference "*, pages 283–287, Warsaw, April 2010.

[65] M. Schelbergen. Structural Optimisation of multi-megawat, offshore vertical axis wind turbine rotors, 2013.

[66] Uwe Schmidt Paulsen, Helge Aagaard Madsen, Knud Abildgaard Kragh, Per Hrlyk Nielsen, and Ismet Baran. The 5 mw deepwind floating offshore vertical wind turbine concept design - status and perspective. *Proceedings - EWEA 2014*, 2014.

[67] S. Sheng. Report on Wind Turbine Subsystem Reliability - A Survey of Various Databases. Technical Report NREL/PR-5000-59111, National Renewable Energy Laboratory, 2013.

[68] G. Sieros, P.K. Chaviaropoulos, P. Jamieson, B.H. Bulder, and J.D. Sorensen. Upscaling Wind Turbines: theoretical and practical aspects and their impact on the cost of energy. *WIND ENERGY*, 15:3–17, 2012.

[69] P.J. Tavner, F. Spinato, G.J.W. Van Bussel, and E. Koutoulakos. Reliability of different wind turbine concepts with relevance to offshore application. *European Wind Energy Conference and Exhibition 2008*, 4:2311–2319, 2008.

[70] S. Tegen, E. Lantz, M. Hand, B. Maples, A.Smith, and P. Schwabe. 2011 Cost of Wind Energy Review. Technical Report NREL/TP-5000-56266, National Renewable Energy Laboratory, March 2013.

[71] Det Norske Veritas. Dnv-os-j103: Design of floating wind turbine structures. 2013.

[72] Luca Vita. *Offshore Vertical Axis Wind Turbine with Floating and Rotating Foundation.* Ph.D. Thesis, RisøDTU, National Laboratory for Sustainable Energy, Rosklide, Denmark, 2011.

[73] Michael Wilkinson, Keir Harman, Ben Hendriks, Fabio Spinato, and Thomas van Delft. Measuring Wind Turbine Reliability- results of the reliawind project. 2011.

[74] W. Xudong, W. Z. Shen, W. J. Zhu, J. N. Sorensen, and C. Jin. Shape Optimization of Wind Turbine blades. *'Wind Energy" - Chichchester*, 12(8):781–803, 2009. ISSN 1095-4244.

[75] M. Zaaijer. *Great Expectations for Offshore Wind Turbines: Emulation of wind farm design to anticipate their value for customers.* Ph.D. Thesis, Delft University of Technology, Delft, Netherlands, 2013.

Appendix A

Existing Cost Models

A.1 Definitions

1. **Levelised cost of energy**: is the constant unit cost (per kWh or MWh) of a payment stream that has the same present value as the total cost of building and operating a generating plant over its life.
2. **Balance of Plant**: BoP is the cost of all offshore engineering infrastructure such as electrical, foundation,permits, installation equipment, foundation and turbine installation
3. **Initial Capital Costs**: This is the summation of the turbine capital costs and balance of station costs.
4. **Turbine Capital Costs**: is the cost of all the components of a wind turbine which comprise into a finished product delivered by a manufacturer. for the floating concept this can or can not include the Floater and mooring system.

A.2 Review of CoE Models

Elaborating on the CoE models introduced in section 2.8 , a review of the main state-of-the-art in cost modelling is presented here. These projects summate the more prominent public research projects researching the promise of upscaling current wind turbine technology in terms of CoE. These projects along with research funded by the DoE in the USA have delivered cost models based on theoretical implications of up scaling derived from empirical models for the weight, cost and loads as a function of power capacity.

A.2.1 UpWind

The UpWind Project was the first initiative taken under the EU FP6 framework to look into the effects of up-scaling wind turbines to 8-10 MW or higher and wind farms above 500 MW respectively for both onshore and offshore applications. The aim of the project was to determine whether “Economies of Scale” hold valid for turbine technology and wind farm size growth, pushing down the CoE for larger machines and wind farms. The goal of the project was to present a framework of the different technological improvements developed in the UpWind project and determine the areas where more work was needed to decrease cost of energy as described by Sieros et al. [68].

Process Two different up-scaling methods for weight, cost and loads were compared; geometric theoretical up-scaling and empirical regression models based on data trends. Both indicated that technology breakthroughs are prerequisites for further up-scaling in a cost-efficient way Sieros et al. [68]. Finally, an optimisation framework was made to output hypothetical optimal designs based on life cycle cost analysis using generic cost models as functions of design parameters with technology growth adjusted up-scaling laws. This involved using *WindFarmer* ® (wind farm emulator) with integrated look up tables from a database of turbulence induced fatigue loads to study the affects on costs (failure) of critical components, Heath [41]. The effects of external factors on cost were studied in the complete design loop, focused on wind farm layout optimisation to achieve a better cost effectiveness, while the RNA was taken as a standard entry. The RNA component optimisation module used a simplified first cost model composed of two elements, one related to *mass* scaling and the other to manufacturing, *technology.* Technology is chosen as the factor that determines the learning curve for innovation and improvement over the years allowing for the theoretical 10-20 MW turbines to become more cost effective designs. The formulation created for the components CAPEX cost scaling was based on one main design parameter, *Rotor diameter.*

Results Based on current technology levels, up-scaling results in unfavourable weight increase. The linearised weighted cost model predicted that the levelised production cost of components increases with turbine size using the current state of technology. The overall optimisation gave a minimal cost of energy for the turbine at a larger optimum scale than the result of the component optimisation.Sieros et al. [68].

A.2.2 InnWind

The InnWind.EU project is a successor to the UpWind project under the context of the FP7 European Commission protocol. The goal was to formulate an innovative design of beyond state of the art 10-20 MW offshore wind turbines. A framework was established where different design for large offshore wind turbines (depth > 50 m) are compared based on *key performance indicators.* The LCoE targets stipulated under the EWII call for a 20% reduction in LCoE from 106.9 [€/MWh] in 2010 to 84.77 [€/MWh] by 2020.

Process The LCoE and its main components are discretised based on the technology used in the turbines along with the external factors driving the CoE. Sensitivities are established amongst its constituent elements to determine key components where "innovation in design" can result in lower CoE. Conventional *Square-Cube* up-scaling techniques Chaviaropoulos [22] are disregarded for mass scaling methods based on load estimations for larger turbines while maintaining a factor for "innovation in design", Chaviaropoulos et al. [23]. The focus to reduce LCoE is by optimising MW specific CAPEX for up-scaled turbines and improving operational efficiency of the wind farm. Investigations on OPEX are not sought with values taken from EWII assumptions while "Balance of Station" costs are varied as a combined exponent value. The turbine CAPEX and OPEX costs are adjusted for an discount rate of 5.4 % over the economic life time of a wind farm. The main parameters based on which load trends are scaled

1. rotational speed, ω
2. Tower Nacelle mass and
3. Rotor design thrust,

Results Up-scaling exponents for cost for the *Innovative Design* turbines of capacity 10, 15 and 20 MW were calculated to be 2.42, 2.80 and 2.90 respectively, figure A.1. The innovation calls for reduced costs and weight reduction in future designs based on technology improvement trends as compared to "classical up-scaling" which uses existing technology standards. This innovation stems from a higher rotational velocity with reduced loading (less thrust) and less specific Tower Nacelle mass resulting in a higher net wind farm capacity factor (+7%), reduced LCoE, decreasing BoP CAPEX and increased IRR, [figure A.2]. The proposed EWII 20% reduction in LCoE is presumed achievable by 2020 based on the presumption that technological improvements and innovation developments continue to increase over the years.

A.2.3 NREL

NREL carried out an array of extensive studies focused on the different systems of a wind turbine across a series of power ratings. These studies developed scaling relations for the systems, components and cost elements.

Limitations : Scaling functions for machines larger than 2MW's based on conceptual designs. It was inspired from the Sunderland model, where scaling relations of the components were determined as parametric functions from compiled empirical results. Baseline model is the GE 1.5 MW machine. Based on value of 2002 Dollar. Some cost elements dependant on the cost of the material which are de-scaled against a PPI. The costs for other aspects are based on the general inflation index. The Blades materials are only for fibreglass.

Components of CoE :

- Fixed Charge Rate: discount rate, taxes, financing fees, depreciation, return ond debt/equity = .1158/yr
- Initial Capital Costs: All systems and components cost of the WT including Balance of station costs, Control and safety system
- Operation and Maintenance costs
- AEP

Where Producer Price index is used per material as a component cost escalation and a GDP-general inflation escalation: Labour intensive components such as Rotor and Electrical components include a labour cost escalator, specified as the general inflation index.

A.3 Figures

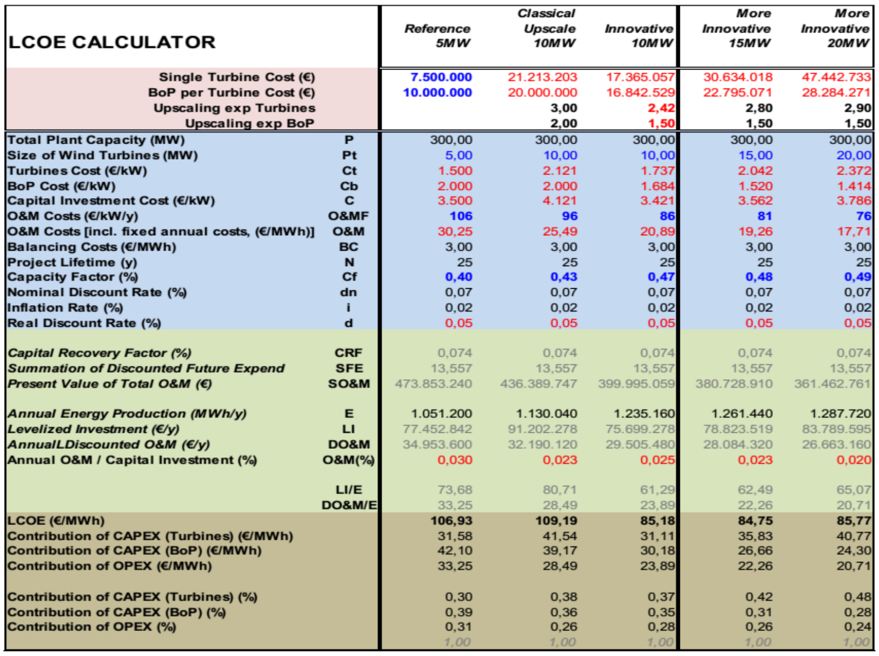

LCOE CALCULATOR		Reference 5MW	Classical Upscale 10MW	Innovative 10MW	More Innovative 15MW	More Innovative 20MW
Single Turbine Cost (€)		7.500.000	21.213.203	17.365.057	30.634.018	47.442.733
BoP per Turbine Cost (€)		10.000.000	20.000.000	16.842.529	22.795.071	28.284.271
Upscaling exp Turbines			3,00	2,42	2,80	2,90
Upscaling exp BoP			2,00	1,50	1,50	1,50
Total Plant Capacity (MW)	P	300,00	300,00	300,00	300,00	300,00
Size of Wind Turbines (MW)	Pt	5,00	10,00	10,00	15,00	20,00
Turbines Cost (€/kW)	Ct	1.500	2.121	1.737	2.042	2.372
BoP Cost (€/kW)	Cb	2.000	2.000	1.684	1.520	1.414
Capital Investment Cost (€/kW)	C	3.500	4.121	3.421	3.562	3.786
O&M Costs (€/kW/y)	O&MF	106	96	86	81	76
O&M Costs [incl. fixed annual costs, (€/MWh)]	O&M	30,25	25,49	20,89	19,26	17,71
Balancing Costs (€/MWh)	BC	3,00	3,00	3,00	3,00	3,00
Project Lifetime (y)	N	25	25	25	25	25
Capacity Factor (%)	Cf	0,40	0,43	0,47	0,48	0,49
Nominal Discount Rate (%)	dn	0,07	0,07	0,07	0,07	0,07
Inflation Rate (%)	i	0,02	0,02	0,02	0,02	0,02
Real Discount Rate (%)	d	0,05	0,05	0,05	0,05	0,05
Capital Recovery Factor (%)	CRF	0,074	0,074	0,074	0,074	0,074
Summation of Discounted Future Expend	SFE	13,557	13,557	13,557	13,557	13,557
Present Value of Total O&M (€)	SO&M	473.853.240	436.389.747	399.995.059	380.728.910	361.462.761
Annual Energy Production (MWh/y)	E	1.051.200	1.130.040	1.235.160	1.261.440	1.287.720
Levelized Investment (€/y)	LI	77.452.842	91.202.278	75.699.278	78.823.519	83.789.595
AnnualLDiscounted O&M (€/y)	DO&M	34.953.600	32.190.120	29.505.480	28.084.320	26.663.160
Annual O&M / Capital Investment (%)	O&M(%)	0,030	0,023	0,025	0,023	0,020
	LI/E	73,68	80,71	61,29	62,49	65,07
	DO&M/E	33,25	28,49	23,89	22,26	20,71
LCOE (€/MWh)		**106,93**	**109,19**	**85,18**	**84,75**	**85,77**
Contribution of CAPEX (Turbines) (€/MWh)		31,58	41,54	31,11	35,83	40,77
Contribution of CAPEX (BoP) (€/MWh)		42,10	39,17	30,18	26,66	24,30
Contribution of OPEX (€/MWh)		33,25	28,49	23,89	22,26	20,71
Contribution of CAPEX (Turbines) (%)		0,30	0,38	0,37	0,42	0,48
Contribution of CAPEX (BoP) (%)		0,39	0,36	0,35	0,31	0,28
Contribution of OPEX (%)		0,31	0,26	0,28	0,26	0,24
		1,00	1,00	1,00	1,00	1,00

Figure A.1: *Levelised Cost of Energy Calculation for classical and innovation based up-scaling,([23, 51])*

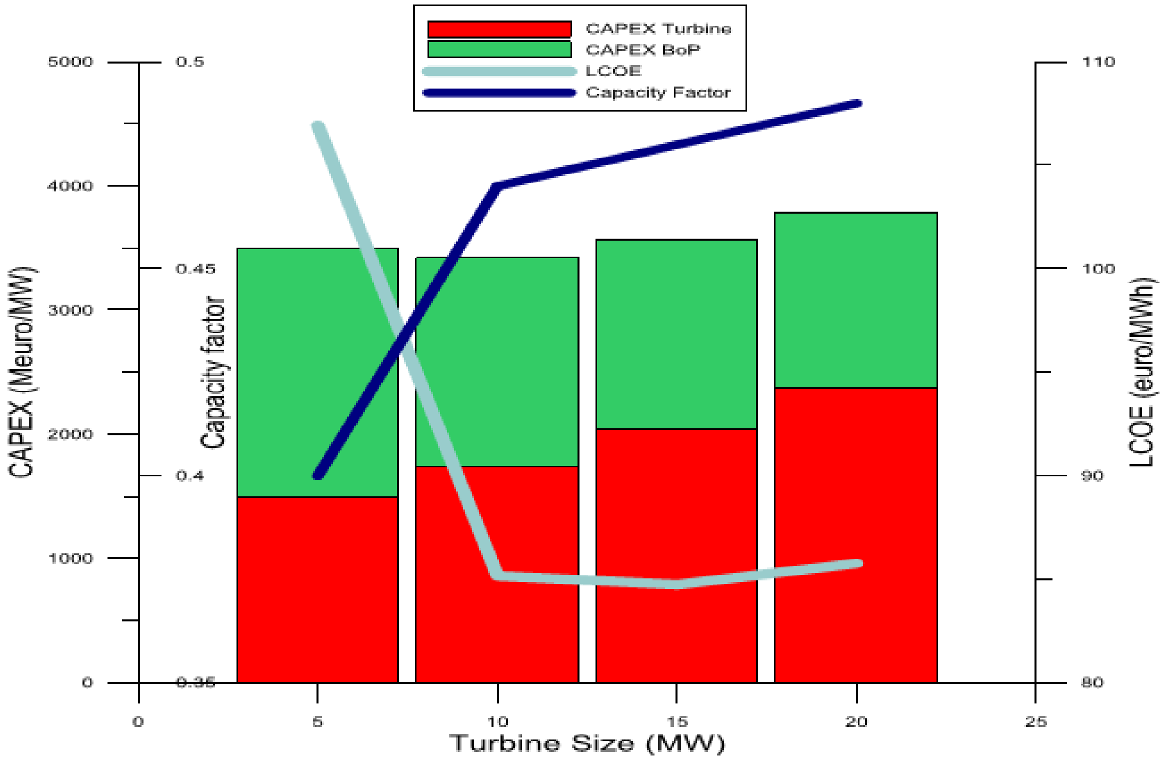

Figure A.2: *Turbine Size influence on LCoE and its main drivers,([23, 51])*

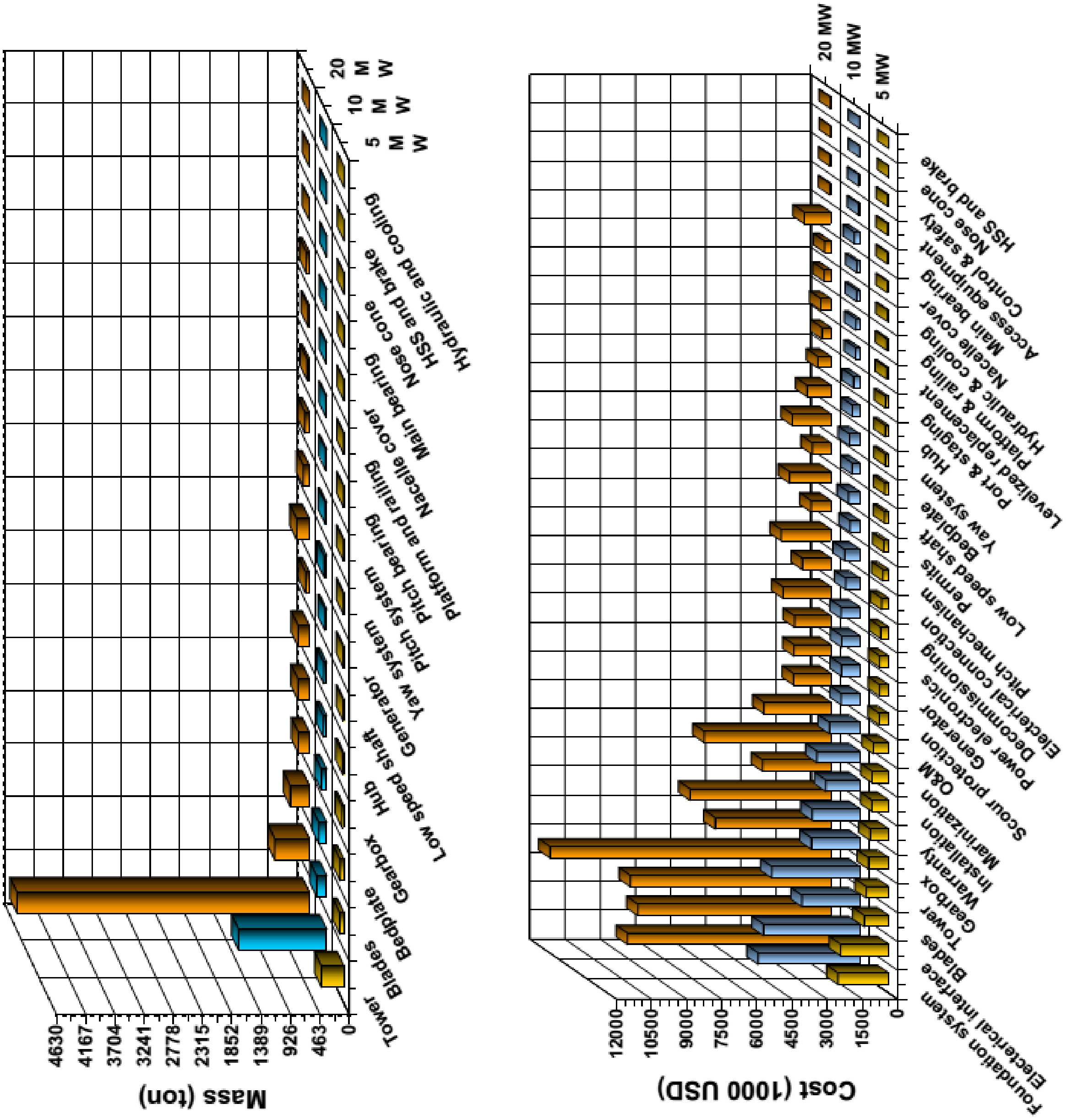

(a) Mass Trends

(b) Cost Trends

Figure A.3: *Mass breakdown and Cost elements for Optimised 5,10 and 20 MW* HAWT *derived by Ashuri [8]*

.

Appendix B

Model Estimations

B.1 Area Mapping

In this section, an area estimation is formulated of the VAWT blade cross section for the *spar*, *shear*, *skin* to subsequently determine the volume of each the segments. However, the following modelling is limited to symmetrical airfoils from the NACA 4 digit series. Based on the illustration given in figure 4.15, the ellipse is constraint such that

- The major axis is equal to half the chord, $2b = 0.5 \cdot C$
- The origin of the ellipse 'O_e' is presumed to be located at the quarter chord, $c_e = 0.25 \cdot C$.
- The shear web is be fixed at the quarter chord with the other shear web is fixed at the half chord length

These presumptions allow for simplifications in area estimation. By placing two concentric ellipses with an origin at the quarter chord, the semi-minor 'a' value becomes equal to half the airfoil thickness 't_{af}'. Thus $(t/C) \cdot C = 2a$. For the given t/C of the airfoil, the eccentricity is determined using the scaling fit from figure 4.14

$$\epsilon = -2.739(t_{AF})^2 + 0.239t_{AF} + 0.983 \tag{B.1}$$

The assumed value of 'a' can be confirmed to be $\approxeq b \cdot \sqrt{1-\epsilon^2}$. The respective skin thickness t_{skin} is subtracted from the axes to get dimensions of inner ellipse a_{in}, b_{in}.

$$A_{le} = \pi \cdot (ab - a_{in}b_{in}) \tag{B.2}$$

The area of the spar and shear web is taken separately rather than as a difference in area of two concentric rectangles. This was to allow different material specifications for the spar and shear webs during cost calculations.

$$\begin{align} A_{spar} &= 2b \cdot (a - (a - t_{spar})) \tag{B.3} \\ A_{shear} &= 2a \cdot (b - (b - 2t_{shear})) \tag{B.4} \\ & \tag{B.5} \end{align}$$

The trailing section of the airfoil from $0.5 > C < 1$, a triangle is assumed. With the height (h_t) equal to $C/2$ and base equal to '$2a$', the angle between the shear web and skin is $\theta = \tan^{-1}\left(\frac{h_t}{a}\right)$.

$$A_{tail} = \frac{1}{2}\left((h_t \cdot 2a) - (a - t_{skin} \cdot \tan(\theta))\right) \tag{B.6}$$

Error Sources

Mapping the blade cross section using simple geometric constraints does add some minor error in accurately predicting the volume of the blade. The differences from actual values arise due to two main reasons

- as the airfoils get thicker airfoils ($t/C \geq 35\,\%$) the curvature in the mid section renders approximation with an orthogonal shape less feasible. Thus, the base of the tail region is also no longer equal to '$2a$'
- The Constraint on the chord-wise location of the shear webs. For larger wind turbines, the blade structure is designed with more shear webs at further distances

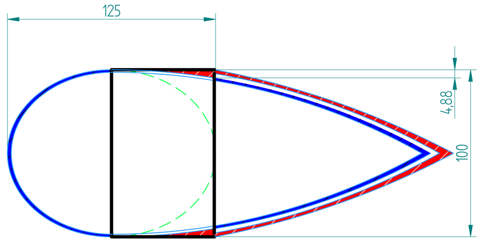

Figure B.1: *Illustration of area estimation error using box beam for mid section*

To determine the error percentage, an example case for NACA0040 was considered. A calculation of the difference in area estimated for a box beam and the tail segment was as compared to the actual area determined from a *CAD* model. The combined error in Area came out to be $\approx 7\%$. This was not considered a sufficient inaccuracy to render the large inconsistencies. Hence the area mapping method was not altered but a tolerance of $\triangle\varepsilon = \pm 5\%$ was considered in the mass estimations. In figure B.1, the red portion marks the area of error

B.2 Estimation of Production Price

The system production prices for a conventional HAWT glass fibre blades were obtained from the DOWEC project (Bussel et al. [18]) , WindPACT studies (Griffin [38]) and corrected for inflation to present day cost. A compilation of the annual inflation rates for countries with a strong wind energy sector figure B.2 were used to escalate the cost of production against the consumer price index, (inf [2]).

The inflation rate is based on the consumer price index. From the figure , the effective inflation for the EU from 2000 - 2014 is estimated at 30.11 % and for USA at 35.81 %. The correction of back dated cost data is done using the cumulative inflation rate till present from the date in question.

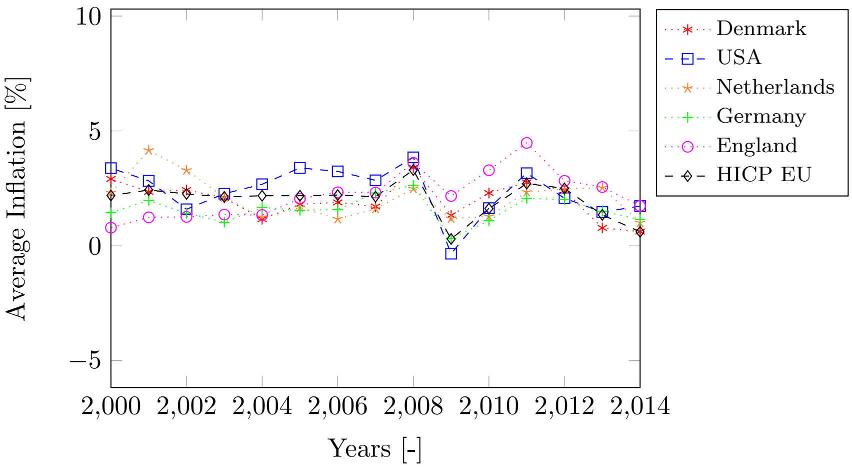

Figure B.2: *historic average annual inflation rates for major wind turbine manufacturing countries , inf [2]*

Rotor For the blades, the production prices and adjustment from various sources is given in table B.3. The blades material was glass fibre reinforced plastics with foam and wood-epoxy layers.

An inflation escalation of 27.04(Denmark), 30.87(Netherlands), 32.43 and 23.06(USA) were used row wise in table B.3, giving an average cost per kg to make a GFRP blade at about €11-13/kg. An However, as the size of wind turbines has increased drastically over the years, cost scales with a higher power than mass with increasing diameter, (Sec 2.8). Thus, despite the advances in technology, the larger sizes of turbine rotors have contributed to an increase of production cost of a wind turbine blade instead of decreasing according to the economies of scale. This is attributed to the used of better materials to cope with higher loads, higher indirect costs such as installation, transportation and impacts from economic recession. To improve on the estimate for the Cost/kg of a wind turbine blade, the cost breakdown for a conventional horizontal axis wind turbine is used from table B.1 to decipher system production cost for modern wind turbines.

Based on this breakdown, the cost of rotor for the following 3 bladed turbines is deciphered from the known costs and mass of certain turbines.

NREL 5MW (Ashuri [8])	63.5 m, Material: GFRP	68553 kg	€3173 k
NREL 5MW (Ashuri [8])	63.5 m, Material: CFRP	53220 kg	€3187 k
Drijfwind (drijfwind report)	55 m, Material: GFRP	110000 kg	€2875 k

Based on these, the cost per kg for one blade of a HAWT for different materials comes out to be

GFRP	€15.43 (2009), €9 (2002)
CFRP	€19.9 (2009)

The cost of GFRP material is generally between €5-7 and for CFRP material is around €18-20 per kg as understood from KBE and Design [31]. The compilation of blade SPP costs given in table B.3 and results presented above, the final production price taken after inflation correction for a rotor blade made out of GFRP is at **€10.5/kg** and **€22/kg** for CFRP.

Floater & Mooring The source of cost estimations taken for the Floaterand mooring system included a detailed study for the "Drijfwind" project and the "NREL" TLP study from an ECN presentation (B.H.Bulder [14]) in figure B.3.

Component	**Cost Fraction 1**	**Cost Fraction 2**
Blade	0.182	0.222
Hub assembly	0.025	0.015
Gearbox	0.169	0.129
Generator	0.066	0.07
Yaw System	0.030	0.018
Nacelle Cover	0.012	0.013
Mainframe	0.034	0.028
Tower	0.0157	0.263
Power electronics	0.097	0.086
Pitch System	0.064	0.046
Rotor Brake	0.015	0.013
Couplings	0.01	0.01
Main Shaft	0.03	0.019
Bearings	0.03	0.012
Misc	0.065	0.056
Total	1.0	1.0

Table B.1: HAWT *Cost fraction distribution from win, Blonk [6, 16]*

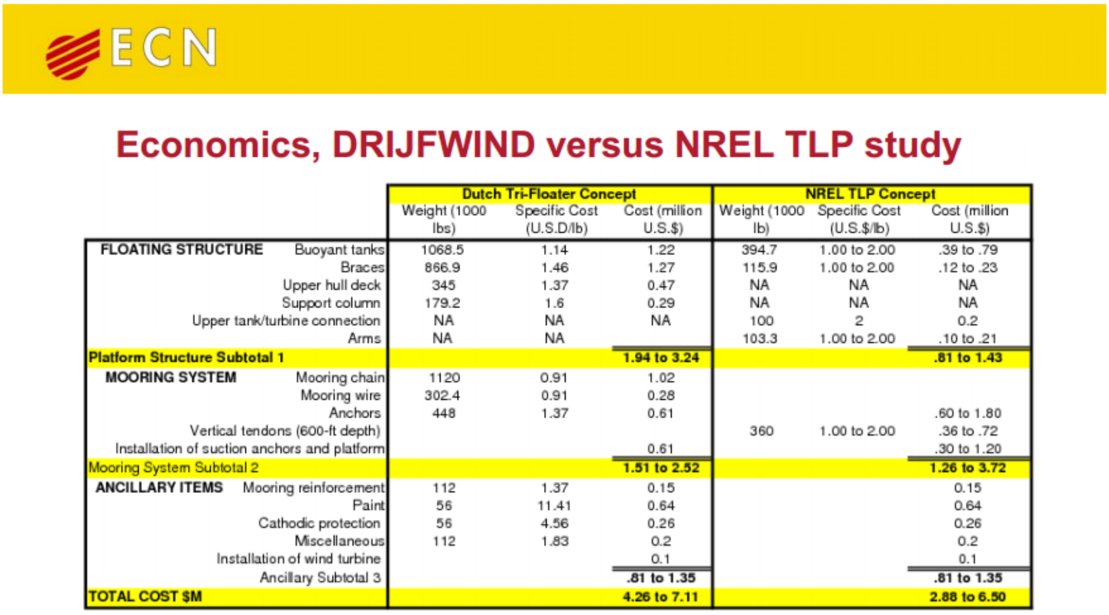

Economics, DRIJFWIND versus NREL TLP study

		Dutch Tri-Floater Concept			NREL TLP Concept		
		Weight (1000 lbs)	Specific Cost (U.S.D/lb)	Cost (million U.S.$)	Weight (1000 lb)	Specific Cost (U.S.$/lb)	Cost (million U.S.$)
FLOATING STRUCTURE	Buoyant tanks	1068.5	1.14	1.22	394.7	1.00 to 2.00	.39 to .79
	Braces	866.9	1.46	1.27	115.9	1.00 to 2.00	.12 to .23
	Upper hull deck	345	1.37	0.47	NA	NA	NA
	Support column	179.2	1.6	0.29	NA	NA	NA
	Upper tank/turbine connection	NA	NA	NA	100	2	0.2
	Arms	NA	NA		103.3	1.00 to 2.00	.10 to .21
Platform Structure Subtotal 1				**1.94 to 3.24**			**.81 to 1.43**
MOORING SYSTEM	Mooring chain	1120	0.91	1.02			
	Mooring wire	302.4	0.91	0.28			
	Anchors	448	1.37	0.61			.60 to 1.80
	Vertical tendons (600-ft depth)				360	1.00 to 2.00	.36 to .72
	Installation of suction anchors and platform			0.61			.30 to 1.20
Mooring System Subtotal 2				**1.51 to 2.52**			**1.26 to 3.72**
ANCILLARY ITEMS	Mooring reinforcement	112	1.37	0.15			0.15
	Paint	56	11.41	0.64			0.64
	Cathodic protection	56	4.56	0.26			0.26
	Miscellaneous	112	1.83	0.2			0.2
	Installation of wind turbine			0.1			0.1
	Ancillary Subtotal 3			**.81 to 1.35**			**.81 to 1.35**
TOTAL COST $M				**4.26 to 7.11**			**2.88 to 6.50**

Figure B.3: *System production costs for Floater and mooring system*

These costs are for tri-floater for the Drijfwind project M.J.Wolf [54] and a floating tension leg platform Matha et al. [52] which are assumed to have same cost structure as compared to floating spar. The costs per unit mass were adjusted to present day values using the GDP inflation given in figure B.2.

The cost of the ballast is taken from Marintek report on the DeepWind project (Berthelsen [12]) as €50/tonne. The material within the ballast is water saturated olivine with a density of 2600 kg/m^3.

B.2.1 Other Cost Parameters

The fixed cost fraction and mature production process level or technology growth factor are terms first introduced in the cost model from Griffin [38] and subsequently implemented by Chaviaropoulos et al. [23] and Heath [41]. Although in the UPWIND and INNWIND project, the MPL is modified as a time dependant technology learning factor which drives down the cost factor of the system being produced through innovation and economies of scale. FCF is a function of power while MPL is a function of the number of blades produced or the years of process experience is held. In this case, it depends on the number of wind turbines in the wind farm.

Table B.2: *Fixed cost and mature production process level fractions*

Power (MW)	FCF[%]	MPL [%]	Year
5	2.2	1.24	3
10	4.08	1.14	5
15	5.96	1.07	10

The producer price index, PPI was tabulated from the bureau of labor statistics for the relevant materials used in the structure.

Table B.3: *System production prices corrected for inflation based on location of study, EU or USA.*

Source	Type	SPP [Cost/kg]	Adjusted SPP [Cost/kg]
Rotor blade			
NEG Micon (2001)	50 - 80 [m]	€10.9	€13.8
Bladopt (2000)	50 - 90 [m]	€9.0	€11.8
WindPACT- (2001)	40 - 60 [m]	$9.5	$12.9
NREL- LM Blades (2005)	70 - 90 [m]	$11.1	$13.7
Power Train			
Leban [49] (2014)	Copper Windings	€15	–
	Sintered Iron	€36	–
	Rare Earth Elements	€50	–
Floater			
Drijfwind Study (2005)	Buoyancy tank	$2.51	$2.96
	Braces	$3.2	$3.77
	Support column	$3.0	$3.53
Marintek (2013)	Ballast liquid	€0.05	€0.05
	General Steel	€3.75	€3.75
DOWEC (2003)	Protection Coating	€3.0/m^2	€3.63/m^2
Mooring System			
Drijfwind Study (2005)	Mooring chain	$2.0	$2.36
	Mooring wire	$2.0	$2.36
	Anchors	$3.0	$3.53
	Installation (fixed)	$0.61 M	$0.718 M
NREL TLP (2005)	Anchor arms	$3.3	$4.06

B.2.2 Labour Percentage estimations

Accounting for labour costs is very dependent on the labour market being considered. Constructions costs in different regions have different rates and thus constitute to different percentages of the total wind turbine CAPEX. A study was done in Lantz et al. [48] on the cost comparison between wind turbines constructed in two European countries, Spain and Denmark and USA. The labour costs were levelised from 2002 till 2008 and reduced a fraction per installed capacity.

The labour cost fraction per installed MW was approximately 9.14 % per kW while the least was for Spain with a labour cost fraction of 4.6% per kW. Both these values define the range of variation of labour costs on the total wind turbine CAPEX.

B.3 Cost Driven Optimisation Framework

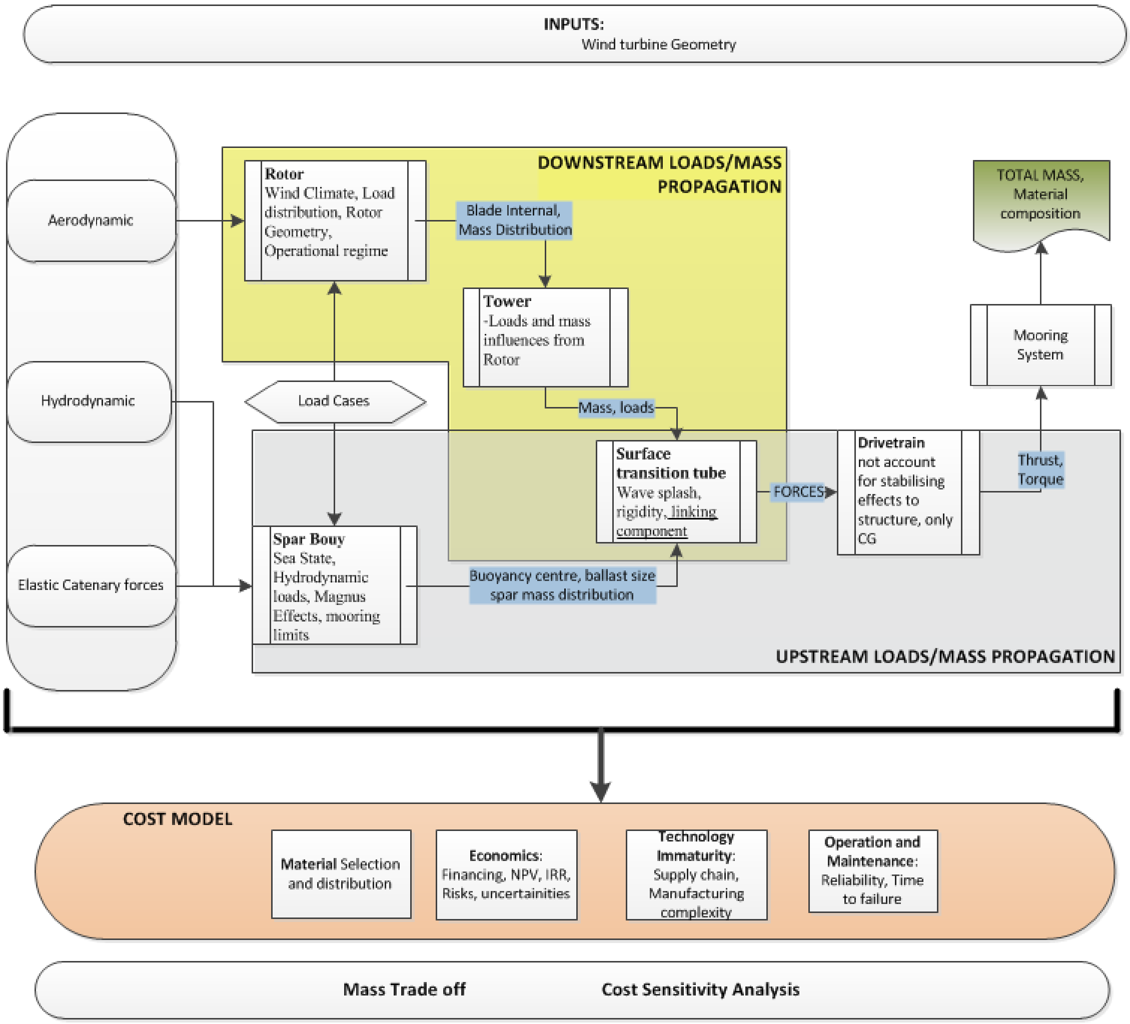
INPUTS:
Wind turbine Geometry
Aerodynamic
Hydrodynamic
Elastic Catenary forces
DOWNSTREAM LOADS/MASS PROPAGATION
Rotor
Wind Climate, Load distribution, Rotor Geometry, Operational regime
Blade Internal, Mass Distribution
Tower
-Loads and mass influences from Rotor
Load Cases
Mass, loads
Surface transition tube
Wave splash, rigidity, linking component
FORCES
Drivetrain
not account for stabilising effects to structure, only CG
Spar Bouy
Sea State, Hydrodynamic loads, Magnus Effects, mooring limits
Buoyancy centre, ballast size spar mass distribution
TOTAL MASS, Material composition
Mooring System
Thrust, Torque
UPSTREAM LOADS/MASS PROPAGATION
COST MODEL
Material Selection and distribution
Economics: Financing, NPV, IRR, Risks, uncertainities
Technology Immaturity: Supply chain, Manufacturing complexity
Operation and Maintenance: Reliability, Time to failure
Mass Trade off
Cost Sensitivity Analysis

Figure B.4: VAWT *Cost Driven Design framework presented by Sarwar [63]*

K13 Site, 245 MW FO-VAWT Wind Farm

Park Specifications

# of turbines	49	Type of Turbine	DeepWind	Electricity base (SDE)	0.05
Site Area	30.1	Power Rating(MW)	5	Assumed Electicity price	0.13
AEP	18.018	Total Power output (MW)	245	**Select Wind turbine rating**	5MW
AEP_p50	15.144	AEP Multiplier	1		
AEP WF(GwH)	8.83E+02	Capex Multiplier	1		

Period	**years**	**20**	**E Price**
Capital cost	**€**	**6.19E+08**	
Approx O&M running Cost	**€/kWh**	**0.058**	
Production	**kWh/year**	**8.83E+08**	
Revenue Potential 1	**€**	**7.39E+07**	**8.37E-02**
Revenue Potential 2	**€**	**9.30E+07**	**1.05E-01**
Revenue Potential 3	**€**	**1.01E+08**	**1.15E-01**
Revenue Potential 4	**€**	**1.16E+08**	**1.32E-01**
Discount rate	**%**	**7**	0.07
Capacity factor	**%**	**41.1369863**	
Full load hours		**3603.6**	
O&M old method	**/year**	**3.59E+07**	
O&M OMCE	**€/year**	**4.18E+07**	
Electricity sales	**€/year**	**1.16E+08**	
Net income	**€/year**	**7.44E+07**	
NPV @ r = 7%	**€**	**1.69E+08**	
PBT(fixed)	**€**	**8.32E+00**	
LCoE	**€**	**0.11357**	
CoE	**€/KwH**	**0.075409323**	
NPV (Excel)	**€**	**1.69E+08**	
IRR (Excel)	**%**	**10%**	

Capital costs (Mil. €)	
Turbines	504.17674
BoP	115.2616
O & M	4.43E+02
flt	187.8428
Balance of Plant	303.10441
Turbine Capital Costs	316.33394
decommissioning	19.358322
Mil. € / MW	2.52831977
Total	619.438343

LINKED TABLE	**5MW**	**10 MW**	**15 MW**
GFRP 5MW (Mil)	1.03E+07	2.24E+07	3.47E+07
CFRP 5MW (Mil)	1.08E+07	2.40E+07	3.77E+07
WF installed Capacity	245	250	240
Number of Turbines	49	25	16
floater Mooring cost	3.83E+06	7.53E+06	1.17E+07
BoP Cost	1.15E+08	9.77E+07	8.83E+07
AEP p50_max	18.02	37.57	57.96
AEP p50_min	15.14	31.58	48.71
O &M effort [1 yr] (Mil)	4.18E+01	4.56E+01	4.78E+01
O &M effort / turbine/yr	8.53E-01	1.82E+00	2.99E+00
O&M cost per kW-yr	1.71E+02	1.82E+02	1.99E+02
Decommisioning	1.94E+07	1.18E+07	9.15E+06
Annual Opex (Eurocents/	4.28	4.44	4.67

Discounted Cash Flow

Years	Costs	Revenue	Fixed Bal	Discount	PV	Discnt Bal	opex dscnt	rev discnt	dsnt Elec	dicnt LEC	CRF	NPV_C*CRF
year -2	2.06E+08	0.00E+00	-2.06E+08	1.0000	-2.06E+08	-2.06E+08	-2.06E+08	0.00E+00				
year -1	2.06E+08	0.00E+00	-2.06E+08	1.0000	-2.06E+08	-2.06E+08	-2.06E+08	0.00E+00				
0	2.06E+08	0.00E+00	-2.06E+08	1.0000	-2.06E+08	-6.19E+08	-2.06E+08	0.00E+00		6.19E+08	1	6.19E+08
1	4.18E+07	1.16E+08	7.44E+07	0.9346	6.96E+07	-5.50E+08	-3.91E+07	1.09E+08	1.07E+08	3.91E+07	1.0700	4.18E+07
2	4.18E+07	1.16E+08	7.44E+07	0.8734	6.50E+07	-4.85E+08	-3.65E+07	1.02E+08	1.00E+08	3.65E+07	0.5531	2.02E+07
3	4.18E+07	1.16E+08	7.44E+07	0.8163	6.08E+07	-4.24E+08	-3.41E+07	9.49E+07	9.37E+07	3.41E+07	0.3811	1.30E+07
4	4.18E+07	1.16E+08	7.44E+07	0.7629	5.68E+07	-3.67E+08	-3.19E+07	8.87E+07	8.76E+07	3.19E+07	0.2952	9.41E+06
5	4.18E+07	1.16E+08	7.44E+07	0.7130	5.31E+07	-3.14E+08	-2.98E+07	8.29E+07	8.18E+07	2.98E+07	0.2439	7.27E+06
6	4.18E+07	1.16E+08	7.44E+07	0.6663	4.96E+07	-2.65E+08	-2.79E+07	7.74E+07	7.65E+07	2.79E+07	0.2098	5.84E+06
7	4.18E+07	1.16E+08	7.44E+07	0.6227	4.64E+07	-2.18E+08	-2.60E+07	7.24E+07	7.15E+07	2.60E+07	0.1856	4.83E+06
8	4.18E+07	1.16E+08	7.44E+07	0.5820	4.33E+07	-1.75E+08	-2.43E+07	6.76E+07	6.68E+07	2.43E+07	0.1675	4.07E+06
9	4.18E+07	1.16E+08	7.44E+07	0.5439	4.05E+07	-1.35E+08	-2.27E+07	6.32E+07	6.24E+07	2.27E+07	0.1535	3.49E+06
10	4.18E+07	1.16E+08	7.44E+07	0.5083	3.78E+07	-9.67E+07	-2.12E+07	5.91E+07	5.83E+07	2.12E+07	0.1424	3.03E+06
11	4.18E+07	1.16E+08	7.44E+07	0.4751	3.54E+07	-6.13E+07	-1.99E+07	5.52E+07	5.45E+07	1.99E+07	0.1334	2.65E+06
12	4.18E+07	1.16E+08	7.44E+07	0.4440	3.30E+07	-2.83E+07	-1.86E+07	5.16E+07	5.10E+07	1.86E+07	0.1259	2.34E+06
13	4.18E+07	1.16E+08	7.44E+07	0.4150	3.09E+07	2.63E+06	-1.73E+07	4.82E+07	4.76E+07	1.73E+07	0.1197	2.08E+06
14	4.18E+07	1.16E+08	7.44E+07	0.3878	2.89E+07	3.15E+07	-1.62E+07	4.51E+07	4.45E+07	1.62E+07	0.1143	1.85E+06
15	4.18E+07	1.16E+08	7.44E+07	0.3624	2.70E+07	5.85E+07	-1.52E+07	4.21E+07	4.16E+07	1.52E+07	0.1098	1.66E+06
16	4.18E+07	1.16E+08	7.44E+07	0.3387	2.52E+07	8.37E+07	-1.42E+07	3.94E+07	3.89E+07	1.42E+07	0.1059	1.50E+06
17	4.18E+07	1.16E+08	7.44E+07	0.3166	2.36E+07	1.07E+08	-1.32E+07	3.68E+07	3.63E+07	1.32E+07	0.1024	1.36E+06
18	4.18E+07	1.16E+08	7.44E+07	0.2959	2.20E+07	1.29E+08	-1.24E+07	3.44E+07	3.40E+07	1.24E+07	0.0994	1.23E+06
19	4.18E+07	1.16E+08	7.44E+07	0.2765	2.06E+07	1.50E+08	-1.16E+07	3.21E+07	3.17E+07	1.16E+07	0.0968	1.12E+06
20	4.18E+07	1.16E+08	7.44E+07	0.2584	1.92E+07	1.69E+08	-1.08E+07	3.00E+07	2.97E+07	1.08E+07	0.0944	1.02E+06
	8.33E+08	**2.32E+09**	**1.49E+09**		**0.00E+00**		**-4.43E+08**	**0.00E+00**	1.22E+09	1.06E+09		**7.49E+08**
								CoE		1.14E-01		8.49E-01

Appendix C

Balance of Plant Cost Simulations

The costs associated with wind farms for different turbine ratings and overall capacity were evaluated with the site conditions for Horns Rev. Hoowever as no wake model is implemented, thus no AEP calculations are performed as part of the simulation. This nullifies any constraints from the meteorological data and the impact on BoP costs for grid infrastructure and installation become a direct consequence of the turbine rating and wind farm geometry.

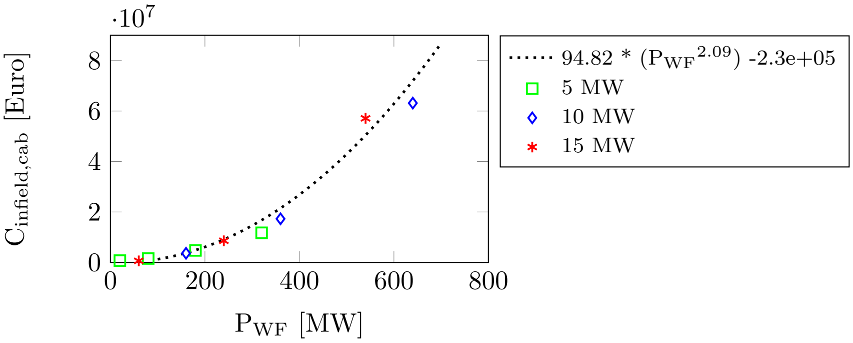

(a) 5ϕ spacing

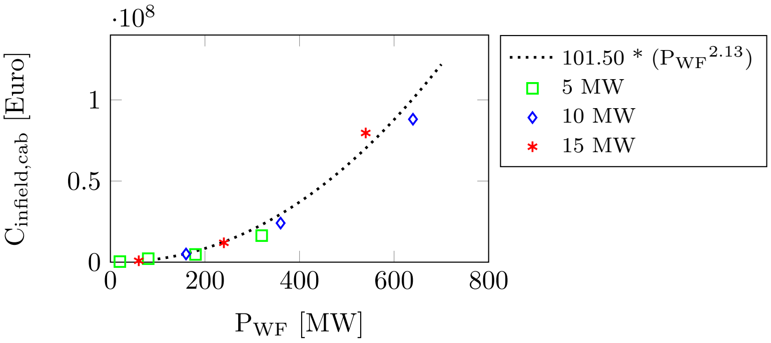

(b) 7ϕ spacing

Figure C.1: *Scaling fit for BoP cable costs vs increasing WF power capacity*

To generate the initial estimates for the BoP costs as a function of the components mentioned in

Section (5.3), the following assumptions were made.

1. The infield cable voltage was fixed at 45kV while transmission cable was fixed at 220 kV for all WF's in Table 5.2
2. The Generator voltage values are taken from Leban [49], kept at a constant 13500 [V]

From the figure C.1, it can be seen that for an equal spacing, the cables capex costs are independent of size of turbine but more dependant on power rating of wind farm. This seems reasonable as for a fixed voltage level, the mass of a cable is dictated by the maximum current flowing through it for certain power capacity. Establishing a trend for the internal grid cable installation cost, a dependency of the cable length was made to power intensity ((P_I)) for a wind farm. As $C_{cab,ins}$ varied linearly with increasing wind farm power capacity and area, a ratio of the two was used to define a parametric function against which the cable length (proportional cable installation cost) is scaled. For each wind turbine power rating, the graphs how similar behaviour, however with a specific offset.

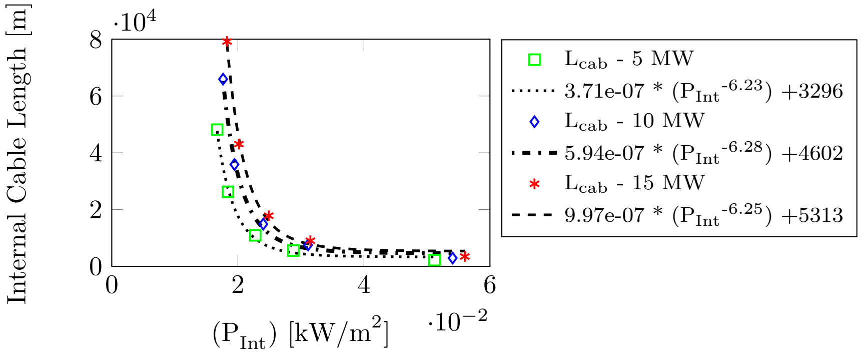

(a) 5ϕ spacing

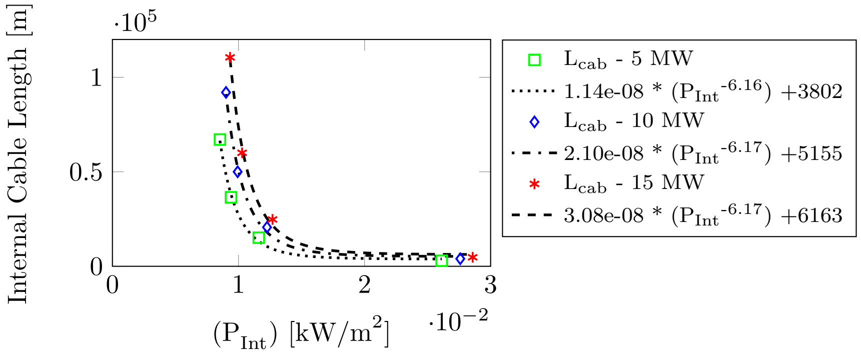

(b) 7ϕ spacing

Figure C.2: *Power relations depicting the scaling of infield cable length with WF Power Intensity.*

Sizing	**5D**	Values in 2012 Eur	**FIXED**											
Decom %	0.91	Turb Rating	5MW				10MW				15 MW			
WF size	Wind Farms are square grids		4	16	36	64	4	16	36	64	4	16	36	64
	Efficiency	Electrical	0.98	0.971	0.977	0.984	0.977	0.978	0.987	0.989	0.975	0.978	0.987	0.989
	Area	m^2	390625	3515625	9765625	19140625	739600	6656400	18490000	36240400	1071225	6656400	18490000	36240400
Cable length	infield	m	2173	10920	26241	48137	2914	14875	35882	65935	3467	17820	43061	79189
	transmission	m	24978	24978	24978	24978	24978	24978	24978	24978	24978	24978	24978	24978
Power		MW	20	80	180	320	40	160	360	640	#REF!	240	540	960
PROCUREMENT	Electrical system	infield cables	720249	1555117	4755930	11743940	415031	3629012	17283304	63145625	628268	8583506	57109012	253579581
		transmission cable	7991218	8591123	11959195	23842104	7923894	11040495	29691237	129119839	8219729	15714812	78608714	489497134
		shunt reactors	344579	373219	481983	698552	341161	456861	773469	1474591	355677	566157	1186694	2728921
		offshore transfomer	789082	1215780	2235886	3444948	722256	2046533	3763687	5798912	979646	2775340	5104003	7864006
		turbine transformee	165946	295016	663786	1180063	143800	575198	1294196	2300794	213845	855381	1924607	3421524
		switch gear	1495709	2317026	3622548	5412276	1495709	2317026	3622548	5412276	1495709	2317026	3622548	5412276
	TOTAL		**11506783**	**14347281**	**23719328**	**46321883**	**11041851**	**20065125**	**56428441**	**207252037**	**11892874**	**30812222**	**1.48E+08**	**762503442**
	Aux	Measuring Tower	2484745	2484745	2484745	2484745	2484745	2484745	2484745	2484745	2484745	2484745	2484745	2484745
		Onshore Premises	1818106	1818106	1818106	1818106	1818106	1818106	1818106	1818106	1818106	1818106	1818106	1818106
		Offshore Platform	1119432	4013453	8855741	15644957	2082502	7886315	17584310	31136728	3047307	11765203	26302018	46562168
	TOTAL		**5422283**	**8316304**	**13158592**	**19947808**	**6385353**	**12189166**	**21887161**	**35439579**	**7350158**	**16068054**	**30604869**	**50865019**
INSTALL	RNA + tower	offshore works	1415186	5660746	12736678	2262984	1664675	6658702	14982079	26634808	1850465	7401861	16654186	29607442
	Aux	Measuring tower	666639	666639	666639	666639	666639	666639	666639	666639	666639	666639	666639	666639
		Port staging	382532	1530127	3442785	6120507	765063	3060254	9885571	12241015	1147595	4590381	10328356	18361522
	TOTAL		**2464357**	**7857512**	**16846102**	**9050130**	**3096377**	**10385595**	**25534289**	**39542462**	**3664699**	**12658881**	**27649181**	**48635603**
	Electrical	infield cables	892150	2044032	4061679	6945093	989809	2564877	5331239	9288895	1062533	2952740	6276656	11034280
		transmission cables	4079834	4079834	4079834	4079834	4079834	4079834	4079834	4079834	4079834	4079834	4079834	4079834
	TOTAL		**4971984**	**6123866**	**8141513**	**11024927**	**5069643**	**6644711**	**9411073**	**13368729**	**5142367**	**7032574**	**10356490**	**15114114**
PROJECT		Management	1242197	3290980	6787198	11968376	1640029	4967469	11157923	22823807	2062943	6882934	17477993	45856673
		engineering	689952	2759808	9209567	11039231	1379904	5519615	12419134	22078461	2069856	8279423	18628702	33117692
	TOTAL		**1932149**	**6050788**	**15996765**	**23007607**	**3019933**	**10487084**	**23577057**	**44902268**	**4132799**	**15162357**	**36106695**	**78974365**
DE-COMMISIONING		Turbine	1287819.3	5151279	11590377	2059315	1514854	6059419	13633692	24237675	1683923	6735694	15155309	26942772
		infield cable	89728	450969	1083723	1987989	120355	614311	1481869	2723027	143162	735949	1778360	3270396
		transmission cable	956270	956270	956270	956270	956270	956270	956270	956270	956270	956270	956270	956270
		Off platform + mete	519118	519118	519118	519118	519118	519118	519118	519118	519118	519118	519118	519118
		site clearance	49960	199841	449642	799364	49960	199841	449642	799364	49960	199841	449642	799364
	TOTAL		**2902895.3**	**7277477**	**14599130**	**6322056**	**3160557**	**8348959**	**17040591**	**29235454**	**3352433**	**9146872**	**18858699**	**32487920**

Sizing	**7D**	Values in 2012 Eur	**FIXED**											
Decom %	0.91	Turb Rating	5MW				10MW				15 MW			
WF size	Wind Farms are square grids		4	16	36	64	4	16	36	64	4	16	36	64
	Efficiency	Electrical	0.98	0.971	0.977	0.984	0.977	0.978	0.987	0.989	0.975	0.978	0.987	0.989
	Area	m^2	765625	6890625	19140625	37515625	1449616	13046544	36240400	71031184	2099601	18896409	52490025	102880449
Cable length	infield	m	2173	10920	26241	48137	2914	14875	35882	65935	3467	17820	43061	79189
	transmission	m	24978	24978	24978	24978	24978	24978	24978	24978	24978	24978	24978	24978
Power		MW	20	80	180	320	40	160	360	640	60	240	540	960
PROCUREMENT	Electrical system	infield cables	355383	2154336	4755930	16363304	569629	5041511	24080815	88096859	865050	11939701	79633745	353984853
		transmission cable	7695879	8591123	11959195	23842104	7923894	11040495	29691237	129119839	8219729	15714812	78608714	489497134
		shunt reactors	329008	373219	481983	698552	341161	456861	773469	1474591	355677	566157	1186694	2728921
		offshore transfomer	429069	1215780	2235886	3444948	722256	2046533	3763687	5798912	979646	2775340	5104003	7864006
		turbine transformeer	73754	295016	663786	1180063	143800	575198	1294196	2300794	213845	855381	1924607	3421524
		switch gear	1495709	2317026	3622548	5412276	1495709	2317026	3622548	5412276	1495709	2317026	3622548	5412276
	TOTAL		**10378802**	**14946500**	**23719328**	**50941247**	**11041851**	**21477624**	**63225952**	**232203271**	**12129656**	**34168417**	**1.7E+08**	**862908714**
	Aux	Measuring Tower	2484745	2484745	2484745	2484745	2484745	2484745	2484745	2484745	2484745	2484745	2484745	2484745
		Onshore Premises	1818106	1818106	1818106	1818106	1818106	1818106	1818106	1818106	1818106	1818106	1818106	1818106
		Offshore Platform	1119432	4013453	8855741	15644957	2082502	7886315	17584310	31136728	3047307	11765203	26302018	46562168
	TOTAL		**5422283**	**8316304**	**13158592**	**19947808**	**6385353**	**12189166**	**21887161**	**35439579**	**7350158**	**16068054**	**30604869**	**50865019**
INSTALL	RNA + tower	offshore works	1415186	5660746	12736678	2262984	1664675	6658702	14982079	26634808	1850465	7401861	16654186	29607442
	Aux	Measuring tower	666639	666639	666639	666639	666639	666639	666639	666639	666639	666639	666639	666639
		Port staging	382532	1530127	3442785	6120507	765063	3060254	6885571	12241015	1147595	4590381	10328356	18361522
	TOTAL		**2464357**	**7857512**	**16846102**	**9050130**	**3096377**	**10385595**	**22534289**	**39542462**	**3664699**	**12658881**	**27649181**	**48635603**
	Electrical	infield cables	996042	2598122	4061679	9438500	1132764	3327305	7189658	12719823	1234578	3870314	8513242	15163362
		transmission cables	4079834	4079834	4079834	4079834	4079834	4079834	4079834	4079834	4079834	4079834	4079834	4079834
	TOTAL		**5075876**	**6677956**	**8141513**	**13518334**	**5069643**	**7407139**	**11269492**	**16799657**	**5314412**	**7950148**	**12593076**	**19243196**
PROJECT		Management	1248154	3325580	6883479	12181759	1648956	5032716	11417601	23675272	2075208	7011147	18220832	48992703
		engineering	689952	2759808	6209567	11039231	1379904	5519615	12419134	625927164	2069856	8279423	18628702	33117692
	TOTAL		**1938106**	**6085388**	**13093046**	**23220990**	**3019933**	**10552331**	**23836735**	**649602436**	**4145064**	**15290570**	**36849534**	**82110395**
DE-COMMISIONING		Turbine	1287819.3	5151279	11590377	2059315	1514854	6059419	13633692	24237675	1683923	6735694	15155309	26942772
		infield cable	122310	624737	1507282	2769944	165187	853416	2064686	3798999	197117	1023709	2479775	456315
		transmission cable	956270	956270	956270	956270	956270	956270	956270	956270	956270	956270	956270	956270
		Off platform + metec	519118	519118	519118	519118	519118	519118	519118	519118	519118	519118	519118	519118
		site clearance	49960	199841	449642	799364	49960	199841	449642	799364	49960	199841	449642	799364
	TOTAL		**2935477.3**	**7451245**	**15022689**	**7104011**	**3160557**	**8588064**	**17623408**	**30311426**	**3406388**	**9434632**	**19560114**	**29673839**

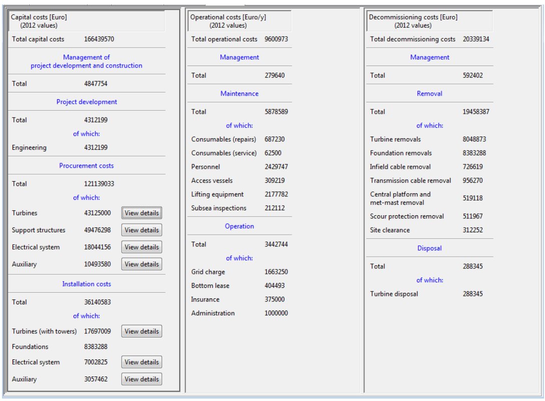

Capital costs [Euro] (2012 values)		
Total capital costs	166439570	
Management of project development and construction		
Total	4847754	
Project development		
Total	4312199	
of which:		
Engineering	4312199	
Procurement costs		
Total	121139033	
of which:		
Turbines	43125000	View details
Support structures	49476298	View details
Electrical system	18044156	View details
Auxiliary	10493580	View details
Installation costs		
Total	36140583	
of which:		
Turbines (with towers)	17697009	View details
Foundations	8383288	
Electrical system	7002825	View details
Auxiliary	3057462	View details

Operational costs [Euro/y] (2012 values)	
Total operational costs	9600973
Management	
Total	279640
Maintenance	
Total	5878589
of which:	
Consumables (repairs)	687230
Consumables (service)	62500
Personnel	2429747
Access vessels	309219
Lifting equipment	2177782
Subsea inspections	212112
Operation	
Total	3442744
of which:	
Grid charge	1663250
Bottom lease	404493
Insurance	375000
Administration	1000000

Decommissioning costs [Euro] (2012 values)	
Total decommissioning costs	20339134
Management	
Total	592402
Removal	
Total	19458387
of which:	
Turbine removals	8048873
Foundation removals	8383288
Infield cable removal	726619
Transmission cable removal	956270
Central platform and met-mast removal	519118
Scour protection removal	511967
Site clearance	312252
Disposal	
Total	288345
of which:	
Turbine disposal	288345

(a) 5 MW, 5 x 5

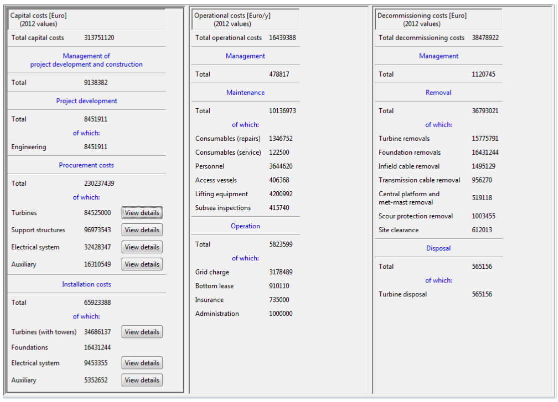

Capital costs [Euro] (2012 values)		
Total capital costs	313751120	
Management of project development and construction		
Total	9138382	
Project development		
Total	8451911	
of which:		
Engineering	8451911	
Procurement costs		
Total	230237439	
of which:		
Turbines	84525000	View details
Support structures	96973543	View details
Electrical system	32428347	View details
Auxiliary	16310549	View details
Installation costs		
Total	65923388	
of which:		
Turbines (with towers)	34686137	View details
Foundations	16431244	
Electrical system	9453355	View details
Auxiliary	5352652	View details

Operational costs [Euro/y] (2012 values)	
Total operational costs	16439388
Management	
Total	478817
Maintenance	
Total	10136973
of which:	
Consumables (repairs)	1346752
Consumables (service)	122500
Personnel	3644620
Access vessels	406368
Lifting equipment	4200992
Subsea inspections	415740
Operation	
Total	5823599
of which:	
Grid charge	3178489
Bottom lease	910110
Insurance	735000
Administration	1000000

Decommissioning costs [Euro] (2012 values)	
Total decommissioning costs	38478922
Management	
Total	1120745
Removal	
Total	36793021
of which:	
Turbine removals	15775791
Foundation removals	16431244
Infield cable removal	1495129
Transmission cable removal	956270
Central platform and met-mast removal	519118
Scour protection removal	1003455
Site clearance	612013
Disposal	
Total	565156
of which:	
Turbine disposal	565156

(b) 5 MW, 7 x 7

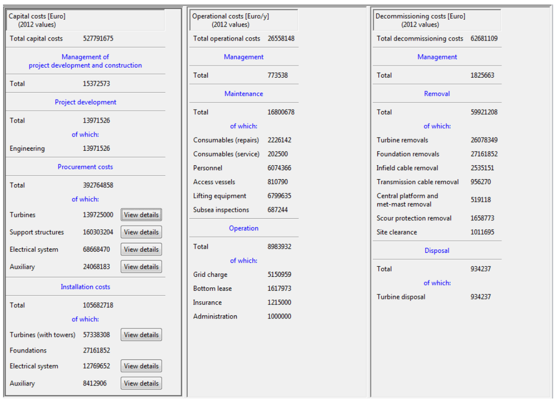

Capital costs [Euro] (2012 values)		
Total capital costs	527791675	
Management of project development and construction		
Total	15372573	
Project development		
Total	13971526	
of which:		
Engineering	13971526	
Procurement costs		
Total	392764858	
of which:		
Turbines	139725000	View details
Support structures	160303204	View details
Electrical system	68668470	View details
Auxiliary	24068183	View details
Installation costs		
Total	105682718	
of which:		
Turbines (with towers)	57338308	View details
Foundations	27161852	
Electrical system	12769652	View details
Auxiliary	8412906	View details

Operational costs [Euro/y] (2012 values)	
Total operational costs	26558148
Management	
Total	773538
Maintenance	
Total	16800678
of which:	
Consumables (repairs)	2226142
Consumables (service)	202500
Personnel	6074366
Access vessels	810790
Lifting equipment	6799635
Subsea inspections	687244
Operation	
Total	8983932
of which:	
Grid charge	5150959
Bottom lease	1617973
Insurance	1215000
Administration	1000000

Decommissioning costs [Euro] (2012 values)	
Total decommissioning costs	62681109
Management	
Total	1825663
Removal	
Total	59921208
of which:	
Turbine removals	26078349
Foundation removals	27161852
Infield cable removal	2535151
Transmission cable removal	956270
Central platform and met-mast removal	519118
Scour protection removal	1658773
Site clearance	1011695
Disposal	
Total	934237
of which:	
Turbine disposal	934237

(c) 5 MW, 9 x 9

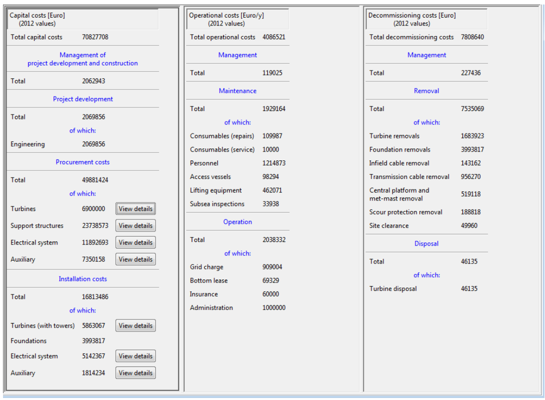

Capital costs [Euro] (2012 values)		
Total capital costs	70827708	
Management of project development and construction		
Total	2062943	
Project development		
Total	2069856	
of which:		
Engineering	2069856	
Procurement costs		
Total	49881424	
of which:		
Turbines	6900000	View details
Support structures	23738573	View details
Electrical system	11892693	View details
Auxiliary	7350158	View details
Installation costs		
Total	16813486	
of which:		
Turbines (with towers)	5863067	View details
Foundations	3993817	
Electrical system	5142367	View details
Auxiliary	1814234	View details

Operational costs [Euro/y] (2012 values)	
Total operational costs	4086521
Management	
Total	119025
Maintenance	
Total	1929164
of which:	
Consumables (repairs)	109987
Consumables (service)	10000
Personnel	1214873
Access vessels	98294
Lifting equipment	462071
Subsea inspections	33938
Operation	
Total	2038332
of which:	
Grid charge	909004
Bottom lease	69329
Insurance	60000
Administration	1000000

Decommissioning costs [Euro] (2012 values)	
Total decommissioning costs	7808640
Management	
Total	227436
Removal	
Total	7535069
of which:	
Turbine removals	1683923
Foundation removals	3993817
Infield cable removal	143162
Transmission cable removal	956270
Central platform and met-mast removal	519118
Scour protection removal	188818
Site clearance	49960
Disposal	
Total	46135
of which:	
Turbine disposal	46135

(d) 15 MW, 2 x 2

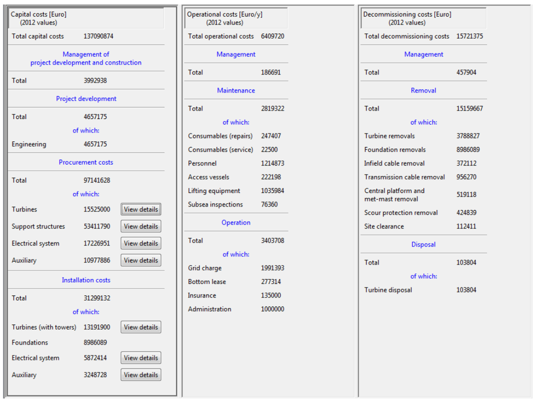

Capital costs [Euro] (2012 values)		
Total capital costs	137090874	
Management of project development and construction		
Total	3992938	
Project development		
Total	4657175	
of which:		
Engineering	4657175	
Procurement costs		
Total	97141628	
of which:		
Turbines	15525000	View details
Support structures	53411790	View details
Electrical system	17226951	View details
Auxiliary	10977886	View details
Installation costs		
Total	31299132	
of which:		
Turbines (with towers)	13191900	View details
Foundations	8986089	
Electrical system	5872414	View details
Auxiliary	3248728	View details

Operational costs [Euro/y] (2012 values)	
Total operational costs	6409720
Management	
Total	186691
Maintenance	
Total	2819322
of which:	
Consumables (repairs)	247407
Consumables (service)	22500
Personnel	1214873
Access vessels	222198
Lifting equipment	1035984
Subsea inspections	76360
Operation	
Total	3403708
of which:	
Grid charge	1991393
Bottom lease	277314
Insurance	135000
Administration	1000000

Decommissioning costs [Euro] (2012 values)	
Total decommissioning costs	15721375
Management	
Total	457904
Removal	
Total	15159667
of which:	
Turbine removals	3788827
Foundation removals	8986089
Infield cable removal	372112
Transmission cable removal	956270
Central platform and met-mast removal	519118
Scour protection removal	424839
Site clearance	112411
Disposal	
Total	103804
of which:	
Turbine disposal	103804

(e) 15 MW, 3 x 3

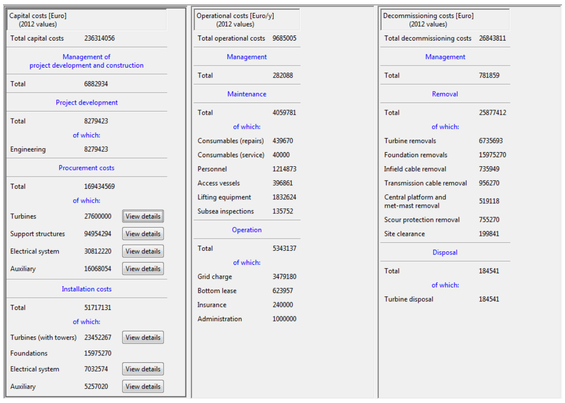

Capital costs [Euro] (2012 values)		
Total capital costs	236314056	
Management of project development and construction		
Total	6882934	
Project development		
Total	8279423	
of which:		
Engineering	8279423	
Procurement costs		
Total	169434569	
of which:		
Turbines	27600000	View details
Support structures	94954294	View details
Electrical system	30812220	View details
Auxiliary	16068054	View details
Installation costs		
Total	51717131	
of which:		
Turbines (with towers)	23452267	View details
Foundations	15975270	
Electrical system	7032574	View details
Auxiliary	5257020	View details

Operational costs [Euro/y] (2012 values)	
Total operational costs	9685005
Management	
Total	282088
Maintenance	
Total	4059781
of which:	
Consumables (repairs)	439670
Consumables (service)	40000
Personnel	1214873
Access vessels	396861
Lifting equipment	1832624
Subsea inspections	135752
Operation	
Total	5343137
of which:	
Grid charge	3479180
Bottom lease	623957
Insurance	240000
Administration	1000000

Decommissioning costs [Euro] (2012 values)	
Total decommissioning costs	26843811
Management	
Total	781859
Removal	
Total	25877412
of which:	
Turbine removals	6735693
Foundation removals	15975270
Infield cable removal	735949
Transmission cable removal	956270
Central platform and met-mast removal	519118
Scour protection removal	755270
Site clearance	199841
Disposal	
Total	184541
of which:	
Turbine disposal	184541

(f) 15 MW, 4 x 4

Figure C.3: *Cost Results for BoP simulations for 5MW and 15 MW* VAWT *in a rectangular grid*

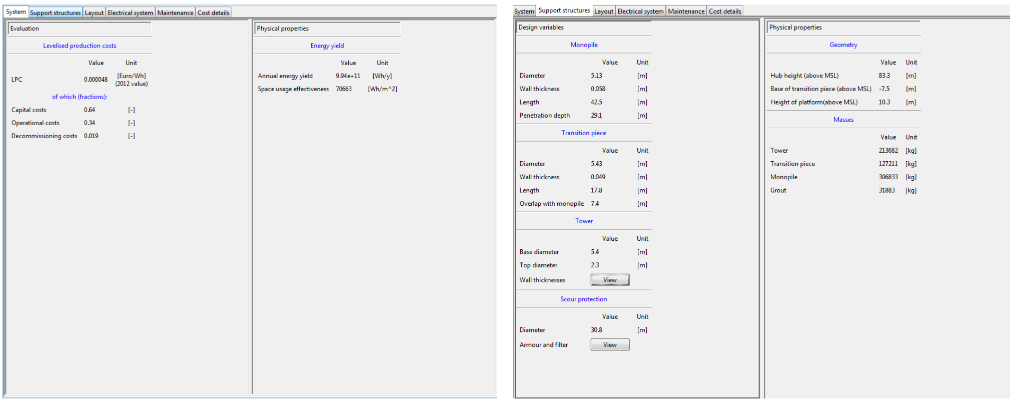

Evaluation

Levelised production costs

	Value	Unit
LPC	0.000048	[Euro/Wh] (2012 value)
of which (fractions):		
Capital costs	0.64	[-]
Operational costs	0.34	[-]
Decommissioning costs	0.019	[-]

Physical properties

Energy yield

	Value	Unit
Annual energy yield	9.94e+11	[Wh/y]
Space usage effectiveness	70663	[Wh/m^2]

Design variables

Monopile

	Value	Unit
Diameter	5.13	[m]
Wall thickness	0.058	[m]
Length	42.5	[m]
Penetration depth	29.1	[m]

Transition piece

	Value	Unit
Diameter	5.43	[m]
Wall thickness	0.049	[m]
Length	17.8	[m]
Overlap with monopile	7.4	[m]

Tower

	Value	Unit
Base diameter	5.4	[m]
Top diameter	2.3	[m]
Wall thicknesses	View	

Scour protection

	Value	Unit
Diameter	30.8	[m]
Armour and filter	View	

Physical properties

Geometry

	Value	Unit
Hub height (above MSL)	83.3	[m]
Base of transition piece (above MSL)	-7.5	[m]
Height of platform(above MSL)	10.3	[m]

Masses

	Value	Unit
Tower	213682	[kg]
Transition piece	127211	[kg]
Monopile	306833	[kg]
Grout	31883	[kg]

(a) LCoE and WF performance

(b) Support Structure mass

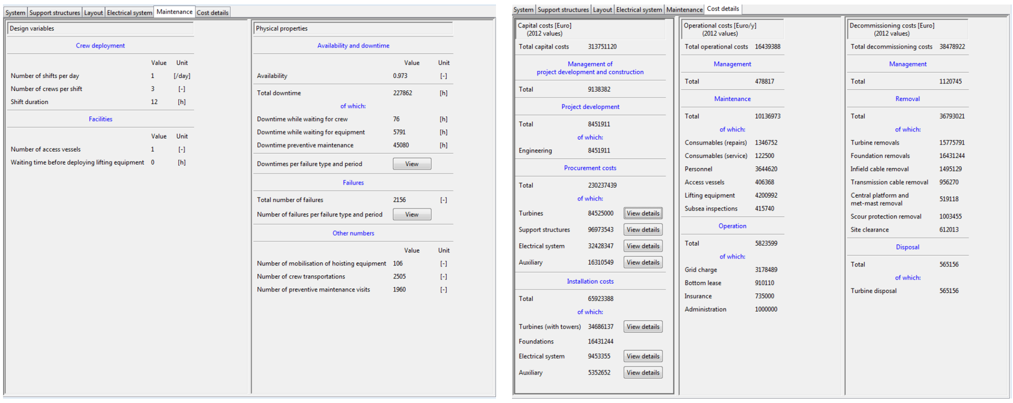

Design variables

Crew deployment

	Value	Unit
Number of shifts per day	1	[/day]
Number of crews per shift	3	[-]
Shift duration	12	[h]

Facilities

	Value	Unit
Number of access vessels	1	[-]
Waiting time before deploying lifting equipment	0	[h]

Physical properties

Availability and downtime

	Value	Unit
Availability	0.973	[-]
Total downtime	227862	[h]
of which:		
Downtime while waiting for crew	76	[h]
Downtime while waiting for equipment	5791	[h]
Downtime preventive maintenance	45080	[h]
Downtimes per failure type and period	View	

Failures

Total number of failures	2156	[-]
Number of failures per failure type and period	View	

Other numbers

	Value	Unit
Number of mobilisation of hoisting equipment	106	[-]
Number of crew transportations	2505	[-]
Number of preventive maintenance visits	1960	[-]

Capital costs [Euro]
(2012 values)

Total capital costs	313751120	
Management of project development and construction		
Total	9138382	
Project development		
Total	8451911	
of which:		
Engineering	8451911	
Procurement costs		
Total	230237439	
of which:		
Turbines	84525000	View details
Support structures	96973543	View details
Electrical system	32428347	View details
Auxiliary	16310549	View details
Installation costs		
Total	65923388	
of which:		
Turbines (with towers)	34686137	View details
Foundations	16431244	
Electrical system	9453355	View details
Auxiliary	5352652	View details

Operational costs [Euro/y]
(2012 values)

Total operational costs	16439388
Management	
Total	478817
Maintenance	
Total	10136973
of which:	
Consumables (repairs)	1346752
Consumables (service)	122500
Personnel	3644620
Access vessels	406368
Lifting equipment	4200992
Subsea inspections	415740
Operation	
Total	5823599
of which:	
Grid charge	3178489
Bottom lease	910110
Insurance	735000
Administration	1000000

Decommissioning costs [Euro]
(2012 values)

Total decommissioning costs	38478922
Management	
Total	1120745
Removal	
Total	36793021
of which:	
Turbine removals	15775791
Foundation removals	16431244
Infield cable removal	1495129
Transmission cable removal	956270
Central platform and met-mast removal	519118
Scour protection removal	1003455
Site clearance	612013
Disposal	
Total	565156
of which:	
Turbine disposal	565156

(c) O & M

(d) Cost Details

Figure C.4: *Cost Results for* OWFDE*simulations for 5MW bottom founded*HAWT *in a 7 x 7 rectangular grid*

Appendix D

Operation and Maintenance

D.1 Repair Classes

For any repair class, there are four assumed different types of maintenance process that can be executed in the repair class.These can either be or a combination of *remote reset*,*inspection*, *repair* and *replacement*, de Pieterman et al., de Pieterman et al. [28, 29]. For each of these maintenance processes, sequential phases are involved, each which have specified time intervals constituting of a fixed portion or/and the time defined due to the repair class.

Remote reset	No resources utilisation; Execution time = fixed at restart procedure from control room at TSO substation
Inspection	Technicians and a single access vehicle need; Launch time = default; travel time = vessel dependant, weather dependant; Execution time = default
Repair	Modelled identically to *Inspection*, Allows use of support vessels such as crane's etc to execute the repair
Replacement	Multiple resource utilisation based on number of vessels; Launch time = *Inspection* phase; Travel time = vessel dependant, weather dependant; Execution time = preparation (default [6 hr]) + Positioning (RC dependant) + finalisation

A Default time specification denotes a fixed time which is presumed into the OMCE tool during initialisation of general properties. Unless otherwise specified during the Repair class definition, it is kept at the default value. For the replacement maintenance phase, upto four vessels can be simultaneously alloted, each adding their own constraints based on immobilisation time and weather related constraints. Before a replacement maintenance phase can be executed in a repair class, a preceding inspection phase is necessary. The total time taken to carry out a Repair Type may stretch over a few days depending on the weather and resource availability and work hours.

Unplanned Corrective maintenance	Repair Classes: RC 1 to RC 12
Condition based maintenance	Repair Classes: RC 13 to RC 15
Calendar based maintenance	Repair classes: RC 16 to RC 19

Class	Repair type	Modifications	Explanation of modifications
RC1	Remote Reset	None	Similar to Default Model
RC2	4h inspection/small repair inside	Procedure	• Procedure - The ROV is used to inspect the spar bouy and the mooring system depending on what alarm was triggered - The technicians mount turbine. Two take the elevator down to generator while one stays on the platform - Fix fault
RC3	6h Inspection/small repair outside	Time Procedure	• Time: reduced by 33% as two blades instead of three • Procedure - Two technicians take elevator up to top of turbine - Equipment also transported under elevator (<1MT) - Repair done by hanging off the side of the blade with harnesses and pulleys - Crane in middle section between top and bottom direction elevators
RC4	8h Replacement parts(subsea) internal	Procedure	These include small replacements in the generator section in the lower part of the spar bouy where the power train is housed. • Procedure - Items (<2MT) picked up by crane, put in lower elevator - Two technicians and equipment lowered
RC5	16h Replacement parts internal (sub sea) (< 2MT)	None	Same as above, just takes longer
RC6	24h Replacement parts external (sub sea) (< 2 MT)	Procedure	Same as RC4 but takes longer • Procedure - Uses ROV as well and involves 4 technicians - An ROV is utilised to do external work and small replacements
RC7	24 hr replacement parts external (<100MT)	Vessel Procedure	• Vessel: Dynamic Positioning Crane instead of Jack-up • Procedure - Inspection of blades by work boat team, 3 technicians - Assess damage and give report - Preparation time where Items ordered, take 16 hrs - Use of Dynamic positioning crane - Work boat vessel with 6 technicians - Replacement procedure take approximately 24

			hrs - An additional repair assessment is initiated after the replacement phase
RC8	48 hr replacement parts external (subsea)(<100MT)	Time Vessel Procedure	Mother vessel also used for diving support (4 divers). Used for replacement of lowest parts of the sparbouy/overhaul of large components. Modular system where whole generator/Bearing and mooring and are not attached in a series manner where they are coupled but can be removed independently. • Time: Longer by 33% • Vessel: Support Mother Vessel, Workboat ROV • Procedure -Inspection Same as above, - The whole unit is removed as a modular - Technicians free the generator from the inside - Use of 4 divers, 4 technician and submarine ROV
RC9	8h BoP transformer repair	None	Focused on repairing Transformer substation Results in 50% of wind farm out of operation
RC10	48h BoP transformer/ Mooring repair	Name Vessel Procedure	Similar to RC9, Focused on Transformer substation repair, use of helicopter removed • Vessel: Support Mother Vessel, Workboat ROV • Procedure - Inspection: work boat and 3 technicians, 4 hr - Repair: Mother vessel and 4 technicians, 44 hrs, small items but complicated operation(< 2MT)
RC11	10h BoP mooring repair	New Repair Class	• Time: Longer by 25% • Vessel: Support Mother Vessel, Workboat ROV • Procedure - Work boat, 6 hr organisation time, 4 hrs inspection - Mother vessel , organisation time 6 hr (assumed items on board always) - Travel time 2 hrs Mother vessel travels to wind farms - Lowers part to bottom with crane - ROV makes change - Replacement phase to finalise work and check it
RC12	32 BoP cable replacement	None	
RC13	8 hr Pitch motor replacement	Removed	**There are no Pitch or Yaw motors in the DeepWind wind turbine**
RC14	16 hr yaw motor replacement	Removed	

RC13	8 hr BoP Repair (TSO)	New Repair Class	Similar to RC 9 and RC 10 Costs and logistics equipment removed Based on the pretence that for foar offshore wind farms, a offshore distribution point will be provided by the TSO. This is maintained and operated by the TSO and any problem incurred results in a time delay of operation for 50 % of the wind farm
RC14	48 hr BoP Repair (TSO)	New Repair Class	
RC15	160h BoP transformer repair	Vessel	Focused on inspection of the underwater transformer module system. Due to lack of knowledge on transformer design of Wind Turbine, left unaltered and used as given in Default model • Vessel: Support Mother Vessel
RC16	24h WT preventive maintenance	None	Similar to Default model
RC17	48h WT preventive maintenance	None	
RC18	6h BoP preventive maintenance-Inspection	New Repair Class	Two similar Repair classes for Calendar based maintenance focused on the bi annually inspection and if needed, restorative repair/replacement of the highly loaded mooring system of all the turbines. It is assumed that 50% of the turbines need some sort of maintenance while the rest are inspected and found fit. This is modelled in the WT system “Mooring bearing” instead of the BoP system “Mooring system” so that each turbine can be individually checked • Time: 6 h • Vessel: Workboat ROV, 2 technicians • Procedure - Work boat picks up technicians from mother vessel - The inspection process is for half the turbines which do not need any repair • Time: 4 h + 6 hr • Vessel: Workboat ROV, 2 technicians • Procedure - Work boat picks up technicians from mother vessel The inspection process is for other half the turbines which do need repair is 2 hours less as the same workboat performs the repair which takes 6 hrs - Items used are consumable and small moving items which are present on the workboat.
RC19	12 h BoP preventive maintenance-Inspection	New Repair Class	

D.2 Failure Frequencies

A number of studies have compiled the failure rates from various turbines and wind farms. Most of the studies are based on the results from onshore wind turbines. Thus the difference in technology and operational regime creates a slight bias against modern HAWT offshore turbine failure rates. According to Polinder et al. [61], Tavner et al. [69] [67], modern turbines which incorporate newer technologies to counter the intrinsic failure problems with hydraulic and gearbox assemblies suffer from a substantial increase in failure rate in electrical related sub assemblies, in some cases to a factor of almost double [69].Considering this eventuality, in the ECN default model, the associated failure frequency is kept much higher than what is reported from the LWK and WMEP surveys. There is also some disparity on how whether the results from the LWK and WMEP surveys are directly applicable to OWT's. Especially because the failures in the BoS are not readily available while the reliability of Danish onshore turbines is quite high, [69].

This compilation was meant to study the distribution of the failure frequencies over the different WT systems. The different studies used different classification methods for the failures. To summarise the distributions into a homogeneous terminology, the following classification was used

- Auxiliary Equipment : Electrical Protection and Safety system, Hydraulic, Cooling, Crane
- Control and Comm systems : Sensor, transmitters, receivers, safety chain, controllers (Power train and rotor)
- Drive Train : Gear Box assembly, shafts, bearings, brake
- Nacelle : Yaw System, Frame, Bed-plate
- Power-Train : converter + switch, generator, transformer, transmission cables, machinery enclosure
- Rotor : Blade,Pitching system, hub assembly, slip rings
- Structure : Tower, foundation(onshore)
- Misc

Wind Turbine Reliability Study

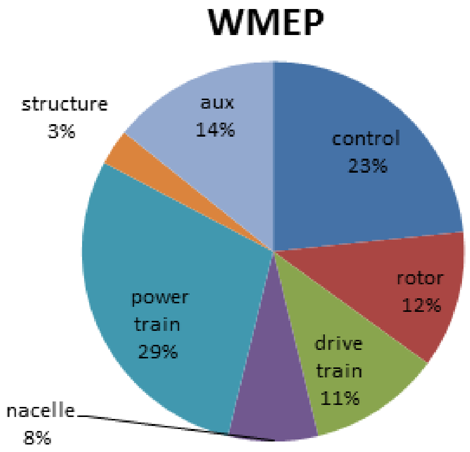

- Large monitoring programme operated by Fraunhofer IWES
- Sampling time = 1989 to 2006
- Data from 1500 onshore turbines reported operating for 15400 turbine years
-
- Overall mean failure frequency/turbine = **2.356**

Wind Turbine Reliability Study

The R80 FMECA wind turbine is a generic 2MW,(ϕ: 80 m) wind turbine configuration which is optimised to increase system reliability until a subsystem level

It was a work package of the ReliaWind project which used Failure mode effects and criticality analysis of different WT designs to predict the WT reliability

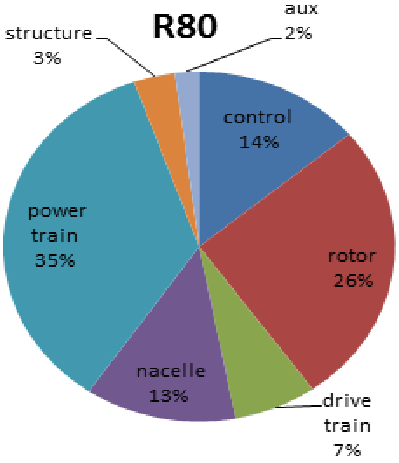

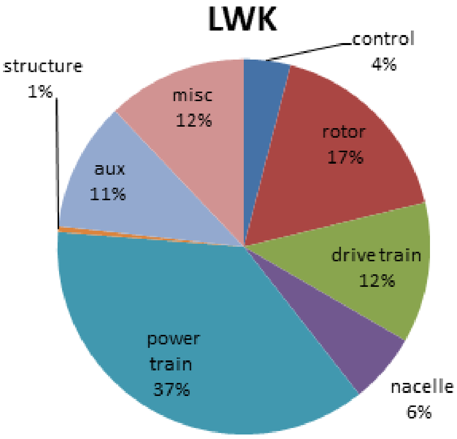

- Failure statistics published *Landwirtschaftskammer Schleswig-Holstein*
- Sampling time = 1993 to 2006
- 650 onshore turbines reported operating for 5800 turbine years
- WT size from 225 kW to 1.8 MW
- Both stall, pitch regulated and as well as Direct-Drive and drive-train types surveyed
-
- Overall mean failure frequency/turbine = **1.813**

OMCE's default model was based mainly on the results from the Reliawind project and *in-house knowledge* as collected from de Pieterman et al. [28]. The difference in failure distribution is attributed towards the classification overlap compared to the source of information for the Reliawind and what is suggested in the OMCE default model

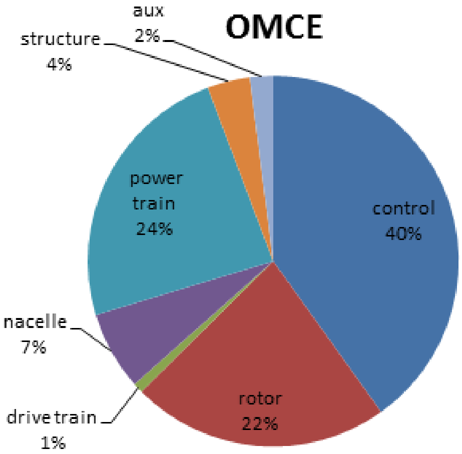

Wind Turbine Reliability Study	
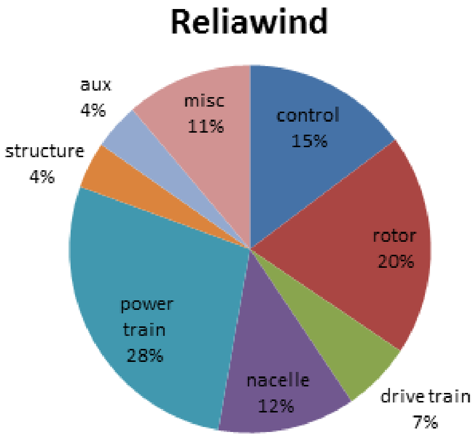	• European Union project involving 10 industrial and academic partners • Sampling time = 2006 to 2011 • 350 pitch regulated turbines , less than 6 yrs old • WT size ≥ 850 kW • • Overall mean failure frequency/turbine **unpublished**

Table D.1: *Review of failure frequencies from three European reliability surveys, a turbine manufacturer data and in-house knowledge at ECN*

In the WMEP database, large variation of turbines were assessed. There was a sharp change of technology during the late 90s towards Direct drive machines. This significantly increases the rate of failures as compared to having a gearbox with conventional generator technology. The control modules are accounted for together for both the power train and rotor.

From the LWK database, Failure rate is low for realistic estimation. The data might be biased as the sample size for each type of turbine might not be same. Reliability tends to decrease from small to large group, representing mature to less mature technologies. Benefits from direct-drive WTs over geared WTs not conclusive; need more data collection to evaluate. The power train controller and rotor controller are considered with the subsystems and not individually

The ReliaWind database indicates that the drive train components only account for a smaller portion of both the total amount of failures. This can be accounted to that pitch regulated wind turbines tend have fewer Drive train failures and also that a larger majority of the sampled turbines are direct drive machines.

The OMCE failure application of the Reliawind results indicates that there is a large failure portion attributed to the control and protection systems for the turbine and the generator. This seems a little inconsistent with the other databases results.

DTU Wind Energy is a department of the Technical University of Denmark with a unique integration of research, education, innovation and public/private sector consulting in the field of wind energy. Our activities develop new opportunities and technology for the global and Danish exploitation of wind energy. Research focuses on key technical-scientific fields, which are central for the development, innovation and use of wind energy and provides the basis for advanced education at the education.

We have more than 240 staff members of which approximately 60 are PhD students. Research is conducted within nine research programmes organized into three main topics: Wind energy systems, Wind turbine technology and Basics for wind energy.

Danmarks Tekniske Universitet
DTU Vindenergi
Nils Koppels Allé
Bygning 403
2800 Kgs. Lyngby
Telefon 45 25 25 25

info@vindenergi.dtu.dk
www.vindenergi.dtu.dk